The impact of interspecific hybridization on fungal plant pathogens:

a case study on the emerging pathogen *Verticillium longisporum*

Jasper R. L. Depotter

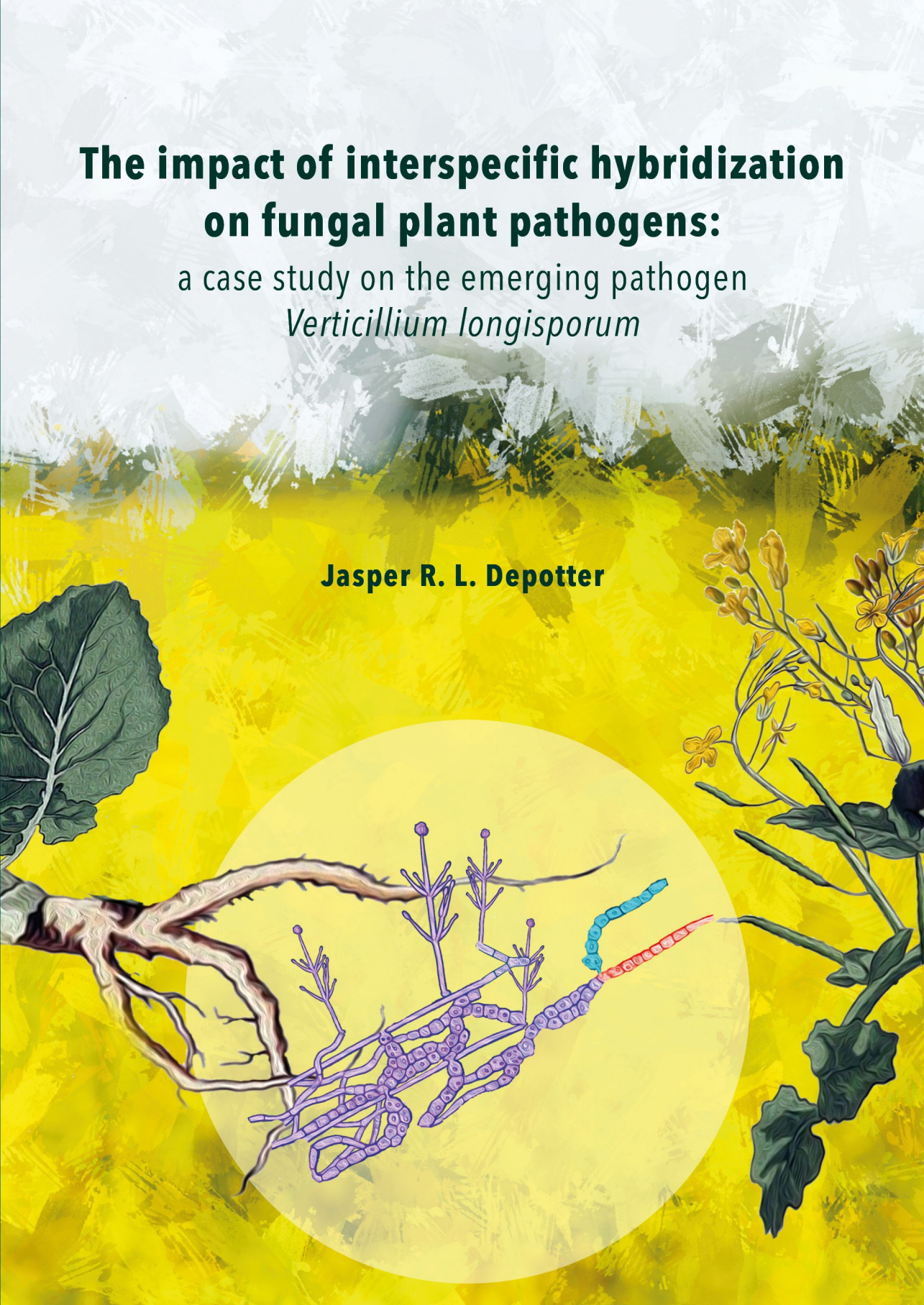

Propositions

1. Interspecific hybridization is an important evolutionary mechanism to evade host immunity.
   (this thesis)

2. A previously established *Verticillium longisporum* population caused the recent emergence of Verticillium stem striping in the UK.
   (this thesis)

3. Microorganisms should not be used as bio-control agents against pathogens.

4. Sex is overrated as a mechanism to generate genetic diversity.

5. Durable resistance can only be achieved by alternating expression of different resistance genes.

6. Exercising contributes to food waste.

7. Internationalization of higher education increases the quality of academic courses.

Propositions belonging to the thesis, entitled

'The impact of interspecific hybridization on fungal plant pathogens:
a case study on the emerging pathogen *Verticillium longisporum*'.

Jasper Robert Lisette Depotter
Wageningen, 14 September 2018

The impact of interspecific hybridization on fungal plant pathogens:

a case study on the emerging pathogen *Verticillium longisporum*

Jasper R. L. Depotter

Thesis committee

Promotor
Prof. Dr B.P.H.J. Thomma
Professor of Phytopathology
Wageningen University & Research

Co-promotors
Dr T.A. Wood
Senior Molecular Pathologist
National Institute of Agricultural Botany, Cambridge, UK

Dr M.F. Seidl
Assistant Professor, Laboratory of Phytopathology
Wageningen University & Research

Other members
Prof. Dr J.A.G.M. de Visser, Wageningen University & Research
Prof. Dr V. Lipka, Georg-August-University Goettingen, Germany
Prof. Dr M. Rep, University of Amsterdam
Dr G. Bonnema, Wageningen University & Research

This research was conducted under the auspices of the Graduate School Experimental Plant Sciences.

The impact of interspecific hybridization on fungal plant pathogens:

a case study on the emerging pathogen *Verticillium longisporum*

Jasper R. L. Depotter

Thesis
submitted in fulfilment of the requirements for the degree of doctor
at Wageningen University
by the authority of the Rector Magnificus,
Prof. Dr A.P.J. Mol,
in the presence of the
Thesis Committee appointed by the Academic Board
to be defended in public
on Friday 14 September 2018
at 4 p.m. in the Aula.

Jasper R.L. Depotter
The impact of interspecific hybridization on fungal plant pathogens: a case study on the emerging pathogen *Verticillium longisporum*,
202 pages.

PhD thesis, Wageningen University, Wageningen, The Netherlands (2018)
With references, with summary in English

DOI: 10.18174/453468
ISBN: 978-94-6343-299-3

Table of contents

1

General introduction

Plant disease emergences

Emerging plant diseases, i.e. diseases that have suddenly increased in incidence or are newly recognized, pose a threat to agricultural and natural ecosystems (Fisher *et al.*, 2012). A notorious example is the emergence of the potato late blight disease during the mid-nineteenth century, which caused the infamous Irish potato famine leading to mass emigration and death of millions of people in Ireland (Bourke, 1964; Ristaino, 2002). The majority of emerging diseases originate from pathogen introductions into new geographic regions (Anderson *et al.*, 2004). Conceivably, the absence of co-evolution between a local ecosystem and a newly introduced pathogen may result in abundant pathogen proliferation, potentially developing into an epidemic (Anderson *et al.*, 2004). Pathogen introductions can occur through natural dispersal of propagules across large distances. For instance, rust pathogens are notorious for their long distance dispersal by airborne spores (Bowden *et al.*, 1971; Brown and Hovmøller, 2002). This mobility can facilitate/drive the emergence of new rust lineages, as illustrated by the recent discovery of the yellow rust (*Puccinia striiformis* f. sp. *tritici*) Warrior-lineage in European wheat fields, likely originating from the center of yellow rust diversity in Asia (Hovmøller *et al.*, 2016; Hubbard *et al.*, 2015). Long distance dispersal of plant pathogens can also be facilitated through human transport and trade of plant commodities (Brasier, 2008; Wellings *et al.*, 1987). The collateral effects of such global distribution is exemplified by the introduction of the American conifer pathogen *Heterobasidion irregulare* into Italy upon the movement of US troops into Europe during World War II (Garbelotto and Gonthier, 2013; Gonthier *et al.*, 2004).

In addition to novel introductions into new geographic areas, other factors play a role in the emergence of plant diseases. Plant diseases embody interactions between pathogen, environment and host (Scholthof, 2007). Consequently, alterations in any of these three factors can cause a shift in balance, potentially leading to the emergence of a novel disease. Firstly, disease emergence can be driven by genomic alterations in pathogens that result in evasion of host immunity or in increased virulence. For instance, different microbial species can exchange genetic material through horizontal gene transfer, leading to changes in pathogenic traits (Soanes and Richards, 2014). *Pyrenophora tritici-repentis*, the causal agent of wheat tan spot, gained pathogenicity on wheat through the acquisition of a gene from the fungal wheat pathogen *Phaeosphaeria nodorum*, enabling the production of the host-specific toxin ToxA (Friesen *et al.*, 2006). Furthermore, plant hosts can also play a major role in the emergence of plant diseases, as a high abundance of susceptible hosts facilitates pathogen proliferation. In comparison to natural ecosystems, agro-ecosystems are characterized by their homogeneity over large spatial scales, which further facilitates the emergence and dissemination of pathogens (McDonald and Stukenbrock, 2016). These pathogen-conducive properties of agro-ecosystems enable disease outbreaks to develop into epidemics. For instance, global dessert banana production is characterized

by extreme homogeneity, as commercial production is based exclusively on the single Cavendish banana cultivar (Ploetz *et al.*, 2015). Cavendish monocultures give leeway to the spread of diseases, such as the Panama disease caused by *Fusarium oxysporum* f.sp. *cubense,* of which the Tropical Race 4 currently threatens global banana production (Ordonez *et al.*, 2015). Finally, environmental factors also play a pivotal role in plant disease development (Colhoun, 1973). Consequently, weather data are an important parameter in plant disease simulation models such as LATEBLIGHT that predicts late blight disease development on potato (Andrade-Piedra *et al.*, 2005). The far-reaching influence of environmental conditions on plant diseases cause on-going concerns for food security, especially in the light of global warming, as its impact on plant diseases is hard to predict (Chakraborty and Newton, 2011).

New plant pathogens emerge upon hybridization

Hybridization is a powerful evolutionary mechanism, as the (re-)combination of adaptive traits of distinct lineages can increase the adaptive potential of organisms, including plant pathogens (Seehausen, 2004). Plant pathogens engage in continuing arms races with their hosts for continued symbiosis (Cook *et al.*, 2015). The increased adaptive potential of hybridization can be used by plant pathogens to overcome host immunity responses. Hence, new plant pathogens can quickly emerge upon hybridization (Stukenbrock, 2016a). Recently, hybridization enabled a new pathogen to emerge on the cereal crop triticale that was only introduced in the 1960s (Menardo *et al.*, 2016). Two *formae speciales* of the powdery mildew pathogen *Blumeria graminis* hybridized, eventually leading to the triticale-infecting lineage *B. graminis* f. sp. *triticale*.

Plant pathogen hybrids can occur through sexual reproduction, when gametes of different microbes fuse into viable zygotes (Stukenbrock, 2016b). In general, these hybrids have the same ploidy as their parents and create genomic variation by sexual recombination between parental chromosome sets. For instance, sexual recombination between races of the Brassicaceae pathogen *Albugo candida* resulted in genomes where 25% of the genetic material has a different racial origin (McMullan *et al.*, 2015). Consequently, effector repertoires have been exchanged between host-specific *A. candida* races enabling host infection of normally non-infecting races. Alternatively, plant pathogens can also double their genome content upon hybridization (allopolyploidization). For instance, the grey-mould neck rot pathogen *Botrytis allii* is an allodiploid hybrid between *Botrytis aclada* and *Botrytis byssoidea* (Staats *et al.*, 2005). Apart from novel combinations of parental alleles, the redundancy of an additional gene copy number in allopolyploid hybrids provides an additional source for niche adaptation (Van de Peer *et al.*, 2017).

Study system: the hybrid fungal pathogen *V. longisporum*

Interspecific hybridization allowed a new pathogenic species to emerge in the ascomycete genus *Verticillium*: *Verticillium longisporum* (Inderbitzin *et al.*, 2011b). *V. longisporum* has distinct disease properties from haploid *Verticillium* spp., as it generally infects brassicaceous plants, whereas the other *Verticillium* spp. generally do not colonize plants of this family (Eynck *et al.*, 2007; Inderbitzin and Subbarao, 2014). Similar to other pathogenic *Verticillium* spp., *V. longisporum* causes wilting symptoms on the majority of its host species (Isaac, 1957; Koike *et al.*, 1994). However, *V. longisporum* induces no wilting symptoms on oilseed rape, but rather early senescence and stem striping symptoms towards the end of the growing season (Heale and Karapapa, 1999). *V. longisporum* consists of three lineages, each representing a separate hybridization event between two *Verticillium* spp. (Inderbitzin *et al.*, 2011b). The most virulent lineage on oilseed rape originates from a hybridization between *Verticillium* spp. A1 and D1, species that have hitherto never been found in their haploid state (Inderbitzin *et al.*, 2011b; Novakazi *et al.*, 2015). As a consequence of hybridization, the nuclear genome size of *V. longisporum* is approximately double that of *V. dahliae,* as numerous genes are present in two copies of different parental origin (Inderbitzin *et al.*, 2011b; Karapapa *et al.*, 1997).

Case study: emergence of Verticillium stem striping in the UK

Over the last five decades, oilseed rape production has boomed in the United Kingdom (UK). Before 1970 the crop was virtually unknown, whereas currently approximately 700,000 hectares are grown annually (Wood *et al.*, 2013). Stem canker (*Leptosphaeria* spp.) and light leaf spot (*Pyrenopeziza brassicae*) are considered the most important diseases for oilseed rape grown in the UK (Fitt *et al.*, 2006). However, in 2007 a new disease was observed in UK oilseed rape fields as Verticillium stem striping symptoms were reported for the first time (Gladders *et al.*, 2011). The reported fields were located in the counties Kent and Herefordshire, where 32 and 10% of the plants were affected, respectively (Gladders *et al.*, 2011). The following year, higher incidences of Verticillium stem striping symptoms were observed in oilseed rape fields in the same locations, despite the fact that other cultivars were grown (Gladders *et al.*, 2011). Between 2009 and 2011, more extensive screens for Verticillium stem striping symptoms were performed in oilseed rape fields in England (Gladders *et al.*, 2013). Verticillium stem striping was found to be distributed all over England, yet was most prevalent in parts of the eastern region (Gladders *et al.*, 2013). The cause of the sudden, large-scale emergence of Verticillium stem striping in the UK still remains unknown. *V. longisporum* strains that are particularly virulent on oilseed rape may have been introduced into the UK through the international seed trade as suggested by Gladders *et al.* (2013). Alternatively, the UK *V. longisporum* population may have been latently present and only recently emerged

as a disease on oilseed rape, especially as *V. longisporum* was already reported in the UK in the 1950s, yet on a different host: Brussels Sprout (Isaac, 1957). In this case, alterations in the environment, plant host or pathogen are likely to be responsible for the Verticillium stem striping outbreak.

Research questions

Emerging plant diseases pose a threat to natural and agricultural ecosystems. In the last decade, Verticillium stem striping has emerged as a new disease in UK oilseed rape production. By using a combination of field trials, glasshouse experiments and genetic screens I addressed the first question:

1. What is the origin and impact of Verticillium stem striping disease on UK oilseed rape cultivation?

Interspecific hybridization resulted in the emergence of the new *Verticillium* pathogen, *V. longisporum*. By using high-quality genome and transcriptome data I investigated the second question:

2. How did *V. longisporum* evolve in the aftermath of hybridization?

Thesis outline

Chapter 2 is a pathogen profile of *V. longisporum* and reviews the evolutionary history and interaction with various hosts. We elaborate specifically on the pathogen's interaction with the economically most import host, oilseed rape. In the last section of this chapter, management strategies to combat *Verticillium* diseases in brassicaceous hosts are further discussed.

In **chapter 3,** a collection of UK *V. longisporum* isolates is genotyped and the relations with strains from other countries are determined. The population structure of the *V. longisporum* lineage A1/D1 is then analyzed. Furthermore, the genomes of two A1/D1 isolates are completely sequenced to more precisely investigate the diversity within the A1/D1 lineage.

In **chapter 4**, to further characterize the UK *V. longisporum* population, the virulence and colonization of multiple UK *V. longisporum* strains are tested on various *Brassica* hosts. These are then compared to virulence and colonization patterns of previously studied *V. longisporum* strains from different countries.

Little is known about the economic significance of *V. longisporum* on oilseed rape production. Field experiments were hitherto unable to show yield reductions due to Verticillium stem striping (Dunker *et al.*, 2008). **Chapter 5** addresses the impact of Verticillium stem striping on economic parameters under UK field conditions.

Hybridization, especially in combination with whole-genome duplication, is a powerful evolutionary mechanism as it increases genomic variation and contributes to adaptive radiation (Meier *et al.*, 2017; Seehausen, 2004). This increased evolutionary potential of hybrids often leads to successful emergences in new environments. In **chapter 6**, we discuss the impact of hybridization on filamentous pathogens and how it can contribute to evasion of host immunity.

As a consequence of hybridization, *V. longisporum* received two chromosome sets from different *Verticillium* spp. (Inderbitzin *et al.*, 2011b; Karapapa *et al.*, 1997). Although the hybridization event is well described, little is known about the genome evolution of *V. longisporum* in the aftermath of hybridization. In general, allopolyploid genomes are highly dynamic and encounter abundant alterations including extensive gene loss (Albalat and Cañestro, 2016). **Chapter 7** describes the current state of the *V. longisporum* genome and the evolutionary mechanisms that played a prominent role in the genomic aftermath of hybridization. Furthermore, we investigate alterations in gene evolution and expression between *V. longisporum* and *V. dahliae*.

Chapter 8 describes the genome evolution of haploid *Verticillium* spp. We investigated sequence divergence of lineage-specific regions in the haploid *V. dahliae*. Lineage-specific regions are hallmarked by their dynamic evolution and reside genes important for pathogenicity.

Chapter 9 discusses the most important findings of my work, in the broader context of genome evolution in filamentous plants pathogens.

2

Verticillium longisporum, the invisible threat to oilseed rape and other brassicaceous plant hosts

Jasper R.L. Depotter
Silke Deketelaere[†]
Patrik Inderbitzin[†]
Andreas von Tiedemann[†]
Monica Höfte[#]
Krishna V. Subbarao[#]
Thomas A. Wood[#]
Bart P.H.J. Thomma

[†]These authors contributed equally
[#]These authors contributed equally

Abstract

The causal agents of Verticillium wilts are globally distributed pathogens that cause significant crop losses every year. Most Verticillium wilts are caused by *Verticillium dahliae*, which is pathogenic on a broad range of plant hosts, whereas other pathogenic *Verticillium* species have more restricted host ranges. Despite its broad host range, *V. dahliae* is generally not considered as a significant pathogen of brassicaceous plants. In contrast, *Verticillium longisporum* appears to prefer brassicaceous plants and poses an increasing problem to oilseed rape production. Interestingly, *V. longisporum* is the only non-haploid species in the *Verticillium* genus, as it is an allodiploid that carries almost twice as much genetic material as the other *Verticillium* species due to interspecific hybridization. *V. longisporum* invades the root tissue of its host and colonizes the shoot xylem vessels, ultimately triggering senescence in the stem tissue where the microsclerotia are formed. There is no effective fungicide treatment to control *Verticillium* diseases, and resistance breeding is the preferred strategy for disease management. However, only few Verticillium wilt resistance genes have been identified, and monogenic resistance against *V. longisporum* has not yet been found. Quantitative resistance exists mainly in the *Brassica* C-genome of parental cabbage lines and may be introgressed in oilseed rape breeding lines. Importantly, detailed knowledge of the impact of *V. longisporum* on crop quality and yield is currently not available. Nevertheless, a thorough understanding of the economic impact of *V. longisporum* may provide impetus for the development of durable resistance and other strategies to control diseases caused by *V. longisporum*. Oilseed rape colonized by *V. longisporum* does not develop wilting symptoms and, therefore, the common name of Verticillium wilt is unsuited for this crop. Therefore, we propose "Verticillium stem striping" as the common name for *V. longisporum* infections of oilseed rape.

Introduction

Verticillium is a relatively small genus of ascomycete fungi that currently comprises ten species (Inderbitzin *et al.*, 2011a). All presently recognized *Verticillium* species are soil-borne fungi, and several of them cause wilt disease on a variety of plant hosts across the world (Pegg and Brady, 2002). Although symptoms may vary considerably between plant hosts, the most frequently observed disease symptoms of Verticillium wilt include wilting, stunting, chlorosis, vascular discoloration and early senescence (Fradin and Thomma, 2006). The economic impact of *Verticillium* diseases can be severe, with an estimated annual loss of €3 billion worldwide in the 20 most affected hosts (Siebold and von Tiedemann, unpublished data). *Verticillium dahliae* is the most economically important species of the *Verticillium* genus, and has the ability to infect more than 200 plant host species (Inderbitzin *et al.*, 2011a; Pegg and Brady, 2002). *Verticillium albo-atrum*, *Verticillium alfalfae*, *Verticillium non-alfalfae* and *Verticillium longisporum* also constitute vascular pathogens, albeit with a more restricted host range. Members of the genus reproduce asexually and a sexual stage has not yet been described for any *Verticillium* spp. (Short *et al.*, 2014).

Taxonomy and morphology

Verticillium belongs to the family *Plectosphaerellaceae* (Zare *et al.*, 2007) in the subclass *Hypocreomycetidae* of the class *Sordariomycetes*, which is part of the phylum *Ascomycota* (Zhang *et al.*, 2006). *Verticillium* is subdivided into two major groups: Clade Flavexudans and Clade Flavnonexudans (Inderbitzin *et al.*, 2011a). *V. longisporum* is a member of the Flavnonexudans lineage and thus lacks the ability to produce yellow hyphal pigmentation. The taxonomic history of *Verticillium,* including *V. longisporum,* is complicated due to name changes and taxonomic disagreements. *V. longisporum* was first described as a variety of *V. dahliae,* as *V. dahliae* var. *longisporum* (Stark, 1961), and was then elevated to species rank 37 years later (Karapapa *et al.*, 1997). Although first contested, the name *V. longisporum* is now widely adopted (Inderbitzin and Subbarao, 2014). The evolutionary history of *V. longisporum* is unique among *Verticillium* spp., as *V. longisporum* is an allodiploid hybrid that evolved repeatedly by hybridization among four different ancestors (Inderbitzin *et al.*, 2011b; Ingram, 1968).

Differentiation of *V. longisporum* from related species may be based on morphological and cultural features (Table 1, Figure 1), but those may not consistently discriminate *V. longisporum* from *V. dahliae*. In general, *V. longisporum* conidia are longer than those of its close relative *V. dahliae* (Karapapa *et al.*, 1997; Stark, 1961), and with respect to *V. dahliae, V. longisporum* was reported to have elongated microsclerotia and a tendency towards the presence of three phialides in each whorl (Karapapa *et al.*, 1997). But for some *V. longisporum* strains, the conidia size ranges overlap with

those of *V. dahliae,* microsclerotia are rounded, and there are more than three phialides per whorl (Inderbitzin *et al.*, 2011a). Also, no morphological characteristics allow for the differentiation of the different hybrid lineages in *V. longisporum.* Therefore, the identity of *V. longisporum* strains and other *Verticillium* spp. should be confirmed with molecular techniques, such as DNA amplification with species discerning primers (Inderbitzin *et al.*, 2013) or DNA sequence determination of species-specific gene regions (Inderbitzin *et al.*, 2011a).

Table 1. Non-molecular criteria for the taxonomic discrimination of *V. longisporum* and *V. dahliae*.

Parameters*	*V. dahliae*	*V. longisporum*
Microsclerotia shape[1,3,6]	Mostly rounded or spherical	Mostly elongated
Conidia size[1,5,6]	Mostly short (3.5-5.5µm)	Mostly long (7.1-8.8µm)
Extracellular polyphenol oxidase activity[1,3,5]	Mostly strong	Mostly none
Culture filtrate fluorescence[1]	No	Yes
Host range[1,2,4]	Broad (vegetables, trees, legumes, ornamental crops)	Mainly restricted to crucifers

[1]Karapapa *et al.* 1997; [2]Bhat and Subbarao, 1999; [3]Zeise and von Tiedemann, 2001; [4]Zeise and von Tiedemann, 2002; [5]Steventon *et al.,* 2002; [6]Inderbitzin *et al.,* 2011b

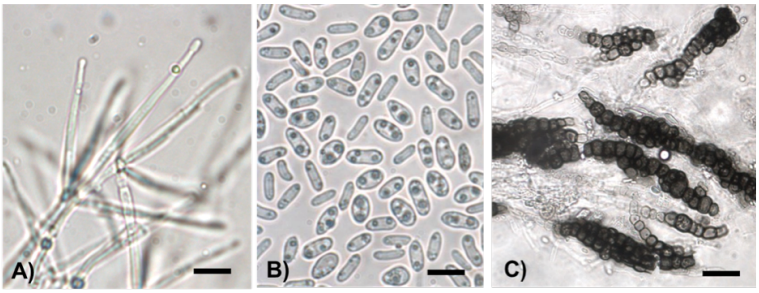

Figure 1 | Microscopic appearance of *V. longisporum in vitro*. (A) verticillate conidiophores (bar = 20 µm), (B) conidia (bar = 10 µm) and (C) young microsclerotia (bar = 25 µm).

Evolutionary history, genomics and pathogenicity

The typical life cycle of ascomycete fungi is dominated by the haploid state, whereas *V. longisporum* is allodiploid due to hybridization between two haploid ancestors. Phylogenetic analysis separates *V. longisporum* isolates into three lineages with different ancestors (Inderbitzin *et al.*, 2011b). Hitherto, four parental lines are known that belong to three different *Verticillium* spp. The parents include two *V. dahliae* genotypes, the *V. dahliae* lineage D2 and *V. dahliae* lineage D3, and two unknown species that were provisionally called Species A1 and Species D1. Based on ribosomal internal transcribed

spacer (ITS) sequences and intron-rich portions of the five protein-encoding genes *actin* (*ACT*), *elongation factor 1-alpha* (*EF*), *glyceraldehyde-3-phosphate dehydrogenase* (*GPD*), *mitochondrial oxaloacetate transport protein* (*OX*) and *tryptophan synthase* (*TS*), it was determined that all characterized *V. longisporum* isolates contain alleles derived from the Species A1 parent, in combination with Species D1, *V. dahliae* lineage D2 or *V. dahliae* lineage D3 alleles, to form the A1xD1, A1xD2 and A1xD3 hybrids, respectively (Figure 2).

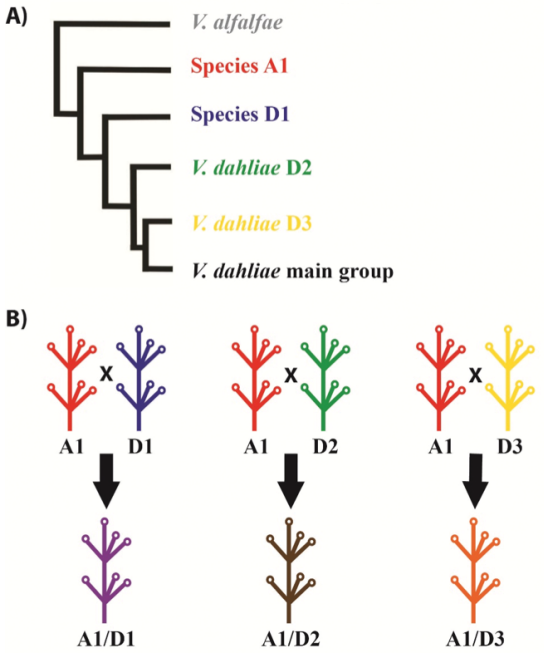

Figure 2 | The genetic constitution of the three lineages of *V. longisporum*. A: Phylogenetic relationship between the parents of *V. longisporum* (adjusted from Inderbitzin and Subbarao, 2014). **B:** The three hybridization events that resulted in the hybrid species *V. longisporum*. A1 and D1 progenitors are unknown and provisionally named haploid *Verticillium* spp., whereas progenitors D2 and D3 are both *V. dahliae* lineages. A1 is a parent of all three *V. longisporum* lineages, as it hybridized with D1, D2 and D3, respectively, resulting in the three *V. longisporum* lineages A1/D1, A1/D2 and A1/D3.

V. longisporum has also been referred to as a 'near-diploid', since its nuclear DNA content is ± 1.7-1.8 times that of *V. dahliae,* depending on the isolate, although the amount may vary considerably between isolates (Collins *et al.*, 2003; Karapapa *et al.*, 1997; Steventon *et al.*, 2002). The DNA content of some isolates can be over twice the amount of others (Steventon *et al.*, 2002). This genome size difference may be due to variation in DNA content between ancestors, may reflect the genomic plasticity of fungi (Zolan, 1995), or may indicate DNA loss associated with hybridization, as in the endophyte *Neotyphodium uncinatum* (Craven *et al.*, 2001; Moon *et al.*, 2004). However,

two copies have so far been found for all nuclear genes examined in *V. longisporum* (Inderbitzin *et al.*, 2011b; Tran *et al.*, 2013), with the exception of the nuclear ribosomal region (rDNA), of which only one type was detected in each lineage (Inderbitzin *et al.*, 2011b; Tran *et al.*, 2013). The *V. longisporum* lineage A1/D3 rDNA region was derived from *V. dahliae*, whereas the *V. longisporum* lineage A1/D1 and A1/D2 rDNA regions were derived from Species A1. In addition to DNA loss, concerted evolution could also account for the loss of one rDNA type in each of the *V. longisporum* lineages.

Several suggestions have been made regarding the origin of *V. longisporum*. Parasexual recombination was proposed as the underlying mechanism (Karapapa *et al.*, 1997), although parasexual processes generally end with chromosome loss to regain a haploid state after fusion of hyphae and nuclei (Caten, 1981). Thus, the stability of *V. longisporum* as a hybrid makes the hypothesis of interspecific hyphal fusion followed by nuclear fusion more plausible than parasexual processes (Inderbitzin *et al.*, 2011b).

The relative karyotypic stability of *V. longisporum* is unusual within *Verticillium*, as artificially induced hybrids between *Verticillium* spp. tend to be unstable (Fordyce and Green, 1964; Hastie, 1973; Typas and Heale, 1976), and undergo parasexual processes. In contrast, in a *V. longisporum* strain maintained in culture for 51 years, no gene loss was observed (Inderbitzin *et al.*, 2011b). The allodiploid nature of *V. longisporum* also explains why auxotrophic mutants for the study of vegetative compatibility groups could not be generated (Bhat and Subbarao, 1999; Joaquim and Rowe, 1990; Nagao *et al.*, 1994; Puhalla, 1979; Subbarao *et al.*, 1995; Zeise and von Tiedemann, 2001).

Individual *V. longisporum* lineages are genetically homogenous, as only a single substitution was found across seven nuclear loci. This suggests a recent origin of *V. longisporum* (Inderbitzin *et al.*, 2011b). But there are differences in pathogenicity and virulence between the lineages. Lineage A1/D1 is the most pathogenic lineage on oilseed rape, whereas lineage A1/D3 isolates are generally not pathogenic on this crop (Novakazi *et al.*, 2015; Tran *et al.*, 2013). Lineage A1/D2 is known only from horseradish in Illinois (USA) (Eastburn and Chang, 1994; Inderbitzin *et al.*, 2011b), and was the most virulent lineage on this crop (Novakazi *et al.*, 2015).

Disease cycle

Verticillium wilts are monocyclic diseases (Klosterman *et al.*, 2011) (Figure 3). Like *V. dahliae*, *V. longisporum* produces melanized microsclerotia (Stark, 1961) for survival to bridge the gap between hosts. Microsclerotia are clusters of melanized, thick-walled fungal cells, which are derived from hyphal cells through lateral budding of the hyaline mycelium (Klebahn, 1913). In the absence of a host, *V. dahliae* microsclerotia remain dormant and viable in the soil for more than ten years (Wilhelm, 1955), which may be

similar for *V. longisporum*. Root exudates stimulate the germination of *V. longisporum* microsclerotia, after which hyphae grow towards the root of the plant. Subsequently, hyphae colonize the surface of the root hairs and grow towards the root surface (Eynck *et al.*, 2007; Zhou *et al.*, 2006). On oilseed rape (*Brassica napus*), the fungus enters the root by direct penetration of rhizodermal cells of lateral roots or root hairs. Once inside the root, hyphae initially grow both intercellularly and intracellularly in the root cortex towards the central cylinder, where the pathogen enters the xylem (Eynck *et al.*, 2007). Next, conidia may be produced that are carried upward with the transpiration stream. Conidia that get trapped in pit membranes or at vessel end walls may germinate and penetrate into adjacent vessels (Garber and Houston, 1966). The colonization induces occlusions of the vessels, which may disturb sap stream in the xylem (Kamble *et al.*, 2013). Only during senescence does the pathogen grow out of the xylem vessels, invade the stem parenchyma and form microsclerotia beneath the stem epidermis and in the stem pith. The microsclerotia are released into the soil during tissue decomposition (Heale and Karapapa, 1999). Clear evidence for transmission of *V. longisporum* by seeds has not been provided so far.

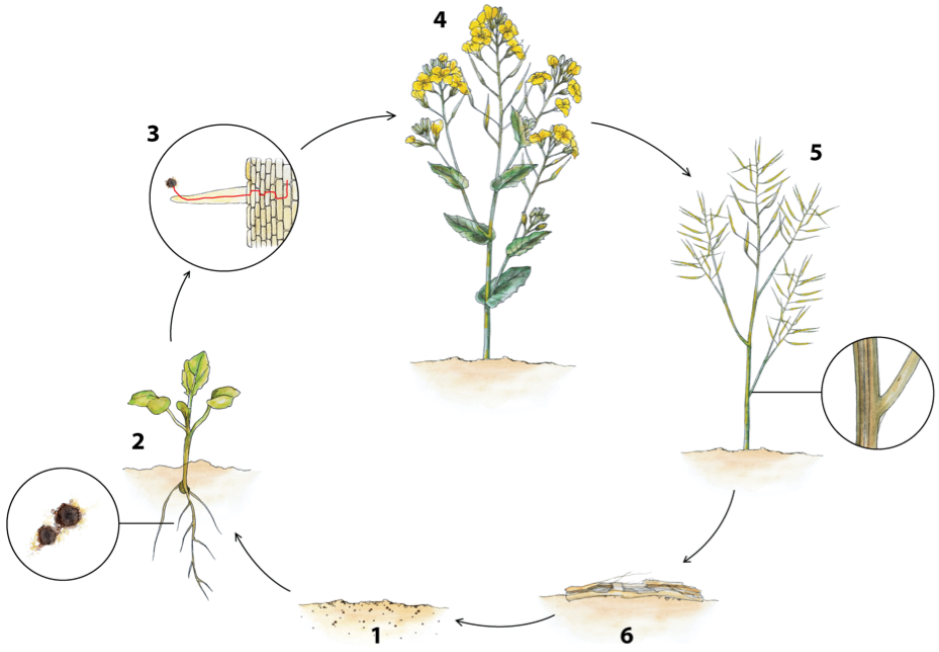

Figure 3 | Disease cycle of *V. longisporum* on oilseed rape. 1: Microsclerotia are persistent resting structures that reside in the soil and bridge the gap between hosts. **2:** Triggered by root exudates, microsclerotia start to germinate and hyphae grow towards the root of the plant. **3:** The fungus enters the root through wounds, or by direct penetration of epidermal cells of lateral roots or root hairs. In the root, hyphae grow intercellularly and intracellularly towards the central cylinder and enter the xylem. **4:** No disease symptoms are observed during the major part of the growing season. **5:** Dark unilateral striping develops on the stem of oilseed rape during the ripening of the crop. Ultimately, black microsclerotia are formed in the stem cortex. **6:** Microsclerotia are released in the soil upon decomposition of plant debris.

Susceptible crops

The currently known *V. longisporum* isolates are mainly found on brassicaceous hosts, whereas *V. dahliae* infects this plant family relatively infrequently (Inderbitzin and Subbarao, 2014). The most likely first description of a *V. longisporum* infection on a brassicaceous host is from Brussels sprout in England (Isaac, 1957). Oilseed rape was first reported as host of *V. longisporum* in the west and south of Scania, southern Sweden, in 1969 (Kroeker, 1970). The hybridization events that resulted in the novel species *V. longisporum* may have facilitated this shift in host preference (Inderbitzin, *et al.*, 2011b; Mallet, 2007), as *V. longisporum* is more pathogenic on brassicacious hosts than *V. dahliae* (Novakazi *et al.*, 2015). However, clear host range segregation is not found between *V. dahliae* and *V. longisporum*, as examples of hosts to both species include oilseed rape (Steventon *et al.*, 2002), horseradish (*Armoracia rusticana*) (Babadoost *et al.*, 2004), sugar beet (*Beta vulgaris*) (Jackson and Heale, 1985) and the model plant *Arabidopsis thaliana* (Fradin *et al.*, 2011; Yadeta *et al.*, 2011).

Pathogenicity tests confirm that *V. longisporum* has the capacity to infect non-brassicaceous plants (Bhat and Subbarao, 1999; Novakazi *et al.*, 2015; Qin *et al.*, 2006; Zeise and von Tiedemann, 2002). Moreover, *V. longisporum* lineages can be more or equally virulent than *V. dahliae* on non-brassicaceous hosts, such as eggplant, tomato, lettuce and watermelon (Novakazi *et al.*, 2015). This either suggests that non-brassicaceous plant species may be a host for certain *V. longisporum* lineages in nature, or that natural infection of *V. longisporum* encounters a barrier that is not encountered in pathogenicity tests. Also, pathogenicity tests performed in these studies involve the inoculation of plants by root-dipping in a conidia suspension, which may differ from natural infections that originate from microsclerotia.

Oilseed rape is economically the most important crop affected by *V. longisporum*. The oil from the seeds is used for human consumption and biodiesel, while by-products become a protein source used in animal feed (Berry *et al.*, 2014). Oilseed rape is the second most important arable oilseed crop, after soybean, and comprises spring and winter cultivars (Berry *et al.*, 2014; Diepenbrock, 2000). Winter oilseed rape is sown between mid-August and mid-September in North-West Europe and has a higher yield than spring oilseed rape, which is sown between March and April (Christen *et al.*, 1999). In 2013, the worldwide annual production of oilseed rape was over 72 megatons with China, Canada, India and Germany as the leading producers (FAOSTAT, 2018). *V. longisporum* is one of the major pathogens of oilseed rape and is found in Europe (Gladders *et al.*, 2011; Karapapa *et al.*, 1997; Steventon *et al.*, 2002; Zeise and von Tiedemann, 2002), Russia (Pantou *et al.*, 2005) and recently in Canada (CFIA, 2015).

V. longisporum is also pathogenic on a broad range of brassicaceous horticultural crops. The pathogen was found on several diseased *Brassica oleracea* species including

cauliflower (Debode *et al.*, 2005a; Koike *et al.*, 1994), cabbage (Inderbitzin *et al.*, 2011b; Subbarao *et al.*, 1995) and Brussels sprout (Isaac, 1957; Karapapa *et al.*, 1997; Karapapa and Typas, 2001). *V. longisporum* was also reported in Japan on other brassicaceous vegetables: Chinese cabbage (*Brassica rapa* var. *pekinensis*) (Narisawa *et al.*, 2004; Watanabe *et al.*, 1973), turnip (*B. rapa* var. *rapa*) (Carder and Barbara, 1994) and wild radish (*Raphanus sativus* var. *hortensis* f. *raphinistroides*) (Okoli *et al.*, 1994).

Interestingly, not all *Brassica* crops are susceptible to *V. longisporum*. Typical Verticillium wilt symptoms are not observed on broccoli grown in infested soil. *V. longisporum* is able to colonize the cortical surface of the roots of this crop, but does not progress into the vascular system (Njoroge *et al.*, 2011; Shetty *et al.*, 2000). However, resistance of broccoli to Verticillium wilt is not consistently observed if the plants are inoculated by root-dipping in a conidiospore suspension (Zeise and von Tiedemann, 2002). Nevertheless, cultivars from the US demonstrated resistance against 15 isolates from different hosts using this root-dipping inoculation method (Bhat and Subbarao, 2001).

Development of disease symptoms and impact

Most field research on *V. longisporum* has been conducted on oilseed rape and on cauliflower. Although both crops are *Brassica* species, the disease symptoms on these crops differ. Infected oilseed rape develops dark, unilateral striping on the stem late in the growing season, indicating the necrosis of cortical tissue (Heale and Karapapa, 1999) (Figure 4). Symptom development coincides with increased pathogen colonization of root and shoot tissues (Dunker *et al.*, 2008). In the final stages of the disease, the fungus forms black microsclerotia in the stem cortex. In contrast to the disease caused by this pathogen on other crops, conventional wilting symptoms are typically not observed on oilseed rape. Rather, the crop ripens prematurely, making disease symptoms difficult to distinguish from natural senescence. Strikingly, not much is known about the impact of *Verticillium* infection on the yield of oil seed rape under field conditions. *V. longisporum* symptoms can be omnipresent with a disease incidence of up to 80% (Dixelius *et al.*, 2005). Under practical conditions, yield losses due to *V. longisporum* have been suggested to range between 10 and 50%, but this has not yet been experimentally verified (Dunker *et al.*, 2008). A study showed no significant effect on the "thousand-seed-weight" (TSW) yield or on oil content of the crop after artificial inoculation of the soil (Dunker *et al.*, 2008). Although there was no effect on the whole-plot yield, disease symptoms of single plants in the field negatively correlate with yield.

Figure 4 | Typical disease symptoms caused by *V. longisporum* on oilseed rape. Dark unilateral striping appears on the stems of apparently healthy looking plants at the end of the growing season (**A**), indicating the necrosis of cortical tissue. The necrosis develops further in a later stage of the disease, which may lead to stem cracks (**B**). Finally, microsclerotia are formed in the stem cortex beneath the epidermis (**C**).

Interestingly, disease development in oilseed rape upon artificial inoculation differs from disease development under field conditions. Whereas symptoms in the field involve dark unilateral striping on the stem late in the growing season, upon root-dip inoculation in the seedling stage, oilseed rape plants exhibit chlorosis, vascular discoloration and stunting at an early stage (Eynck *et al.*, 2007, 2009b; Floerl *et al.*, 2008; Zeise and von Tiedemann, 2002). Moreover, clear biomass reduction is observed whereby roots are significantly more affected than shoots (Keunecke, 2009). Recent studies have demonstrated that extensively increased branching of the shoot occurs on inoculated plants (Lopisso *et al.*, 2017). It is currently not understood why these differences in disease development occur.

In contrast to oilseed rape, cauliflower displays typical wilting symptoms upon infection with *V. longisporum*, which starts with chlorosis and necrosis of the lower leaves (Koike *et al.*, 1994). At maturity, stunting of the plants and wilting can be observed. Furthermore, *V. longisporum* infection may lead to an increase in the number of cauliflower leaves (Subbarao *et al.*, 1995), although this is not universally observed across cultivars (Debode *et al.*, 2005b; Xiao and Subbarao, 1998).

The symptom development of the disease caused by *V. longisporum* in cauliflower and oilseed rape seems to be temperature-dependent. Cauliflower grown as a winter crop in infested fields remained unaffected, while more disease was observed at higher temperatures (Koike *et al.*, 1994). At the same time, increased temperatures may also be non-conducive to *V. longisporum* infection, as infected cauliflower did not display any symptoms when grown in a greenhouse where temperatures were elevated to the range

of 27-35°C. More recently, studies in a soil heating facility demonstrated a significant increase in *V. longisporum* colonization of winter oilseed rape when soil temperatures were elevated by 1.6 or 3.2°C with respect to ambient temperature, indicating a higher vulnerability of spring-sown crops growing into the warmer season (Siebold and von Tiedemann, 2013).

The incidence and severity of disease caused by *V. longisporum* on cauliflower and oilseed rape is not always correlated with inoculum density, although symptoms on cauliflower can occur earlier at higher inoculum densities (França *et al.*, 2013; Johansson *et al.*, 2006a; Xiao and Subbarao, 1998). In contrast, in a study on oilseed rape, the disease incidence and severity were positively correlated to inoculum level (Dunker *et al.*, 2008).

Plant responses

Chemical and mechanical responses

The influence of plant secondary metabolites on the interaction between *V. longisporum* and its host plants has not yet been extensively explored, but glucosinolate concentrations in infected hosts have been investigated. Glucosinolates are constitutively expressed sulfur-containing phytochemicals that are predominantly found in brassicaceous plants (Wittstock and Halkier, 2002). In general, they are grouped in aliphatic, aromatic and indole glucosinolates, depending on whether they originate from aliphatic amino acids, aromatic amino acids or tryptophan. Upon tissue damage, glucosinolates are hydrolysed with the formation of biologically active and sometimes toxic compounds. Interestingly, concentrations of aliphatic glucosinolates are generally higher in the roots of infected broccoli than in the shoots, while the opposite is observed in cauliflower, which may be implicated in the resistance of broccoli towards *V. longisporum* (Njoroge *et al.*, 2011). Levels of glucosinolates in the roots of *V. longisporum*-infected *Arabidopsis* plants are higher than in non-inoculated plants. However, the increase in glucosinolates is not accompanied by an increase in glucosinolate breakdown products in the roots (Witzel *et al.*, 2015). *V. longisporum* infection induces transcriptional activation of genes involved in tryptophan biosynthesis and tryptophan-derived secondary metabolism. Furthermore, genetic disruption of tryptophan-derived secondary metabolism leads to enhanced susceptibility. However, no increase in antifungal indole glucosinolate breakdown products was observed and the tryptophan-derived phytoalexin, camalexin did not significantly contribute to defense against *V. longisporum* in roots either (Iven *et al.*, 2012). This indicates that other, as-yet unidentified, tryptophan-derived metabolites play an important role in fungal defense in roots. In contrast to the protective role of the tryptophan-derived secondary metabolites, monoterpenes produced by the monoterpene synthase TPS23/27 stimulate *in vitro* conidial germination and subsequent invasion of *V. longisporum* in *Arabidopsis* roots (Roos *et al.*, 2015).

In leaf tissue of *Arabidopsis thaliana,* soluble phenylpropanoids rather than tryptophan-derived metabolites were found to accumulate in response to *V. longisporum* infection. Mutant analysis and *in vitro* growth assays revealed that sinapate glucose and coniferin are involved in restricting the pathogen (König *et al.*, 2014). Also, the phenylpropanoid pathway is important for defense of *B. napus* against *V. longisporum*, as more phenolic compounds were produced by a resistant line of *B. napus* upon infection with *V. longisporum* when compared with a susceptible line (Eynck *et al.*, 2009a). Moreover, concentrations of phenylpropanoids are correlated with *V. longisporum* resistance in *B. napus* (Obermeier *et al.*, 2013).

The ability of *V. longisporum* to synthesize aromatic amino acids and cross-pathway control of amino acid biosynthesis are required for pathogenicity. Silencing mutants impaired in chorismate synthase or CPC1, the conserved transcription factor of cross-pathway control, caused less disease and showed reduced growth in the hypocotyl of *B. napus* and *Arabidopsis*. Chorismate is essential for the biosynthesis of tryptophan, phenylalanine and tyrosine, while cross-pathway control allows fungi to increase amino acid biosynthesis upon amino acid starvation (Singh *et al.*, 2010; Timpner *et al.*, 2013). *Brassica napus* xylem sap contains only low concentrations of amino acids and aromatic amino acids are especially scarce (Singh *et al.*, 2010). An increased production of plant secondary metabolites in response to *V. longisporum* infection probably further depletes amino acid concentrations in the xylem. Hence, the fungus needs a functional cross pathway control to overcome the imbalance in amino acid supply in the xylem.

Drought stress tolerance increases when *Arabidopsis* plants are challenged with *V. longisporum,* which may be the result of pathogen-induced reduction of stomatal apertures or *de novo* xylem formation (Reusche *et al.*, 2012; Roos *et al.*, 2014). Reduction in stomatal apertures may be linked to increased abscisic acid (ABA) levels in *Arabidopsis* leaves in response to *V. longisporum*, as ABA is a known central regulator of the stomatal apparatus (Acharya and Assmann, 2009; Roos *et al.*, 2014). Furthermore, *V longisporum* infection induces transdifferentiation of bundle sheath cells into functional xylem elements in *A. thaliana* and *B. napus*. *V. longisporum* also causes reinitiation of cambial activity and transdifferentiation of xylem parenchyma in *A. thaliana*, resulting in xylem hyperplasia (Reusche *et al.*, 2012, 2014).

Micrornas

It was recently demonstrated that *V. longisporum* interferes with plant miRNAs to reprogram plant gene expression. Sixty-two miRNAs were responsive to *V. longisporum* infection in *B. napus*, the majority of which were downregulated. Important targets of downregulated miRNAs include auxin response factors (ARFs), which control transcription of genes in response to auxin. The resulting increase in ARFs may suppress plant defense responses by enhancing auxin signaling. Another downregulated miRNA targets a positive regulator of leaf senescence. At early infection stages, the greatest

suppression was observed for miR168, which interferes with Argonaute 1 (AGO1) (Shen *et al.*, 2014). AGO1 is an RNA-binding protein involved in RNA silencing that regulates diverse physiological processes including a number of PAMP-triggered immune responses (Li *et al.*, 2010). AGO1 mutants were clearly more resistant to *V. longisporum*, suggesting a key role of AGO1 in the compatible interaction with *V. longisporum* (Shen *et al.*, 2014).

Plant hormones

So far, the involvement of typical plant hormone signaling pathways in the interaction with *V. longisporum* remains unclear, and the role of the various plant hormones in the defense of *A. thaliana* and *B. napus* towards *V. longisporum* appears to be different (Ratzinger *et al.*, 2009). *V. longisporum* infection increases the level of jasmonic acid (JA) in *A. thaliana* and activates the corresponding marker genes *VSP2* and *PDF1.2,* while biosynthesis and signaling mutants do not show major differences in disease susceptibility when compared with wild type plants (Johansson *et al.*, 2006b; Ralhan *et al.*, 2012). This suggests that JA does not contribute to *V. longisporum* resistance in *A. thaliana*. However, treating *Arabidopsis* plants with methyl jasmonate (MeJA) resulted in enhanced resistance towards *V. longisporum* (Johansson *et al.*, 2006b). Moreover, *V. longisporum* requires JA-independent CORONATINE INSENSITIVE1 (COI1) function in the roots to elicit disease symptoms in *A. thaliana* shoots (Ralhan *et al.*, 2012). In oilseed rape, JA concentrations increase over time in both healthy and infected plants, which is likely caused by aging-related processes as JA acts in senescence (He *et al.*, 2002; Ratzinger *et al.*, 2009).

In *Arabidopsis*, metabolites of the salicylic acid (SA) pathway, salicylic acid glucoside (SAG) and dihydroxybenzoic acid, increase after *V. longisporum* infection and the SA marker genes *PR1* and *PR2* are activated. However, mutants in the SA pathway (*eds1-1*, *NahG*, *npr1-3*, *pad4-1* and *sid2-1*) do not exhibit enhanced susceptibility, indicating that SA-signaling may not contribute to *V. longisporum* resistance in *Arabidopsis* (Johansson *et al.*, 2006b; Ralhan *et al.*, 2012). In contrast, SA appears to play a role in *B. napus* susceptibility to *V. longisporum* infection (Ratzinger *et al.*, 2009). Concentrations of SA and SAG in the xylem sap of *B. napus* plants increase upon *V. longisporum* infection and correlate with disease severity; a strong correlation between SAG levels in the shoot and the amount of *V. longisporum* DNA in hypocotyls was found. However, the exact role of the enhanced levels of SA and SAG in xylem sap after infection with *V. longisporum* is not clear (Ratzinger *et al.*, 2009).

Ethylene (ET) production and the expression of ET-dependent plant defenses were induced by *V. longisporum* in *Arabidopsis*. Moreover, pretreatment with the ET precursor 1-aminocyclopropane-1-carboxylic acid (ACC) enhances host resistance to *V. longisporum*. The *Arabidopsis* mutants impaired in ET signaling, *ein4-1, ein2-1* and *ein6-1*, were more susceptible to *V. longisporum* than the wild type. In contrast,

the *Arabidopsis* mutant *etr1-1* showed enhanced resistance and a higher chlorophyll content compared with the wild type, indicating that prolonged ET perception via ETR1 enhances susceptibility via induction of senescence (Johansson *et al.*, 2006b; Veronese *et al.*, 2003). Reusche *et al.*, (2013) found that *V. longisporum* triggers early senescence in *Arabidopsis* by actively decreasing cytokinin levels in the leaves. Senescing tissue may provide easy access to nutrients for the development of microsclerotia during the last phase of the life cycle of *V. longisporum*. Stabilization of cytokinin levels inhibits fungal growth and reduces disease symptom development (Reusche *et al.*, 2013).

Abscisic acid levels increase after infection with *V. longisporum* in *Arabidopsis* (Ralhan *et al.*, 2012; Roos *et al.*, 2014). The ABA-deficient mutant *aba2-1* is susceptible to *V. longisporum* and accumulates less anthocyanin than wild type plants, whereas ABA insensitive mutants do not show enhanced susceptibility (Johansson *et al.*, 2006b; Veronese *et al.*, 2003). In *B. napus*, however, ABA concentrations in xylem sap are not affected by *V. longisporum* infection (Ratzinger *et al.*, 2009).

Disease management

Chemical control, heat treatments and solarization

Management of Verticillium wilts is challenging, as current disease control strategies do not provide appropriate protection. Consequently, a combination of management techniques is necessary to contain the disease. Protective or curative control by conventional fungicides has not been an option for *V. longisporum*. Soil fumigation is a successful strategy to reduce the inoculum density of *V. dahliae* in the soil (Powelson and Carter, 1973), but is no longer available for agricultural use because of its detrimental effects on stratospheric ozone (Subbarao, 2002). Although heat-treatment of the soil can similarly reduce microsclerotia viability, steam-mediated heat treatment and most other heat treatment methods are energy consuming and not cost-effective in most commercial field production systems (Pullman *et al.*, 1981). However, soil solarization by heating the soil under a tarpaulin may be economically feasible and effective depending on the temperature and duration of the treatment (Pullman *et al.*, 1981), and is currently only commercially practiced in Mediterranean, desert, and tropical climates (Stapleton, 2000) because these climates allow the accumulation of adequate heat units to neutralize the pathogen.

Weed management and crop rotation

The more confined host range of *V. longisporum*, in comparison to *V. dahliae*, theoretically facilitates the use of crop rotation as a disease management strategy. However, persistence of microsclerotia, potential non-brassicaceous reservoir plants (Johansson *et al.*, 2006a), and inadequate weed management may jeopardize the

effects of crop rotation. Brassicaceous weeds may act as a reservoir for *V. longisporum* as *Verticillium* isolates have been recovered from *B. rapa* spp. *campestris*, shepherd's purse (*Capsella bursa-pastoris*), annual wall-rocket (*Diplotaxis muralis*), clasping pepperweed (*Lepidium perfoliatum*), tumble mustard (*Sisymbrium altissimum*), *Descurainia hartwegiana*, field pennycress (*Thlaspi arvense*) and charlock (*Sinapis arvensis*) (Johansson *et al.*, 2006a; Vargas-Machuca *et al.*, 1987; Woolliams, 1966). Besides weed management, the prevention of *Brassica* volunteers in subsequent crops is also important; oilseed rape is particularly prone to volunteers due to high seed losses before and during harvest (Price *et al.*, 1996).

Few crop rotation studies have been conducted with *V. longisporum*, and more long-term research is needed to determine if crop rotation could be an effective management strategy. Hitherto, only studies about the impact of fallow treatment in cauliflower fields have been conducted. These suggest that fallow treatment does not reduce microsclerotia accumulation in the soil (França *et al.*, 2013; Subbarao and Hubbard, 1999). The microsclerotia density in the soil after two years of consecutive cauliflower crops is not significantly higher than when a cauliflower crop is followed by a fallow treatment the year after (Subbarao and Hubbard, 1999). Moreover, even a 4 year fallow period after a long history of cauliflower cropping did not reduce the microsclerotia density in the soil (França *et al.*, 2013). The long-term release of microsclerotia from the plant debris of the previous crop may be the reason why fallow does not lead to a significant reduction in the study of Subbarao and Hubbard (1999), as the microsclerotia density keeps increasing during the fallow period. Therefore, a more extended fallow period may be more effective in decreasing microsclerotia densities in the soil. In contrast, França *et al.* (2013) did not report an increase in microsclerotia density in the soil of fallow treated plots, but reported a fluctuation with a seasonal pattern. Interestingly, similar patterns and inoculum levels occur in soil of plots with continuous cauliflower cropping. Possibly, the amount of microsclerotia formed in the cauliflower debris may be affected by the incomplete inflorescence development of cauliflower as the generative phase of the plant is interrupted by the harvest of the curd (França *et al.*, 2013). However, this hypothesis is not in line with the increasing microsclerotial density observed previously (Subbarao and Hubbard, 1999; Xiao *et al.*, 1998).

Bio-control agents and organic soil amendments

Several microorganisms, including bacteria and fungi, have the ability to reduce the colonization by, and deleterious effects of, *V. longisporum* and can thus potentially serve as biological control agents (BCAs), provided an ecologically fit and effective agent is developed. Specific, non-pathogenic *Verticillium* isolates, such as the *V. isaacii* isolate Vt305, are able to suppress disease symptoms caused by pathogenic isolates. The strain Vt305 was isolated from a Verticillium wilt-suppressive cauliflower field

in Belgium (França *et al.*, 2013). Vt305 appears to be an endophyte of cauliflower and shows effective biological control capacities under controlled conditions (Tyvaert *et al.*, 2014). Inoculation of Vt305 one week prior to *V. longisporum* inoculation reduced symptom development and colonization of plant tissue by *V. longisporum*. However, the mechanism by which Vt305 protects cauliflower against Verticillium wilt is unknown, although it has been suggested that competition for infection sites and induced resistance responses are the two most likely possibilities (Tyvaert *et al.*, 2014).

Microsphaeropsis ochracea is another ascomycete and BCA of *V. longisporum* (Stadler and von Tiedemann, 2014). The effectiveness of *M. ochracea* as a BCA is proven *in vitro* and under sterile soil conditions, as it causes high rates of microsclerotia mortality. Nevertheless, *M. ochracea* appears not to have sufficient microbial competitiveness to control *V. longisporum* under field conditions (Stadler and von Tiedemann, 2014).

A large-scale screening for root-colonizing and endophytic fungi with BCA capacities has led to the isolation of two *Phialocephala fortinii* isolates, one *Heteroconium chaetospira* isolate, and one *Meliniomyces variabilis* isolate (Narisawa *et al.*, 1998, 2000, 2004; Ohtaka and Narisawa, 2008). All isolates reduced the symptoms of *V. longisporum* on *in vitro*-grown Chinese cabbage when the colonization of the plant by the BCA preceded *V. longisporum* infection. Only the *H. chaetospira* and *M. variabilis* isolates were able to reduce disease severity and incidence of Verticillium wilt in Chinese cabbage under field conditions.

Besides fungal BCAs, the plant beneficial bacterium *Serratia plymuthica* HRO-C48 also reduces *Verticillium* symptoms in oilseed rape (Müller and Berg, 2008). A biological product based on *Serratia plymuthica* HRO-C48 was developed called RhizoStar® (E-nema, Raisdorf, Germany). Furthermore, certain *Bacillus amyloliquefaciens* strains are BCAs towards several fungal pathogens of oilseed rape including *V. longisporum* (Danielsson *et al.*, 2007). *B. amyloliquefaciens* subsp. *plantarum* UCMB5113 was the most effective strain against *V. longisporum* and also had plant growth promoting activity. Strain UCMB5113 produces antibiotic compounds and bio-surfactants, which likely are involved in the bio-control properties of the bacterium (Danielsson *et al.*, 2007; Niazi *et al.*, 2014). However, its BCA capacities can also act indirectly and be caused by plant defense priming (Sarosh *et al.*, 2009). The latter hypothesis is supported by the observation that the soil-borne isolate UCMB5113 confers resistance to airborne pathogens, where the spatial separation of the BCA and the pathogen prevents direct interaction between the two (Sarosh *et al.*, 2009).

Amendments of organic material to soils can suppress soil-borne fungal diseases (Bonanomi *et al.*, 2007). Several crop residues are able to reduce microsclerotium viability in naturally infested cauliflower fields (Debode *et al.*, 2005a; França *et al.*, 2013). The incorporation of ryegrass and corn residues is more effective than brassicaceous plant material. However, the reduction of primary inoculum does not reduce the incidence or severity of the disease. Other publications report a Verticillium

wilt-suppressive effect by broccoli residues (Subbarao and Hubbard, 1996, 1999). The broccoli amendments reduce disease abundance and microsclerotium viability in naturally infested soils (Xiao *et al.*, 1998). Moreover, broccoli residues may even inhibit the cauliflower root-colonization ability of surviving microsclerotia (Njoroge *et al.*, 2011; Shetty *et al.*, 2000). The lignin content of the incorporated crop residues seems to be a key determinant for the effectiveness of *Verticillium* control. The 'lignin-melanin hypothesis' proposes that enzymes involved in lignin biodegradation also degrade fungal melanin (Butler and Day, 1998; Debode *et al.*, 2005a; Shetty *et al.*, 2000). Melanin protects microsclerotia against biotic and abiotic stress during the period between hosts (Bell and Wheeler, 1986). Therefore, soil amendments with relatively high lignin content may stimulate microbial organisms that decompose lignin and that simultaneously reduce microsclerotia viability.

Resistance breeding

Resistance breeding is the most favored means of *Verticillium* disease management, and several crops with polygenic *V. longisporum* resistance have been reported (Fradin and Thomma, 2006; Kemmochi *et al.*, 2000; Rygulla *et al.*, 2008). Unfortunately, a genuine resistance (*R*) gene against *V. longisporum* has not yet been found, and *Ve1* presently remains the only *R* gene that has been described against Verticillium wilts (Fradin *et al.*, 2009, 2011). Whereas *Ve1* was initially identified in tomato (Kawchuk *et al.*, 2001), functional *Ve1* homologs have been identified in other plant species as well, such as *Nicotiana glutinosa* (Zhang *et al.*, 2013), lettuce (Hayes *et al.*, 2011) and cotton (Zhang *et al.*, 2011, 2012). Tomato *Ve1* confers resistance against race 1 isolates of *V. dahliae* and *V. albo-atrum* (presently: *V. alfalfae*) that contain the *Ave1* gene (de Jonge *et al.*, 2012). *Ave1* encodes an effector protein that activates *Ve1*-mediated resistance, but *Ave1* contributes to fungal virulence in susceptible plants that lack *Ve1*. Thus far, functionality of *Ve1*-mediated resistance could not be demonstrated against *V. longisporum*, which was attributed to the observation that the currently investigated isolates do not carry the *Ave1* gene (Fradin *et al.*, 2011). However, there are genetic resources that may be used to reduce susceptibility of brassicaceous plants against *V. longisporum*. For instance, constitutive expression of the *Enhancer of vascular Wilt Resistance 1* (*EWR1*) gene enhances the resistance against Verticillium wilt caused by *V. albo-atrum* (presently: *V. alfalfae*), *V. dahliae* and *V. longisporum* in *Arabidopsis* (Yadeta *et al.*, 2011, 2014). *EWR1* encodes a putatively secreted protein of unknown function and has homologs that are only found within the Brassicaceae family (Yadeta *et al.*, 2014). *EWR1* homologs facilitate enhanced *Verticillium* resistance in transformed *A. thaliana*. Interestingly, the brassicaceous-specific *EWR1* homologs can also be used to increase resistance against Verticillium wilts in non-brassicaceous plants, as *Nicotiana benthamiana* displays resistance against *V. dahliae* when Brassicaceae *EWR1* homologs are over-expressed.

Current European oilseed rape cultivars possess a low level of *Verticillium* resistance, and the availability of novel germplasm for resistance breeding is limited due to the narrow genetic basis of currently used cultivars (Cowling, 2007; Seyis *et al.*, 2003). However, three quantitative trait locus (QTL) alleles that significantly correlate with *V. longisporum* resistance were identified, one on the C1 and two on the C5 chromosomes, of the partly resistant oilseed rape cultivar Express 617 (Obermeier *et al.*, 2013). These QTL indicate sources of quantitative resistance available in the C-genome derived from oilseed rape parental cabbage lines. Interestingly, the QTL co-localize with loci for two soluble phenylpropanoids that are negatively correlated with disease severity during *V. longisporum* infection, while a positive correlation exists with precursors of cell wall bound phenols related to lignin. This is in agreement with the higher constitutive and induced levels of cell wall-bound phenols in roots and hypocotyls of resistant rapeseed genotypes. The resistance genotypes were identified in *V. longisporum* resistance screenings of *B. napus* accessions (Eynck *et al.*, 2009b). One of the identified accessions with quantitative resistance to *V. longisporum* tolerates root invasion but hinders the pathogen from colonizing the shoot by means of vascular occlusions, and strongly enhances accumulation of phenols in the xylem parenchyma at the hypocotyl interface (Eynck *et al.*, 2009a). In spite of these specific observations, the genuine mechanism of quantitative resistance is not entirely clear.

Resistance traits in *B. oleracea* and *B. rapa* can be applied in oilseed rape resistance breeding, as *B. napus* is an interspecific hybrid between these two plant species (Eynck *et al.*, 2009b; Happstadius *et al.*, 2003; Obermeier *et al.*, 2013; Rygulla *et al.*, 2007a, 2007b, 2008). Cultivars of *B. oleracea* crops have been screened for *V. longisporum* susceptibility, with differences in susceptibility found among cauliflower cultivars (Debode *et al.*, 2005b) and dominant polygenic resistance occurring in cabbage (Kemmochi *et al.*, 2000).

In addition to breeding, resistance sources from outside the Brassicaceae may improve resistance of current *V. longisporum* hosts. These include sugar beet, whose *BvGLP-1* gene reduces *V. longisporum* disease symptoms in *Arabidopsis*. *BvGLP-1* has high sequence homology to a set of plant germin-like proteins, and is highly induced after nematode (*Heterodera schachtii*) infection of resistant sugar beet plants containing the single dominant resistance gene $Hs1^{pro-1}$ (Knecht *et al.*, 2010).

Conclusions

Verticillium longisporum is becoming a global problem in oilseed rape production. Recently, the disease was reported outside continental Europe in two important oilseed rape production areas: the UK in 2011 (Gladders *et al.*, 2011) and Canada in 2015 (CFIA, 2015). To improve management of the *V. longisporum* disease of oilseed rape and other crops, several steps could be implemented. Firstly, the search for sources of resistance should be intensified. Host resistance is generally considered to be the most desirable

control strategy, but *R* genes such as *Ve1* in tomato against *V. dahliae* are unknown for *V. longisporum*. Therefore, more *B. napus*, *B. oleracea* and *B. rapa* germplasm should be screened for resistance traits for introgression into new, improved cultivars. *R* genes should be deployed cautiously and combined with other resistance traits and management measures to improve durability of the resistance. Secondly, phytosanitary measures should be expanded to prevent the spread of *V. longisporum* with contaminated soil and equipment to new areas. *V. longisporum* is a soil-borne pathogen and cannot move autonomously over great distances. Therefore, international trade and travel are likely to be responsible for *V. longisporum*'s continually expanding geographic range. Finally, accurate assessments of the impact of *V. longisporum* infections on crop quality and yield under field conditions are required. These would determine the economic relevance of the pathogen, and provide a solid economic basis for disease management decisions.

V. longisporum on oilseed rape is not a causal agent of wilt and, therefore, the use of "Verticillium wilt" as the common name of *V. longisporum* on oilseed rape is incorrect. Perhaps, *V. longisporum* mainly has an endophytic lifestyle in oilseed rape, which causes symptoms on the stem that do not result in reduced crop quality or yield losses. Therefore, we propose "Verticillium stem striping" as the common name to describe *V. longisporum* on oilseed rape.

Acknowledgements

The authors would like to thank the Marie Curie Actions program of the European Commission that financially supports the research that will investigate the threat *V. longisporum* poses to the British oilseed rape production. Work in the laboratory of B.P.H.J.T. is supported by the Research Council Earth and Life Sciences (ALW) of the Netherlands Organization of Scientific Research (NWO). We highly appreciate the drawing of the disease cycle diagram of *V. longisporum* on oilseed rape (Figure 3) by Hannah R. Pritchard.

3

A distinct and genetically diverse lineage of the hybrid fungal pathogen *Verticillium longisporum* population causes stem striping in British oilseed rape

Jasper R.L. Depotter[†]
Michael F. Seidl[†]
Grardy C.M. van den Berg
Bart P.H.J. Thomma[#]
Thomas A. Wood[#]

[†]These authors contributed equally
[#]These authors contributed equally

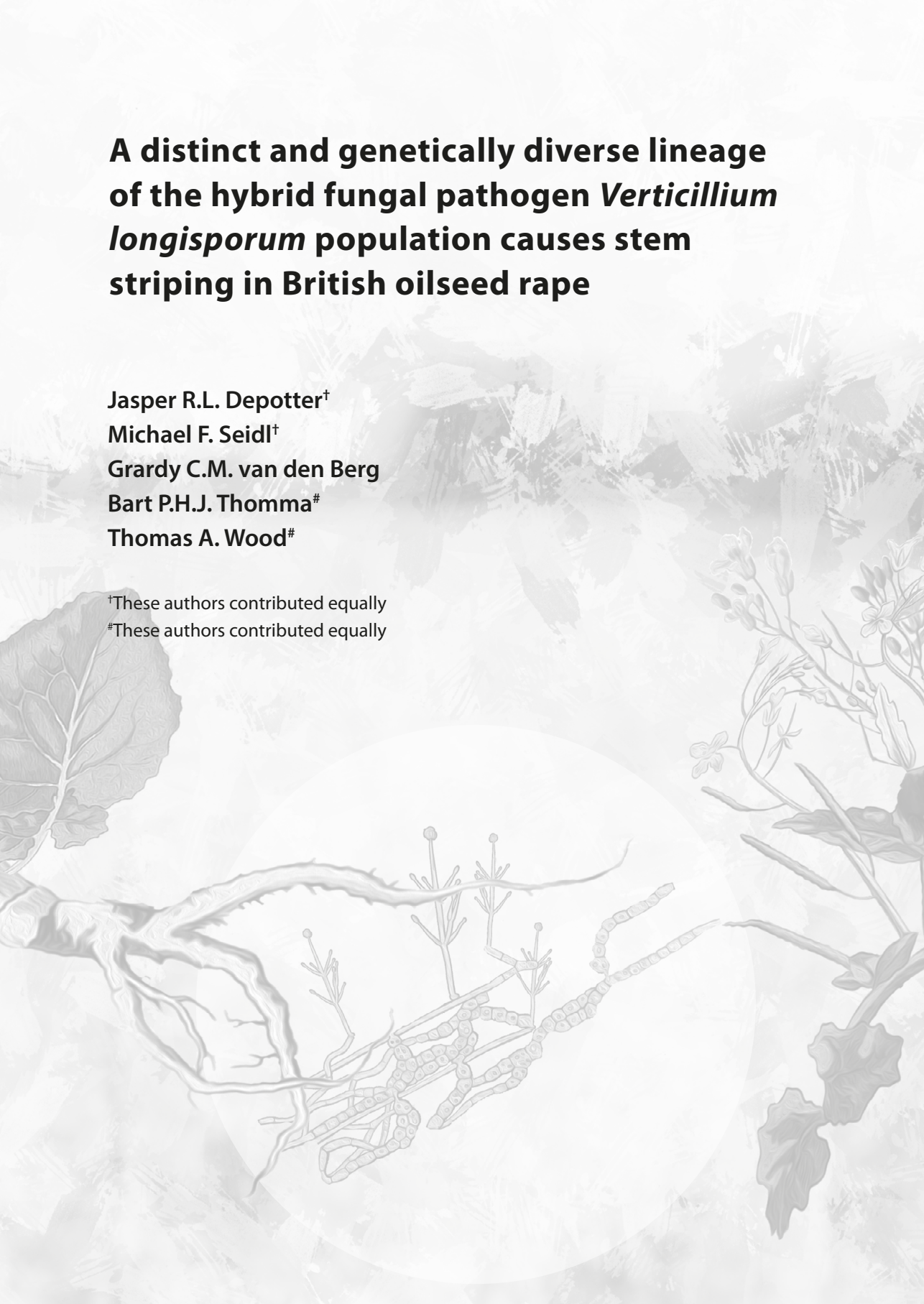

Abstract

Population genetic structures illustrate evolutionary trajectories of organisms adapting to differential environmental conditions. Verticillium stem striping disease on oilseed rape was mainly observed in continental Europe, but has recently emerged in the United Kingdom. The disease is caused by the hybrid fungal species *Verticillium longisporum* that originates from at least three separate hybridization events, yet hybrids between *Verticillium* progenitor species A1 and D1 are mainly responsible for Verticillium stem striping. We reveal a hitherto un-described dichotomy within *V. longisporum* lineage A1/D1 that correlates with the geographic distribution of the isolates with an "A1/D1 West" and an "A1/D1 East" cluster. Genome comparison between representatives of the A1/D1 West and East clusters excluded population distinctiveness through separate hybridization events. Remarkably, the A1/D1 West population that is genetically more diverse than the entire A1/D1 East cluster caused the sudden emergence of Verticillium stem striping in the UK, whereas in continental Europe Verticillium stem striping is predominantly caused by the more genetically uniform A1/D1 East population. The observed genetic diversity of the A1/D1 West population argues against a recent introduction of the pathogen into the UK, but rather suggests that the pathogen previously established in the UK and remained latent or unnoticed as an oilseed rape pathogen until recently.

Introduction

Verticillium species are causal agents of wilt diseases on many economically important crops, with a total estimated annual loss of €3 billion worldwide in the 20 most affected hosts, including cotton and olive (Depotter *et al.*, 2016a). *Verticillium dahliae* is the most notorious wilt agent of this genus and is characterized by its extremely broad host range that encompasses hundreds of host species (Fradin and Thomma, 2006; Inderbitzin and Subbarao, 2014). *V. dahliae* propagates mainly asexually and genomic variation is mostly established by mechanisms different from meiotic recombination, such as large-scale genomic rearrangements, horizontal gene transfer and transposon activity (Faino *et al.*, 2016; de Jonge *et al.*, 2012, 2013; Seidl and Thomma, 2014). Moreover, particular *Verticillium* spp. experienced more intrusive genomic evolution by interspecific crosses within the genus leading to an approximate doubling of the genome size. Interspecific *Verticillium* hybrids gave rise to new diseases such as Verticillium stem striping on oilseed rape (Depotter *et al.*, 2016a; Inderbitzin *et al.*, 2011b). At least three hybridization events between two separate *Verticillium* spp. have occurred that have been classified under the same species name, *V. longisporum* (Inderbitzin *et al.*, 2011b; Karapapa *et al.*, 1997). The three hybrid lineages have been named after their respective hybridization parents: A1/D1, A1/D2 and A1/D3 (Inderbitzin *et al.*, 2011b). A1 and D1 are hitherto un-described *Verticillium* species, whereas D2 and D3 are presumed *V. dahliae* isolates. Similar to other hybrid pathogens, hybridization appears to have altered the host range of *Verticillium* (Depotter *et al.*, 2016b; Inderbitzin *et al.*, 2011b). *V. longisporum* is highly adapted to brassicaceous hosts, such as oilseed rape and cauliflower, whereas *V. dahliae* generally does not colonize these plants (Depotter *et al.*, 2016a; Inderbitzin and Subbarao, 2014). Moreover, differences in pathogenicity are also observed between hybrid lineages, as *V. longisporum* A1/D1 and A1/D3 are often found on multiple brassicaceous hosts, whereas lineage A1/D2 has hitherto only been found on horseradish (Inderbitzin *et al.*, 2011b; Yu *et al.*, 2016). Furthermore, lineage A1/D1 is predominantly found on oilseed rape and responsible for the Verticillium stem striping disease as this lineage is the most virulent on this crop (Novakazi *et al.*, 2015).

In the past, *V. longisporum* and *V. dahliae* were considered a single species, and only at the end of the 1990s *V. longisporum* was proposed as a separate species from *V. dahliae* (Karapapa *et al.*, 1997). While adequate characterization of *V. longisporum* strains in predating publications is obscured by this name change and taxonomic disagreements, Verticillium stem striping is exclusively caused by *V. longisporum* (Eynck *et al.*, 2007). This oilseed rape disease was first reported in the west and south of Scania, southern Sweden, in 1969 (Kroeker, 1970). Until recently, Verticillium stem striping was only present in north-central Europe, but over the last decade other important oilseed rape production regions have also been affected (CFIA, 2015; Gladders *et al.*, 2011). Verticillium stem striping was noticed in UK oilseed rape production for the first time in 2007, in the counties Kent and Herefordshire (Gladders *et al.*, 2011). Currently,

V. longisporum is present throughout England, yet the disease is most prevalent in the east (Gladders *et al.*, 2013). The main causal agent of Verticillium stem striping, lineage A1/D1, has also been found outside Europe in Japan and the USA, albeit on different crops than oilseed rape (Carder and Barbara, 1994; Heale and Karapapa, 1999; Subbarao *et al.*, 1995). The wide-spread occurrence of *V. longisporum* A1/D1 suggests the importance of human activity in the spread of this disease as, similar to other *Verticillium* spp. (Atallah *et al.*, 2012), *V. longisporum* is considered soil-borne without the long-distance dispersal of air-borne spores (Depotter *et al.*, 2016a). Dispersal of *Verticillium* by the trade of plant commodities has been observed for *V. dahliae*, which has facilitated the intercontinental spread of the pathogen (Atallah *et al.*, 2012).

The aim of this study is to reveal population structures within Verticillium stem striping lineage A1/D1 by screening of rapidly evolving DNA regions. Microsatellites or simple sequence repeat (SSR) loci are hyper-variable genome regions of simple DNA motifs repeated in tandem. The repetitive character of these regions makes them more prone to mutation than non-repetitive sequences due to unequal crossing-over and replication slippage, generally revealing high degrees of polymorphism (Levinson and Gutman, 1987). Several population studies previously used SSR loci to describe diversity within *Verticillium* populations (Atallah *et al.*, 2010, 2012; Short *et al.*, 2014). However, hitherto, no population studies have been performed on *V. longisporum*. Here, we assessed the genetic diversity within a broad geographic range of the *V. longisporum* lineage A1/D1 isolates and found clear population structuring. The origin of these distinct populations was further elucidated by genealogical analysis and genome comparison. Here, established Verticillium stem striping populations (e.g. from Germany and Sweden) were compared with populations from a recent disease outbreak in the UK, in order to link the population dynamics with the expansion of Verticillium stem striping.

Material and methods

Isolate collection, DNA extraction and lineage characterization

In total 88 isolates from nine different countries were used in this study (Table S1). Mycelium was harvested from two-week-old potato dextrose broth cultures and DNA was extracted according to DNA extraction protocol A from Ribeiro and Lovato (2007). The lineage and mating type to which the respective isolates belong was determined previously for several isolates (Table S1) (Inderbitzin *et al.*, 2011b, 2013). The hitherto uncharacterized isolates were screened for the presence of a marker that is specific for lineage A1/D1. To this end, the primer pair D1f/AlfD1r was used for PCR to amplify a fragment from the *GPD* locus according to Inderbitzin *et al.* (2013). Amplicons were displayed by gel electrophoresis on a 1% agarose gel. Furthermore, isolates were screened for *MAT1-1* and *MAT1-2* idiomorphs with the primer pairs Alf/MAT11r and HMG21f/MAT21r, respectively, according to Inderbitzin, *et al.* (2011b). Amplicons were displayed by gel electrophoresis on a 1.5% agarose gel.

SSR loci

A genome-wide screening for polymorphic SSR loci was done with unpublished draft genome sequences from several *V. longisporum* isolates. INDELs between genomes were extracted from the whole-genome alignments using the mummer package (v3.1) (Kurtz *et al.*, 2004). Gene sequence variations were received by the variant call format tool (Danecek *et al.*, 2011). Insertions and deletions between 5 and 20 nucleotides were selected and screened for recurrent patterns that are typical for SSR loci. Primers were developed for 61 putative polymorphic SSR loci with the Primer3 software (Untergasser *et al.*, 2012). Additional polymorphic SSR markers for lineage A1/D1 were used in this study. VD1, VD8 and VD12 from Atallah *et al.* (2010) were originally designed for *V. dahliae* and were found to be polymorphic between *V. longisporum* isolates. In addition, VDA783, VDA787 and VDA823 from Barbara *et al.* (2005), designed for *V. longisporum*, were used. SSR loci were labelled and amplified with an M13 fluorescent tag according to Schuelke (Schuelke, 2000). The PCRs consisted of a 2 min initial denaturation step at 95°C, 30 cycles of 35 sec at 95°C, 45 sec at 62°C, and 1 min at 72°C, followed by 8 cycles of 30 sec at 95°C, 45 sec at 53°C and 1 min at 72°C, followed by an extension of 10 min at 72°C. The PCR mix contained 8 pmol of each reverse and M13 tagged universal sequence primer and 2.5 pmol of the forward primer in a final 10µl reaction volume: 1X GoTaq® Flexi Buffer Mg-free, 2.5mM $MgCl_2$, 0.2mM each dNTP, 100ng template DNA, DNA polymerase, 1.25 u GoTaq® polymerase (Promega, Madison, WI, USA). The labelled PCR products were then combined with Hi-Di formamide and LIZ-500 size standard and resolved on a 3730XL DNA Analyzer (Applied Biosystems, Foster City, CA, USA). The results were processed using GeneMapper v4.0 software (Applied Biosystems, Foster City, CA, USA).

Population structure

V. longisporum isolates were individually clustered based on polymorphic SSR loci using the software Structure version 2.3 (Pritchard *et al.*, 2000). Data were analyzed as for a haploid organism as all markers only gave a single polymorphic signal. The population was tested for containing 1 up to 6 genetic clusters (K). For every cluster, 10 runs were performed with a burn-in period of 500,000 generations and 1,000,000 Markov Chain Monte Carlo (MCMC) simulations. The admixture model was chosen and the loci were considered independent. The most likely number of genetic clusters in the population was determined with the ad-hoc statistic ΔK (Evanno *et al.*, 2005) using Structure Harvester (Earl and vonHoldt, 2012). Hereby, the amount of clusters in a population is determined based on the rate of change in the log probability of data between successive K values. Furthermore, the results from Structure were permuted and aligned in the program CLUMPP 1.1.2 (method Greedy, random input order, 1,000,000 repeats) (Jakobsson and Rosenberg, 2007) and visualized with the software Distruct 1.1 (Rosenberg, 2004). The correlation between the clusters and the country of origin of the isolates was determined with the Spearman's rank correlation coefficient

(ρ) with Hmisc package in R 3.2.3 (Harrell and Dupont, 2016; R Core Team, 2015). The standardized index of association I_A^s gives an indication for the recombination rate between organisms. In outcrossing populations, no linkage disequilibrium is present and an I_A^s of 0 is expected (Burt *et al.*, 1996). I_A^s was computed to test the recombination potential within the *V. longisporum* lineage A1/D1 population using the software LIAN version 3.7 (Haubold and Hudson, 2000). A Monte Carlo simulation of 100,000 iterations was chosen. The genetic clusters identified by Structure were evaluated using an analysis of molecular variance (AMOVA) with the software GenAlEx version 6.502 (Peakall and Smouse, 2006, 2012). The variance within the genetic clusters was compared with the variance between the genetic clusters with an analogue of Wright's fixation index (Φ_{PT}) (Excoffier *et al.*, 1992). The population diversity was assessed for populations with a minimum of 10 representatives, excluding isolates with missing data. Multi-locus genotype (MLG) diversity and the allelic richness (*AR*) were determined for each population using software Contrib 1.4, using rarefaction size 5 (Petit *et al.*, 1998). Nei's (1973) genetic diversity corrected for sample size (H_s) values were generated in GenoDive (Meirmans and van Tienderen, 2004). Genealogical relationships among the different MLGs haplotypes in the *V. longisporum* population were inferred using the median-joining method (Bandelt *et al.*, 1999), implemented in the software Network 5.0.0.0 (http://www.fluxus-engineering.com). All SSR loci were weighed equally (10) and an epsilon = 0 was chosen. The hypervariable SSR locus VD12 was not included in the analysis to reduce the amount of MLGs, and MLGs with missing data were excluded as well.

Genome sequencing and assembly of two *Verticillium longisporum* isolates

Genomic DNA of *V. longisporum* isolates VL20 and VLB2 was isolated from conidia and mycelium fragments that were harvested from 10-day-old cultures grown in liquid potato dextrose agar according to the protocol described by Seidl *et al.* (2015). The PacBio libraries for sequencing on the PacBio RSII machine (Pacific Biosciences of California, CA, USA) were constructed using ~20 µg of *V. longisporum* DNA, similary as described previously by Faino *et al.* (2015). Briefly, DNA was mechanically sheared, and size selected using the BluePippin preparation system (Sage Science, Beverly, MA, USA) to produce ~20 kb insert size libraries. The sheared DNA and final library were characterized for size distribution using an Agilent Bioanalyzer 2100 (Agilent Technology, Inc., Santa Clara, CA, USA). The PacBio libraries were sequenced on six SMRT cells per *V. longisporum* isolate at KeyGene N.V. (Wageningen, the Netherlands) using the PacBio RS II instrument. Sequencing was performed using the P6-C4 polymerase-Chemistry combination and a >4h movie time and stage start. Post filtering, a total of 344,906 (N50 ~20 kb) and 358,083 (N50 ~19 kb) polymerase reads were obtained for *V. longisporum* isolates VLB2 and VL20, respectively. Filtered sub-reads for VLB2 and VL20 (457,986; N50 ~14 kb and 466,673; N50 ~13.7 kb, respectively) were assembled using the HGAP v3 protocol (Chin *et al.*, 2013). Subsequently, the HGAP3 assemblies underwent additional polishing using Quiver (Chin *et al.*, 2013).

The *de novo* assemblies were further upgraded using FinisherSC, and the upgraded assemblies were polished with Quiver (Lam *et al.*, 2015). Lastly, contigs that displayed very low or exceptionally high PacBio read coverage, as well as the contig representing the mitochondrial DNA, were removed from the final assemblies. *De novo* repetitive elements in the genomes of *V. longisporum* were identified using RepeatModeler (v1.0.8), and repetitive elements were subsequently masked using RepeatMasker (v4.0.6; sensitive mode).

Genome comparisons between *V. longisporum* and *V. dahliae* strains

To place the newly sequenced *V. longisporum* isolates in context of 74 previously analyzed *Verticillium* spp., we identified the alleles (A1 or D1) of four previously used protein-coding genes *actin* (*ACT*), *elongation factor 1-alpha* (*EF*), *glyceraldehyde-3-phosphate dehydrogenase* (*GPD*) and *tryptophan synthase* (*TS*) in the genome assemblies of VLB2 and VL20 using blastn searches (Inderbitzin *et al.*, 2011a). Sequences were extracted from the genome assemblies and aligned to the four genes in the 74 *Verticillium* isolates using mafft (LINSi; v7.271) (Katoh and Standley, 2013). A phylogenetic tree was reconstructed using PhyML using the GTR nucleotide substitution model and four discrete gamma categories (Guindon and Gascuel, 2003). The robustness of the phylogeny was assessed using 500 bootstrap replicates.

Whole-genome comparisons between *V. longisporum* strains VLB2 and VL20 and between *V. dahliae* strains JR2 and VdLs17 (Faino *et al.*, 2015) were performed with nucmer (maxmatch), which is part of the mummer package (v3.1) (Kurtz *et al.*, 2004). Small polymorphisms (SNPs and INDELs) between genomes were extracted from the whole-genome alignments using show-snps (excluding ambiguous alignments), which is part of the mummer package (v3.1). Lineage-specific regions per individual *Verticillium* strain were determined by extracting nucmer alignments and subsequently identifying genomic regions that lack alignments with the other isolate (bedtools genomecov) (Quinlan and Hall, 2010).

To tentatively assign the individual sub-genomes, the repeat-masked genome of *V. dahliae* strain JR2 was compared to the repeat-masked *V. longisporum* genomes using nucmer (maxmatch), of which only 1-to-1 alignments longer than 5 kb where retained. Genomic regions were assigned to parental sub-genomes based on the average identity of consecutive alignments (defined by location and/or strand), where regions with average identity >95% were assigned to D1 and < 95% identity to A1, respectively. The pairwise identity between A1 and D1 parents within and between *V. longisporum* strains was calculated using nucmer (mum), with dividing the respective query sequences into non-overlapping windows of 500 bp.

Sequence data

SSR data have been deposited as GenBank accessions KY828946-KY828954. The *Verticillium longisporum* genome sequence data have been desposited as SRP102600 (VLB2) and SRP102606 (VL20).

Results

Population structure analysis

A geographically diverse collection of *V. longisporum* isolates was obtained in order to assess the population diversity and to genotypically link isolates from different origins. In total, 88 *V. longisporum* isolates from 9 different countries were screened for SSR polymorphisms in order to determine the population structure (Table S1). Sixty-one putative polymorphic SSR markers were developed based on unpublished draft *V. longisporum* genome sequence data and tested on the *V. longisporum* collection, of which 9 displayed polymorphisms (Table 1). Our analysis was performed as for a haploid organism as all markers only gave a single polymorphic signal.

The population structure was assessed based on the polymorphisms of these nine SSR loci that are dispersed over the genome (Table 1). The acquired multi-locus genotype (MLG) data were used to determine the most likely amount of genetic clusters in the *V. longisporum* population, allowing individual isolates to admix between different genetic clusters. The ad-hoc statistic ΔK was maximized for 3 genetic clusters in the population (K = 3), indicating that 3 is the most likely number of genetic clusters for the complete data set (Figure 1, S1). Four isolates that were previously determined to belong to lineage A1/D3 (Inderbitzin *et al.*, 2011b) formed one genetic cluster, whereas isolates known to belong to lineage A1/D1 showed two distinct clusters: one that includes samples from the USA and Japan, and another with samples from Germany and Sweden (Figure 1, S1). The hitherto uncharacterized isolates all grouped together with one of these two A1/D1 clusters, indicating that they belong to the A1/D1 lineage (Figure 1, S1). Indeed, successful amplification of the lineage A1/D1 specific primers D1f/AlfD1r (Inderbitzin *et al.*, 2013) confirmed that these isolates belong to the A1/D1 lineage (Figure S2). In addition, similar to all tested *V. longisporum* isolates, all uncharacterized isolates contained *MAT1-1* idiomorphs and failed to display *MAT1-2* in a mating type idiomorph PCR screen (Inderbitzin *et al.*, 2011b) (Figure S3). Interestingly, the dichotomy within the A1/D1 lineage correlated with the country of origin of the isolates (ρ = -0.51, P = 0.00), as the Belgian, Dutch, UK and USA isolates formed one of the A1/D1 clusters (A1/D1 West; n = 44), whereas the German, Latvian and Swedish formed the other cluster (A1/D1 East; n = 40). These two clusters within lineage A1/D1 are further referred to as "lineage A1/D1 West" and "lineage A1/D1 East" according to their relative geographic location in Europe. Furthermore, isolates from both genetic clusters are found in France and in Japan.

Table 1 | Polymorphic simple sequence repeat markers for *V. longisporum* lineages A1/D1 and A1/D3.

Locus	Size (bp)[1]	GenBank accession#[2]	Marker location[3]	Repeat motif[4]	Allele#[5]	Primer sequence
SSR25	283	KY828946	6	$(TGCC)_{13}$	6	F: AAGGAACCAAAATGCACACC
						R: GGCACTGGCGTAGGTAGGTA
SSR15	318	KY828947	3	$(CGT)_{7}$	2	F: GTCGATTTCGTTTTGGGAAA
						R: TACACAGTCAGCAAGGACGG
SSR159[6]	212	KY828948	11	$(TCT)_{12}$	10	F: ATCCACCATGTCAAACCGTT
						R: ACGAAATGGAAGGCAAACAC
SSR27	294	KY828949	13	$(GTCA)_{7}$	3	F: CTTCTTCTTGTTTGCCGGAG
						R: CACTGTTCAACGACACACCC
SSR135	226	KY828950	30	$(AGC)_{11}$	2	F: ACCATGTCTTCCTGACGGTC
						R: AGGTCCCTGGTAAAGCCACT
SSR70	252	KY828951	14	$(CA)_{15}$	6	F: GCCAGTGCGTTTCTTCCTAG
						R: GACGGACACGGAGATGAACT
SSR84	272	KY828952	3	$(CAG)_{8}$	4	F: TGATTAACTGGGAAGACCGC
						R: GCCAGAGAAACCAGACTGCT
SSR101	363	KY828953	12	TGTTGCTGC	2	F: TCGGATCATCGTAGTAGGCC
						R: TGGCTGAGCATCATTCACTC
SSR219	477	KY828954	13	$(CA)_{13}(A)_{8}$	3	F: ACAACACCTTGCCTAATGCC
						R: GCCAAACATTGTTAACGCCT

[1]: Amplicon length for isolate VLB2
[2]: Amplified sequence for isolate VLB2, acquired from unpublished VLB2 genome sequence
[3]: Contig number of the VLB2 genome sequence (Figure 3)
[4]: Number of repeats identified in genome sequence VLB2
[5]: Numbers of alleles observed in tested population
[6]: No amplification for isolates lineage A1/D3

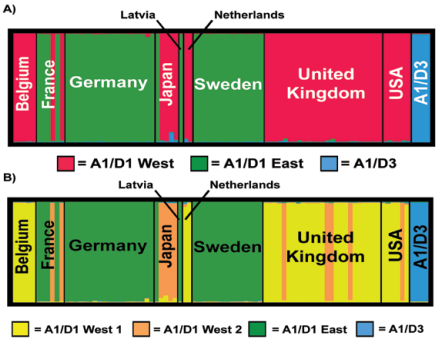

Figure 1 | Clustering of individual *V. longisporum* multi-locus genotypes (MLGs) using 15 polymorphic simple sequence repeat markers. Population clustering was executed on the whole data set for (A) three genetic clusters (K = 3) and (B) four genetic clusters (K = 4) with by the software Structure version 2.3 (Pritchard *et al.*, 2000). The thick vertical bars separate the MLGs by country of origin. The bar width of every country is relative to the amount of samples: Belgium (n = 5), France (n = 6), Germany (n = 19), Japan (n = 5), Latvia (n = 1), the Netherlands (n = 2), Sweden (n = 15), UK (n = 25), USA (n = 6) and the cluster with isolates from the A1/D3 lineage (n = 4). The different colors represent separate genetic clusters. In A: red = lineage A1/D1 West, green = lineage A1/D1 East, and blue = lineage A1/D3. Lineage A1/D1 West is subdivided in section B, where yellow = A1/D1 West cluster 1, and orange = A1/D1 West cluster 2.

In order to confirm the dichotomy within lineage A1/D1 and to reveal more potential sub-structuring in the population, six additional published polymorphic SSR loci were used in the analysis (Table 2) (Atallah *et al.*, 2010; Barbara *et al.*, 2005). The SSR marker VDA817 from Barbara *et al.* (2005) also revealed polymorphisms, but was targeting the same SSR locus as VDA783. Thus, VDA817 was excluded from the population analysis. In total, 13 SSR loci were polymorphic for lineage A1/D1 as two of the nine previously mentioned SSR loci (SSR101 and SSR135) only differentiated between the A1/D1 and A1/D3 lineages (Table 1). The dichotomy within lineage A1/D1 was confirmed with these additional SSR loci, as the most likely number of genetic clusters was two for the A1/D1 population (Figure 1A, S3). Here, nine of the 13 polymorphic SSR loci for lineage A1/D1 subdivided the population significantly into the A1/D1 West and East dichotomy based on the analysis of molecular variance (AMOVA) (Φ_{PT} statistic, Table 2). Moreover, isolates of A1/D1 West and A1/D1 East lineages have no alleles in common for the loci SSR25, SSR70, SSR219, VD8 and VDA823. All SSR loci combined, over 59% of the total genotypic variability within the A1/D1 population can be explained by the A1/D1 West and East dichotomy. Based on this, the dichotomy within A1/D1 is considered significant (Φ_{PT} = 0.590; P = 0.001).

Table 2 | The cluster determining capacities of the A1/D1 polymorphic simple sequence repeat loci.

Locus	Marker location[1]	Repeat motif[2]	Allele #[3]	A1/D1 West[4]	A1/D1 East[5]	Φ_{PT}[6]	p
SSR25	6	$(TGCC)_{13}$	5	4	1	0.827	0.001
SSR15	3	$(CGT)_{7}$	2	0	0	-0.005	0.468
SSR159	11	$(TCT)_{12}$	10	7	2	0.537	0.001
SSR27	13	$(GTCA)_{7}$	2	1	0	-0.002	1.000
SSR70	14	$(CA)_{15}$	5	3	2	0.610	0.001
SSR84	3	$(CAG)_{8}$	3	2	0	0.006	0.492
SSR219	13	$(CA)_{13}(A)_{8}$	2	1	1	1.000	0.001
VD1	9	$(GCCT)_{8}$[7]	2	0	1	0.951	0.001
VD8	11	$(TGA)_{13}$	5	3	2	0.662	0.001
VD12	6	$(CTTT)_{19}$	9	1	1	0.267	0.002
VDA783[8]	6	$(CGT)_{22}$	5	1	2	0.026	0.092
VDA787	4	$(GAC(AGC)_{2})_{7}$	2	1	0	0.735	0.001
VDA823	5	$(CCG)_{8}$	2	1	1	1.000	0.001

[1]: Contig number of the VLB2 genome sequence (Figure 3)
[2]: Number of repeats identified in genome sequence VLB2
[3]: Numbers of alleles observed in tested A1/D1 population
[4]: Number of alleles exclusive for A1/D1 West
[5]: Number of alleles exclusive for A1/D1 East
[6]: Computed with GenAlEx version 6.502 (Peakall and Smouse, 2006, 2012)
[7]: Different repeat motif than reported for *V. dahliae* in Atallah *et al.* (2010)
[8]: Targets same locus as VDA817 from Barbara *et al.* (2005)

Although our data divided the A1/D1 population into two genetic clusters, an additional population structure analysis was performed for lineage A1/D1 West and A1/D1 East separately to reveal putative sub-structuring. For the A1/D1 West population, the ad-hoc statistic ΔK was maximized for 2 genetic clusters in the population (K = 2), indicating that 2 is the most likely number of genetic clusters within the A1/D1 West cluster (Figure 1, S4). Here, the Belgian and Dutch isolates formed one genetic cluster that segregated from the French/Japanese isolates. The UK and USA populations both resided in A1/D1 West clusters. In addition, AMOVA analysis also confirmed this sub-division within A1/D1 West as almost 34% of the genotypic variability within A1/D1 West can be explained by this dichotomy (Φ_{PT} = 0.338; P = 0.001). Further genetic clustering of the A1/D1 West population (K > 2) did not reveal any more subdivisions in A1/D1 West as isolates were then assigned to more than one genetic cluster. Furthermore, no further genetic clusters were present in lineage A1/D1 East as isolates were more or less equally subdivided between two clusters when K = 2. In conclusion, the *V. longisporum* lineage A1/D1 population contained 3 genetic clusters with no apparent intermixing between clusters, although intermixing between genetic clusters was enabled in the Structure analysis. The lack of intermixing between the genetic clusters within lineage A1/D1 indicates an exclusively clonal reproduction (Figure 1). The standardized index of association I_A^s was calculated to investigate linkage disequilibrium between loci of *V. longisporum* lineage A1/D1. I_A^s was significantly different from 0 (I_A^s = 0.3081, $P < 1.00 \times 10^{-5}$) indicating that *V. longisporum* is not out-crossing.

Population diversity and genealogy

The *V. longisporum* A1/D1 collection contained 40 different MLGs derived from 79 isolates with a complete genotype, of which 31 were unique (Table 3). The diversity between the UK isolates was higher than between the German and Swedish ones as Nei's corrected gene diversity (H_s) was 0.163, 0.110 and 0.085, respectively (Table 3). In agreement with this, the diversity of the whole A1/D1 West (H_s = 0.176) cluster was higher than A1/D1 East (H_s = 0.109). The difference in diversity between A1/D1 West and A1/D1 East is also clearly depicted in the genealogical network of the isolates; excluding locus VD12 to reduce the total amount of MLGs to 31 MLGs (Figure 2). The A1/D1 West and A1/D1 East populations were segregated from each other by a minimal of 10 mutations between MLG 3 and MLG 17. The A1/D1 East network was centred on the modal MLG 6 that represents more than half of the isolates (n=22) from four different countries (France, Germany, Sweden and Latvia). In contrast, A1/D1 West had a less centralized population network with MLGs 15, 23 and 26 being the most represented with 8, 9 and 7 individuals, respectively. MLG 15 contains exclusively UK isolates, whereas MLG23 and MLG26 have representatives from multiple countries (Belgium, Netherlands, UK and USA).

Table 3 | Diversity within the German, Swedish, UK, A1/D1 West, A1/D1 East and A1/D1 population.

Population	# Isolates	# MLG	H_s [1]	MLG [2] diversity	AR [2]
Germany	18	10	0.110	0.810	2.683
Sweden	13	7	0.085	0.885	2.979
United Kingdom	23	11	0.163	0.893	3.071
A1/D1 West	42	24	0.176	0.933	3.405
A1/D1 East	37	16	0.109	0.872	2.988
A1/D1	79	40	0.307	0.954	3.575

[1] Nei's corrected gene diversity (H_s) values were generated in GenoDive (Meirmans and van Tienderen, 2004).
[2] Multi-locus genotype (MLG) diversity and allelic richness (AR) were determined using the software Contrib 1.4 (Petit *et al.*, 1998).

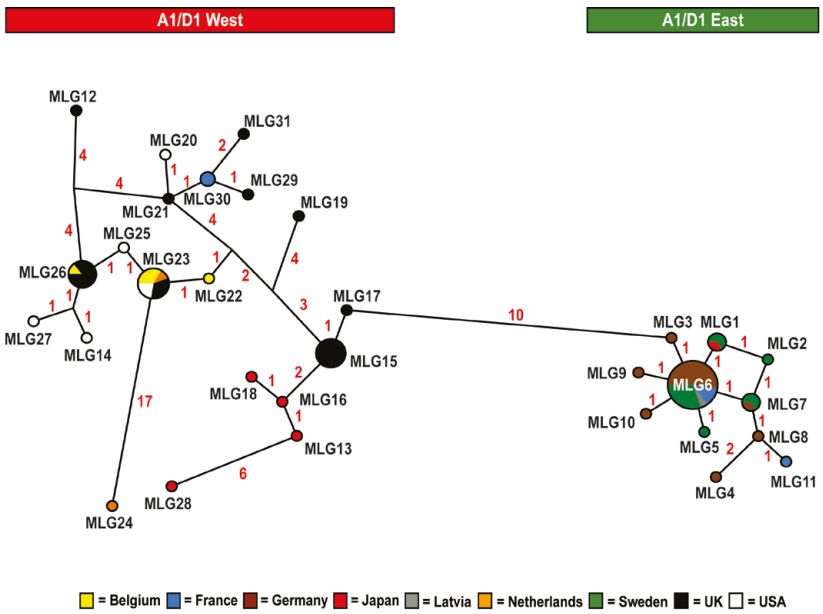

Figure 2 | Genealogical relationships of *V. longisporum* A1/D1 population based on 12 polymorphic simple sequence repeat (SSR) loci. Genealogical relationships were calculated based on 12 SSR loci (Table 2 except marker VD12) using the software Network 5.0.0.0 (Bandelt *et al.*, 1999). The median-joining (MJ) network algorithm was chosen whereby SSR loci were weighted equally (10) and epsilon = 0 was used. Every circle represents a different multi-locus genotype (MLG) and the radius is relative to the MLG's occurrence in the population. The lines connecting the MLGs depict the genealogical relationship between them, whereby the number of mutations between MLGs is written next to the lines. All MLGs on the left of the figure (under the green bar) clustered to the previous determined lineage A1/D1 East, whereas all the MLGs on the right (under the red bar) are members of the A1/D1 West cluster. MLGs with missing data were excluded.

Population origin

The origin of the dichotomy within lineage A1/D1 (Figure 1) can either point to two independent hybridization events, giving rise to the two subpopulations within A1/D1, or to a single hybridization event followed by evolutionary diversification, leading to the emergence of two sub-populations. To gather additional evidence supporting either hypothesis, we selected one *V. longisporum* isolate of A1/D1 West (VLB2) and one of A1/D1 East (VL20) for single-molecule real-time (SMRT) sequencing using the PacBio RSII platform, which has been previously demonstrated to deliver high quality genome assemblies of *V. dahliae* and *Verticillium tricorpus* (Faino *et al.*, 2015; Seidl *et al.*, 2015). We generated 466,673 and 457,986 filtered subreads (~67x coverage) for *V. longisporum* strain VL20 and VLB2 that were assembled into 74 and 83 contigs, respectively (Table S2). Subsequent manual curation yielded a final assembly of 44 and 45 contigs with a total assembled genome length of 72.3 and 72.9 Mb for *V. longisporum* VL20 and VLB2, respectively (Table S2), which represents approximately twice the size of the recently assembled complete, telomere-to-telomere assemblies of *V. dahliae* strains JR2 (36.2 Mb) and VdLs17 (36.0 Mb) (Faino *et al.*, 2015).

To place the sequenced *V. longisporum* strains into the context of other *Verticillium* spp., we extracted the alleles of four protein-coding genes, namely *actin* (*ACT*), *elongation factor 1-alpha* (*EF*), *glyceraldehyde-3-phosphate dehydrogenase* (*GPD*) and *tryptophan synthase* (*TS*) (Inderbitzin *et al.*, 2011b), from the two genome assemblies and performed maximum likelihood phylogenetic analyses (Figure S6), confirming that both *V. longisporum* isolates belong to the A1/D1 lineage.

In order to obtain further evidence for their evolutionary origin and to fully utilize the genome assemblies of the two *V. longisporum* isolates, we performed whole-genome comparisons between *V. longisporum* VL20 and VLB2 (Figure 3A). Whole-genome alignments between *V. longisporum* VL20 and VLB2 revealed large-scale synteny between both genomes, where a single genomic region in one of the genome aligns to two regions in the other genome. Moreover, as expected from an interspecific hybrid, the alignments of one of these regions generally displays >99% identity, while the identity of the second region is lower, ranging from 90 to 95% (Figure 3B). Notably, comparisons between *V. longisporum* strains VL20 and VLB2 only identified 140 kb and 450 kb, respectively, of genomic material that is absent in the other strain (Figure 3B). Furthermore, ~1,000 SNPs and ~3,800 indels between VL20 and VLB2 were revealed. Thus, the two *V. longisporum* strains are genetically highly similar and do not display marked differences between their individual lineage-specific (LS) regions; a likely scenario if the two *V. longisporum* strains emerged from the same hybridization event.

To obtain further evidence the evolutionary origin of the two *V. longisporum* strains, we extracted the individual A1 and D1 sub-genomes based on their sequence identity to *V. dahliae* strain JR2, as parent D1 only recently diverged from *V. dahliae* (Figure

S6) (Inderbitzin *et al.*, 2011b). Moreover, genome comparisons between *V. dahliae* and *V. longisporum* indicated that 95% sequence identity allows discriminating A1 from D1 sub-genome. The extracted A1 and D1 sub-genomes of *V. longisporum* strain VL20 comprised 32.8 Mb and 34.2 Mb, respectively, while 5.2 Mb could not be assigned. Similarly, the A1 and D1 sub-genomes of *V. longisporum* strain VLB2 comprised 32.5 Mb and 34.7 Mb, respectively, while 5.7 Mb could not be assigned. As expected, within and between the *V. longisporum* strains the average identity between A1 and D1 sub-genomes was ~93% (Figure 3C). Notably, however, the average identity between the A1 sub-genomes as well as between the D1 sub-genomes of both *V. longisporum* strains was >99% (Figure 3C), suggesting that the A1 and D1 parental genomes that give rise to *V. longisporum* strain VLB2 and VL20 were identical and that, consequently, A1/D1 West and A1/D1 East are derived from a single hybridization event (Figure 4).

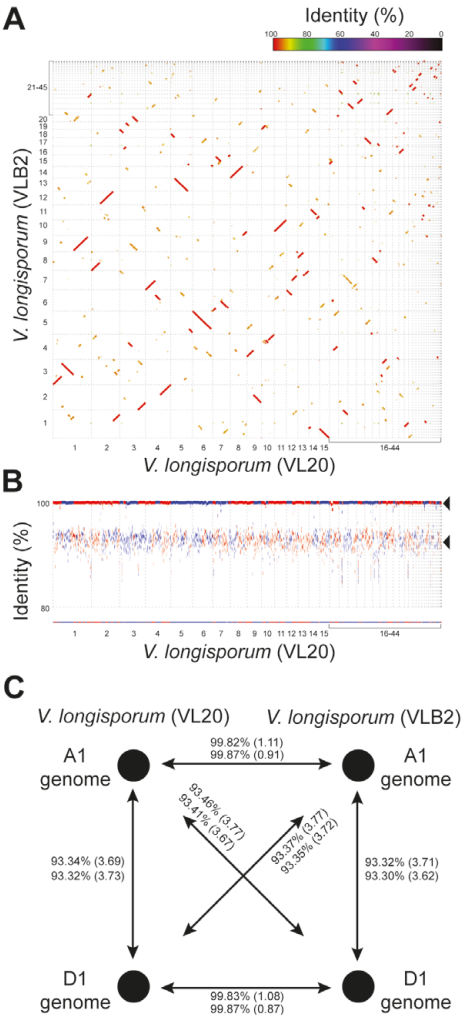

Figure 3 | Whole-genome comparison between *V. longisporum* VL20 and VLB2 reveals a common origin. A) Whole-genome comparison between *V. longisporum* VL20 and VLB2. Aligned genomic regions (>10 kb) are displayed and color indicates sequence identity. Numbers along the axes represent the contigs of the respective isolates. B) Coverage plot displaying the whole-genome alignment (>10 kb) of *V. longisporum* strain VLB2 to that of strain VL20. Since *V. longisporum* is an allodiploid, two genomic regions, one with ~99% and the other with 90-95% sequence identity (indicated by the two black arrow heads), align to the VLB2 genome. Forward-forward alignments are shown in red and forward-reverse alignments (inversions) are shown in blue. C) Sequence identity between the A1 and D1 sub-genomes of *V. longisporum* strains VL20 and VLB2.

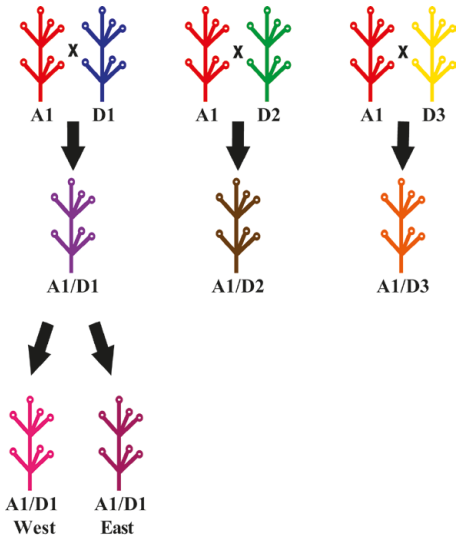

Figure 4 | The evolutionary history of *V. longisporum*. *V. longisporum* consists of three separate hybridization events between two different *Verticillium* spp. Hybrid lineages are named after their parental spp.: A1/D1, A1/D2 and A1/D3. Two A1/D1 populations have segregated from each other fur still unclear reasons. Phylogenetic relationships between parents of *V. longisporum* and other *Verticillium* spp. are depicted in figure S6. (Adjusted from Depotter *et al.* 2016a; Inderbitzin *et al.* 2011b).

Discussion

Population genetic structures reveal information about the evolutionary history of organisms. Genome hybridization can be a major driver for organismal adaptation and has allowed *V. dahliae* that infects brassicaceous species relatively infrequently, to become pathogenic on these hosts as *V. longisporum* (Depotter *et al.*, 2016a). Based on phylogenetic analyses, *V. longisporum* has been subdivided into three lineages: A1/D1, A1/D2 and A1/D3, each representing a separate hybridization event between two *Verticillium* spp. (Inderbitzin *et al.*, 2011b). The Verticillium stem striping pathogen has been emerging as a disease on oilseed rape and is emerging in hitherto unaffected production regions (CFIA, 2015; Gladders *et al.*, 2011). This disease is predominantly caused by the *V. longisporum* lineage A1/D1, which is the most virulent lineage on this crop (Novakazi *et al.*, 2015). In this study, the diversity within the A1/D1 lineage was assessed and population structures within a collection from a diverse geographic origin were elucidated. Isolates from nine different countries (Table S1) were genotyped with newly and previously characterized polymorphic SSR loci (Tables 1, 2). Model-based clustering revealed a hitherto undiscovered dichotomous structuring within *V. longisporum* lineage A1/D1 (Figure 1, S1). Interestingly, the two A1/D1 sub-populations were geographically correlated and were accordingly labeled "A1/D1 West" and "A1/D1 East" based on their relative European location. Geographic population structuring typically indicates adaptation to local climate or to local hosts. Alternatively, the two genetic clusters may also represent two separate hybridization events. In order to test

the latter hypothesis, whole-genome comparisons between two representative genomes of the A1/D1 West and East population were performed. All our evidence points towards a single origin of the two A1/D1 populations (Figure 4). First, the genome sizes of strains VL20 and VLB2 are highly similar, with 72.3 Mb and 72.9 Mb, respectively (Table S2). Then, the two genomes carried only a small proportion of lineage specific sequence: 140 kb and 450 kb for VL20 and VLB2, respectively. Recently, genome-comparisons between multiple *V. dahliae* strains have revealed the presence of extensive (2.5-4.5 Mb) LS regions that are shared by only a subset of the *V. dahliae* isolates and that are enriched for *in planta* induced genes that contribute to fungal virulence (Faino *et al.*, 2016; de Jonge *et al.*, 2013). For example, direct comparisons between the completely assembled genomes of *V. dahliae* strains JR2 and VdLS17 (Faino *et al.*, 2015), two strains that have been shown to be extremely closely related with 99.98% sequence identity (de Jonge *et al.*, 2013), identified four large regions comprising ~2 Mb that display frequent presence/absence polymorphisms (Faino *et al.*, 2016), of which in total ~550 kb and ~620 kb in *V. dahliae* strain JR2 and VdLs17 do not align to the other strain, respectively. Additionally, genome-wide comparison between *V. dahliae* strains JR2 and VdLs17 revealed ~4,700 SNPs and ~10,000 indels, while the *V. longisporum* VL20 and VLB2 strains contain genomes that were relatively low in divergence as only ~1,000 SNPs and ~3,800 indels were found. Finally, the genetic distance between the A1 sub-genomes as well as between the D1-sub-genomes of both *V. longisporum* strains was >99% (Figure 3C), suggesting that the A1 and D1 parental genomes were nearly identical. Thus, we conclude that the observed geographic population structuring is a signature of divergent evolution driven by environmental adaptation.

Presently, environmental conditions responsible for the dichotomous A1/D1 population structure remain elusive. However, strikingly, although all UK A1/D1 isolates were isolated from the same host species, oilseed rape (Table S1), they are more diverse than the German, Swedish and even the whole A1/D1 East population (Table 3). The high diversity of the British population contradicts a recent introduction as genetic bottlenecks can be expected, especially when considering the isolated character of the British island (Nei *et al.*, 1975). Consequently, the A1/D1 West population may have been present in the UK for a longer time without being noticed as Verticillium stem striping pathogen on oilseed rape. Nevertheless, genetic diversity may also be the consequence of multiple introductions. For example, three genetic lineages of the chestnut blight fungus *Cryphonectria parasitica* were separately introduced in France (Dutech *et al.*, 2010).

The A1/D1 West sub-population, partly consisting of UK isolates, is more diverse than its A1/D1 East counterpart (Table 3, Figure 2). Their shared origin along with this difference in diversity indicates that A1/D1 East is a founder population of the originating A1/D1 West population. The more recent origin of A1/D1 East is also depicted in the genealogical network (Figure 2). A1/D1 East has a clear modal MLG (MLG6) with all other A1/D1 East MLGs centered on it. In contrast, the A1/D1 West population lacks a dominating genotype. A1/D1 East may have evolved from A1/D1 West

in order to adapt to different climate conditions, hence the geographic correlation of the two A1/D1 sub-populations. Obviously, population segregation in organisms with symbiotic relationships can be host driven. Genetic co-structuring between pathogen and host can be found due to their co-evolutionary interaction (Croll and Laine, 2016; Feurtey *et al.*, 2016), as pathogens engage in arm races with hosts for continued symbiosis (Cook *et al.*, 2015). Host-pathogen evolution, also with host plants other than oilseed rape and thus even differences in host range compositions, may explain the discrepancy in population diversity and the Verticillium stem striping emergences of the two A1/D1 sub-populations. Interestingly, Verticillium stem striping has been conspicuous in Sweden and Germany since the 1960s, countries with an exclusive A1/D1 East presence (Figure 1) (Daebeler *et al.*, 1988; Kroeker, 1970). Although we cannot exclude that the A1/D1 West lineage was present as an unnoticed oilseed rape pathogen for a long time, this lineage recently emerged as a conspicuous pathogen on oilseed rape in the UK (Figure 1) (Gladders *et al.*, 2011). Oilseed rape must have become susceptible, or at least more sensitive, to A1/D1 West for reasons that presently remain unclear. Considering the large degree of diversity within the A1D1 West population, rather than particular adaptations in the pathogen population, alterations in environmental conditions (e.g. global warming) (Siebold and von Tiedemann, 2012) and oilseed rape cultivars are more likely explanations for the sudden rise of the genomic diverse UK Verticillium stem striping population. Oilseed rape is a relatively new crop in the UK that was virtually unknown in the 1970 but is currently one of the main arable crops with approximate production area of 700,000 hectares (Wood *et al.*, 2013). Intensive breeding efforts have been made to create a broad diversity of oilseed rape oil, such as the modern 00 (canola) type (Wittkop *et al.*, 2009). The novelty of Verticillium stem striping makes that cultivar resistance for this disease was not selected for, hence the possibility that more susceptible oilseed rape varieties have been commercialized over time.

V. longisporum is an interspecific hybrid between two separate *Verticillium* spp. (Depotter *et al.*, 2016a; Inderbitzin *et al.*, 2011b). Interspecific hybrids are regularly found to be impaired in their sexual reproduction (Bertier *et al.*, 2013; Greig, 2009), although this should be of little significance for *V. longisporum,* as a sexual stage has not been described for any of the *Verticillium* spp. (Short *et al.*, 2014). However, mating types, meiosis-specific genes and genomic recombination between clonal lineages have been observed for *V. dahliae* (Milgroom *et al.*, 2014; Short *et al.*, 2014). This suggests that *V. dahliae* may have cryptic or ancestral sexual reproduction. In contrast to population structure studies with *V. dahliae* (Atallah *et al.*, 2010, 2012), no apparent intermixing between genetic clusters was observed for *V. longisporum*. Moreover, the I_A^s was also significantly different from 0 for the *V. longisporum* lineage A1/D1 (I_A^s = 0.3081, $P < 1.00 \times 10^{-5}$), which implies that no linkage equilibrium is present. These data indicate that *V. longisporum* reproduces exclusively in a clonal fashion and has never experienced sexual reproduction. Mechanisms different from meiotic recombination must contribute to genetic diversity in order to achieve evolutionary adaptation (Seidl

and Thomma, 2014). Similar as proposed for several other filamentous pathogens, *V. dahliae* has a two-speed genome with particular genomic (LS) regions that are considerably more dynamic than the core genome (Faino *et al.*, 2016). These rapidly evolving LS regions are enriched in active transposable elements that shape the genome in an active and passive fashion (Faino *et al.*, 2016; de Jonge *et al.*, 2013). Moreover, also horizontal gene transfer contributes to genome evolution of *Verticillium dahliae*, as *Ave1*, an effector gene crucial for aggressiveness, originated by horizontal gene transfer from plants (de Jonge *et al.*, 2012).

Increasing evolutionary ecology knowledge of a pathogen can play a pivotal role in disease management in order to protect ecosystems (Williams, 2010). Population genetic studies are therefore often used to identify origins of newly emerging pathogens and their adaptation pathways (Dutech *et al.*, 2012; Gross *et al.*, 2014). However, not all emerging diseases are preceded by a clearly identified recent introduction. Our study exemplifies that new diseases can emerge from a latent, previously established, microbial population. Thus, factors like weather and farming techniques can also spur disease emergences, especially for fungal pathogens (Anderson *et al.*, 2004). Besides, the two *V. longisporum* populations are generally still geographically bound to specific geographic locations in Europe. The driving forces causing the dichotomous population structure remain elusive, but conceivable differences in pathogenic traits may have contributed to the West/East segregation. A cautious approach is therefore appropriate to prevent further spread of the two populations, as the expansion of the population into new geographic regions may have unpredicted outcomes.

Acknowledgements

The authors would like to thank the Marie Curie Actions program of the European Commission that financially supports the research investigating the threat of *V. longisporum* to UK oilseed rape production. Work in the laboratories of B.P.H.J.T. and M.F.S. is supported by the Research Council Earth and Life Sciences (ALW) of the Netherlands Organization of Scientific Research (NWO). We greatly appreciate all donors of *V. longisporum* isolates: the Dixelius, Höfte, INRA-CIRAD, Norddeutsche Pflanzenzucht, Subbarao and Terres Inovia laboratories. The authors declare no conflict of interest.

Supplementary material

Table S1 | *V. longisporum* isolates used in this study.

Isolate name	Region	Original host	Year	Source
Lineage A1/D1 West				
Belgium				
K1	Klein Brabant	cauliflower	?	Höfte lab collection
O1	Klein Brabant	cauliflower	?	Höfte lab collection
WVL1	West-Vlaanderen	?	?	Höfte lab collection
WVL2	West-Vlaanderen	cauliflower	?	Höfte lab collection
P4	Klein Brabant	cauliflower	?	Höfte lab collection
France				
V654	Doubs	rape	1989	INRA-CIRAD
V544	Ille-et-Vilaine	rape	1987	INRA-CIRAD
Japan				
PD588/CA9	Gunma	cabbage	?	Subbarao lab collection
PD630/84020	?	birdrape	?	Subbarao lab collection
PD591/Dk-1	Chiba	radish	?	Subbarao lab collection
PD590/CA58	Gunma	cabbage	?	Subbarao lab collection
The Netherlands				
VL2	Noord-Groningen	rape	2006	Thomma lab collection
Be1	Waarland	cauliflower	?	Höfte lab collection
United Kingdom				
VLB1	Cambridgeshire	rape	2014	NIAB
VLB2	Leicestershire	rape	2014	NIAB
VLB3	Lincolnshire	rape	2014	NIAB
VLB4	Norfolk	rape	2014	NIAB
VLB6	Lincolnshire	rape	2013	NIAB
VLB7	Bedfordshire	rape	2014	NIAB
VLB8	Bedfordshire	rape	2014	NIAB
VLB9	Suffolk	rape	2014	NIAB
VLB10	Suffolk	rape	2012	NIAB
VLB11	Cambridgeshire	rape	2012	NIAB
VLB12	Cambridgeshire	rape	2014	NIAB
VLB13	Cambridgeshire	rape	2013	NIAB
VLB14	Cambridgeshire	rape	2012	NIAB
VLB15	Lincolnshire	rape	2014	NIAB
VLB16	Northamptonshire	rape	2015	NIAB
VLB17	Buckinghamshire	rape	2015	NIAB
VLB18	Suffolk	rape	2015	NIAB
VLB22	Northamptonshire	rape	2015	NIAB
VLB23	Northamptonshire	rape	2015	NIAB
VLB24	Cambridgeshire	rape	2015	NIAB
VLB25	?	rape	2015	NIAB
VLB26	?	rape	2015	NIAB
VLB27	Lincolnshire	rape	2015	NIAB
VLB28	Cambridgeshire	rape	2015	NIAB
VLB29	Lincolnshire	rape	2015	NIAB

Isolate name	Region	Original host	Year	Source
United States of America				
PD348/Bob.70/90-02	California	cauliflower	1990	Subbarao lab collection
PD330/Boc.74/91-05	California	cabbage	1991	Subbarao lab collection
PD624/90-10	?	cauliflower	?	Subbarao lab collection
PD352/Bob.69	California	cauliflower	1990	Subbarao lab collection
PD329/Bob.71	California	cauliflower	1990	Subbarao lab collection
PD355/Bob.127	California	cauliflower	1997	Subbarao lab collection
Lineage A1/D1 East				
France				
Vl02	Meurthe-et-Moselle	rape	2007	Terres Inovia
Vl04	Aube	rape	2010	Terres Inovia
Vl05	Aube	rape	2010	Terres Inovia
V668	Meurthe-et-Moselle	rape	1989	INRA-CIRAD
Germany				
PD638/Vl 40	Mecklenburg-Vorpommern	rape	1990	Norddeutsche Pflanzenzucht
PD639/Vl 43	Mecklenburg-Vorpommern	rape	1990	Subbarao lab collection
Vl 92	Brandenburg	rape	1999	Norddeutsche Pflanzenzucht
Vl 93	Brandenburg	rape	1999	Norddeutsche Pflanzenzucht
Vl 94	Mecklenburg-Vorpommern	rape	1999	Norddeutsche Pflanzenzucht
Vl 95	Mecklenburg-Vorpommern	rape	1999	Norddeutsche Pflanzenzucht
Vl 96	Mecklenburg-Vorpommern	rape	1999	Norddeutsche Pflanzenzucht
Vl 97	Mecklenburg-Vorpommern	rape	1999	Norddeutsche Pflanzenzucht
Vl 98	Mecklenburg-Vorpommern	rape	1999	Norddeutsche Pflanzenzucht
Vl 99	Mecklenburg-Vorpommern	rape	1999	Norddeutsche Pflanzenzucht
Vl 100	Mecklenburg-Vorpommern	rape	1999	Norddeutsche Pflanzenzucht
Vl 101	Schleswig-Holstein	rape	1999	Norddeutsche Pflanzenzucht
Vl 102	Mecklenburg-Vorpommern	rape	1999	Norddeutsche Pflanzenzucht
Vl 103	Niedersachsen	rape	1999	Norddeutsche Pflanzenzucht
Vl 104	Niedersachsen	rape	1999	Norddeutsche Pflanzenzucht
Vl 105	Schleswig-Holstein	rape	1999	Norddeutsche Pflanzenzucht
Vl 106	Niedersachsen	rape	1999	Norddeutsche Pflanzenzucht
Vl 107	Baden-Württemberg	rape	1999	Norddeutsche Pflanzenzucht
Pf2	Rhineland-Palatinate	?	?	Höfte lab collection
Japan				
PD677/86207	?	wild radish	1980	Subbarao lab collection
Latvia				
VL20	Zemgale	rape	2015	SIA
Sweden				
Vd 6	?	rape	?	Dixelius lab colelction
PD725/Vd 13	?	rape	?	Dixelius lab collection
PD645/Vd 11/CBS 110220	?	rape	?	Dixelius lab collection
PD641/Vd 1	?	rape	?	Subbarao lab collection
PD644/Vd 4	?	rape	?	Subbarao lab collection
PD723/40-2	?	rape	?	Subbarao lab collection
PD721/43-3	?	rape	?	Subbarao lab collection
PD724/42-1	?	rape	?	Subbarao lab collection
PD726/37-1	?	rape	?	Subbarao lab collection
PD643/Vd 02:50	Västmanland	rape	?	Subbarao lab collection

Isolate name	Region	Original host	Year	Source
PD722/Vd 12	?	rape	?	Subbarao lab collection
PD720/44-4	?	rape	?	Subbarao lab collection
PD676/161	?	sugar beet	1981	Subbarao lab collection
PD642/Vd 01:43	Landskrona	rape	?	Subbarao lab collection
CBS 649.85	?	*Brassica rapa*?		Thomma lab collection
Lineage A1/D3				
Germany				
PD614/MD73	?	rape	?	Subbarao lab collection
PD715/Vl 32	Mecklenburg-Vorpommern	rape	1988	Subbarao lab collection
PD687/CBS 124.64	Niedersachsen	horseradish	1959	Subbarao lab collection
Japan				
PD589/CA10	Gunma	cabbage	?	Subbarao lab collection

Table S2 | *V. longisporum* strain VL20 and VLB2 genome assemblies.

Matric		VL20	VLB2
SMRT cells		6	6
Filtered subreads		466,673	457,986
Coverage (n-fold)		67.7x	66.4x
HGAP3 assembly	Size (bp)	72,495,102	73,489,504
	Contigs	74	83
	Longest contig	5,837,573	5,411,788
	N_{50} (bp)	2,718,091	2,899,830
	No of Ns/100 kb	0	0
FinisherSC assembly	Size (bp)	72,433,856	73,098,666
	Contigs	52	56
	Longest contig	7,148,864	5,411,733
	N_{50} (bp)	2,718,187	3,135,754
	No of Ns/100 kb	0	0
Final assembly	Size (bp)	72,271,822	72,894,593
	Contigs	44	45
	Longest contig	7,148,928	5,411,750
	N_{50} (bp)	2,718,243	3,135,757
	No of Ns/100 kb	0	0

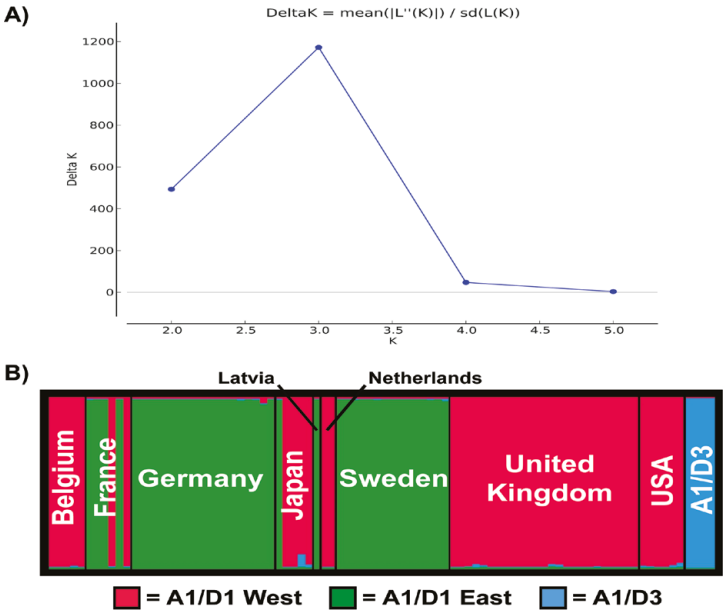

Figure S1 | Genetic clusters within the *V. longisporum* population using the 9 newly designed polymorphic simple sequence repeat (SSR) markers. Isolate genotyping was based on 9 SSR loci (Table 1). (A) Output of the ad-hoc statistic ΔK calculated for the different genetic clusters within *V. longisporum* population with a maximum for K = 3 (Earl and vonHoldt, 2012). (B) Genetic clustering of individual *V. longisporum* multi-locus genotypes (MLGs) devided the whole data set into three groups using Structure version 2.3 (Pritchard *et al.*, 2000). The thick vertical bars separate the MLGs by country of origin. The bar width of every country is relative to the amount of samples: Belgium (n = 5), France (n = 6), Germany (n = 19), Japan (n = 5), Latvia (n = 1), the Netherlands (n = 2), Sweden (n = 15), UK (n = 25), the USA (n = 6) and the cluster with isolates from the A1/D3 lineage (n = 4). The different colors represent separate genetic clusters: red = lineage A1/D1 West, green = lineage A1/D1 East, and blue = lineage A1/D3.

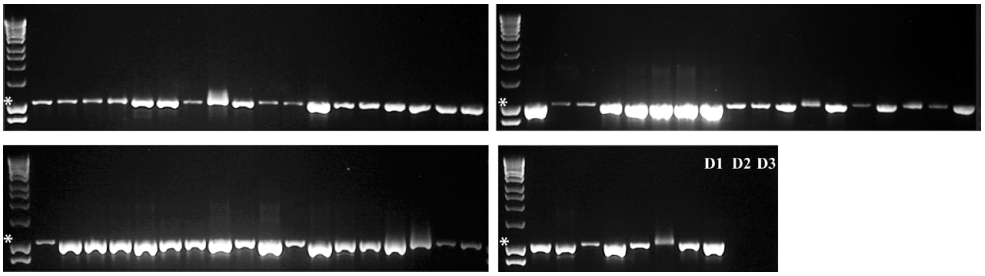

Figure S2 | Lineage characterization of *V. longisporum* isolates. Agarose gels show the selective amplification of markers obtained with the lineage A1/D1 specific primers D1f/AlfD1r (Inderbitzin *et al.*, 2013) for hitherto uncharacterized *V. longisporum* isolates. Gels are deliminated by ladders where the 1000 bp size marker is indicated by '*'. Isolates with an 1020 bp amplicon belong to the A1/D1 lineage. The three lanes indicated by 'D1', 'D2' and 'D3' are controls, in which previously characterized isolates were used from lineage A1/D1, A1/D2 and A1/D3 respectively. Isolates used from top left to bottom right: K1, O1, WVL1, WVL2, P4, Vl02, Vl04, Vl05, V654, V668, V544, Pf2, Vl 40, Vl 92, Vl 93, Vl 94, Vl 95, Vl 96, Vl 97, Vl 98, Vl 99, Vl 100, Vl 101, Vl 102, Vl 103, Vl 104, Vl 105, Vl 106, Vl 107, Vl 43, PD677, VL20, Be1, VL2, CBS 649.85, Vd 6, VLB1, VLB2, VLB3, VLB4,VLB6,VLB7, VLB8, VLB9, VLB10, VLB11, VLB12, VLB13, VLB14, VLB15, VLB16, VLB17, VLB18, VLB22, VLB23, VLB24, VLB25, VLB26, VLB27, VLB28, VLB29, Vd 11, PD356 and PD715.

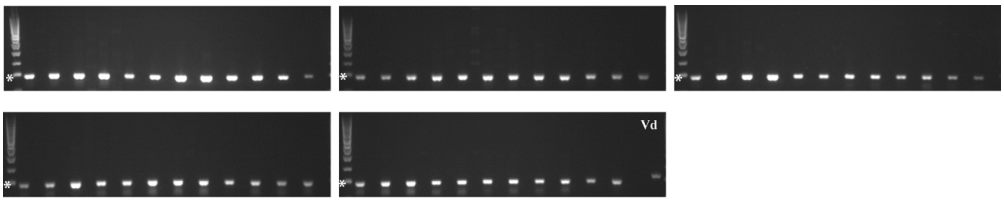

Figure S3 | Mating type characterization of *V. longisporum* isolates. Agarose gels shows alternatingly the presence/absence of the mating type idiomorphs *MAT1-1* and *MAT1-2* according to Inderbitzin, *et al.* (2011b) for hitherto uncharacterized *V. longisporum* isolates. Gels are deliminated by ladders where the 300 bp size marker is indicated by '*'. The *MAT1-1* and *MAT1-2* specific amplicons have a length of 291 and 330 bp, respectively. The last two lanes function as a positive control for *MAT1-2* as *V. dahliae* (Vd) DNA of isolate JR2 was used as template. Isolates used from top left to bottom right: K1, O1, WVL1, WVL2, P4, Vlo2, Vlo4, Vlo5, V654, V668, V544, Pf2, Vl 92, Vl 93, Vl 94, Vl 95, Vl 96, Vl 97, Vl 98, Vl 99, Vl 100, Vl 101, Vl 102, Vl 103, Vl 104, Vl 105, Vl 106, Vl 107, Vl 43, PD677, VL20, Be1, VL2, CBS 649.85, Vd 6, VLB1, VLB2, VLB3, VLB4,VLB6,VLB7, VLB8, VLB9, VLB10, VLB11, VLB12, VLB13, VLB14, VLB15, VLB16, VLB17, VLB18, VLB22, VLB23, VLB24, VLB25, VLB26, VLB27, VLB28, VLB29 and JR2.

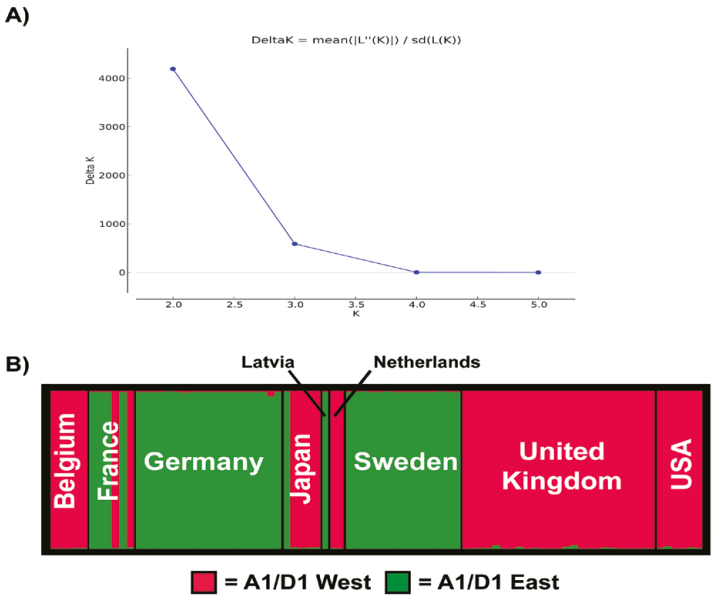

Figure S4 | Genetic clusters within the *V. longisporum* A1/D1 population using 13 polymorphic simple sequence repeat (SSR) markers. Isolate genotyping was based on 13 SSR loci (Table 2). (A) Output of the ad-hoc statistic ΔK calculated for the different genetic clusters within *V. longisporum* population with a maximum for K = 2 (Earl and vonHoldt, 2012). (B) Genetic clustering of individual *V. longisporum* multi-locus genotypes (MLGs) into 2 groups determined by Structure version 2.3 (Pritchard *et al.*, 2000). The thick vertical bars separate the MLGs by country of origin. The bar width of every country is relative to the amount of samples: Belgium (n = 5), France (n = 2), Japan (n = 5), the Netherlands (n = 2), UK (n = 25) and USA (n = 6). The different colors represent separate genetic clusters: red = A1/D1 West cluster and green = A1/D1 East cluster.

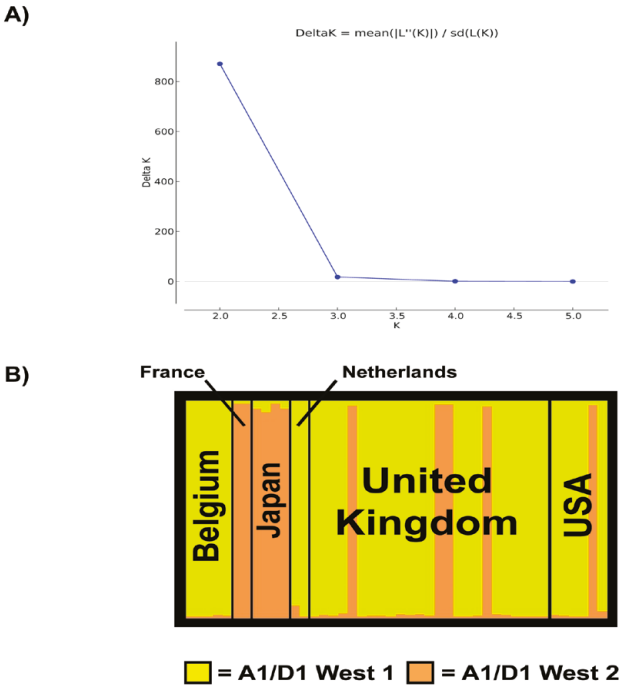

Figure S5 | Genetic clusters within the *V. longisporum* A1/D1 West population using 11 polymorphic simple sequence repeat (SSR) markers. Isolate genotyping was based on 11 SSR loci (Table 2 except markers SSR219 and VDA823). (A) Output of the ad-hoc statistic ΔK calculated for the different genetic clusters within *V. longisporum* population with a maximum for K = 2 (Earl and vonHoldt, 2012). (B) Genetic clustering of individual *V. longisporum* multi-locus genotypes (MLGs) into 2 groups determined by Structure version 2.3 (Pritchard *et al.*, 2000). The thick vertical bars separate the MLGs by country of origin. The bar with of every country is relative to the amount of samples: Belgium (n = 5), France (n = 2), Japan (n = 4), the Netherlands (n = 2), UK (n = 25) and USA (n = 6). The different colors represent separate genetic clusters: yellow = A1/D1 West cluster 1 and orange green = A1/D1 West cluster 2.

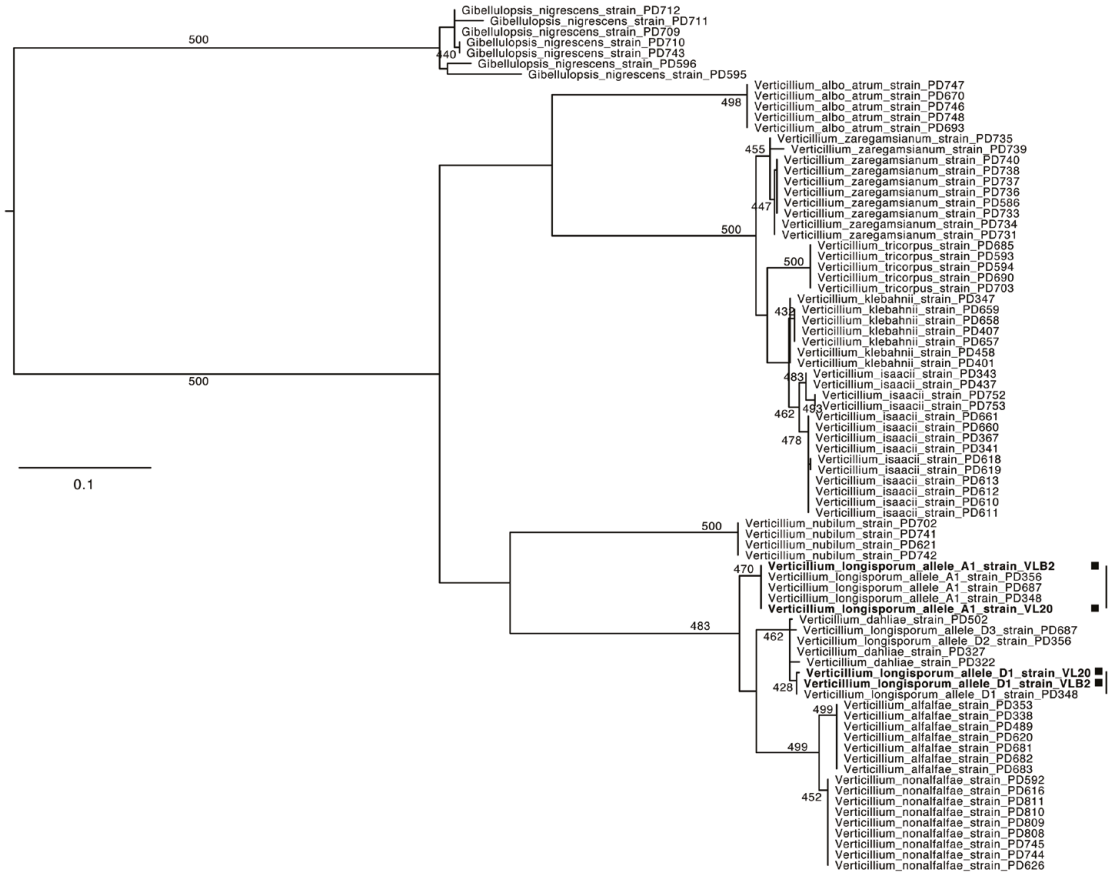

Figure S6 | Phylogenetic relationships between *V. longisporum* A1/D1 West and East parents with the other *Verticillium* species. Phylogenetic relationships are based on the sequence of four previously used protein-coding genes: *actin* (*ACT*), *elongation factor 1-alpha* (*EF*), *glyceraldehyde-3-phosphate dehydrogenase* (*GDP*) and *tryptophan synthase* (*TS*) (Inderbitzin, *et al.*, 2011a). The phylogenetic tree was reconstructed using PhyML using the GTR nucleotide substitution model and four discrete gamma categories (Guindon and Gascuel, 2003). The robustness of the phylogeny was assessed using 500 bootstrap replicates. VLB2 and VL20 were used as a representative for the lineage A1/D1 West and East, respectively (Table S1). These were included together with 74 previously characterized *Verticillium* and *Verticillium*-related isolates in the phylogenetic analysis.

4

The emerging British *Verticillium longisporum* population consists of aggressive *Brassica* pathogens

Jasper R.L. Depotter
Luis Rodriguez-Moreno
Bart P.H.J. Thomma[†]
Thomas A. Wood[†]

[†]These authors contributed equally

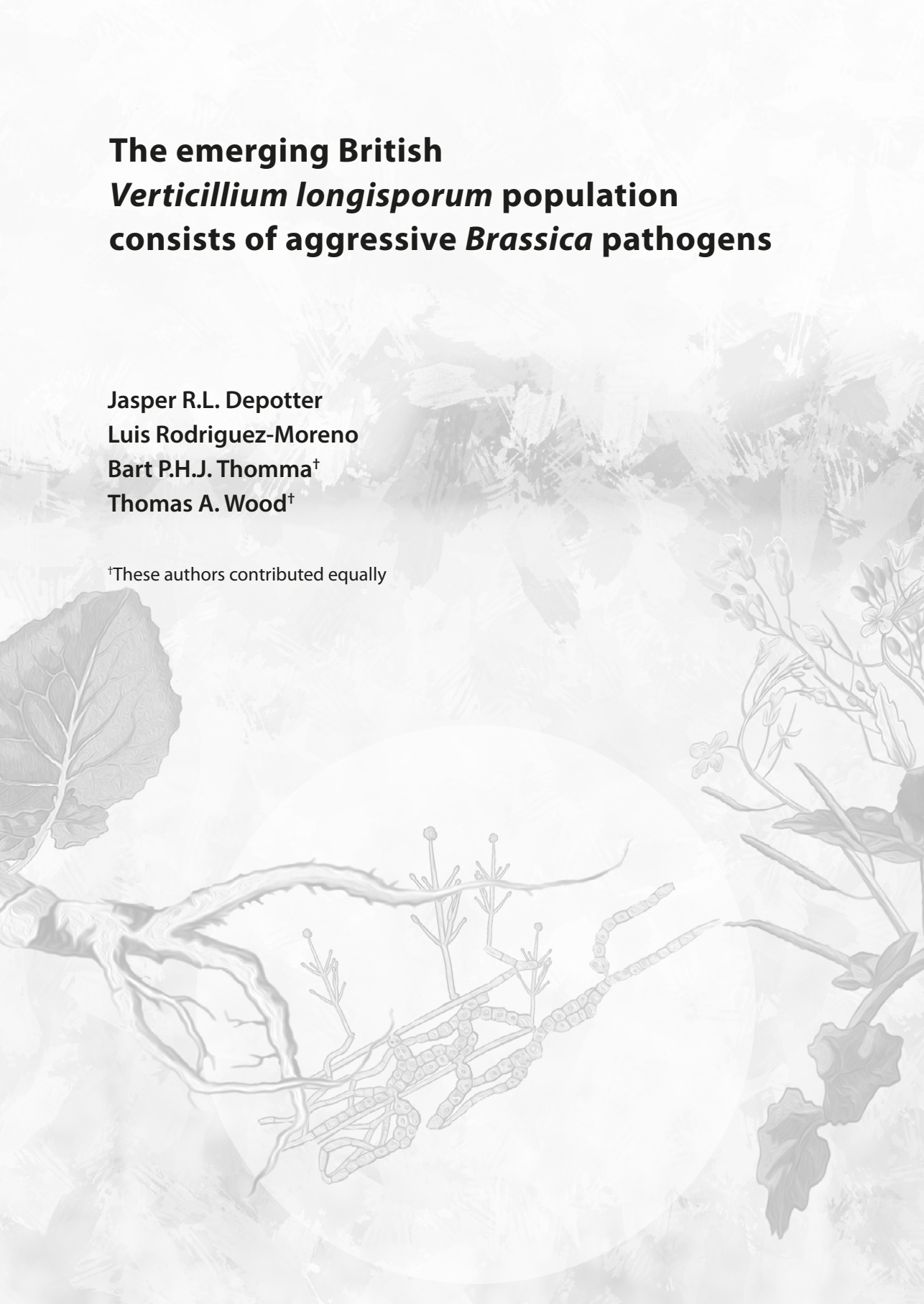

Abstract

V. longisporum is an economically important fungal pathogen of brassicaceous crops that originated from at least three hybridization events between different *Verticillium* spp., leading to the hybrid lineages A1/D1, A1/D2 and A1/D3. Isolates of lineage A1/D1 generally cause stem striping on oilseed rape (*Brassica napus*), which has recently been reported for the first time to occur in the UK. Intriguingly, the emerging UK population is distinct from the north-central Europe stem striping population. Little is known about the pathogenicity of the newly emerged UK population; hence pathogenicity tests were executed to compare British isolates to previously characterized reference strains. Besides on the model plant *Arabidopsis thaliana*, the pathogenicity of four British isolates was assessed on four cultivars of three *Brassica* crop species: oilseed rape (cv. Quartz and Incentive), cauliflower (cv. Clapton) and Chinese cabbage (cv. Hilton). To this end, vascular discoloration of the roots, plant biomass accumulations and fungal stem colonization upon isolate infection were evaluated. The British isolates appeared to be remarkably aggressive, as plant biomass was significantly impacted and severe vascular discoloration was observed. The British isolates were successful stem colonizers and the extent of fungal colonization negatively correlated with plant biomass of cauliflower and oilseed rape cv. Quartz. However, in Quartz, the fungal colonization of A1/D1 isolates was significantly lower than that of the virulent reference isolate from lineage A1/D3, PD589. Moreover, despite similar levels of stem colonization as A1/D1 strains, PD589 did not cause significant disease on Incentive. Thus, A1/D1 isolates, including British isolates, are aggressive oilseed rape pathogens despite limited colonization levels in comparison to a virulent A1/D3 isolate.

Introduction

Verticillium fungi cause wilt diseases on hundreds of plant species of which many are economically important crops. *Verticillium dahliae* is the most notorious member of these fungi and can cause severe yield losses in crops like olive and cotton (Fradin and Thomma, 2006; Levin *et al.*, 2003; Melero-Vara *et al.*, 1995). Despite a wide host range that comprises hundreds of plant species, *V. dahliae* generally does not infect brassicaceous plants (Inderbitzin and Subbarao, 2014; Zeise and von Tiedemann, 2002). In contrast, *V. longisporum* is specialized on Brassicaceae hosts, with oilseed rape as its most economically important target (Depotter *et al.*, 2016a; Inderbitzin *et al.*, 2011b). In contrast to all other *Verticillium* spp, including *V. dahliae*, *V. longisporum* is not a haploid organism but rather an allodiploid as a consequence of interspecific hybridization. The species *V. longisporum* consists of three lineages, each representing a separate hybridization event. Four parental lines, including two *V. dahliae* isolates (D2 and D3), contributed to the different hybridization events. The two remaining parental lines represent two previously uncharacterized *Verticillium* spp. that have been provisionally called species A1 and species D1 (Inderbitzin *et al.*, 2011b). Species A1 participated in all three hybridization events and hybridized with D1, D2 and D3 to form the lineages A1/D1, A1/D2 and A1/D3, respectively. Conceivably, the allodiploid genome of *V. longisporum* contributed to the host range shift such that *V. longisporum* gained the capacity to infect Brassicaceae (Depotter *et al.*, 2016b; Inderbitzin *et al.*, 2011b). The separate hybridization events seem to have impacted the pathogenicity of *V. longisporum* lineages differently. Lineages A1/D1 and A1/D3 are found on various Brassicaceae species, whereas lineage A1/D2 is only known from horseradish in the USA (Inderbitzin *et al.*, 2011b; Yu *et al.*, 2016). Furthermore, A1/D1 is the predominant lineage on oilseed rape and is also the most pathogenic *V. longisporum* lineage on this crop (Novakazi *et al.*, 2015).

In addition to its different genetic constitution, *V. longisporum* is unique amongst *Verticillium* species for its disease symptom display on oilseed rape. *Verticillium* pathogens are xylem colonizers inducing occlusions in the vessels, which hampers the water transport in the xylem (Fradin and Thomma, 2006). In response, *Verticillium* infections generally develop wilting symptoms. However, these symptoms are lacking from *V. longisporum* infections on oilseed rape. Rather, black unilateral stripes appear on the plant stem at the end of the growing season and, in a later stage, microsclerotia appear on the cortex under the stem epidermis (Heale and Karapapa, 1999). Hence, the new common name "Verticillium stem striping" was coined to describe the *V. longisporum* disease on oilseed rape (Depotter *et al.*, 2016a). Intriguingly, Verticillium stem striping symptoms fail to appear during pathogenicity tests when oilseed rape plants are grown under controlled conditions and seedlings are inoculated by dipping the roots in a spore suspension (Eynck *et al.*, 2007, 2009b; Floerl *et al.*, 2008; Zeise and von Tiedemann, 2002). Under those conditions, plants exhibit chlorosis, vascular

discoloration and stunting at an early stage. The reasons for these differences in symptom development are currently unknown. Nevertheless, despite differences in disease symptomatology, it has previously been determined that root-dip pathogenicity tests in the glasshouse are a good proxy for oilseed rape cultivar resistance under field conditions (Knüfer *et al.*, 2017).

In the past, *V. dahliae* and *V. longisporum* were considered a single species, and only at the end of the 1990s *V. longisporum* was proposed as a separate taxon (Karapapa *et al.*, 1997). Hence, adequate characterization of *V. longisporum* strains in predating publications is hampered. However, on oilseed rape, Verticillium stem striping is exclusively caused by *V. longisporum* and thus trustworthy species assumptions can be made on this crop (Eynck *et al.*, 2007). Verticillium stem striping was first reported in 1969 in the south of Sweden and became prevalent in north-central Europe the following years (Heale and Karapapa, 1999; Kroeker, 1970; Steventon *et al.*, 2002; Zhou *et al.*, 2006). Recently, the geographic range of Verticillium stem striping has expanded as oilseed rape production in Canada and the UK are now affected as well (CFIA, 2015; Gladders *et al.*, 2011). In the UK, Verticillium stem striping was reported for the first time in 2007, and is currently widespread (Gladders *et al.*, 2011, 2013). Intriguingly, *V. longisporum* was most likely described earlier in the UK but on a different host: Brussels sprout (Isaac, 1957). In congruence with other geographic regions, characterized *V. longisporum* strains from UK oilseed rape belong to the A1/D1 lineage (Depotter *et al.*, 2017b). However, the UK population is distinct from the A1/D1 population in north-central Europe, where Verticillium stem striping is predominantly found (Depotter *et al.*, 2017b). According their relative geographic distribution in Europe, British isolates have been assigned to the "A1/D1 West" population, whereas German and Swedish A1/D1 isolates have been assigned to "A1/D1 East".

The recent emergence of Verticillium stem striping makes that little is known about the pathogenicity of the British *V. longisporum* strains. Moreover, British strains belong to a distinct population from most other previously characterized *V. longisporum* strains isolated from oilseed rape. Hence, we performed pathogenicity tests to compare four British *V. longisporum* strains with five reference stains from different countries (Belgium, Germany, Japan and USA) including all hybrid lineages. Pathogenicity was assessed thoroughly based on visual symptoms, biomass accumulation and fungal colonization in the stem.

Material and methods

Pathogenicity tests

Pathogenicity tests were conducted in order to compare the virulence of 9 *V. longisporum* strains (Table 1). Three different *Brassica* crops were used: oilseed rape (*B. napus* var. *oleifera*), cauliflower (*B. oleracea* var. *botrytis*) and Chinese cabbage (*B. rapa* subsp. *Pekinensis*). Winter oilseed rape cultivars comprise open pollinating and hybrid types of which one of each was tested: cv. Quartz and cv. Incentive, respectively. Furthermore, one Chinese cabbage cultivar (cv. Hilton), and one cauliflower cultivar (cv. Clapton) were also included. Thus, in total, four *Brassica* cultivars were tested. Importantly, because of limited greenhouse space availability, pathogenicity tests on the different crops were not performed all at the same time. Plants were grown in climate-controlled glasshouses under a 16 hrs light/ 8 hrs dark cycle with temperatures maintained between 20 and 28°C during the day, and a minimum of 15°C overnight. Before sowing, seeds were surface-sterilized during 1 min in 70% ethanol, followed by 15 min in 1% commercial bleach and then rinsed four times with sterile water. These sterilized seeds were then sown in trays with sterile compost and kept in the glasshouse for 14 days. These two-week old seedlings were inoculated by dipping the roots for 30 min in a suspension of $1x10^6$ conidiospores ml^{-1}. Conidiospores were obtained from three-week old cultures grown on potato dextrose agar plates. Fifteen plants were inoculated for every *V. longisporum* strain and 15 control plants were dipped in sterile water instead of a conidiospore suspension. Individual seedlings were planted in 9 cm square pots with 4:1:1 compost:sand:loam mixture and pots were placed according to a random block design. The potting mixture had been autoclaved twice for 60 min with 24h between each treatment. Plants were grown for 6 weeks before harvesting. Plants were harvested by cutting the stem just above the hypocotyls and pooled in 5 groups of three plants. For every pooled sample, the aboveground dry weight was subsequently determined by drying the samples at 100°C for a minimum of 12 h. Furthermore, vascular discoloration of individual roots was scored at six weeks according to Tyvaert *et al.* (2014). A scale was used from 0 to 4: 0 = no vascular discoloration, 1 = vascular discoloration of 1-25% of the root length, 2 = vascular discoloration of 26-50% of the root length, 3 = 51-75% vascular discoloration of the root length and 4 = 76-100% vascular discoloration of the root length. Pathogenicity tests were executed twice to confirm the virulence responses of the different strains. In addition to root vascular discoloration and dry weight, fungal stem colonization was evaluated. To this end, stems were removed at the hypocotyl, pooled in groups of three, and fungal colonization was assessed in the 1 cm section adjacent to the hypocotyl. The remainders of the stems were used for dry weight determination. During the repeat experiment, Quartz plants were only grown until 25 days after inoculation to guarantee sufficient plant biomass to extract DNA from as longer growth periods could lead to complete decay of the plants (Figure S1). Furthermore, in the second pathogenicity test, due to limited conidiospore availability, Chinese cabbage plants were inoculated with a water suspension of $5x10^5$ conidiospores ml^{-1}.

Arabidopsis thaliana (Col-0) plants were grown in a different glasshouse where the temperature was kept between 19 and 21°C and the same light/dark regime was used (16h/8h). Four plants of every treatment were grown. Plant inoculation occurred three weeks after sowing and roots were dipped for 10 min in a water suspension of 10^6 conidiospores ml^{-1}. Aboveground plant material was harvested for real-time PCR analysis three weeks after inoculation.

Relative fungal quantification

Samples were taken for fungal biomass quantification and ground in liquid nitrogen. Approximately 200 mg ground plant material was dissolved in 500 µl of CTAB buffer (55 mM CTAB, 0.1 M Tris pH 8.0, 20 mM EDTA pH 8.0, 1.25 NaCl and 0.25 mM PVP 40). The buffer/plant extract was incubated for 30 min at 65°C. Samples were centrifuged and supernatant was subsequently transferred to a clean tube and 250 µl chloroform:isoamyl alcohol solution (24:1) was added. Samples were mixed thoroughly by inversion and subsequently centrifuged. Next, the supernatant was transferred into 50 µl ammonium acetate (7.5M) and 500 µl ethanol. After mixing, DNA was precipitated and the supernatant was removed. DNA pellets were washed twice with 70% ethanol and dissolved in DNase free water.

The amount of *V. longisporum* DNA in stems was quantified relatively to the amount of plant DNA by real-time PCR using QuantStudio™ Flex Real-Time PCR System (Applied Biosystems, CA, USA). Fungal DNA was amplified with the *V. longisporum* specific primer pair: VlTubF2/ VlTubR1 (GCAAAACCCTACCGGGTTATG / AGATATCCATCGGACT-GTTCGTA) (Debode *et al.*, 2011) and the RuBisCO sequence targeting primer pair RubF/ RubR (TATGCCTGCTTTGACCGAGA / AGCTACTCGGTTAGCTACGG) for plants. Real-time PCR was performed in reactions of 10 µl containing 500 nM of every primer and 5 µl of Power SYBR Green Master Mix (Applied Biosystems, Foster City, CA, USA). The thermal program of the real-time PCR started with an initial denaturation step at 95°C for 10 min, followed by 40 cycles of 15 s at 95°C, 1 min at 62°C and 30 s at 72°C. Specific amplification was verified running a melting curve: samples were heated to 95°C for 15 s, cooled down to 60°C for 1 min and heated again to 95°C for 15 s. Signals above 36 cycles are considered below the detection limit.

DNA of the *Arabidopsis* plants was isolated according to Fulton *et al.* (1995). Relative *V. longisporum* colonization was quantified according to Ellendorff *et al.* (2009) using the qPCR core kit (Eurogentec, Liège, Belgium). Real-time PCR was executed on an ABI7300 PCR System (Applied Biosystems, Foster City, CA, USA) with following thermal conditions: an initial 95 °C denaturation step for 4 min, 30 cycles of denaturation for 15 s at 95 °C, annealing for 30 s at 60 °C, and extension for 30 s at 72 °C.

Data analysis

Significance levels were determined with the Mann-Whitney U-test. Correlations were calculated with the Pearson correlation coefficient (*r*). Data from the vascular discoloration consisted of too many ties for adequate *P*-value calculation. Hence, significant differences were calculated based on 5000 bootstrap replicates of the median difference between random disease scores of two treatments.

Results

The pathogenicity of four British *V. longisporum* isolates was compared with that of five previously characterized isolates, including isolates of all three *V. longisporum* hybridization lineages (Table 1). The four British isolates are adequate population representatives as their genotypes approximate the range of diversity within the British *V. longisporum* population (Table 1; Depotter *et al.* 2017b). The isolates were tested on four different *Brassica* cultivars: two oilseed rape (cv. Incentive and cv. Quartz), one cauliflower (cv. Clapton) and one Chinese cabbage (cv. Hilton). Pathogenicity tests were repeated twice and similar pathogenicity outcomes for the different *V. longisporum* strains were obtained on both occasions. Pathogenic *V. longisporum* isolates stunted plant growth and leaves displayed chlorosis and necrosis (Figure S1-4). Moreover, the more aggressive isolates caused complete decay of Quartz plants within 6 weeks of inoculation (Figure S1). Furthermore, the pathogenicity of the British strains was also tested on the model plant *Arabidopsis thaliana* (Col-0): VLB1, VLB2 and VLB9 induced leaf curling and necrosis (Figure S5). The same symptoms were observed for VLB3, but the plants were also heavily stunted indicating that VLB3 is more aggressive than the other British strains on *Arabidopsis*.

Table 1 | *V. longisporum* isolate information.

Isolate name	Region of origin	Country of origin	Original host	Collection year	Lineage	MLG[1]	Reference*
PD639	Mecklenburg	Germany	Rape	1990	A1/D1	MLG6	(Novakazi *et al.*, 2015)
O1	Klein Brabant	Belgium	Cauliflower	/	A1/D1	MLG23	(Tyvaert *et al.*, 2014)
PD356	Illinois	USA	Horseradish	1997	A1/D2	/	(Novakazi *et al.*, 2015)
PD715	Mecklenburg-Vorpommern	Germany	Rape	1988	A1/D3	/	(Novakazi *et al.*, 2015)
PD589	Gunma	Japan	Cabbage	/	A1/D3	/	(Novakazi *et al.*, 2015)
VLB1	Cambridgeshire	UK	Rape	2014	A1/D1	MLG26	(Depotter *et al.*, 2017b)
VLB2	Leicestershire	UK	Rape	2014	A1/D1	MLG15	(Depotter *et al.*, 2017b)
VLB3	Lincolnshire	UK	Rape	2014	A1/D1	MLG26[2]	(Depotter *et al.*, 2017b)
VLB9	Suffolk	UK	Rape	2014	A1/D1	MLG17	(Depotter *et al.*, 2017b)

[1] Multi-locus genotype (MLG) of the A1/D1 isolates based on 12 polymorphic simple sequence repeat loci determined by Depotter *et al.* (2017b).

[2] The allele of locus SSR25 could not be determined, but all other loci resembled MLG26 (Depotter *et al.*, 2017b).

The British *V. longisporum* isolates were pathogenic on all tested *Brassica* cultivars. Their vascular root tissues were discolored, which was generally significantly different from the control plants displaying no such symptoms (Figure 1). Severe discoloration was similarly observed in the two A1/D1 reference strains. In contrast, the strain of lineage A1/D2, PD356, failed to induce vascular discoloration significantly different from the control treatment. Intriguingly, vascular discoloration varied for lineage A1/D3 depending on the strain and host. No significant root discoloration was observed in Incentive (Figure 1B), whereas roots of Quartz, Clapton and Hilton displayed discolorations ranging from nothing to severe (Figure 1A-C-D). Disease symptoms such as stunted growth and necrosis were in correspondence with the vascular discoloration of the roots and led to significant aboveground biomass reductions (Figure 2). Here, reductions in biomass accumulations were amongst the highest for the British *V. longisporum* strains. Similarly, severe biomass reductions were observed for the two A1/D1 representatives (PD639 and VLO1), illustrating the high virulence of this lineage on *Brassica* hosts (Figure 2). In contrast, PD356 was the least virulent *V. longisporum* strain, especially on oilseed rape, where no significant reductions in biomass accumulation were observed upon inoculation (Figure 2A-B). PD356 inoculation significantly reduced the plant biomass of Clapton and Hilton but nevertheless it was one of the least aggressive isolates (Figure 2C-D). Disease responses of the two A1/D3 representatives (PD715 and PD589) were, in contrast to the two A1/D1 representatives, dissimilar (Figure 2). The German isolate PD715 was a weak pathogen unable to cause significant biomass reduction on Incentive (Figure 2B) and was amongst the weakest strains tested on Quartz, Clapton and Hilton (Figure 2A-C-D). In contrast, the Japanese A1/D3 isolate, PD589, strongly affected *Brassica* crops as PD589 was amongst the most severe isolates in Quartz, Clapton and Hilton (Figure 2A-C-D). In contrast to the devastating outcome on the oilseed cultivar Quartz, no significant biomass reduction was observed when Incentive was infected with PD589 (Figure 2B).

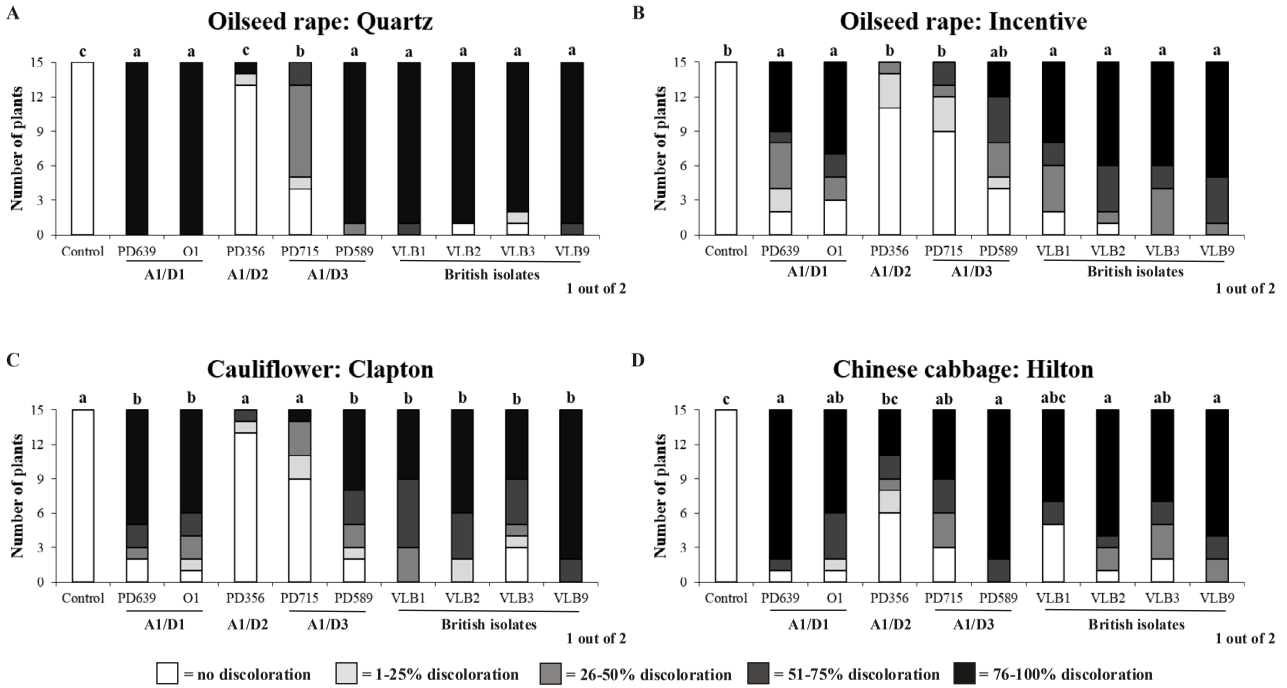

Figure 1 | Vascular discoloration in the roots of various *Brassica* crops upon inoculation with *V. longisporum*. The color of the bar represents the length of the root with vascular discoloration at 6 weeks for the cultivars: Quartz (A), Incentive (B), Clapton (C) and Hilton (D). In total, 15 plants were assessed for every treatment and the data represent one out of two experiments. Significance levels were calculated based on 5000 bootstrap replicates of the median difference between random scores of two treatments ($p<0.05$). Different letter labels indicate significant differences.

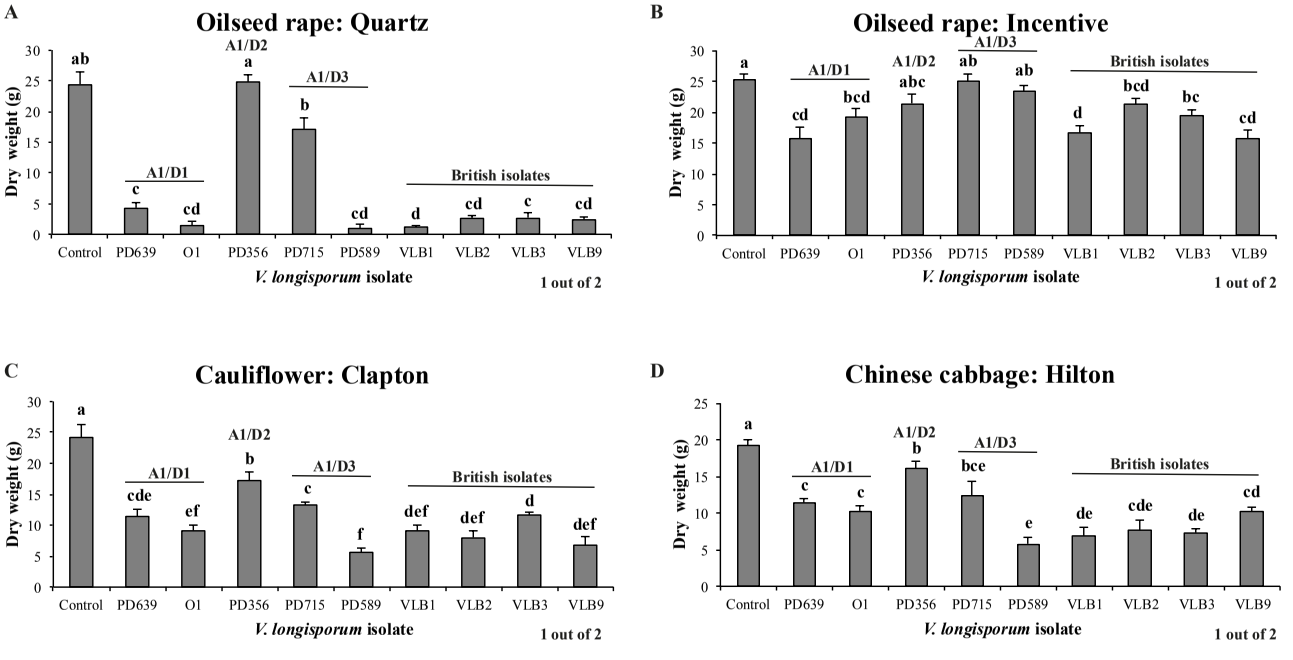

Figure 2 | Aerial plant biomass accumulation of various *Brassica* crops upon inoculation with *V. longisporum*. The bars indicate the median aboveground dry weight at 6 weeks after inoculation for the cultivars Quartz, Incentive, Clapton and Hilton: A, B, C and D, respectively. The figure represents one out of two experiments conducted. Every treatment consists of five pooled samples of three plants. Significance levels were calculated with the Mann-Whitney U-test ($p<0.05$). Error bars represent the standard error. Different letter labels indicate significant differences.

To determine to what extent the symptomatology correlates with the amount of *V. longisporum* biomass inside the plant, *V. longisporum* DNA was quantified inside the stems relative to the amount of plant DNA. Verticillium spp. are xylem colonizers, hence stem colonization is a good indication of strain aggressiveness. In correspondence with the observed disease symptoms, PD356 and PD715 were weak *Brassica* colonizers, as both strains were generally not detected in the stem, except for Hilton where PD715 was detected in four of the five samples (Figure 3). In contrast, all other *V. longisporum* isolates could be detected in most cases. In Quartz, PD589 was clearly the best colonizer, whereas the British and the A1/D1 strains were approximately present in equal levels (Figure 3A). The colonization of the detected isolates was negatively correlated with the aboveground biomass of Quartz plants (r = -0.6526, P = 2.148x10^{-5}). In Incentive, significant differences in the colonization of the pathogenic isolates were observed, although these were not significantly correlated to plant biomass (r = -0.2745, P = 0.1105) (Figure 3B). Intriguingly, although no significant biomass reduction was observed upon infection of PD589 on Incentive (Figure 2B), PD589 was able to colonize the stem to a similar extent as the A1/D1 strains. In Clapton, high differences in colonization of the same isolates were observed between biological replicates (Figure 3C). Similar to observations in Quartz, PD589 had the highest median colonization level, which was significantly higher than that of PD639 and VLB3. The fungal colonization of the detected isolates was also negatively correlated to the aboveground biomass of the cauliflower plants (r = -0.4793 P = 4,127 x10^{-3}). Hilton was the only *Brassica* cultivar with detection for PD715, however, no differences in colonization between the isolates were observed (Figure 3D). Similarly, PD715 was also detected in *Arabidopsis* for half of the inoculated plants and no significant differences in colonization were found between the treatments (Figure 4).

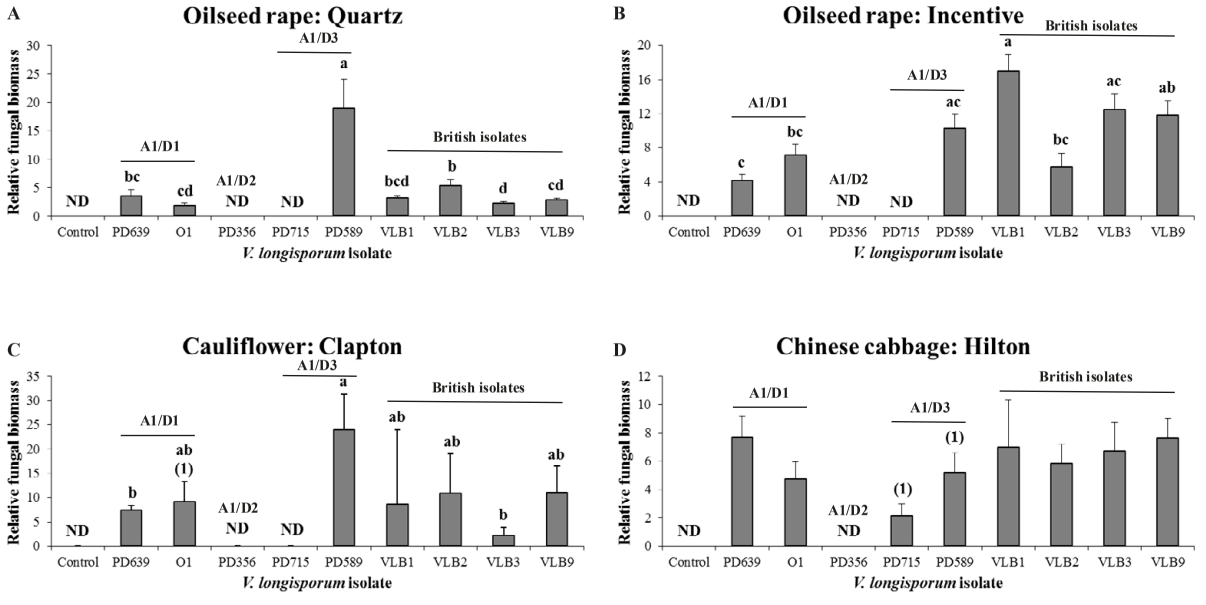

Figure 3 | Fungal biomass accumulation of various *V. longisporum* strains in plant stems. The bars indicate the median *V. longisporum* biomass relatively to the stem biomass. Isolates with no bar and ND in the graph were not detected in all 5 biological replicates. Significant differences were calculated with the Mann-Whitney U-test ($p<0.05$) and depicted by different letter labels. No significant differences in colonization between isolates were found in Chinese cabbage cultivar Hilton. The number between brackets gives the amount of samples without detection. No number is given if the fungal colonization in all replicates was detected. Error flags represent the standard error.

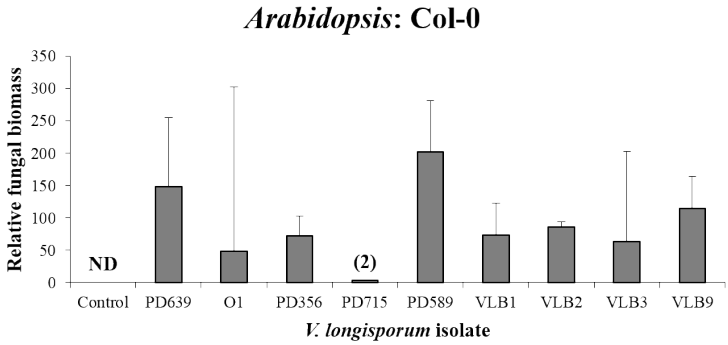

Figure 4 | Fungal biomass accumulation of various *V. longisporum* strains in *Arabidopsis* plants. The bars indicate the median *V. longisporum* biomass relative to plant biomass. Isolates with no bar and ND in the graph were not detected in all 5 biological replicates. No significant differences in colonization of the different isolates were found (Mann-Whitney U-test, $p<0.05$). The number between brackets gives the amount of samples without detection. No number is given if the fungal colonization in all replicates was detected. Error flags represent the standard error.

Discussion

The majority of emerging diseases originate from the introduction of pathogens in new geographic regions (Anderson *et al.*, 2004). However, the recent outbreak of Verticillium stem striping in the UK originates from a previously established population (Depotter *et al.*, 2017b). Similar to other newly emerging diseases, Verticillium stem striping is threatening for British oilseed rape, as the impact on yield is still relatively uncertain. In this study the pathogenicity of four British *V. longisporum* isolates from four different counties was compared with five previously characterized strains including strains from all *V. longisporum* lineages (Table 1). The British isolates were aggressive pathogens as they caused vascular discoloration and aerial biomass reduction, and were able to successfully colonize plant stem tissue (Figure 1-4). The disease level of British isolates resembled those of the other two A1/D1 isolates (PD639 and VLO1) as plant colonization caused significant vascular discoloration and yield reductions on all *Brassica* crops (Figure 1,2). This corresponds with a previous *V. longisporum* pathogenicity test that considered A1/D1 as the most virulent *V. longisporum* lineage on oilseed rape and cauliflower (Novakazi *et al.*, 2015). Thus, despite the genotypic differentiation, all A1/D1 West isolates (O1, VLB1, VLB2, VLB3, VLB9) induced similar disease responses as A1/D1 East reference strain PD639 (Depotter *et al.*, 2017b). However, further pathogenicity studies including more strains and host spp. are needed to confirm that this is a general pattern for the two populations.

The unification of A1/D1 as a lineage of aggressive pathogens is in sheer contrast with the disease symptoms caused by reference strains from lineages A1/D2 and A1/D3. Lineage A1/D2 has hitherto only been found on horseradish and causes the severest disease on this crop of all *V. longisporum* strains (Novakazi *et al.*, 2015; Yu *et al.*, 2016). Isolate PD356 is a relatively poor colonizer of *Brassica* crops and caused no to little disease symptoms (Figure 1-3). Thus, the lack of disease in *Brassica* crops indicates that lineage A1/D2 is rather specialized on horseradish. However, A1/D2 came out as the most virulent *V. longisporum* lineage on cabbage (*B. oleracea* convar. *capitata* var. *alba*, cv. Brunswijker) during pathogenicity tests of Novakazi *et al.* (2015) indicating that pathogenicity may vary within different varieties or crop sub-species. Previously, lineage A1/D3 was considered non-pathogenic on oilseed rape (Zeise and von Tiedemann, 2002). However, a recent pathogenicity study identified a highly virulent strain on oilseed rape within lineage A1/D3; isolate PD589 (Novakazi *et al.*, 2015). Accordingly, in this study lineage A1/D3 isolate PD715 was a weak pathogen on oilseed rape, whereas PD589 caused severe disease symptoms in Quartz (Figure 1,2). Intriguingly, the biomass reductions of PD589 in Quartz were in contrast to the symptoms on Incentive that, despite extensive stem colonization, tolerated infection by PD589 (Figure 1-3).

Virulence of *Verticillium* isolates is generally associated with successful host colonization (de Jonge *et al.*, 2013). For example, *V. dahliae* impaired in the production of effector proteins that are important for virulence colonizes its host plant to a lesser extent than the wild type strain. Accordingly, *V. longisporum* colonizes more susceptible oilseed rape cultivars more successfully than less susceptible cultivars (Knüfer *et al.*, 2017). In this study, the weak pathogens PD356 and PD715 were generally not detected in the host stem, which can explain the weak symptom development (Figure 1-3). Furthermore, the extent of colonization in the stem was negatively correlated with the aboveground biomass of the cultivars Quartz and Clapton. The correlation for Incentive was not significant and in Hilton no significant differences in fungal colonization were observed between isolates. The lack of correlation in Incentive may be caused by the lower biomass reduction upon infection. This can be due to higher resistance of Incentive to *V. longisporum* when compared with the other *Brassica* cultivars. However, the contribution of different environmental conditions to the different disease responses cannot be excluded, as pathogenicity tests were performed at different time points. Remarkably, although A1/D1 isolates and PD589 caused similar disease symptoms, PD589 clearly colonized Quartz plants better than A1/D1 isolates (Figure 2A, 3A). Moreover, PD589 colonized Incentive to a similar extent as A1/D1 isolates, but neither caused significant vascular discoloration nor plant biomass reduction (Figure 2B, 3B). Thus, fungal colonization may be a misleading indicator for virulence comparison, as hosts may tolerate particular pathogen strains better than others. Interspecific hybridization is an intrusive evolutionary mechanism as hybrid organisms experience a so-called "genomic shock" that incites major genomic rearranges and changes in gene

expression patterns (Doyle *et al.*, 2008). Conceivably, hybridization may have impacted the *V. longisporum* lineages differently, which may have led to different pathogenic features between lineages. However, more studies that investigate colonization patterns must be performed in order to relate colonization patterns with specific *V. longisporum* lineages more thoroughly.

Hybrid pathogens can have devastating outcomes on ecosystems. For example, the hybrid pathogen *Phytophthora xalni*, lead to an epidemic of alder decline in riparian ecosystems of Europe since the early 1990s (Brasier *et al.*, 1995). The hybrid fungus *V. longisporum* is currently gaining momentum as it is causing Verticillium stem striping in previously unaffected regions (CFIA, 2015; Gladders *et al.*, 2011). A decade since the first report of Verticillium stem striping in the UK, the extent to which this disease may contribute to losses in British oilseed rape is better understood. Although tested on a limited amount of isolates, yet adequately comprising the general genotypic diversity, the British *V. longisporum* population consists of strong pathogens that are as virulent as a previously characterized A1/D1 strain from oilseed rape. Given the similar climatic constraints, Verticillium stem striping is therefore expected to have similar outcomes as in countries where the disease was previously established such as Germany. However, the British *V. longisporum* population is genotypically more diverse than the ones in Germany and Swedish (Depotter *et al.*, 2017b). Conceivably, the heterogeneous character of the British populations may therefore hamper disease management strategies more. Nevertheless, these recent findings should be an incentive in oilseed rape breeding programs to select for Verticillium stem striping resistance, especially as protective or curative control by conventional fungicides is not possible for *Verticillium* diseases.

Acknowledgments

The authors would like to thank the Marie Curie Actions program of the European Commission that financially supports the research investigating the threat of *V. longisporum* to UK oilseed rape production. Work in the laboratory of B.P.H.J.T. is supported by the Research Council Earth and Life Sciences (ALW) of the Netherlands Organization of Scientific Research (NWO).

Supplementary material

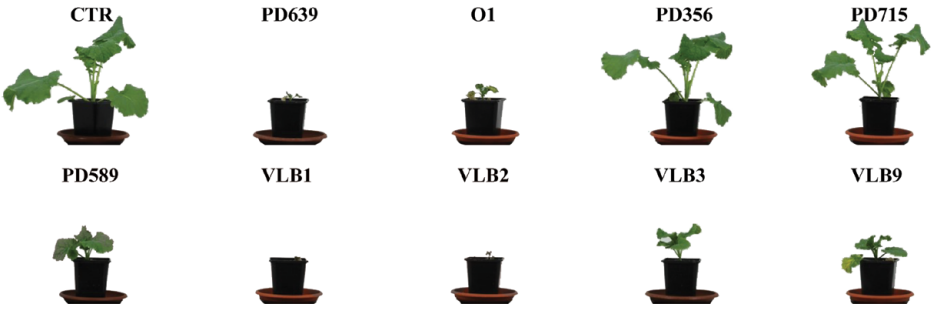

Figure S1 | Symptoms induced by *V. longisporum* on the oilseed rape cultivar Quartz at 3 weeks after inoculation. Two-week old seedlings were inoculated by root-dip inoculation with the following isolates: PD639, O1, PD356, PD715, PD589, VLB1, VLB2, VLB3 and VLB9.

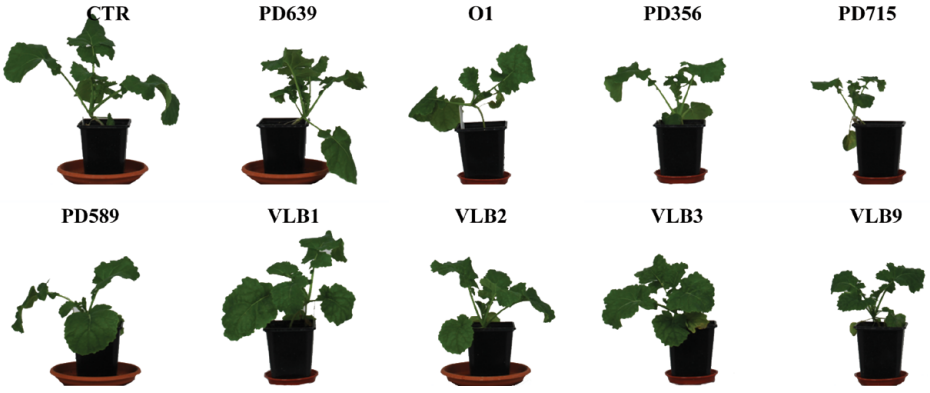

Figure S2 | Symptoms induced by *V. longisporum* on the oilseed rape cultivar Incentive at 3 weeks after inoculation. Two-week old seedlings were inoculated by root-dip inoculation with the following isolates: PD639, O1, PD356, PD715, PD589, VLB1, VLB2, VLB3 and VLB9.

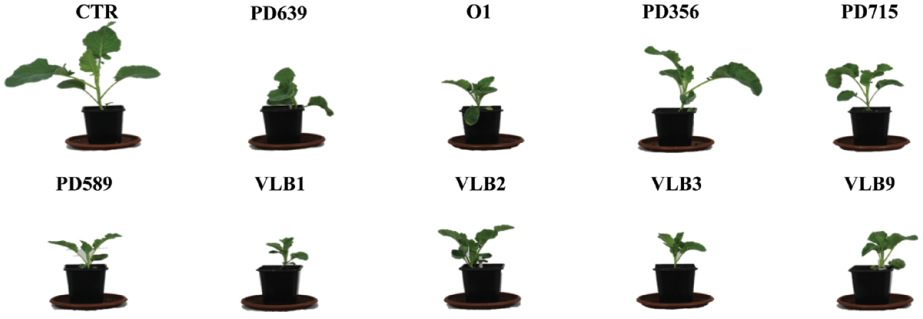

Figure S3 | Symptoms induced by *V. longisporum* on the cauliflower cultivar Clapton at 3 weeks after inoculation. Two-week old seedlings were inoculated by root-dip inoculation with the following isolates: PD639, O1, PD356, PD715, PD589, VLB1, VLB2, VLB3 and VLB9.

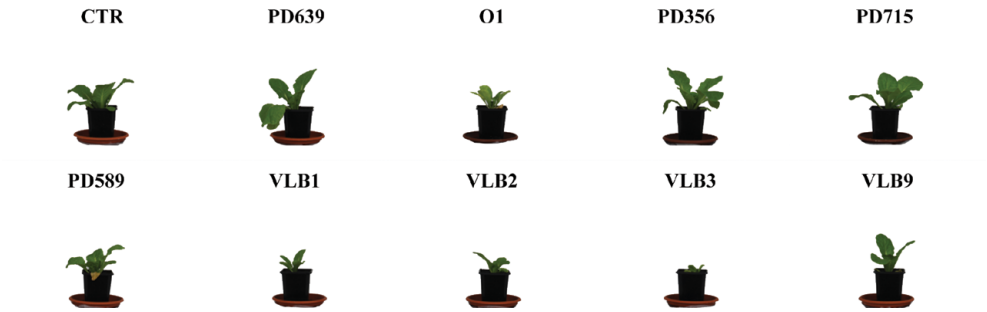

Figure S4 | Symptoms induced by *V. longisporum* on the Chinese cabbage cultivar Hilton at 3 weeks after inoculation. Two-week old seedlings were inoculated by root-dip inoculation with the following isolates: PD639, O1, PD356, PD715, PD589, VLB1, VLB2, VLB3 and VLB9.

Figure S5 | Symptoms induced by *V. longisporum* on *A. thaliana* (Col-0) at 3 weeks after inoculation. Two-week old seedlings were inoculated by root-dip inoculation with the following isolates: PD639, O1, PD356, PD715, PD589, VLB1, VLB2, VLB3 and VLB9.


5

Measuring the impact of *Verticillium longisporum* on oilseed rape (*Brassica napus*) yield in field trials in the United Kingdom

Jasper R.L. Depotter
Bart P.H.J. Thomma[†]
Thomas A. Wood[†]

[†]These authors contributed equally

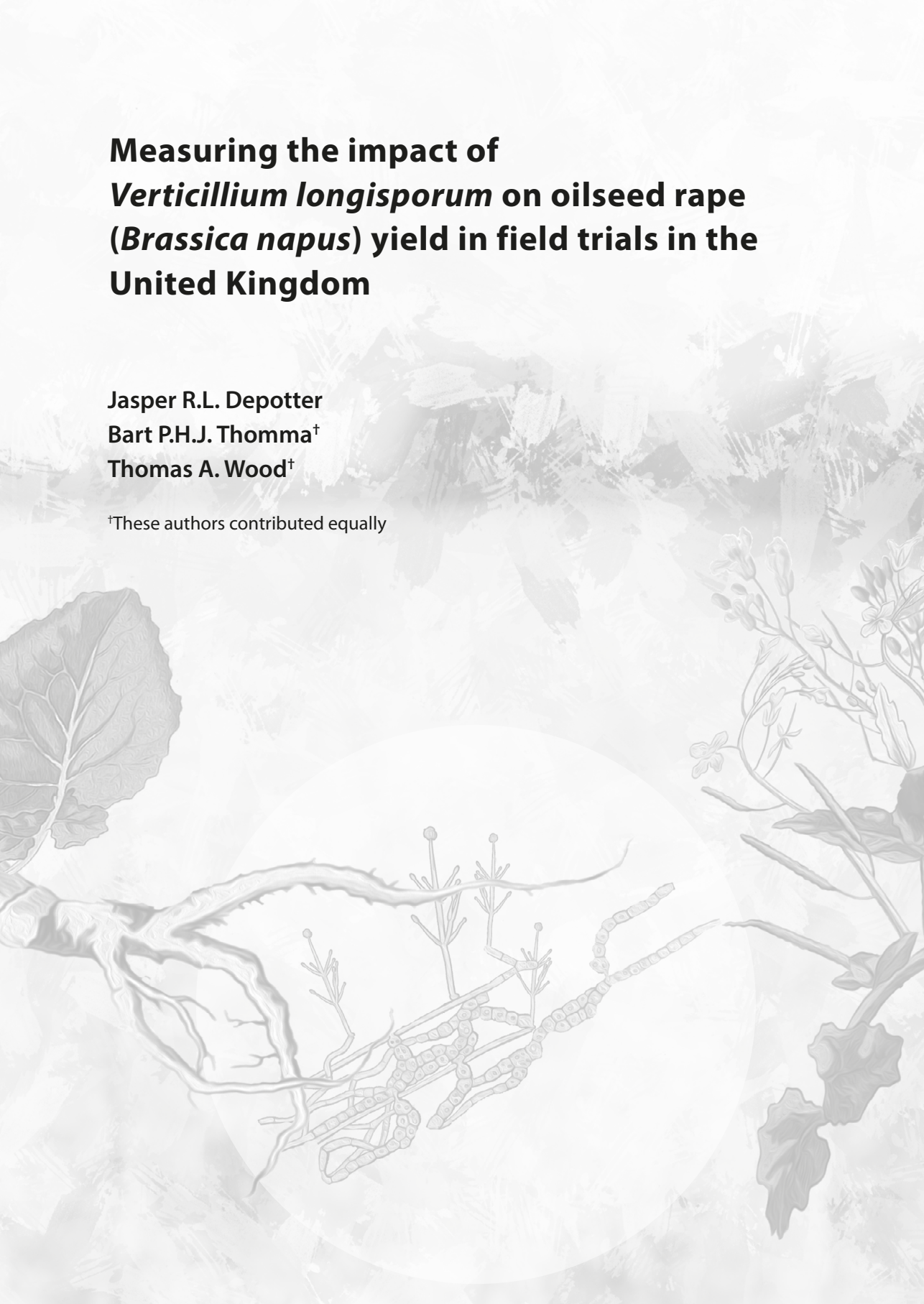

Abstract

Verticillium longisporum causes black stem striping on oilseed rape, which appears towards the end of the cropping season. Thus far, the impact of *V. longisporum* infection on oilseed yield remains unclear. In this study, we assessed the impact of Verticillium stem striping on British oilseed rape production. To this end, four cultivars (Incentive, Vision, Harper and Quartz) were grown in field plots with different levels of *V. longisporum* disease pressure at different locations over two consecutive years. Whereas Incentive and Vision developed relatively few stem striping symptoms, Harper and especially Quartz showed severe symptoms during these field experiments. Furthermore, higher inoculum levels induced more severe symptoms in these cultivars. Significant yield reductions upon *V. longisporum* infection only occurred in a single field trial on all tested oilseed rape cultivars. These preliminary data suggest that Verticillium stem striping does not consistently impact oilseed rape yield, despite the occurrence of abundant disease symptoms.

Verticillium stem striping is caused by the fungal pathogen *Verticillium longisporum*, one of the ten species of the *Verticillium* genus (Depotter *et al.*, 2016a; Inderbitzin *et al.*, 2011b). In contrast to other *Verticillium* spp., *V. longisporum* generally infects brassicaceous plants (Inderbitzin and Subbarao, 2014; Novakazi *et al.*, 2015; Zeise and von Tiedemann, 2002). On these hosts, *V. longisporum* causes wilting symptoms (Koike *et al.*, 1994). However, no wilting symptoms are observed on oilseed rape (Heale and Karapapa, 1999). Rather, dark unilateral striping is induced at the end of the cropping season before the onset of maturation, approximately 3-4 weeks before harvest. This coincides with the formation of black microsclerotia by the fungus in the stem cortex underneath the epidermis. Limited studies investigated the impact of Verticillium stem striping on crop quality and quantity (Dunker *et al.*, 2008). Yield losses by Verticillium stem striping have been anticipated to range from 10 to 50%, yet experimental verifications of such estimations are lacking (Dunker *et al.*, 2008). In contrast, Verticillium stem striping did not impact yield significantly in previous field studies despite the presence of stem striping symptoms (Dunker *et al.*, 2008).

To investigate the impact of Verticillium stem striping on oilseed rape production, we performed field experiments in two consecutive years at different locations in the United Kingdom (UK). In harvest year 2016, field plots were located in Hinxton, Cambridgeshire, UK, whereas in harvest year 2017 fields were situated in Higham, Suffolk, UK. Previously, winter oilseed rape cultivars were screened for their resistance against Verticillium stem striping under field conditions (not published). We selected four cultivars of this screen for our field experiments: two open-pollinated cultivars Vision and Quartz, and two hybrid types: Incentive and Harper. In the screen, Incentive and Vision displayed few symptoms, whereas Harper and Quartz displayed stem-striping symptoms abundantly. These differences in susceptibility were also confirmed by pathogenicity tests under controlled greenhouse conditions, where Quartz displayed more severe disease symptom development upon *V. longisporum* inoculation compared to Incentive (Depotter *et al.*, 2017a). To monitor putative dosage effects, plots were inoculated with different quantities of *V. longisporum* inoculum. To this end, a mix of British *Verticillium* strains were cultured in bags containing a sterile, moist medium of vermiculite (800 ml) and maize meal (26 g) for approximately four weeks and then dried at room temperature for a week prior to inoculation. The plots were either not inoculated, or inoculated by homogenously spreading 0.25 l or 2.5 l of thoroughly mixed, colonized vermiculite/maize meal medium. To enable homogenous dispersion, the 0.25 l of inoculum was first mixed with 0.75 l sand. Inoculations were performed the 16th of September 2015 for the field trial at Hinxton and the 26th of September 2016 for the trial at Higham. As four different cultivars and three different inoculum levels were tested in four replicates, the field trial comprised of 48 plots, which were arranged in a semi-randomized block design and were 24 m^2 (12 m x 2 m) in size. The field plots were sown the 5th and 21st September, and harvested on the 31th and 26th July for the field trials at Hinxton and Higham, respectively. To this end, a central strip of 18 m^2 was harvested using a combine and used for analysis.

We assessed the Verticillium stem striping disease symptoms by monitoring severity and incidence. Disease symptom severity was measured based on the fraction of stem circumference that displayed Verticillium stem striping symptoms. For every plot at each time point, 20 stems were randomly chosen and scored on a 0-10 scale, with each interval representing a 10% increase in dark unilateral striping of the stem circumference at knee-height (eg. score 2 = 20% striping). Disease incidence was the fraction of the stems containing disease symptoms with a minimal score of 1. The symptoms were scored four times each year starting from the end of June with a 7-day interval with the first assessment on 30th June and 27th June for year 2016 and 2017, respectively. In this way, area under disease progress curve (AUDPC) could be calculated by trapezoidal integration to compare disease severities over time (Shaner and Finney, 1977).

In correspondence to the unpublished cultivar screen, cultivars Incentive and Vision displayed equally few disease symptoms at the end of both cropping seasons (Table 1). Consequently, little to no progress in disease symptoms was monitored in both years (Figure 1). In contrast, Harper displayed more extensive disease symptoms in both consecutive trial years (Table 1). Altogether, disease symptom development was similar in harvest years 2016 and 2017 (Figure 1). Higher inoculum levels resulted in increasing incidence and symptom severity in Harper for the 2016 trial (Table 1). However, whereas disease levels of the inoculated plots were higher than in control plots, symptoms levels between the lower and higher inoculum treatments could not be distinguished in 2017 (Table 1). Furthermore, Quartz displayed the most severe disease symptoms of the four tested cultivars upon *V. longisporum* challenge (Table 1). The area under disease progress curves (AUDPCs) for the lower and higher inoculum treatments were similar for both years (Figure 1). Higher inoculum levels resulted in increasing incidence and symptom severity in Quartz for both cropping years (Table 1). Thus, in general, the symptom development of the four cultivars was consistent for the harvest years 2016 and 2017.

Table 1 | Impact of Verticillium stem striping on oilseed rape: disease symptoms, yield, and oil content. Data of disease incidence and symptom severity were assessed on 21 July and 18 July for year 2016 and 2017, respectively. Lower case letters indicate significant differences between treatments of the same cultivar in the same year, whereas capital letters indicate significant differences between cultivars of the same treatment in the same year. The treatment abbreviations "CTR", "LOW" and "HIGH", represent the data for plots were no, lower and higher amounts of *V. longisporum* inoculum were applied, respectively.

Cultivar	Treatment	Disease incidence (%)[a]						Disease symptom severity (0-10)[b]						Yield (ton/ha)[c]						Oil content (%)[d]			
		2016			2017			2016			2017			2016			2017			2016		2017	
Incentive	CTR	6.3	3.1	aA	3.8	2.4	aA	0	[0,0]	aA	0	[0,0]	abA	3.23	0.08	a	3.24	0.08	a	46.3	a	48.9	a
	LOW	10.0	2.0	aA	10.0	2.0	aA	0	[0,0]	abA	0	[0,0]	aA	3.03	0.12	ab	3.48	0.14	a	45.8	a	48.4	a
	HIGH	16.3	3.1	aA	22.5	5.2	bA	0	[0,0]	bA	0	[0,0]	bA	2.88	0.05	b	3.17	0.21	a	45.5	a	48.9	a
Vision	CTR	13.8	2.4	aAB	5.0	2.0	aA	0	[0,0]	aA	0	[0,0]	aA	3.17	0.06	a	3.08	0.08	a	44.8	a	46.9	a
	LOW	13.8	5.5	aA	15.0	4.1	aA	0	[0,0]	aA	0	[0,0]	bA	2.97	0.12	ab	2.76	0.11	a	43.6	a	47.4	a
	HIGH	27.5	4.8	aA	30.0	4.6	bA	0	[0,1]	bA	0	[0,2]	cA	2.74	0.09	b	3.13	0.18	a	44.3	a	47.6	a
Harper	CTR	25.0	6.1	aB	7.5	4.3	aA	0	[0,0]	aA	0	[0,0]	aA	3.30	0.04	a	3.73	0.10	a	45.6	a	49.3	a
	LOW	47.5	3.2	bB	48.8	6.6	bB	0	[0,7]	bB	0	[0,4]	bA	3.14	0.12	a	3.82	0.16	a	45.7	a	48.7	a
	HIGH	73.8	2.4	cB	60.0	4.1	bB	6	[0,9]	cB	2	[0,6]	bB	2.80	0.05	b	3.62	0.09	a	45.5	a	49.2	a
Quartz	CTR	27.5	4.3	aB	11.3	4.7	aA	0	[0,1]	aA	0	[0,0]	aA	3.40	0.09	a	3.38	0.09	a	46.2	a	48.8	a
	LOW	67.5	7.5	bB	55.0	9.8	bB	4	[0,8]	bC	3	[0,6]	bB	2.81	0.13	b	3.42	0.03	a	45.5	ab	48.5	a
	HIGH	85.0	4.6	bB	93.8	2.4	cC	9	[3,10]	cC	8	[5,10]	cC	2.23	0.12	c	3.06	0.15	a	44.5	b	48.5	a

[a] First column shows average disease incidence, second column standard error and third column statistical differences performed with ANOVA ($P<0.05$).

[b] First column shows median disease severity, second column the interquartile range and the third column statistical differences performed with Wilcoxon rank-sum test ($P < 0.05$).

[c] First column shows average yield standardised on 9% moisture content, second column standard error and the third column statistical differences performed with ANOVA ($P<0.05$).

[d] First column shows median oil content on dry matter basis and the second column statistical differences performed with a 5,000 bootstrap replications of median differences ($P<0.05$).

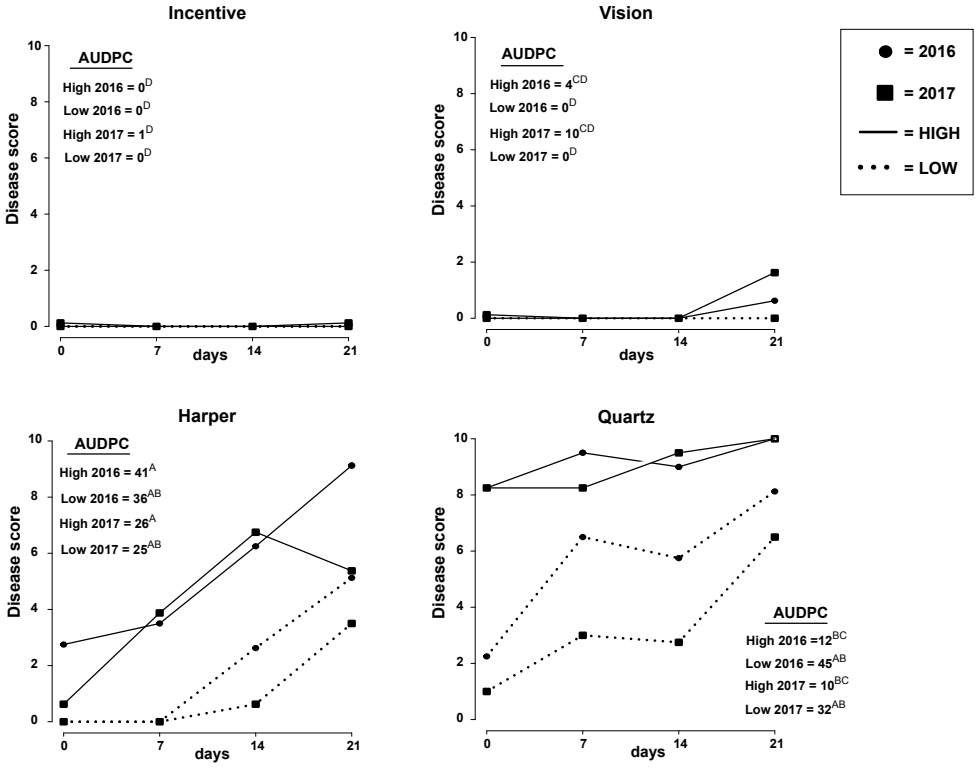

Figure 1 | Verticillium stem striping progression during the end of the cropping season. The Y-axis represents the median of the upper quartile plot disease score. The X-axis represents the number of days after the first scoring: 30th June and 27th June for harvest years 2016 and 2017, respectively. The area under progress disease curve (AUPDC) was calculated and letters present significance levels for all panels collectively calculated with 50,000 bootstrap replications of median differences (P<0.05).

In order to evaluate whether the different symptom development between cultivars corresponded with economically important crop parameters, seed yield and oil content were measured. To this end, yield of oilseed rape were adjusted to 9% moisture content and oil content of the seeds was determined by Nuclear Magnetic Resonance (NMR) spectroscopy (Benchtop NMR Analyser – MQC, Oxford Instruments, UK). Differences in oilseed rape cultivar and trial year impacted significantly on seed yield and oil content, whereas differences in the level of inoculum only impacted on yield and not oil content (Table 2). However, the impact of inoculum level was inconsistent between the two cropping years as significant differences in yield and oil content could only be found in the 2016 field trial (Table 1). In 2016, plots with the higher inoculum rate yielded significantly less than control plots for all tested oilseed rape cultivars. The highest yield impact was for Quartz that demonstrated a 34% reduction compared to the un-inoculated control, which is within the range of previously made estimates of 10 to 50% (Table 1) (Dunker *et al.*, 2008). Despite the presence of only mild disease

symptoms, the yield in 2016 was also significantly lower for Incentive (-11%) and Vision (-14%). The degree of yield reduction was similar for Harper (-15%), despite the observation that disease incidence and severity are significantly higher on this cultivar (Table 1). This indicates that stem striping is a poor indicator for predicting yield losses by *V. longisporum*. Yield for plots inoculated with the lower amount of inoculum only showed significant reduction for Quartz (-17%) while the other cultivars did not suffer from measurable yield losses (Table 1). Across all cultivars, the median disease symptom severity negatively correlated to yield (ρ = -0.53, P = 0.0001). Similarly, the average disease incidence also correlated negatively with yield (r = -0.57, P = 0). In contrast to the observations in 2016, the relationship between Verticillium stem striping symptoms and yield was different in the 2017 trial, since no significant differences between the different inoculum treatments were observed in yield for any of the cultivars assessed (Table 1). Verticillium stem striping symptoms, incidence (r = 0.05, P = 0.73) and severity (ρ = 0.09, P = 0.52) did not correlate with yield. Thus, although these data comprise only two cropping years, this indicates that the impact of *V. longisporum* is inconsistent despite the occurrence of abundant disease symptoms. This might be due to differences in host colonization patterns of *V. longisporum* between the two years (Siebold and von Tiedemann, 2013). Different weather conditions between the two years may have an effect on yield reduction by *V. longisporum*. Elevated temperatures can enhance the *V. longisporum* colonization on oilseed rape, however, this effect is not consistently observed (Siebold and von Tiedemann, 2013). Watering regimes were previously shown not to impact *V. longisporum* disease levels if grown under controlled greenhouse conditions (Lopisso *et al.*, 2017).

Table 2 | Analysis of variance for effects on seed yield and oil content. Multivariate ANOVA was used: Yield/Oil content ~ Cultivar + Year + Inoculum level + Repeat.

	Yield					Oil content				
	Df	**Sum Sq**	**Mean Sq**	***F*-value**	***P*-value**	**Df**	**Sum Sq**	**Mean Sq**	***F*-value**	***P*-value**
Main effects										
A: Cultivar	3	2.53	0.84	10.19	8.28×10^{-6}	3	33.81	11.27	16.21	1.95×10^{-8}
B: Year	1	2.93	2.93	35.39	5.66×10^{-8}	1	253.27	253.27	364.32	$< 2 \times 10^{-16}$
C: Inoculum	2	2.14	1.07	12.94	1.22×10^{-5}	2	1.19	0.60	0.86	0.43
D: Repeat	3	0.38	0.13	1.55	0.21	3	9.59	3.19	4.58	5.02×10^{-3}
Residuals	86	7.12	0.08			86	59.79	0.70		

The significant yield impact in harvest year 2016 showed that *V. longisporum* pathogen can be of economic significance in oilseed rape production. However, our inability to reproduce these yield reductions and the absence of significant oilseed rape yield reductions in a previous study indicate that significant yield reductions upon *V. longisporum* field inoculation only sporadically occur. As this study only

comprises data from two consecutive cropping years, more field studies are needed to have a general assessment of the economic importance of Verticillium stem striping. Furthermore, weather data in combination with fungal colonization patterns should also be integrated in further studies to investigate the impact of the environment on yield reduction outcomes. The collection of yield data instead of striping symptoms in field trials would lead to a more genuine assessment of Verticillium stem striping resistance in oilseed rape cultivars, as we observed that striping symptoms can be untruthful predictors of final yielding outcomes.

Acknowledgements

The authors would like to thank the Marie Curie Actions program of the European Commission that financially supports the research of J.R.L.D. Work in the laboratory of B.P.H.J.T. is supported by the Research Council Earth and Life Sciences (ALW) of the Netherlands Organization of Scientific Research (NWO).

6

Interspecific hybridization impacts host range and pathogenicity of filamentous microbes

Jasper R.L. Depotter
Michael F. Seidl
Thomas A. Wood
Bart P.H.J. Thomma

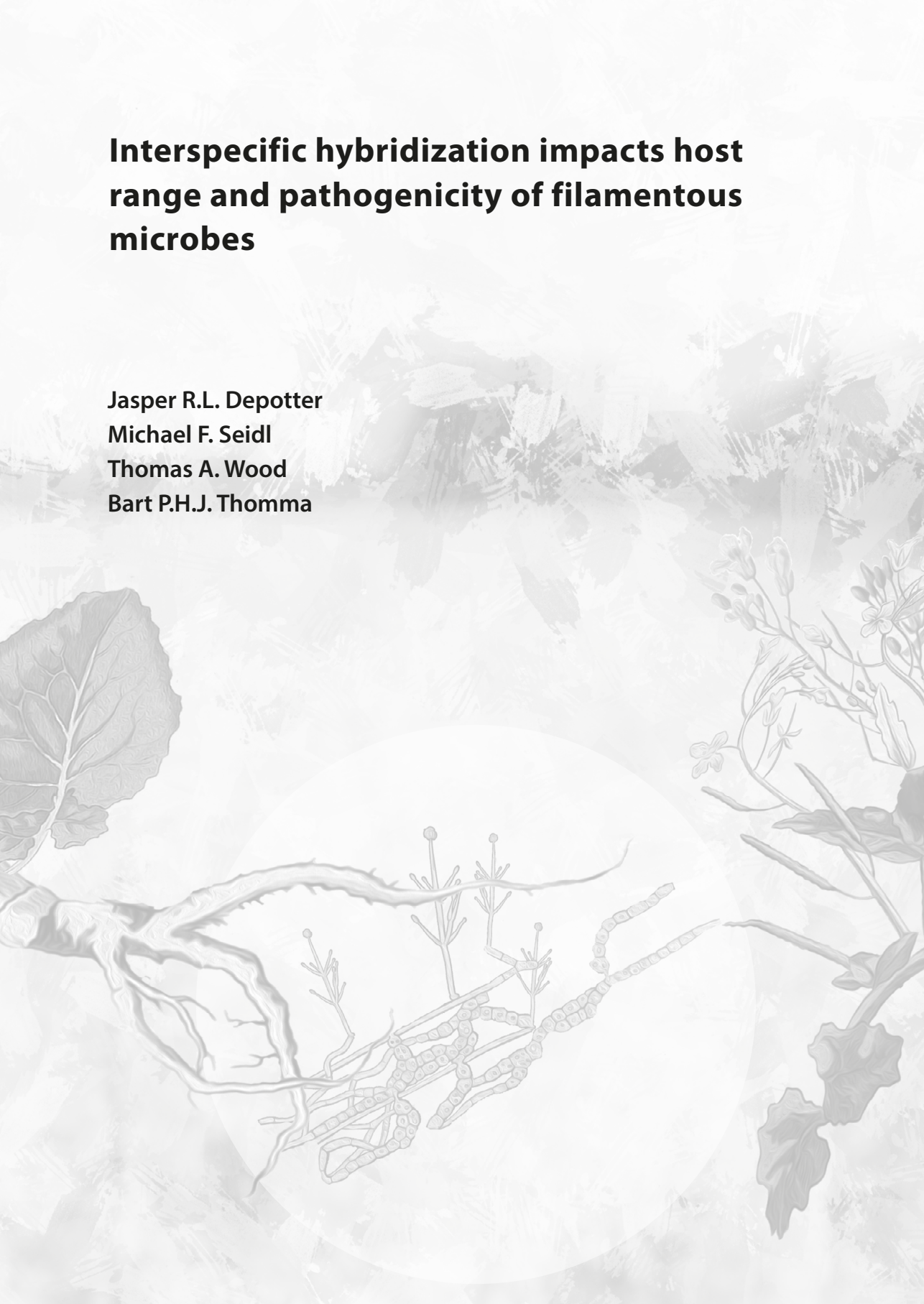

Abstract

Interspecific hybridization is widely observed within diverse eukaryotic taxa, and is considered an important driver for genome evolution. As hybridization fuels genomic and transcriptional alterations, hybrids are adept to respond to environmental changes or to invade novel niches. This may be particularly relevant for organisms that establish symbiotic relationships with host organisms, such as mutualistic symbionts, endophytes and pathogens. The latter group is especially well-known for engaging in everlasting arms races with their hosts. Illustrated by the increased identification of hybrid pathogens with altered virulence or host ranges when compared with their parental lineages, it appears that hybridization is a strong driver for pathogen evolution, and may thus significantly impact agriculture and natural ecosystems.

Introduction

Genomes continuously evolve through mechanisms such as mutation, recombination, duplication and uptake of novel DNA upon horizontal gene transfer (HGT). Such plasticity allows organisms to adapt to environmental changes, which is considered particularly important for microbial pathogens that engage in arms races with hosts for continued symbiosis (Cook *et al.*, 2015). As a consequence, many pathogens have evolved two-speed genomes with genomic regions implicated in pathogenicity displaying accelerated evolution (Croll and McDonald, 2012; Raffaele and Kamoun, 2012). Interspecific hybridization often concerns two species within the same genus, and is considered an important driver for genome evolution. Hybridizations have been widely observed within various eukaryotic taxa such as plants, insects, birds, mammals and fungi (Mallet, 2005; Morales and Dujon, 2012), and since the 1990s various interspecific hybrids of filamentous plant pathogens have been described (Table 1). In this review we discuss the impact of interspecific hybridization on the pathogenicity of filamentous microbes.

Hybridization mechanisms

Hybrids may originate from parasexual reproduction, a nonsexual process thought to occur widely in fungi for transferring genetic material without development of sexual structures or meiosis. Parasexual reproduction typically involves hyphal fusion of two strains, followed by nuclear fusion, mitotic recombination and chromosome loss to restore the parental ploidy state (Karapapa *et al.*, 1997). Consequently, interspecific hybrids may originate from nuclear fusion without subsequent immediate chromosome loss (Inderbitzin *et al.*, 2011b). However, interspecific hybridization can also occur through sexual reproduction, when gametes of different species fuse into a viable zygote. For example, hybrids between the sexually compatible causal agents of anther smut disease of different weeds, *Microbotryum lychnidis-dioicae* and *Microbotryum silenes-dioicae*, are regularly found in nature (Gladieux *et al.*, 2011; Refrégier *et al.*, 2010).

Hybridization results in allopolyploidy when the ploidy of hybrids increases with respect to that of the normal ploidy of the parental species (Figure 1). Nevertheless, the hybridization is generally followed by loss of genetic material due to the incompatibility of genes or the discard of genomic ballast, eventually leading to the original ploidy status (Bertier *et al.*, 2013). The resulting hybrids are therefore considered stable or transient according to the conservation of parental chromosome sets over time (Figure 1). However, during homoploid hybridization, for instance upon hybridization of the haploid gametes of two diploid species, chromosome numbers do not change. For such a hybrid to be viable, the parental chromosomes need to be very similar, and thus the parents closely related, to allow proper mitosis in the offspring (Ferree and Prasad, 2012). Consequently, homoploid hybrids are often only weakly reproductively isolated from their parents

(Mallet, 2007), which may contribute to reversion of homoploid hybrids to their original parental genomes and making the hybrid phase transient. Ultimately, this may lead to the transfer of genetic material between hybridized lineages, leading to introgression of DNA of one parent into the other parent's genome.

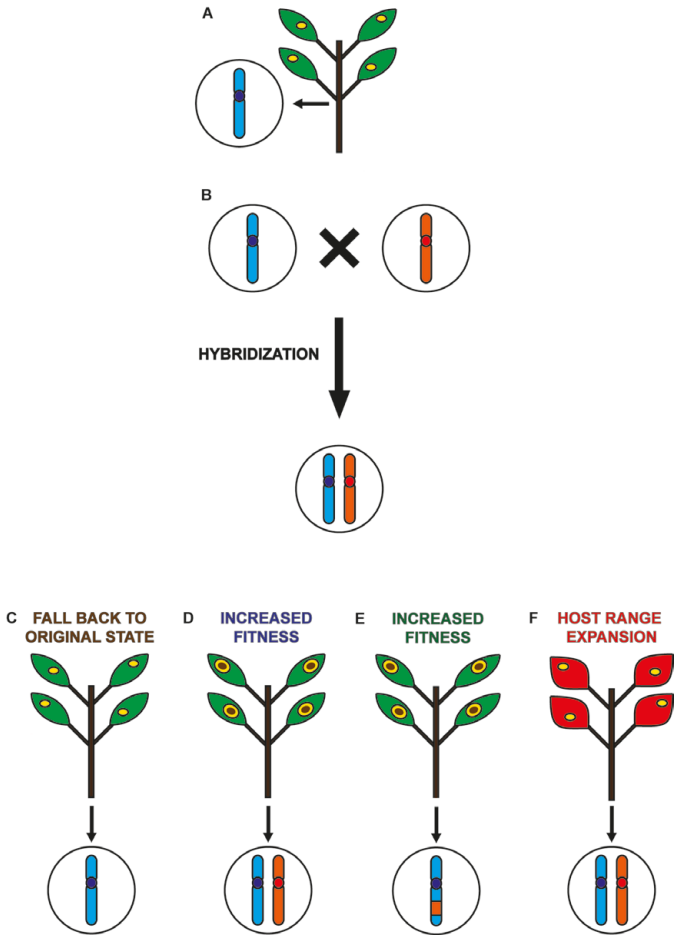

Figure 1 | Evolutionary fate of hybrid pathogen genomes. One of the parental lineages (illustrated as a blue chromosome) causes disease on a particular host plant (**A**). Another, somewhat related, species (illustrated as an orange chromosome) co-occurs in a particular niche, makes physical contact and hybridizes, resulting in a lineage with the cumulative amount of chromosomes (**B**). Hybridizations with disadvantageous outcomes are evolutionary dead ends. These hybrids are not viable or evolve back to their original genomic state by extensive gene loss (**C**). Alternatively, plasticity of the hybrid genome enables that hybrids eventually evolve towards three extreme outcomes. Potentially, the combination of the two parental genomes leads to increased fitness on the original host and the hybrid is able to establish as a stable entity (**D**). Ultimately, this may even lead to displacement of the parental lineage that may consequently even go extinct. Increased aggressiveness may still be accompanied by extensive DNA loss, leading to hybrid pathogen reversion to the original ploidy status while maintaining a proportion of particularly beneficial genetic material (**E**). In some cases, the hybrid gains the capacity to colonize alternative hosts, leading to host range expansion (**F**). Ultimately, this may lead to adaptation on a novel host.

Table 1 | Examples of naturally occurring interspecific hybrid pathogens.

	Hybrid species taxon[1]	Division	Parental species 1	Parental species 2	Reported host genera	Refs
Ascomycota						
Botrytis	*B. allii*		*B. aclada*	*B. byssoidea*	*Allium*	(Staats *et al.*, 2005; Yohalem *et al.*, 2003)
Ophiostoma			*O. novo-ulmi*	*O. ulmi*	*Ulmus*	(Brasier, 2001)
Verticillium	*V. longisporum*	Lineage A1/D1	A1[2]	D1[2]	*Beta, Brassica*, & *Raphanus*	(Inderbitzin *et al.*, 2011b)
		Lineage A1/D2	A1[2]	*V. dahliae*	*Armoracia*	(Inderbitzin *et al.*, 2011b)
		Lineage A1/D3	A1[2]	*V. dahliae*	*Armoracia & Brassica*	(Inderbitzin *et al.*, 2011b)
Basidiomycota						
Cryptococcus			*C. gattii*	*C. neoformans*	*Homo*	(Aminnejad *et al.*, 2012; Bovers *et al.*, 2006)
Melampsora	*M.* xcolumbiana		*M. medusae*	*M. occidentalis*	*Populus*	(Newcombe *et al.*, 2000, 2001)
	M. medusae-populina		*M. medusae*	*M. larici-populina*	*Populus*	(Spiers and Hopcroft, 1994)
Microbotryum			*M. lychnidis-dioicae*	*M. silene-dioicae*	*Silene*	(Gladieux *et al.*, 2011)
Heterobasidion			*H. annosum*	*H. irregulare*	*Pinus*	(Gonthier *et al.*, 2007)
			H. irregulare	*H. occidentale*	*Juniperus*, *Pinus* & *Larix*	(Garbelotto *et al.*, 1996; Lockman *et al.*, 2014)
Oomycota						
Phytophthora	*P. andina*		*P. infestans*	Unknown	*Brugmansia* & *Solanum*	(Goss *et al.*, 2011; Oliva *et al.*, 2010)
	P. xalni		*P.* xmultiformis	*P. uniformis*	*Alnus*	(Husson *et al.*, 2015)
	P. xmultiformis		*Pm1*[2]	*Pm2*[2]	*Alnus*	(Husson *et al.*, 2015)
	P. xpelgrandis		*P. cactorum*	*P. nicotianae*	*Eriobotrya, Spathiphyllum, Pelargonium* & *Primula*	(Hurtado-Gonzales *et al.*, 2009; Man in 't Veld *et al.*, 1998; Nirenberg *et al.*, 2009)
	P. xserendipita		*P. cactorum*	*P. hedraiandra*	*Allium, Dicentra, Idesia, Penstemon, Kalmia* & *Rhododendron*	(Man in 't Veld *et al.*, 2007, 2012)
			P. porri	*P.* taxon parsley	*Allium, Chrysanthemum, Parthenium* & *Pastinaca*	(Bertier *et al.*, 2013)
Pythium			*P. phragmitis*	*P. phragmiticola*	*Phragmites*	(Nechwatal and Lebecka, 2013; Nechwatal and Mendgen, 2009)

[1] Only mentioned if a designated taxon has been provided to the hybrid.
[2] Provisional name for hitherto unknown parental species.

Genomic and transcriptomic consequences of hybridization

Gene flow from closely related species through hybridization is a saltational, fast mean of genome evolution (Stukenbrock, 2016a). Allopolyploidy as a result from hybridization generally leads to chromosomal doubling, thereby inciting major genomic and transcriptomic reorganization also known as genome and transcriptome shock, respectively (Figure 2). In the early stages of allopolyploid evolution, most genes are present in two copies (homeologs), one derived from each parental genome with its own transcriptional regulation. In plant and fungal hybrids, the transcriptional response upon hybridization is often conservative (Cox *et al.*, 2014; Yoo *et al.*, 2013). For instance, in the fungal grass endophyte *Epichloë* polyploid Lp1, an economically important allopolyploid derived from interspecific hybridization between the sexual species *E. typhina* and the asexual relative *Neotyphodium lolii*, over half of the homeologs retained the parental gene expression patterns (Cox *et al.*, 2014). Moreover, if genes were differentially expressed in the parental lineages the difference was often lost in the hybrid, and the vast majority of genes with differential parental expression displayed signs of expression-level dominance, whereby the total homeolog expression level is similar to one of the parents (Cox *et al.*, 2014). While in relatively recently evolved allopolyploids such as *Epichloë* Lp1 gene loss is only observed at low frequency, gene loss is one of the major patterns over longer evolutionary time frames (Figure 2). Arguably, extensive gene loss and close synteny between duplicated gene regions can mask ancestral processes that played a role in genome evolution. For instance, allopolyploidy was recently revealed to be causative to the whole-genome duplication (WGD) in the baker's yeast *Saccharomyces cerevisiae* that had been initially ascribed to doubling of its ancestor DNA (Marcet-Houben and Gabaldón, 2015). Subsequently, *S. cerevisiae* underwent extensive genomic rearrangements and gene loss, eventually resulting in retaining of only ~15% of the duplicated genes (Gordon *et al.*, 2009; Seoighe and Wolfe, 1998; Wong *et al.*, 2002). In fungi and plants, retained genes often functionally diverge, e.g. by increasing differences in gene expression patterns, leading to neo-functionalization when one copy retains the original function while the other copy acquires a novel function, or sub-functionalization when both copies partition the original gene function (Blanc and Wolfe, 2004; Gu *et al.*, 2002).

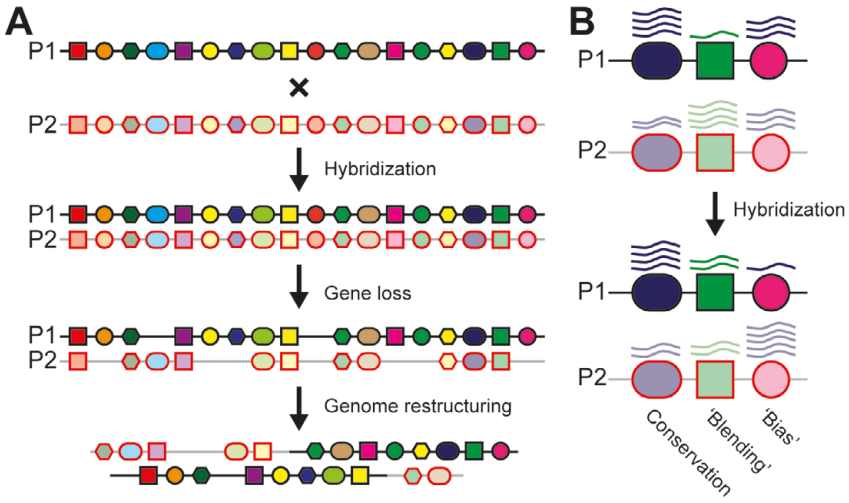

Figure 2 | Potential genomic and transcriptomic consequences of allopolyploidy. (A) Hybridization of two parental genomes (P1 and P2, of which genes (different shapes) are indicated by dark and light colors, respectively), initially leads to two copies for each gene (homeologs) in the hybrid. Over longer evolutionary timescales, gene loss in the hybrid is a major evolutionary pattern that, together with genomic rearrangements, ultimately leads to genomic restructuring. (B) Transcriptional responses in the hybrid lineage when compared with its parental lineages. Expression patterns in the hybrid are often either directly inherited from the parents ('expression conservation') or, if differentially expressed in the parents, expression differences are lost ('expression blending'). Alternatively, if not differentially expressed in the parents, genes in the hybrid display an expression pattern that differs from the pattern observed in the parental lineages ('expression bias').

Hybrid emergence

Although hybridization most frequently occurs between species with a close relationship (Mallet, 2007), it remains a rare phenomenon as closely related species typically evolved barriers to prevent crossing, especially if they evolved in the same geographical area (Brasier, 2000). However, allopatric species that evolved in isolation or in different geographic regions often display less stringent reproductive barriers. It is therefore not surprising that novel hybrid pathogens have often been associated with microbial introductions in new geographical areas. For example, hybrids between two allopatric species of the *Heterobasidion* genus that harbours economically important pathogens of Northern Hemisphere conifer forests, the European *H. annosum* and the American *H. irregulare*, emerged in Italy upon the movement of US troops in Europe during World War II (Garbelotto and Gonthier, 2013; Gonthier *et al.*, 2004). Arguably, increased globalization, trade and traffic promote contact between geographically separated microbial species, therefore enhancing opportunities for hybridization events (Callaghan and Guest, 2015).

Even in the absence of crossing barriers, mating in many fungi (and thus also hybridization) only occurs under very particular, often enigmatic conditions. This is illustrated by the recent discovery of the outbreeding behavior of *S. cerevisiae*, a well-studied model organism of which the reproduction ecology remained largely obscure. Intriguingly, intestines of the social wasp *Polistes dominula* were found to host highly outbred *S. cerevisiae* strains as well as a rare hybrid of *S. cerevisiae* with *S. paradoxus*, the latter of which cannot survive solitarily in wasp intestines and needs to be rescued through interspecific hybridization (Stefanini *et al.*, 2016). Similarly, the occurrence of mosaic *Albugo candida* genomes with intermixed genetic material of different races, remained puzzling as these races are obligate biotrophic parasites on distinct brassicaceous hosts (McMullan *et al.*, 2015). However, infecting sequentially, different races were recently found to be able to colonize the same host, as host-adapted races pave the way for the subsequent colonization by normally avirulent strains. Conceivably, hybrids between *A. candida* strains can arise during such co-colonisations (McMullan *et al.*, 2015).

As hybridization has an enormous impact on pathogen genome characteristics, illustrated by genome and transcriptome shocks (Figure 2), host species may take a relatively long time to intercept hybrid pathogens, sometimes leading to the rapid expansion of emerging hybrid pathogens and resulting in epidemic outbreaks. For example, hybridization is thought to have played a pivotal role in the second Dutch elm disease epidemic that started in the early 1970s in Europe (Brasier, 2001). Hybrids between *Ophiostoma novo-ulmi* and *Ophiostoma ulmi* are thought to have formed a genetic bridge between the two species (Brasier *et al.*, 1998), mediating interspecific gene flow and allowing *O. novo-ulmi* to outcompete *O. ulmi* in Europe eventually (Brasier, 2001). In addition, rapidly expanding hybrids between eastern European and North American *O. novo-ulmi* subspecies *novo-ulmi* and *americana*, respectively, emerged during the geographical overlap of both subspecies during this epidemic (Brasier and Kirk, 2010). The introduced genetic heterogeneity between subspecies may have facilitated the epidemic proliferation of *O. novo-ulmi* even more.

Hybrids need to be fitter towards a given niche than their parental lineages in order to sustain themselves on the same host (Figure 1). For example, the main causal agent of alder decline, *Phytophthora xalni*, is the progeny from hybridization between the generally less aggressive parental lineages *P. xmultiformis* and *P. uniformis* (Brasier and Kirk, 2001; Husson *et al.*, 2015). However, if the increase in fitness is too significant, hybrids may completely outcompete and replace their parental lineages on a particular host, which could eventually lead to the extinction of particular parental lineages (Mallet, 1995). This may be a plausible explanation for unfound parental lineages underlying numerous hybridization events (Bertier *et al.*, 2013; Goss *et al.*, 2011; Inderbitzin *et al.*, 2011b). This is the case for the interspecific hybrid causal agent of stem striping on oilseed rape, *Verticillium longisporum* (Depotter *et al.*, 2016a; Inderbitzin *et al.*, 2011b). This species originates from at least three separate hybridization events

involving three different parental *Verticillium* lineages. One of these lineages has been identified as *V. dahliae*, a species that shows remarkable genomic plasticity (Faino *et al.*, 2015; de Jonge *et al.*, 2013), whereas the two remaining lineages have hitherto not been found. *V. longisporum* is highly adapted to brassicaceous hosts, whereas *V. dahliae* does generally not colonize these plants (Depotter *et al.*, 2016a). Arguably, the unknown *V. longisporum* parents were Brassicaceae-specific pathogens that were outcompeted by the *V. longisporum* hybrid.

Probably the best illustrated example of genome evolution and the impact of hybridization on host range stems from the *Zymoseptoria* genus. *Z. pseudotritici* and *Z. tritici* diverged from the last common ancestor with the domestication of wheat in the Middle East, approximately 10,000 years ago (Stukenbrock *et al.*, 2007). Whereas the wheat-adapted *Z. tritici* spread globally presumably with its host, *Z. pseudotritici* only occurs in the Middle East on various wild grass species. Intriguingly, the genome composition of *Z. pseudotritici* is consistent with a hybridization event that occurred less than 400 sexual generations ago, likely within the last five centuries, due to a sexual cross between two related haploid individuals that both diverged from the *Z. tritici* lineage (Stukenbrock *et al.*, 2012). Similar to *V. longisporum*, the parental species of *Z. pseudotritici* have never been collected, suggesting that they occur on different hosts to the hybrid or got outcompeted (Stukenbrock, 2016b). Thus, hybridization led to the emergence of a unique pathogenic species.

Pathogens on novel hosts through hybridization

As hybridization allows organisms to acquire novel traits to colonise new niches, it may even allow colonization of novel hosts (Figure 1). In the 1960s, a hybrid crop between wheat and rye called triticale was introduced in agriculture. Although initially immune to powdery mildew disease, infections on triticale were reported since the 2000s. It was recently determined that the causal agent, *Blumeria graminis* f.sp. *triticale*, arose upon hybridization of two subspecies of the powdery mildew fungus *B. graminis* that are adapted to wheat and rye, respectively (Menardo *et al.*, 2016). Intriguingly, the mosaic genome of *B. graminis* f.sp. *triticale* was determined to have evolved only within the last 50 years, suggesting that it arose on the novel crop.

Introgression of the apple scab resistance gene *Rvi6* from the wild apple *Malus floribunda* into domestic *Malus* x*domestica* cultivars permitted the invasion of a virulent population of the apple scab pathogen *Venturia inaequalis* into apple orchards, bringing together environmental and agricultural pathogen lineages that diverged in allopatry several thousand years ago (Lemaire *et al.*, 2016). Presently, the *Rvi6* resistance in orchards is overcome by virulent *V. inaequalis* lineages with heterogeneous genomes, indicating a high amount of gene flow between the two allopatric populations due to mating on the common host (Leroy *et al.*, 2016). Thus, the introduction of *Rvi6* resistance in apple seventy years ago led to the transfer of virulence from a non-agricultural pathogen

population into agriculturally relevant pathogen populations showing that, similar to the previous example, modern agricultural practices may generate novel pathogen lineages.

Although the previous examples concern intraspecific hybrids, similar shifts in host range are observed for interspecific hybrids. For example, a hybrid between *Phytophthora cactorum* and *Phytophthora hedraiandra*, called *Phytophthora* x*serendipita*, infects monocot (*Allium*) and dicot (*Idesia* and *Penstemon*) hosts outside the host range of its parents (Man in 't Veld *et al.*, 2007). Similarly, hybrids between the leek and parsley pathogens *P. porri* and *P.* taxon parsley, respectively, expanded their host range with species from the genera *Pastinaca*, *Chrysanthemum* and *Parthenium* (Bertier *et al.*, 2013). Hypothetically, observations of hybrid host range shifts may result from their capacity to invade novel niches (hosts), while they failed to compete with their parental lineages on the traditional host.

More extremely, hybridization of two non-pathogenic lineages may even result into the generation of a novel pathogen. This was recently demonstrated for the opportunistic pathogenic yeast *Candida metapsilosis* where a single hybridization event of two non-pathogenic ancestor lineages resulted in a highly heterozygous species. Presently, *C. metapsilosis* reached worldwide distribution as an emerging pathogen of immunocompromised patients (Pryszcz *et al.*, 2015).

Conclusions

Interspecific hybridization appears to be a successful evolutionary strategy whereby the combination of two dissimilar genomes promotes diversification in a saltational manner, leading to novel (combinations of) traits, including those relevant to pathogenicity. Particularly successful hybridization events may generate hybrid pathogens that are particularly fit in a given niche, and thus have far-reaching effects on agricultural crops or natural ecosystems. Considering that interspecific hybridization was recently revealed to be causative to the WGD in *S. cerevisiae* that had been initially ascribed to doubling of its ancestor DNA (Marcet-Houben and Gabaldón, 2015), the occurrence of interspecific hybridization may currently be underestimated. Additionally, the number of hybridization events resulting in novel pathogen lineages is expected to increase due to the increased globalization, travel and trade, as well as agricultural practices such as large acreages of monocultures and hybrid crops, mediating physical contact between geographically separated organisms. Clearly, interspecific hybridization events do not only impact plant pathogenicity, but may affect pathogens of any organism. In addition to the previously mentioned example of *Candida metapsilosis*, the yeast hybrid that is an emerging pathogen of immunocompromised patients, also interspecific hybrids between *Cryptococcus neoformans* and *C. gattii*, both causal agents of pulmonary cryptococcosis and meningitis in various animals, have been reported to occur in humans (Bovers *et al.*, 2006).

Acknowledgements

J.R.L. Depotter is supported by the Marie Curie Actions program of the European Commission. Work in the laboratory of B.P.H.J.T. is supported by the Research Council Earth and Life Sciences (ALW) of the Netherlands Organization of Scientific Research (NWO). M.F.S. acknowledges receipt of a VENI grant of ALW-NWO. The funders had no involvement in the writing or submission of this review. The authors would like to thank Drs. Melvin Bolton, David Cook and Toni Gabaldón for their critical review and useful suggestions.

7

Genomic and transcriptomic plasticity in the allodiploid fungal plant pathogen *Verticillium longisporum*

Jasper R.L. Depotter
Fabian van Beveren[†]
Luis Rodriguez-Moreno[†]
Grardy C.M. van den Berg
Thomas A. Wood
Bart P.H.J. Thomma
Michael F. Seidl

[†]These authors contributed equally

Abstract

Allopolyploidization, genome duplication through interspecific hybridization, is an important evolutionary mechanism that can enable organisms to adapt to environmental changes or stresses. The increased adaptive potential of allopolyploids can be particularly relevant for plant pathogens in their ongoing quest for host immune response evasion. The allodiploidization that lead to the emergence of the fungal plant pathogen *Verticillium longisporum* has been associated with a host range shift, as *V. longisporum* mainly infects Brassicaceae plants in contrast to haploid *Verticillium* spp. that do not typically infect hosts from this plant family. Here, we investigated the impact of allodiploidization on genome and transcriptome plasticity in *V. longisporum*. Genome evolution of *V. longisporum* is characterized by extensive chromosomal rearrangements, both between as well as within parental chromosome sets, leading to a mosaic genome structure. In comparison to haploid *Verticillium* spp., *V. longisporum* genes encounter more non-synonymous substitutions and display more frequent signs of positive selection. Intriguingly, the expression patterns of the two *V. longisporum* sub-genomes show remarkable resemblance and, in particular, expression levels of genes encoding secreted proteins homogenize upon plant colonization. Collectively, our results illustrate the large adaptive potential of *V. longisporum* mediated by its genomic plasticity and interaction between the sub-genomes, which may have facilitated the host range shift.

Introduction

Cycles of polyploidization are hallmarks of eukaryotic genome evolution, where an initial increase of ploidy is commonly followed by reversions to original ploidy states (Wolfe, 2001). For instance, all angiosperm plants share two rounds of ancient polyploidy (Jiao *et al.*, 2011). The prevalence of polyploidy events in eukaryotic evolution is likely due to the high evolutionary potential of polyploids, as additional chromosome sets give leeway to functional diversification (Van de Peer *et al.*, 2017). Consequently, polyploidy events are often followed by adaptive radiation and are dated near the base of species-rich clades in phylogenies (Hoegg *et al.*, 2004; Soltis *et al.*, 2009). In addition, polyploidy has been associated with increased invasiveness (te Beest *et al.*, 2012) and resistance to environmental stresses (Lohaus and Van de Peer, 2016). For instance, numerous plant species that survived the Cretaceous-Palaeogene mass extinction 66 million years ago underwent a polyploidization event which is thought to have contributed to their increased survival rates (Vanneste *et al.*, 2014a, 2014b). Polyploids may originate from the same species, i.e. autopolyploidization, or from different species as a result of interspecific hybridization, i.e. allopolyploidization. In general, allopolyploids are believed to have a higher adaptive potential than autopolyploids due to the combination of novel or diverged genes from distinct parental species (Van de Peer *et al.*, 2017).

The impact of allopolyploidization has mainly been investigated in plants, as approximately a tenth of all plant species consists of allopolyploids (Barker *et al.*, 2015). In contrast, allopolyploidization in fungi is far less intensively investigated (Campbell *et al.*, 2016). Nonetheless, allopolyploidization impacted the evolution of numerous fungal species, including the economically important baker's yeast *Saccharomyces cerevisiae* (Marcet-Houben and Gabaldón, 2015). The increased adaptive potential enabled allopolyploid fungi to develop desirable traits that can be exploited in industrial bioprocessing (Peris *et al.*, 2017). For instance, at least two recent hybridization events between *S. cerevisiae* and its close relative *Saccharomyces eubayanus* gave rise to *Saccharomyces pastorianus*, a species with high cold tolerance and good maltose/maltotriose utilization capabilities, which is exploited in the production of lager beer that requires barley to be malted at low temperatures (Gibson and Liti, 2015).

Allopolyploid genomes experience a so-called "genome shock" upon hybridization, inciting major genomic reorganizations that can manifest by genome rearrangements, extensive gene loss, transposon activation, and alterations in gene expression (Doyle *et al.*, 2008). These early stage alterations are primordial for hybrid survival, as divergent evolution is principally associated with incompatibilities between the parental genomes (Matute *et al.*, 2010). Additionally, these initial re-organizations and further alterations in the aftermath of hybridization also provide a source for environmental adaptation (Van de Peer *et al.*, 2017). Frequently, heterozygosity is lost for many regions in the allopolyploid genome (Mixão and Gabaldón, 2017). This can be a result of the

direct loss of a homolog of different parental origin (i.e. a homeolog) through deletion or gene conversion whereby one of the copies substitutes its homeologous counterpart (McGrath *et al.*, 2014). Gene conversion and the homogenization of complete chromosomes played a pivotal role in the evolution of the osmotolerant yeast species *Pichia sorbitophila* (Louis *et al.*, 2012). In total, two of its seven chromosome pairs consist of partly heterozygous, partly homozygous sections, whereas two chromosome pairs are completely homozygous. Gene conversion may eventually result in chromosomes consisting of sections of both parental origins as "mosaic genomes" (Stukenbrock *et al.*, 2012). However, mosaic genomes can also arise through recombination between chromosomes of the different parents, such as in the hybrid yeast *Zygosaccharomyces parabailii* (Ortiz-Merino *et al.*, 2017).

The redundancy of having one or more additional homeolog copies for most genes facilitates functional diversification in allopolyploids (Kimura and Ohta, 1974). Consequently, accelerated gene evolution is generally observed upon allopolyploidization (Hellsten *et al.*, 2007; Kimura and Ohta, 1974). Nevertheless, recent allopolyploidization events in the fungal genus *Trichosporon* resulted in a general deceleration of gene evolution (Sriswasdi *et al.*, 2016). Thus, allopolyploidization is not always followed by accelerated gene evolution. Arguably, the environmental exposure upon allopolyploidization plays a pivotal role in the eventual speed and grade of gene diversification (Schranz *et al.*, 2012).

Allopolyploidization typically entails gene expression pattern alterations when parental genomes that evolved distinct transcriptional regulation merge (Grover *et al.*, 2012). Moreover, crosstalk between parental sub-genomes can lead to further gene expression alterations, leading to the emergence of novel expression patterns (Adams *et al.*, 2003; Buggs *et al.*, 2010; Tirosh *et al.*, 2009). Nevertheless, in general, expression patterns are often conservatively inherited upon hybridization as the majority of allopolyploid genes are expressed similarly to their parental orthologs (Yoo *et al.*, 2013). For instance, more than half of the genes in an allopolyploid strain of the fungal grass endophyte *Epichloë* retained their parental gene expression level (Cox *et al.*, 2014).

Plant pathogens are often thought to evolve while being engaged in arms races with their hosts with pathogens evolving to evade host immunity while plant hosts attempt to intercept pathogen ingress (Cook *et al.*, 2015; Jones and Dangl, 2006). Due to the increased adaptation potential, allopolyploidization has been proposed as a potent driver in pathogen evolution (Depotter *et al.*, 2016b). Allopolyploids often have different pathogenic traits than their parental lineages, such as higher virulence (Brasier and Kirk, 2001; Husson *et al.*, 2015) and altered host ranges (Inderbitzin *et al.*, 2011b; Zeise and von Tiedemann, 2002). Within the fungal genus *Verticillium*, allodiploidization resulted in the emergence of the species *Verticillium longisporum* (Depotter *et al.*, 2017b; Inderbitzin *et al.*, 2011b). *V. longisporum* infects brassicaceous plants, whereas other *Verticillium* spp. generally do not typically colonize plants of this family, with the exception of *Arabidopsis thaliana* (Ellendorff *et al.*, 2009; Eynck *et al.*, 2007; Fradin *et*

al., 2011; Inderbitzin *et al.*, 2011b). Similar to haploid *Verticillium* spp., *V. longisporum* is thought to have predominant asexual reproduction as a sexual cycle has never been described and populations are not outcrossing (Depotter *et al.*, 2017b; Short *et al.*, 2014). *V. longisporum* is sub-divided into three lineages, each representing a separate hybridization event (Inderbitzin *et al.*, 2011b). The economically most important lineage A1/D1 originates from hybridization between *Verticillium* species A1 and D1 that have hitherto not been found in their haploid states. *V. longisporum* lineage A1/D1 is the main causal agent of Verticillium stem striping on oilseed rape (Depotter *et al.*, 2016a; Novakazi *et al.*, 2015) and a worldwide emerging pathogen (CFIA, 2015; Gladders *et al.*, 2011). Lineage A1/D1 can be further divided into two genetically distinct populations, which have been named 'A1/D1 West' and 'A1/D1 East' after their relative geographic occurrence in Europe (Depotter *et al.*, 2017b). Nevertheless, both populations originate from the same hybridization event (Depotter *et al.*, 2017b). Conceivably, upon or subsequent to the hybridization event, *V. longisporum* encountered extensive genetic and transcriptomic alterations that might have facilitated a shift towards brassicaceous hosts. Here, we studied the impact of allodiploidization on the evolution of *V. longisporum* by investigating genome, gene and transcriptomic plasticity.

Material and methods

Genome analysis

Genome assemblies of the two *V. longisporum* strains (VLB2 and VL20) and *V. dahliae* strain JR2 were previously published (Depotter *et al.*, 2017b; Faino *et al.*, 2015). Telomeric regions were determined based on the fungal telomeric repeat pattern: TAACCC/GGGTTA (minimum three repetitions) (Faino *et al.*, 2015). Furthermore, additional repeats were identified and characterized using RepeatModeler (v1.0.8). *De novo*-identified repeats were combined with the repeat library from RepBase (release 20170127) (Bao *et al.*, 2015). The genomic coordinates of the repeats were identified with RepeatMasker (v4.0.6). Homologous genes were identified by nucleotide BLAST (v2.2.31+). Here, only hits with a minimal coverage of 80% with each other were selected.

RNA sequencing, gene annotation and function determination

To obtain RNA-seq data for *Verticillium* grown in culture medium, isolates JR2, VLB2 and VL20 were grown for three days in potato dextrose broth (PDB) with three biological replicates for every isolate. To obtain RNA-seq data from *Verticillium* grown *in planta*, two-week-old plants of the susceptible oilseed rape cultivar 'Quartz' were inoculated by dipping the roots for 10 minutes in $1x10^6$ conidiospores ml^{-1} spore suspension of *V. longisporum* isolates VLB2 and VL20, respectively (Depotter *et al.*, 2017a). Similarly, three-week-old *A. thaliana* (Col-0) plants were inoculated with *V. dahliae* isolate JR2, VLB2 and VL20, respectively. After root inoculation, plants were grown in individual

pots in a greenhouse under a cycle of 16 h of light and 8 h of darkness, with temperatures maintained between 20 and 22°C during the day and a minimum of 15°C overnight. Three pooled samples (10 plants per sample) of stem fragments (3 cm) and complete flowering stems were used for total RNA extraction for oilseed rape and *A. thaliana*, respectively. Total RNA was extracted based on TRIzol RNA extraction (Simms *et al.* 1993). cDNA synthesis, library preparation (TruSeq RNA-Seq short-insert library), and Illumina sequencing (single-end 50 bp) was performed at the Beijing Genome Institute (BGI, Hong Kong, China). In total, ~2 Gb and ~1.5 Gb of filtered reads were obtained for the *Verticillium* samples grown in culture medium and *in planta*, respectively.

Using RNA-seq from the in liquid medium grown cultures, gene annotation was performed for JR2, VLB2 and VL20 with the BRAKER1 1.9 pipeline (Hoff *et al.*, 2016) using GeneMark-ET (Lomsadze *et al.*, 2014) and AUGUSTUS (Stanke *et al.*, 2008). Predicted genes with internal stop codons were removed from the analysis. The secretome prediction was done using SingalP4 (v4.1) (Petersen *et al.*, 2011), TargetP (v1.1) (Emanuelsson *et al.*, 2000), and TMHMM (v2.0) (Krogh *et al.*, 2001) as described previously (Seidl *et al.*, 2015). Pfam function domains were predicted using InterProScan (Jones *et al.*, 2014). Subsequently, Pfam enrichments were determined using hypergeometric tests, and significance values were corrected using the Benjamini-Hochberg false discovery method (Benjamini and Hochberg, 1995). Clusters of Orthologous Group (COG) categories were determined for protein sequences using EggNOG (v4.5.1) (Huerta-Cepas *et al.*, 2016).

Parental origin determination

Sub-genomes were divided based on the differences in sequence identities between species A1 and D1 with *V. dahliae*. *V. longisporum* genomes of VLB2 and VL20 were aligned to the complete genome assembly of *V. dahliae* JR2 using NUCmer, which is part of the MUMmer package v3.23 (Faino *et al.*, 2015; Kurtz *et al.*, 2004). Here, only 1-to-1 alignments longer than 10 kb and with a minimum of 80% identity were retained. Subsequent alignments were concatenated if they aligned to the same contig with the same orientation and order as the reference genome. The average nucleotide identity was determined for every concatenated alignment and used to divide the genomes into sub-genome.

The parental origin determination based on sequence identities of the exonic regions of genes was performed by BLAST (v2.6.0+). Here, hits with a minimum subject and query coverage of 80% were used. Furthermore, similar to Louis *et al.* (2012), differences in GC-content between homologous genes present in two copies were calculated accordingly:

$$\mathrm{dGC}_{\mathrm{gene}} = \frac{2 * \mathrm{GCgene}}{\mathrm{GCgene} + \mathrm{GChomolog}}$$

GCgene = GC% of gene

GChomolog = GC% of homolog

dGC_{gene} = GC ratio from the mean GC% value

Gene conversion and genomic rearrangements

Genes occurring in multiple copies were identified using nucleotide BLAST (v2.6.0+) and the sequence identity between these genes was determined. Here, hits with a minimum subject and query coverage of 80% were used. The VLB2 genome assembly was aligned to VL20 to identify synteny breaks using NUCmer, which is part of the MUMmer package v3.23 (Kurtz *et al.*, 2004). Subsequent alignments were concatenated if they aligned to the same contig with the same orientation and order as the reference genome. In order to confirm synteny breaks, filtered *V. longisporum* long sequencing reads of VLB2 (Depotter *et al.*, 2017b) were aligned to the *V. longisporum* VL20 genome with the Burrows-Wheeler Aligner (BWA) (Li, 2013) and further processed with the samtools package (v1.3.1) (Li *et al.*, 2009). Synteny breaks were visualized using the R package Sushi (Phanstiel *et al.*, 2014) and the Integrative Genomics Viewer (Robinson *et al.*, 2011). The association between breaks with repeats was tested through permutation. First, the fraction of synteny breaks flanked by repeats was determined. Here, synteny breaks were assigned to reside in a "repeat-rich" region if a 1 kb window around the break consisted for more than 10% of repeats. The *V. longisporum* VL20 genome assembly was divided into windows of 1 kb using BEDTools (v2.26.0). To estimate the significance of the synteny break/repeat association (Quinlan and Hall, 2010), 10,000 permutations were executed with the same amount of windows as there were synteny breaks to determine the random distribution of repeat-rich regions.

Phylogenetic tree

The following *Verticillium* strains were used as representatives for their species: *V. albo-atrum* = PD747, *V. alfalfae* = PD683, *V. dahliae* = JR2, *V. isaacii* = PD660, *V. klebahnii* = PD401, *V. nonalfalfae* = TAB2, *V. nubilum* = PD621, *V. tricorpus* = PD593 and *V. zaregansianum* = PD739. The phylogenetic tree was constructed based on nucleotide sequences of the Benchmarking Universal Single-Copy Orthologs (BUSCOs) of fungi present in all *Verticillium* spp. and the out-group species *Sodiomyces alkalinus* (Simão *et al.*, 2015). To this end, previously published *Verticillium* and *S. alkalinus* assemblies were used (Depotter *et al.*, 2017b; Faino *et al.*, 2015; Grum-Grzhimaylo *et al.*, 2013; Shi-Kunne *et al.*, 2018). In total, 277 orthologous groups were aligned using mafft (v7.271) (default settings) (Katoh and Standley, 2013). Aligned genes were then concatenated, and the phylogenetic tree was inferred using RAxML with the GTRGAMMA substitution model (v8.2.0) (Stamatakis, 2014). The robustness of the inferred phylogeny was assessed by 100 rapid bootstrap approximations.

Gene divergence

Previously published annotations of the haploid *Verticillium* spp. were used to compare the evolutionary speed of orthologs (Faino *et al.*, 2015; Shi-Kunne *et al.*, 2018). The VESPA (v1.0b) software was used to automate this process (Webb *et al.*, 2017). The coding sequences for each *Verticillium* spp. were filtered and subsequently translated using the VESPA 'clean' and 'translate' function. Homologous genes were retrieved by protein BLAST (v2.2.31+) querying a database consisting of all *Verticillium* protein sequences. Here, only hits with a minimum coverage of 70% were used. Homologous genes were grouped with the VESPA 'best_reciprocal_group' function. Only homology groups that comprised a single representative for every *Verticillium* spp. were used for further analysis. Protein sequences of each homology group were aligned with muscle (v3.8.31) (Edgar, 2004). The aligned protein sequences of the homology groups were conversed to nucleotide sequence by the VESPA 'map_alignments' function. The alignments were used to calculate *Ka*/*Ks* for every branch of the species phylogeny using codeml module of PAML (v4.8) with the following parameters: F3X4 codon frequency model, wag.dat empirical amino acid substitution model and no molecular clock (Yang, 2007). To this end, the previously obtained phylogenetic tree topology was used: (((((*V. klebahnii*, *V. isaacii*), *V. tricorpus*), *V. zaregamsianum*), *V. albo-atrum*), (((*V. dahliae*, species D1), (*V. alfalfae*, *V. nonalfalfae*)), species A1), *V. nubilum*). When comparing the evolutionary speed between *V. dahliae* genes and its orthologs, extreme values *Ka*/*Ks* were discarded from further analysis, i.e. *Ka*/*Ks* < 0.0001 and *Ka*/*Ks* ≥ 2. Significance of positive selection was tested using a Z-test (Stukenbrock and Dutheil, 2012) and Z-values >1.65 were considered significant with $P<0.05$.

Gene expression analysis

The RNA sequencing reads of the *Verticillium* strains VLB2, VL20 and JR2 were uniquely mapped to their previously assembled genomes using the Rsubread package in R (Depotter *et al.*, 2017b; Faino *et al.*, 2015; Liao *et al.*, 2013; R Core Team, 2015). To compare gene expression patterns, gene orthologs were retrieved by protein BLAST (v2.2.31+). Here, only hits with a minimum sequence identity of 70% and of coverage of 80% were used. Only genes in single copy in *V. dahliae* with two orthologs in *V. longisporum* of different parental origin (one A1 copy and one D1 copy) were used for comparative analysis. The comparative transcriptomic analysis was performed with the package edgeR in R (v3.4.3) (McCarthy *et al.*, 2012; R Core Team, 2015; Robinson *et al.*, 2009). Expression patterns were corrected for putative length differences between orthologous genes. Genes are considered differently expressed when *P*-value < 0.05 with a log2-fold-change ≥ 1. *P*-values were corrected for multiple comparisons according to Benjamini and Hochberg (1995).

Results

V. longisporum displays a mosaic genome structure

The genomes of two *V. longisporum* strains were analyzed to investigate the impact of hybridization on the genome structure. Previously, *V. longisporum* strains VLB2 and VL20, belonging to 'A1/D1 West' and 'A1/D1 East', were sequenced with the PacBio RSII platform and assembled into genomes of 72.9 and 72.3 Mb in size, respectively (Depotter *et al.*, 2017b). These genome sizes exceed double the amount of the telomere-to-telomere sequenced *V. dahliae* strains JR2 (36.2 Mb) and VdLs17 (36.0 Mb) (Faino *et al.*, 2015). We used RepeatModeler (V1.0.8; Smit *et al.* 2015) in combination with RepeatMasker to determine that 14.28 and 13.90% of the *V. longisporum* strain VLB2 and VL20 genomes are composed of repeats, respectively (Table S1). Intriguingly, this is more than double the repeat content as in *V. dahliae* strain JR2, for which 6.49% of the genome was annotated as repeat using the same methodology. The *V. longisporum* genomes were also screened for the fungal telomere-specific repeats (TAACCC/GGGTTA) to estimate the number of chromosomes. In total, 29 and 30 telomeric regions were found in the VLB2 and VL20 genomes, respectively, that were consistently situated at the end of sequence contigs, suggesting that *V. longisporum* contains at least 15 chromosomes (Table S1). Six out of 45 and 4 out of 44 sequence contigs in strains VLB2 and VL20, respectively, were flanked on both ends by telomeric repeats and therefore likely represent complete chromosomes (Table S1). For comparison, *V. dahliae* strains have 8 chromosomes (Faino *et al.*, 2015).

In allodiploid organisms, parental origin determination is elementary to investigate genome evolution in the aftermath of hybridization. As species D1 is phylogenetically closer related, and consequently has a higher sequence identity, to *V. dahliae* than species A1, *V. longisporum* genomic regions were previously provisionally assigned to either species D1 or A1 (Depotter *et al.*, 2017b). Here, we determined the parental origin of *V. longisporum* genomic regions more precisely. The difference in phylogenetic distance of species A1 and D1 to *V. dahliae* caused that *V. longisporum* genome alignments to *V. dahliae* displayed a bimodal distribution with one peak at 93.1% and another peak at 98.4% sequence identity that represent the two parents with a dip at 96.0% (Figure S1). In order to separate the two sub-genomes, regions with an average sequence identity to *V. dahliae* of <96% were assigned to species A1, whereas regions with an identity of ≥96% were assigned to species D1 (Figure 1). In this manner, 36.2 Mb of *V. longisporum* strain VLB2 was assigned to species A1 and 35.7 Mb to species D1. For *V. longisporum* strain VL20, 36.3 Mb was assigned to species A1 and 35.2 Mb to species D1. Only 1.0 and 0.8 Mb of strains VLB2 and VL20, respectively, could not be aligned to *V. dahliae* and thus remained unassigned.

To trace the chromosome sets of the original parents of the hybrid, the parental origin of individual contigs was determined. In total, 8 of the 10 largest contigs of *V. longisporum* strain VLB2 as well as strain VL20 consist of regions originating from both species A1 and species D1 (Figure 1). Thus, parental chromosome sets cannot be separated from one another as *V. longisporum* apparently evolved a mosaic genome structure in the aftermath of hybridization.

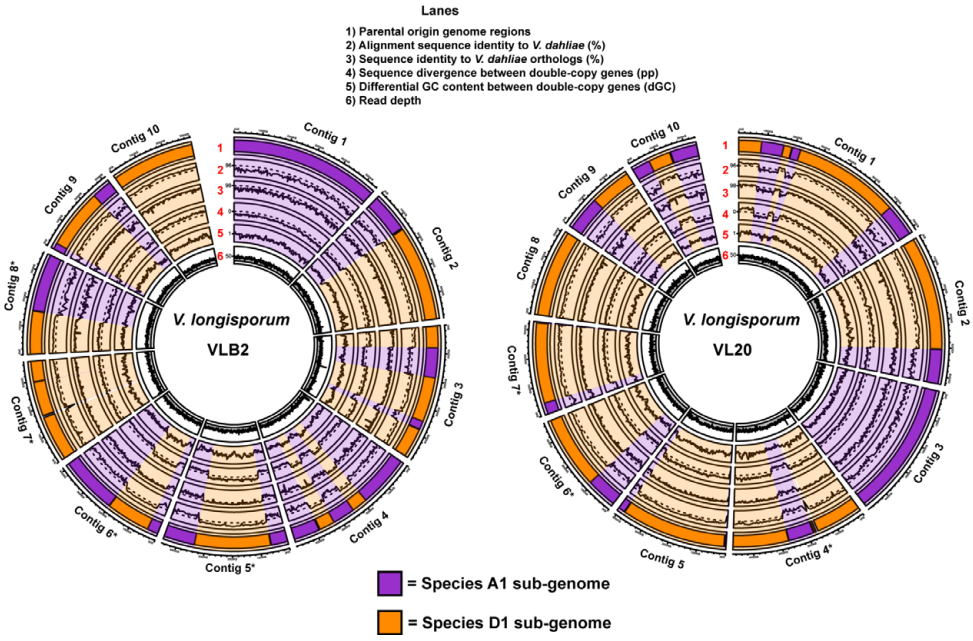

Figure 1 | Determination of parental origin of *V. longisporum* genome sections. The ten largest contigs of the genome assemblies of *V. longisporum* strains VLB2 and VL20 are depicted. Lane 1: regions with a sequence identity of at least 96% were assigned to Species D1 (orange), whereas ones with lower sequence identity to Species A1 (purple). Lane 2: sequence identity of *V. longisporum* alignments to *V. dahliae*. Lane 3: Sequence identity between exonic regions of *V. longisporum* and *V. dahliae* orthologs. Lane 4: Difference in sequence identity in percent point (pp) between exonic regions of *V. longisporum* double-copy genes. Only gene pairs with an ortholog in *V. dahliae* are depicted. Alleles with a higher identity to *V. dahliae* are depicted as a positive pp difference, whereas the corresponding homolog as a negative pp difference. Lane 5: the relative difference in GC content (dGC) between genes in double copy. Lane 6: Read depth with non-overlapping windows of 10 kb. Data points of lanes 3-5 represent the average value of a window of eleven genes, which proceed with a step of one gene.

Genomic rearrangements are responsible for the mosaic genome

Typically, a mosaic structure of a hybrid genome can originate from gene conversion or from chromosomal rearrangements between DNA strands of different parental origin (Mixão and Gabaldón, 2017). To analyze the extent of gene conversion, genes were predicted for the *V. longisporum* strains VLB2 and VL20. To aid gene annotation with the BRAKER1 1.9 pipeline (Hoff *et al.*, 2016), ~2 Gb of filtered RNA-seq reads were generated from fungal cultures in liquid medium. In total, 19,123 and 18,784 genes were

predicted for *V. longisporum* strains VLB2 and VL20 respectively, which is ~90% higher than the amount of genes that were predicted for *V. dahliae* strain JR2 using the same approach (9,909 genes) (Table S1). As to be expected, the divergence of species A1 and D1 could also be observed at the gene level based on sequence identity and GC-content (Figure 1, S1). In total, 9,531 and 9,402 genes were assigned to the species A1 sub-genome of the strains VLB2 and VL20, respectively, whereas the number of genes in the species D1 sub-genomes was 9,468 and 9,243 for these strains, respectively (Table S1). Thus, the amount of genes is similar in the two sub-genomes for both *V. longisporum* strains and similar to the gene number identified in *V. dahliae* strain JR2. Over 80% of the *V. longisporum* genes are present in two copies whereas almost all genes (97-98%) are present in one copy within each of the *V. longisporum* sub-genomes (Figure S2). Moreover, of the 7,620 genes that are present in two copies in VLB2 and VL20, only 5 genes were found to be highly similar (<1% nucleotide sequence diversity) in VLB2, whereas the corresponding gene pair in VL20 was more diverse (>1%) (Figure 2A). In *V. longisporum* strain VL20, no highly similar copies were found that are more divergent in VLB2. Collectively, these findings indicate that the two copies of most genes present in the *V. longisporum* are homeologs and that gene conversion only played a minor role during evolution of the mosaic genome.

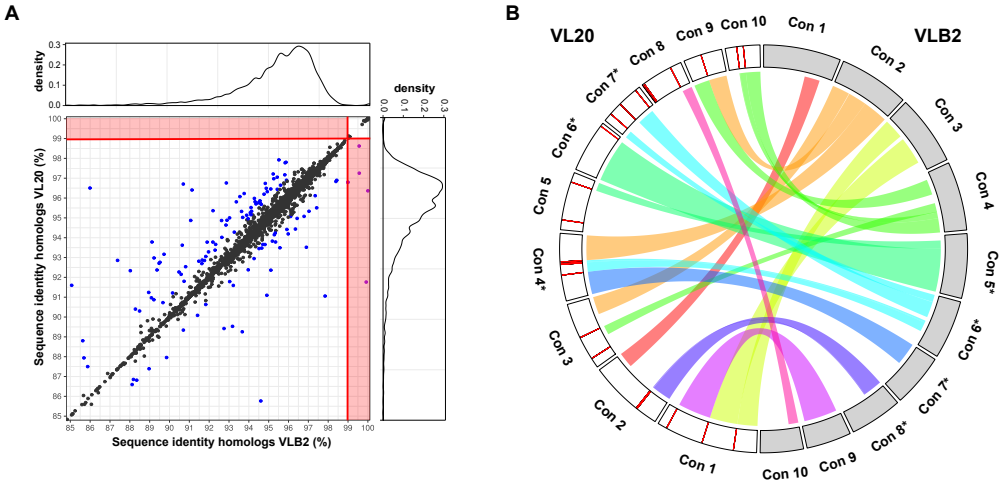

Figure 2 | The origin of the mosaic genome structure of *V. longisporum*. (A) The contribution of gene conversion to *V. longisporum* genome evolution. Sequence identities between genes in copy, present in *V. longisporum* VLB2 and VL20, are depicted. Gene pairs that encountered gene conversion (purple dots in the red zones) have sequence divergence of more than one percent in one *V. longisporum* strain and less than one percent in the other strain. In other cases, pairs that differ less than one percent are depicted as a black dot, whereas a difference greater than one percent is depicted as a blue dot. (B) The contribution of genomic rearrangements to *V. longisporum* genome evolution. The ten largest contigs of the *V. longisporum* strains VLB2 (displayed in grey) and VL20 (displayed in white) are depicted with complete chromosomes indicated by asterisks. Ribbons indicate syntenic genome regions between the two strains. Regions without ribbons do not have homology to regions in the 10 largest contigs of the other isolate. Red bars on the contigs indicate synteny breaks that are confirmed by discontinuity in read alignment of VLB2 to the VL20 genome assembly (Figure S3).

Considering that gene conversion played a minor role during genome evolution, the mosaic genome structure of *V. longisporum* likely originated from rearrangements between homeologous chromosomes. To identify the location of genomic rearrangements, the genome of *V. longisporum* strain VLB2 was aligned to that of strain VL20 (Figure 2B). Extensive chromosomal rearrangements occurred between the two *V. longisporum* strains, as we observed 87 putative syntenic breaks. In order to confirm these breaks, long sequencing reads of VLB2 were aligned to the VL20 genome assembly to assess if synteny breaks were supported by read mapping (Figure S3). In total, 60 synteny breaks could be confirmed by read mapping. As genomic rearrangements are often associated with repeat-rich genome regions (Seidl and Thomma, 2014), the synteny break points were tested for their association to these regions. In total, 34 of the 60 (57%) confirmed synteny break points were flanked by repeats, which is significantly more than expected from random sampling (mean = 18.5%, σ = 0.05%) (Figure S4). In conclusion, it appears that chromosomal rearrangement, rather than gene conversion, is the main driver underlying the mosaic structure of the *V. longisporum* genome.

V. longisporum lost heterozygosity through deletions

In each of the *V. longisporum* isolates, 17% of the genes occur only in a single copy. Although gene conversion played a minor role in the aftermath of hybridization, loss of heterozygosity may occur through gene loss or, alternatively, single-copy genes may originate from parent-specific contributions. However, as 12% of the singly copy genes in strain VLB2 are present in two copies in strain VL20, and 16% of the single copy genes in VL20 are present in two copies in VLB2, gene deletion seems to be an on-going process in *V. longisporum* evolution since both strains are derived from the same hybridization event (Depotter *et al.*, 2017b). Of the genes that were lost in the VLB2 divergence from VL20, 52% resided in the species A1 sub-genome, whereas 47% in the D1 sub-genome (1% remained unassigned). For VL20, 49% and 50% of these lost genes resided in the A1 and D1 sub-genome, respectively. Thus, gene loss occurs evenly across the two sub-genomes. We next determined the fraction of lost genes that encode secreted proteins as pathogen secretomes play pivotal roles in establishing symbioses with plant hosts (Gupta *et al.*, 2015). In total, 12.9% and 8.7% of the genes that encode secreted proteins were lost in the divergence of VLB2 and VL20, respectively. This is a significant enrichment for strain VLB2, where genome-wide 8.9% of the genes encode secreted proteins (Fisher's exact test, P = 0.009) (Table S1). Nevertheless, this enrichment is not found for strain VL20 of which 9.0% of the genes encode secreted proteins (Fisher's exact test, P = 0.45) (Table S1). Nonetheless, in general, *V. longisporum* strains VLB2 and VL20 contain 1.91 and 1.90 times the number of genes encoding secreted proteins compared to *V. dahliae* JR2 with similar contributions of the species A1 and D1 sub-genomes (Table S1). This indicates that, although gene loss occurs, it hitherto impacted the secretome of *V. longisporum* only to a limited extent.

Global acceleration of gene evolution upon allodiploidization

To investigate the evolution of genes subsequent to the allodiploidization event, we determined their rates of non-synonymous (*Ka*) and synonymous (*Ks*) substitutions. Substitution rates were determined for so-called best-reciprocal orthologs, which are genes that are present in a single copy in all *Verticillium* spp. (Figure 3A) and thus, sub-genomes A1 and D1 of *V. longisporum* were considered separately. In total, 5,342 and 5,369 orthologous groups could be constructed using *V. longisporum* strain VLB2 and VL20, respectively. Consequently, for every orthologous group, *Ka*/*Ks* ratios were determined for every branch of the *Verticillium* phylogeny leading to an extant species and consequently compared with the *Ka*/*Ks* ratio obtained for the *V. dahliae* branch. In general, genes in clade Flavexudans spp. displayed higher *Ka*/*Ks* ratios than clade Flavnonexudans spp. (Figure 3, S5). *V. nubilum* and *V. albo-atrum* genes displayed the lowest *Ka*/*Ks* ratios of all *Verticillium* spp., which correlates with their relatively long evolutionary history without divergence of known sister species (Figure 3, S5). Of all *Verticillium* spp., *V. longisporum* sub-genome D1 was the only species of which genes displayed significantly higher *Ka*/*Ks* ratios than *V. dahliae* (Wilcoxon rank-sum test, $P = 9.43e\text{-}12$, VLB2 based). Thus, genes of the *V. longisporum* sub-genome D1 generally evolve faster than genes of other haploid *Verticillium* spp. In contrast, genes of the other *V. longisporum* sub-genome, A1, generally displayed lower *Ka*/*Ks* ratios than *V. dahliae* orthologs (Wilcoxon rank-sum test, $P < 2.2e\text{-}16$, VLB2 based). However, the absence of a phylogenetically closely related A1 sister species hampers the determination of putative differences in gene diversification rate before and after hybridization as *Ka*/*Ks* ratios can vary considerably between genes of haploid *Verticillium* spp. For instance, *V. longisporum* sub-genome A1 displays higher evolutionary speed, expressed by *Ka*/*Ks*, than *V. alfalfae* (Wilcoxon rank-sum test, $P = 3.94e\text{-}14$, VLB2 based) and a similar evolutionary speed to *V. nonalfalfae* (Wilcoxon rank-sum test, $P = 0.09$, VLB2 based), species that have the same last common ancestor with A1 as *V. dahliae* (Figure 3A).

To find evidence for accelerated evolution in both *V. longisporum* sub-genomes, we determined the number of genes under positive selection in every *Verticillium* (sub-) genome using the above formed orthologous groups. Genes under positive selection were determined based on a *Z*-test and varied considerably from 209 in the *V. longisporum* sub-genome A1 to 3 in *V. tricorpus* (Figure S6). Intriguingly, the *V. longisporum* sub-genomes A1 and D1 have the highest number of genes under positive selection (128 genes for species D1). The genomes *V. dahliae* and *V. zaregansianum* contain a considerable number of genes under positive selection; 103 and 99 respectively. To investigate whether particular functional gene properties are associated with genes under positive selection, the fractions of genes that encode secreted proteins were determined (Figure S6). These fractions were not higher in the *V. longisporum* sub-genomes than in *V. dahliae* and *V. zaregansianum*. Furthermore, no major differences in Clusters of Orthologous Group (COG) functional categories could be observed for genes under positive selection between sub-genome A1, sub-genome D1, *V. dahliae* and *V. zaregansianum* (Figure S7). Thus, we conclude that *V. longisporum* genes globally diverge faster than genes of related haploid *Verticillium* spp.

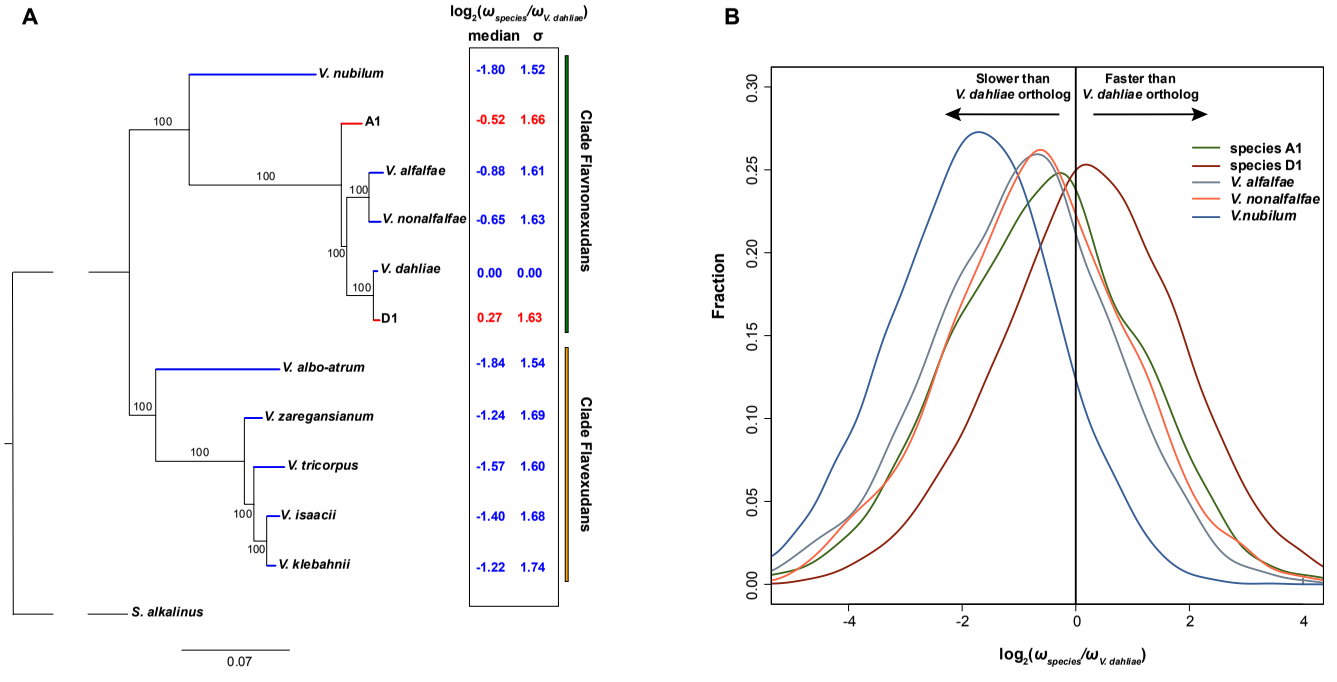

Figure 3 | Comparison of gene divergence between *Verticillium* species. *Ka/Ks* ratios (ω) between *V. dahliae* and other *Verticillium* spp. were compared. (A) Blue branches in the phylogenetic tree represent *Verticillium* species with a haploid evolutionary history, whereas red branches represent species with an allodiploid phase in their evolutionary history. The median difference in evolutionary speed between *V. dahliae* and orthologs was calculated in addition to the standard deviation (σ). (B) The distribution of these differences is depicted for species of the *Verticillium* clade Flavnonexudans. For the *Verticillium* species A1 and D1, *V. longisporum* strain VLB2 was used.

Expression pattern homogenization in the hybridization aftermath

To investigate the impact of allodiploidization on gene expression patterns, the expression of *V. longisporum* genes was compared with *V. dahliae* orthologs of isolates grown in culture medium. To this end, expression of single copy *V. dahliae* genes was compared with *V. longisporum* orthologs that are present in two copies: one in the species A1 sub-genome and one in the species D1 sub-genome. In total, 7,469 and 7,411 of these expressed gene clusters were found for *V. longisporum* strain VLB2 and VL20, respectively. Reads were mapped to the predicted *V. longisporum* genes of which 51% and 50% mapped to species A1 homeologs and 49% and 50% to the species D1 homeologs, for strains VLB2 and VL20, respectively, and thus we observed no general dominance in expression for one of the sub-genomes. Over 60% of the *V. dahliae* genes are not differentially expressed compared to A1 and D1 orthologs, indicating that the majority of the genes did not evolve differential expression patterns (Figure 4). In total, 29.6% and 24.2% of the genes are differently expressed compared to *V. dahliae* orthologs in the species A1 and D1 sub-genomes, respectively (Figure 4, VLB2 based). The significantly higher fraction of differentially expressed A1 genes (Fisher's exact test, $P = 4.3e\text{-}13$) corresponds to the more distant phylogenetic relationship of A1 with *V. dahliae* than of D1. Intriguingly, however, significantly less D1 genes (18.5%, VLB2 based) were differently expressed to A1 homeologs than to *V. dahliae* orthologs despite the larger phylogenetic distance between *Verticillium* species A1 and D1 (Fisher's exact test, $P < 2.2e\text{-}16$). In general, the expression pattern of *V. longisporum* A1 and D1 sub-genomes are more similar to each other ($\rho = 0.90$ for VLB2) than the expression pattern of sub-genome D1 and *V. dahliae* ($\rho = 0.86$ for VLB2) (Figure 5, Table S2). This discrepancy in phylogenetic relationship and expression pattern similarities may indicate that the expression patterns of species A1 and D1 homogenized upon hybridization. Moreover, for *V. longisporum* strains VLB2 and VL20, homeolog expression patterns within the same strain ($\rho = 0.90$ for VLB2) correlated more than A1 and D1 expression patterns of different strains ($\rho = 0.88$ for VLB2 A1 and VL20 D1) (Figure 5, Table S2). Thus, expression patterns of homeologs may have synchronized in the aftermath of hybridization.

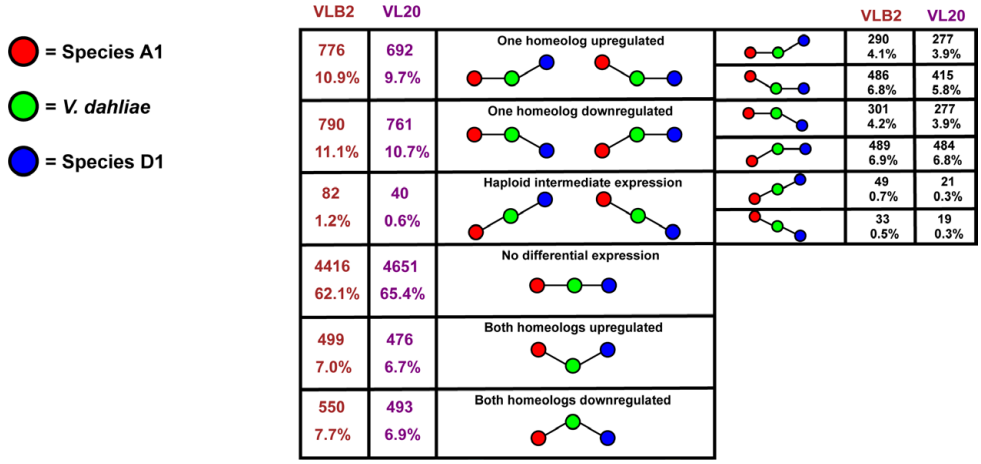

Figure 4 | Global comparison of expression between *V. longisporum* and *V. dahliae* orthologs. Only genes with one copy in *V. dahliae* and two orthologs in the *V. longisporum* strains VLB2 and VL20 (one from sub-genome A1 and one from sub-genome D1) were considered.

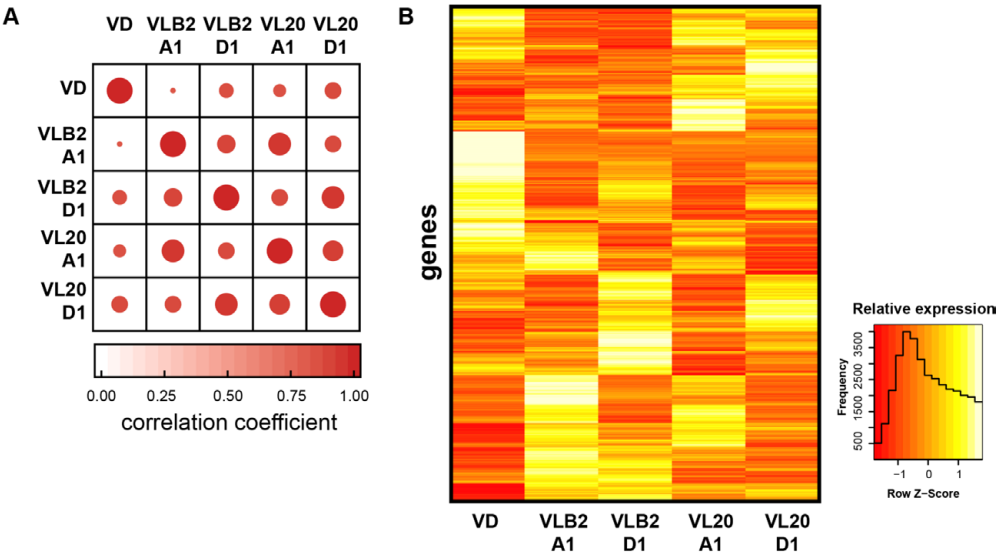

Figure 5 | Expression pattern comparison between *V. longisporum* sub-genomes and *V. dahliae*. Only genes with one copy in *V. dahliae* and two orthologs in the *V. longisporum* strains VLB2 and VL20 (one from sub-genome A1 and one from sub-genome D1) were considered. (A) Pairwise correlations between *Verticillium* expression patterns. Dot size and colour represent the Spearman's correlation coefficient (ρ). (B) Relative expression (Z-scores) between *Verticillium* spp. VD = *V. dahliae*, A1 = *V. longisporum* A1 sub-genome and D1 = *V. longisporum* D1 sub-genome.

In planta secretome homogenization between *V. longisporum* sub-genomes

To assess potential gene expression differences upon host colonization, gene expression patterns of *V. longisporum* and *V. dahliae* orthologs were also investigated *in planta*. To this end, oilseed rape plants were inoculated with VLB2 and VL20, respectively. As observed previously, oilseed rape plants inoculated with VLB2 developed typical *Verticillium* symptoms including stunted plant growth and leaf chlorosis (Depotter *et al.*, 2017a). In contrast, oilseed rape plants inoculated with VL20 did not display any disease symptoms. Accordingly, VLB2 DNA could be detected in oilseed rape stems, whereas VL20 DNA remained under the detection limit. In addition, *A. thaliana* plants were inoculated with *V. dahliae* strain JR2, and *V. longisporum* strains VLB2 and VL20. However, only JR2 DNA could be detected in above-ground plant material. Consequently, total RNA sequencing was performed for oilseed rape plants inoculated with *V. longisporum* strain VLB2 and *A. thaliana* plants inoculated with *V. dahliae* strain JR2. In total, ~1.5 Gb of filtered RNA-seq reads were generated from the *Verticillium* inoculated plant material. Similar to *V. longisporum* grown in culture medium, 49% and 51% of the reads mapped to the A1 and D1 sub-genomes of *V. longisporum*. Thus, also *in planta* there is no expression dominance of one of the *V. longisporum* sub-genomes. Furthermore, 16.4% and 15.1% of the *V. longisporum* genes were differently expressed from *V. dahliae* orthologs in sub-genome A1 and D1, respectively (Figure 6). Thus, in correspondence with *V. longisporum* grown in culture medium, a larger fraction of A1 orthologs was differently expressed to *V. dahliae* orthologs than D1 orthologs (Fisher's exact test, $P = 0.04$).

To elucidate a putative association of gene expression differences between *V. longisporum* and *V. dahliae* with their distinct host ranges, the fraction of differently expressed genes that encode secreted proteins was determined. For *Verticillium* grown in culture medium, 16.5% of the differentially expressed genes between *V. longisporum* and *V. dahliae* encode secreted proteins, whereas this is only 5.3% for genes without differential expression (Figure 6A). This enrichment of genes encoding secreted proteins was also found for isolate VL20 (Figure S8). Correspondingly, *V. longisporum* genes that were differently expressed from *V. dahliae* orthologs were enriched for Pfam domains associated with secretion and host colonization, such as *Hce2* (PF14856), a domain found in putative effectors with homology to *Cladosporium fulvum* effector Ecp2 (Stergiopoulos *et al.* 2012; Table S3). Similarly, genes encoding secreted proteins were also significantly enriched for differentially expressed genes between *V. longisporum* and *V. dahliae in planta* (Figure 6B). However, the fraction of 9.7% was significantly less than 16.5% for *Verticillium* grown in culture medium (Figure 6B). Thus, despite the colonization of *V. longisporum* and *V. dahliae* on a different host species, the enrichment of genes encoding secreted proteins is lower for *Verticillium* grown *in planta* compared with culture medium.

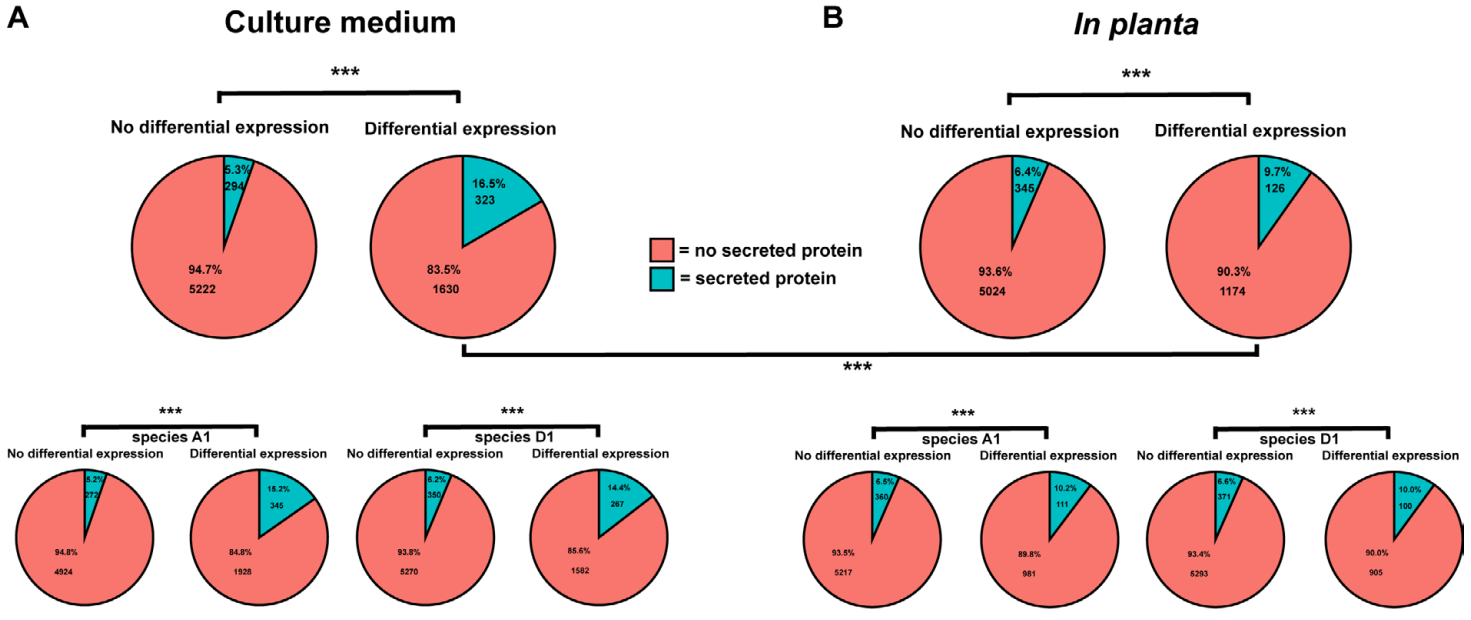

Figure 6 | Differential expression between *V. longisporum* and *V. dahliae* in relation to genes encoding secreted proteins. Differential expression is calculated for species A1, species D1 and *V. longisporum* (cumulative expression A1 and D1 homeologs) with *V. dahliae* orthologs for isolates grown in (A) culture medium and (B) *in planta*. Pie charts show fraction of genes encoding secreted proteins of not-differentially and differentially expressed genes, respectively. Significance of the different distributions was calculated the Fisher's exact test (*** = $P<0.001$).

To see how the different sub-genomes contribute to the enrichment of genes encoding secreted proteins, we compared gene expression patterns of *V. longisporum* sub-genomes. For *V. longisporum* grown in culture medium, 19.4% of the genes that are differentially expressed between the A1 and D1 homeologs encode secreted proteins, whereas this is 5.8% for homeologs with similar expression levels (Figure 7). Thus, similar to *V. longisporum* and *V. dahliae* orthologs, differentially expressed homeologs are enriched for genes that encode secreted proteins. Intriguingly, 7.9% of the genes with differential homeolog expression *in planta* encode secreted proteins, which is a similar fraction as for homeologs without differential expression (8.4%; Figure 7). Thus, upon plant colonization, there is no enrichment of genes that encode secreted proteins for differentially expressed homeologs. This lack of enrichment may be due to increased expression differences *in planta* between homeologs that encode non-secreted proteins. Alternatively, expression levels of homeologs encoding secreted proteins may homogenize *in planta* (Figure 7). In total, 11.2% and 9.5% of the genes that are differently regulated *in planta* from culture medium encode secreted proteins in sub-genome A1 and D1, respectively (Figure 7). This is a significantly larger fraction than for genes without differential expression: 7.2% and 7.9% for sub-genomes A1 and D1, respectively. In sub-genome A1, this enrichment of genes encoding secreted proteins was both present for *in planta* up-regulated (11.6%, Fisher's exact test, $P < 1.74e\text{-}05$) and down-regulated (10.9%, Fisher's exact test, $P < 4.23e\text{-}05$) genes. In contrast, in sub-genome D1, the enrichment was present for *in planta* up-regulated genes (12.3%, Fisher's exact test, $P < 2.27e\text{-}05$), but not for down-regulated genes (7.7%, Fisher's exact test, $P = 0.91$). Thus, in general, genes encoding secreted proteins underwent relatively more frequently expression alterations upon plant colonization compared to genes that encode for non-secreted proteins. Consequently, the lack of enrichment *in planta* is caused by an increased homogenization of homeolog expression patterns of genes encoding secreted proteins.

The expression pattern homogenization is illustrated by genes encoding secreted proteins with a pectate lyase Pfam domain (PF03211), which is associated with host cell-wall degradation (Figure S9) (Marín-Rodríguez *et al.*, 2002). In total, 5 genes (*Pect_ly_1*, *Pect_ly_2*, *Pect_ly_3*, *Pect_ly_4* and *Pect_ly_5*), with a pectate lyase domain were found with two homeologous copies in *V. longisporum* and all of them were predicted to be secreted. There was no differential expression between the homeologs *in planta* for all 5 genes, whereas in culture medium the homeologs are differentially expressed for *Pect_ly_1*, *Pect_ly_4* and *Pect_ly_5*. Homogenization of homeolog expression was achieved through down-regulation for *Pec_ly_1*, as both homeologs were not expressed *in planta*. In contrast, similar levels of homeolog *in planta* expression were achieved for *Pect_ly_4* and *Pect_ly_5* by the relative increase in expression of the D1 and A1 homeolog, respectively.

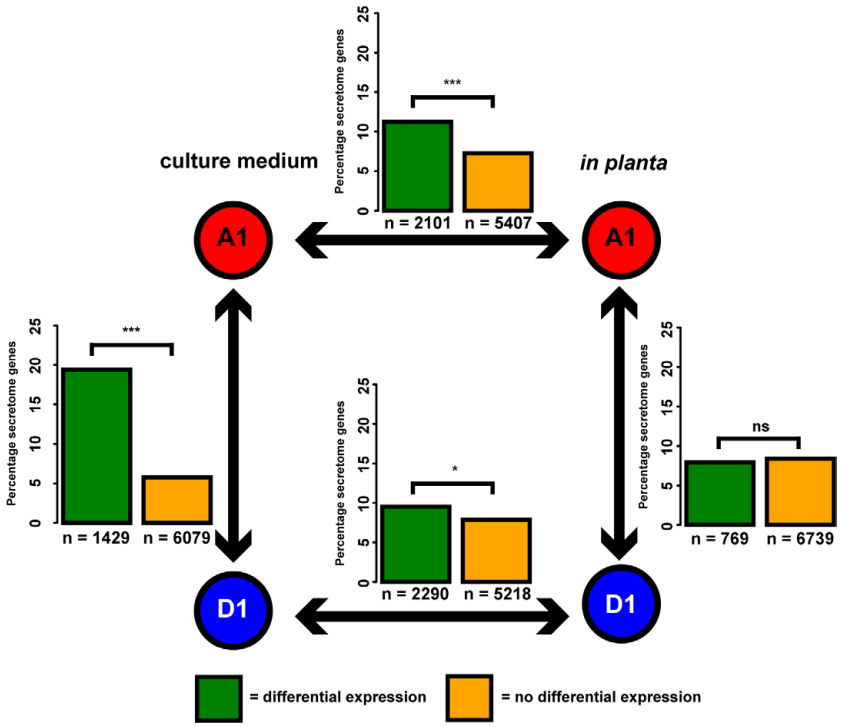

Figure 7 | Differential expression between *V. longisporum* sub-genomes in relation to genes encoding secreted proteins. Gene expression of A1 and D1 homeologs were compared for *V. longisporum* grown in culture medium and *in planta*. Only genes were considered with one copy in *V. dahliae* and two corresponding copies in the *V. longisporum* strains VLB2 (one from sub-genome A1 and one from sub-genome D1). The number below the bar indicates the amount of differently and not differently expressed genes, respectively. Significance of the different distributions was calculated the Fisher's exact test (ns = not significant, * = $P<0.05$, *** = $P<0.001$).

7

Discussion

Hybridization is a powerful evolutionary mechanisms often leading to the emergence of new plant pathogens with distinct pathogenic features from their parents (Depotter *et al.*, 2016b; Stukenbrock, 2016b). We demonstrate the genomic and transcriptomic plasticity of the allodiploid *V. longisporum* pathogen and illustrate its potential for divergent evolution. Firstly, the plastic nature of the *V. longisporum* genome is displayed by its mosaic structure (Figure 1). Mosaicism in *V. longisporum* is not driven by homogenization that played a negligible role in the aftermath of hybridization (Figure 2A). Rather, *V. longisporum* mosaic genome structure is caused by extensive genomic rearrangements after hybridization (Figure 2B). Genomic rearrangements are major drivers of evolution and facilitate adaptation to novel or changing environments (Seidl and Thomma, 2014). Genomic rearrangements are not specific to the hybrid nature of *V. longisporum* as other *Verticillium* spp. similarly encountered extensive chromosomal reshuffling (Faino *et al.*, 2016; de Jonge *et al.*, 2013; Shi-Kunne *et al.*, 2018). As expected,

the majority of the synteny breaks between the genomes of *V. longisporum* strains VLB2 and VL20 reside in repeat-rich genome regions (Figure S4) as, due to their abundance, repetitive sequences are more likely to act as a substrate for unfaithful repair of double-strand DNA breaks (Seidl and Thomma, 2014). Nonetheless, in *V. longisporum*, 43% of the synteny breaks identified are not associated with repeat-rich regions. Conceivably, the presence of two genomes also provides homeologous sequences with sufficient identity to mediate unfaithful repair. Secondly, *V. longisporum* genes globally display accelerated evolution in comparison to orthologs of non-hybrid *Verticillium* spp. This is illustrated by the increased abundance of genes under positive selection and the more divergent evolution of D1 genes in comparison to its sister species *V. dahliae* (Figure 3, S5, S6). The increased rate of divergence is likely a result of having two homeologs of most genes as this redundancy gives leeway to functional diversification (Lynch and Conery, 2001). Previously, 29 genes in *V. dahliae* were determined to evolve under positive selection, whereas in this study more than three times the amount was found (Figure S6) (de Jonge *et al.*, 2013). Here, we obtained higher numbers as a higher *P*-value cut-off was used ($P < 0.05$ and instead of $P < 0.01$). Moreover, we calculated positive selection based on the nucleotide substitutions along the *V. dahliae* species branch, whereas de Jonge *et al.* (2013) determined positive selection based on intraspecific substitutions, which is expected to have lower *Ka*/*Ks* ratios for genes under positive selection than when interspecific mutations are used (McDonald and Kreitman, 1991). Finally, allodiploidization resulted in transcriptomic alterations even though the majority of the *V. longisporum* genes was not differently expressed from *V. dahliae* orthologs (Figure 4). As species A1 and D1 are hitherto unfound in their haploid state, *V. dahliae* was used for expression pattern comparison as it only recently diverged from species D1 and therefore likely resembles D1 gene expression (Inderbitzin *et al.*, 2011b). Unfortunately, species A1 currently lacks a known sister species that could be used in the gene expression comparison (Figure 3A). Despite the absence of the *V. longisporum* parents, expression patterns between the A1 and D1 sub-genomes seem to have homogenized upon hybridization as they show more resemblance than the expression pattern between *V. dahliae* and species D1 (Figure 5, Table S2). *V. longisporum* genes that were differently expressed to *V. dahliae* orthologs are enriched for genes encoding secreted proteins (Figure 6, S8). However, that enrichment is higher for *Verticillium* grown in culture medium compared with *in planta* (Figure 6). This may be a consequence of the disappearance of expression differences between the *V. longisporum* homeologs as homeologs that encode secreted proteins homogenized their expression upon host colonization (Figure 7).

Whole-genome duplication events are usually followed by extensive gene loss, often leading to reversion to the original ploidy state (Maere *et al.*, 2005). However, the so-called 'haploidization' of *V. longisporum* has only proceeded to a limited extent, as 80% of the genes are present in two copies (Figure S2), whereas the haploid *V. dahliae* genome contains only 1% of its genes in two copies. Thus, the *V. longisporum* genome displays the symptoms of a recent allodiploid, with gene loss being an on-going process

that by now has only progressed marginally. However, the retention of both homeolog copies can also be evolutionary advantageous as the presence of an additional gene copy may facilitate functional diversification of *V. longisporum* genes in comparison to haploid *Verticillium* spp. (Figure 3, S5, S6). Gene duplication is an important mechanism for plant pathogens, including *V. dahliae* to evade host immunity (Dutheil *et al.*, 2016; Faino *et al.*, 2016; Fouche *et al.*, 2018). The LS regions of *V. dahliae*, which are enriched for active transposable elements, are derived from segmental duplications (Faino *et al.*, 2016; de Jonge *et al.*, 2013). However, instead of the specific duplication of LS regions, *V. longisporum* hybridization resulted in a whole-genome duplication likely resulting in the global acceleration of gene evolution as genes encoding secreted proteins or genes associated with niche colonization were not enriched in genes that evolve under positive selection (Figure S6, S7).

Expression divergence of a particular gene may evolve through mutations in regulatory sequences of the gene itself (cis effects), such as promoter elements, or alterations in other regulatory factors (trans effects), such as chromatin regulation (Shi *et al.*, 2012; Tirosh *et al.*, 2009). Conceivably, the surprisingly higher correlation of the sub-genome D1 expression pattern with A1 than with *V. dahliae* may originate from the disappearance of differences in trans regulators between species A1 and D1 upon hybridization as in *V. longisporum* they reside in the same nuclear environment (Figure 5, Table S2) (Tirosh *et al.*, 2009). Homogenization of expression patterns of homeologs has been similarly observed in the fungal allopolyploid *Epichloë* Lp1 (Cox *et al.*, 2014). Furthermore, the enrichment in genes encoding secreted proteins for *V. longisporum* genes that are differently regulated upon infection indicates their importance for infection, as secreted proteins play important roles in pathogen-host interactions (Gupta *et al.* 2015; Figure 7). Upon plant infection, expression of homeologs encoding secreted proteins homogenized, illustrating gene expression crosstalk between the different sub-genomes of *V. longisporum* (Figure 7). Ratio changes between homeolog expressions also occurred in synthetic allopolyploid *Arabidopsis* upon cold stress treatment (Akama *et al.*, 2014). Many of these ratio alterations were related to stress responses. Thus, conceivably, alterations in homeolog expression ratios facilitate the adjustment of allopolyploids to different environmental conditions.

Conclusions

Allodiploidization is an intrusive evolutionary mechanism that involves extensive alterations in genome, gene and transcriptome evolution. *V. longisporum* displays signatures of rapid diversifying evolution in the aftermath of hybridization, illustrated by extensive genomic rearrangements and accelerated gene evolution. Furthermore, the regulatory crosstalk between sub-genomes can adjust gene expression depending on the environment. Thus, in comparison to non-hybrid *Verticillium* spp., *V. longisporum* has a high adaptive potential that can contribute to host immunity evasion and to the further specialization towards brassicaceous plant hosts.

Acknowledgements

The authors would like to thank the Marie Curie Actions program of the European Commission that financially supported the research of J.R.L.D. Work in the laboratories of B.P.H.J.T. and M.F.S. is supported by the Research Council Earth and Life Sciences (ALW) of the Netherlands Organization of Scientific Research (NWO). We thank Sander Y.A. Rodenburg for sharing bioinformatics scripts.

Supplementary material

Table S1 | Comparison *V. longisporum* and *V. dahliae* genomes.

	V. longisporum VLB2	*V. longisporum* VL20	*V. dahliae* JR2
Genome size	72.9 Mb	72.3 Mb	36.2 Mb
Number of contigs	45	44	8
Complete chromosomes	6	4	8
Number of genes	19,123	18,784	9,909
Assigned to sub-genome A1	9,531	9,402	/
Assigned to sub-genome D1	9,468	9,243	/
Number of genes encoding secreted proteins	1,711	1,696	894
Assigned to sub-genome A1	850	843	/
Assigned to sub-genome D1	845	831	/
Telomere regions	29	30	16
Repeat content	14.28	13.90	6.49
BUSCO completeness[1]	99.0%	98.3%	98.7%

[1]Based on Ascomycota Benchmarking Universal Single-Copy Orthologs (BUSCOs)

Table S2 | Expression pattern correlation of genes between *V. dahliae* and *V. longisporum* sub-genomes. VD = *V. dahliae*, A1 = *V. longisporum* A1 sub-genome and D1 = *V. longisporum* D1 sub-genome. Correlations are calculated with the Spearman's rank correlation coefficient based on the count per million (CPM) values.

	VD	VLB2 A1	VLB2 D1	VL20 A1	VL20 D1
VD	1.00	0.82	0.86	0.85	0.88
VLB2 A1	0.82	1.00	0.90	0.95	0.88
VLB2 D1	0.86	0.90	1.00	0.88	0.95
VL20 A1	0.85	0.95	0.88	1.00	0.92
VL20 D1	0.88	0.88	0.95	0.92	1.00

Table S3 | Pfam domain enrichment for differentially expressed *V. longisporum* (expression A1 and D1 homeologs combined) and *V. dahliae* orthologs in culture medium

Pfam domain	Description	*P*-value
Strain VL20		
PF07690	*MFS_1*	2e-16
PF00067	*p450*	2e-08
PF00246	*Peptidase_M14*	6e-06
PF00732	*GMC_oxred_N*	1e-05
PF05199	*GMC_oxred_C*	1e-05
PF00083	*Sugar_tr*	5e-05
PF00743	*FMO-like*	2e-04
PF00106	*adh_short*	2e-04
PF04616	*Glyco_hydro_43*	2e-04
PF08031	*BBE*	3e-04
PF01565	*FAD_binding_4*	5e-04
PF00544	*Pec_lyase_C*	1e-03
PF03443	*Glyco_hydro_61*	1e-03
PF07992	*Pyr_redox_2*	1e-03
PF09362	*DUF1996*	2e-03
PF14856	*Hce2*	2e-03
PF13378	*MR_MLE_C*	2e-03
PF13602	*ADH_zinc_N_2*	2e-03
PF13520	*AA_permease_2*	3e-03
PF06422	*PDR_CDR*	4e-03
PF00201	*UDPGT*	5e-03
PF06985	*HET*	5e-03
PF00005	*ABC_tran*	7e-03
PF08240	*ADH_N*	7e-03
PF05572	*Peptidase_M43*	8e-03
PF01061	*ABC2_membrane*	8e-03
PF04828	*GFA*	8e-03
PF00734	*CBM_1*	8e-03
PF00199	*Catalase*	9e-03
PF00355	*Rieske*	9e-03
PF00723	*Glyco_hydro_15*	9e-03
PF06628	*Catalase_rel*	9e-03
PF16499	*Melibiase*	9e-03
PF04389	*Peptidase_M28*	9e-03

Pfam domain	Description	*P*-value
Strain VLB2		
PF07690	*MFS_1*	2e-12
PF01565	*FAD_binding_4*	6e-07
PF00067	*p450*	4e-05
PF00732	*GMC_oxred_N*	8e-05
PF05199	*GMC_oxred_C*	8e-05
PF00083	*Sugar_tr*	1e-04
PF07992	*Pyr_redox_2*	2e-04
PF00246	*Peptidase_M14*	3e-04
PF04479	*RTA1*	6e-04
PF00394	*Cu-oxidase*	8e-04
PF07731	*Cu-oxidase_2*	8e-04
PF01179	*Cu_amine_oxid*	8e-04
PF13561	*adh_short_C2*	1e-03
PF03443	*Glyco_hydro_61*	2e-03
PF00583	*Acetyltrans_1*	2e-03
PF02727	*Cu_amine_oxidN2*	3e-03
PF07732	*Cu-oxidase_3*	3e-03
PF09362	*DUF1996*	3e-03
PF14856	*Hce2*	3e-03
PF00295	*Glyco_hydro_28*	3e-03
PF00264	*Tyrosinase*	4e-03
PF13602	*ADH_zinc_N_2*	4e-03
PF08031	*BBE*	4e-03
PF03171	*2OG-FeII_Oxy*	4e-03
PF14226	*DIOX_N*	4e-03
PF00106	*adh_short*	6e-03
PF13472	*Lipase_GDSL_2*	8e-03

[1]Only *P*-values < 0.01 are reported.

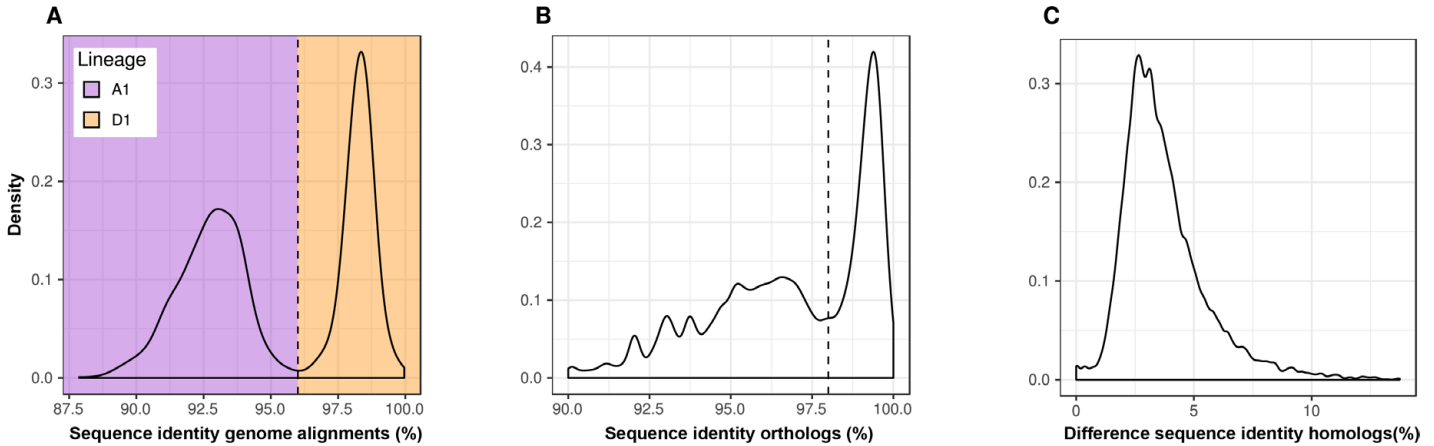

Figure S1 | Lines of evidence for the parental origin of *V. longisporum* genomic regions. (A) Distribution of sequence identity of *V. longisporum* alignments to *V. dahliae*. (B) The distribution of the sequence identity between *V. longisporum* exonic regions of genes and their *V. dahliae* orthologs. (C) Distribution of sequence identity between exonic regions of *V. longisporum* homologs that are present in two copies. Strains VLB2 and JR2 were used for *V. longisporum* and *V. dahliae*, respectively.

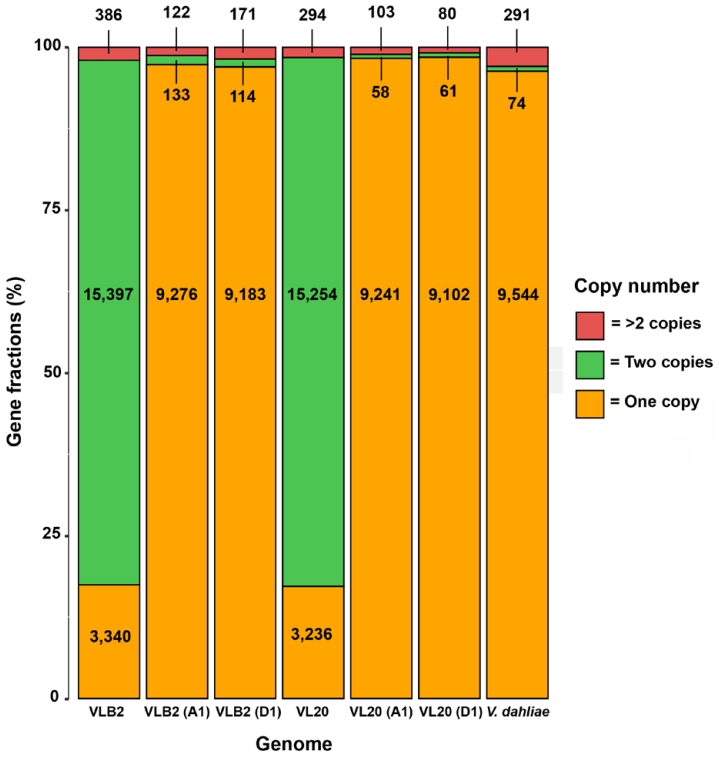

Figure S2 | Gene copy number distribution within *Verticillium* (sub-)genomes. "(A1)" and "(D1)" represent species A1 and D1 sub-genomes, respectively, of the *V. longisporum* strains VLB2 and VL20. For *V. dahliae*, the strain JR2 was used.

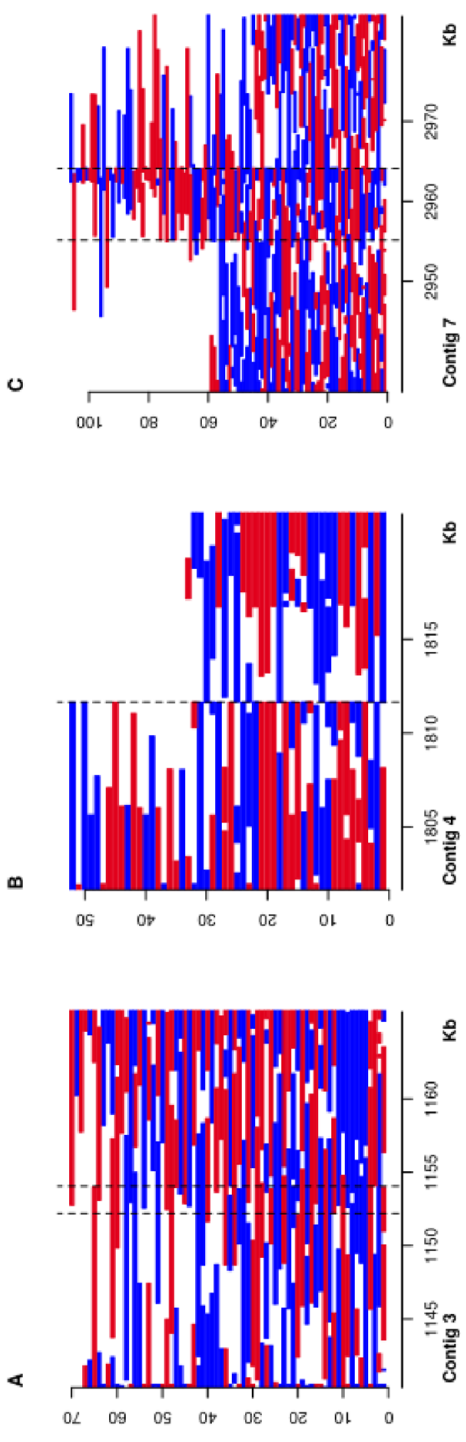

Figure S3 | Synteny break confirmation by mapping *V. longisporum* VLB2 reads to the VL20 genome. Red and blue bars represent forward and reverse aligned VLB2 reads to the VL20 genome. The dashed lines show the suggested position in synteny break through genome alignment. (A) In particular cases, read alignments did not confirm the break in synteny. (B) In other cases, breaks in synteny were confirmed as reads abruptly stopped and started on these genome positions. (C) Breaks were also considered truthful if regions showed overlap in repeat-rich regions where read overlap between adjacent genome regions is lacking.

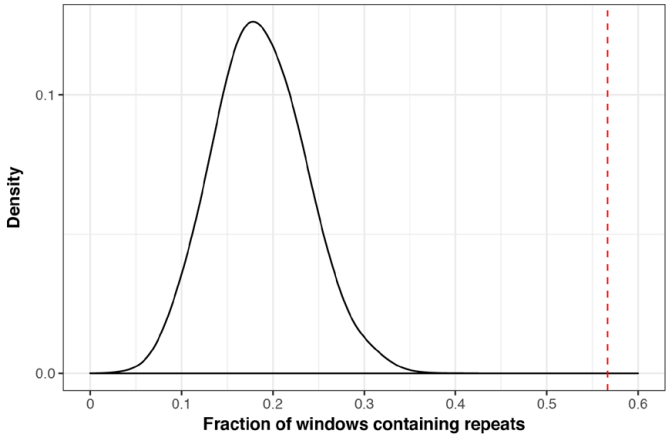

Figure S4 | The association of synteny breaks with repetitive elements. The black curve represents the fraction of 60 randomly chosen 1 kb windows in the *V. longisporum* VL20 that are repeat-rich, which has been permutated 10,000 times. The red line indicates the fraction of true breaks that lay in a 1 kb window enriched for repeats (57%).

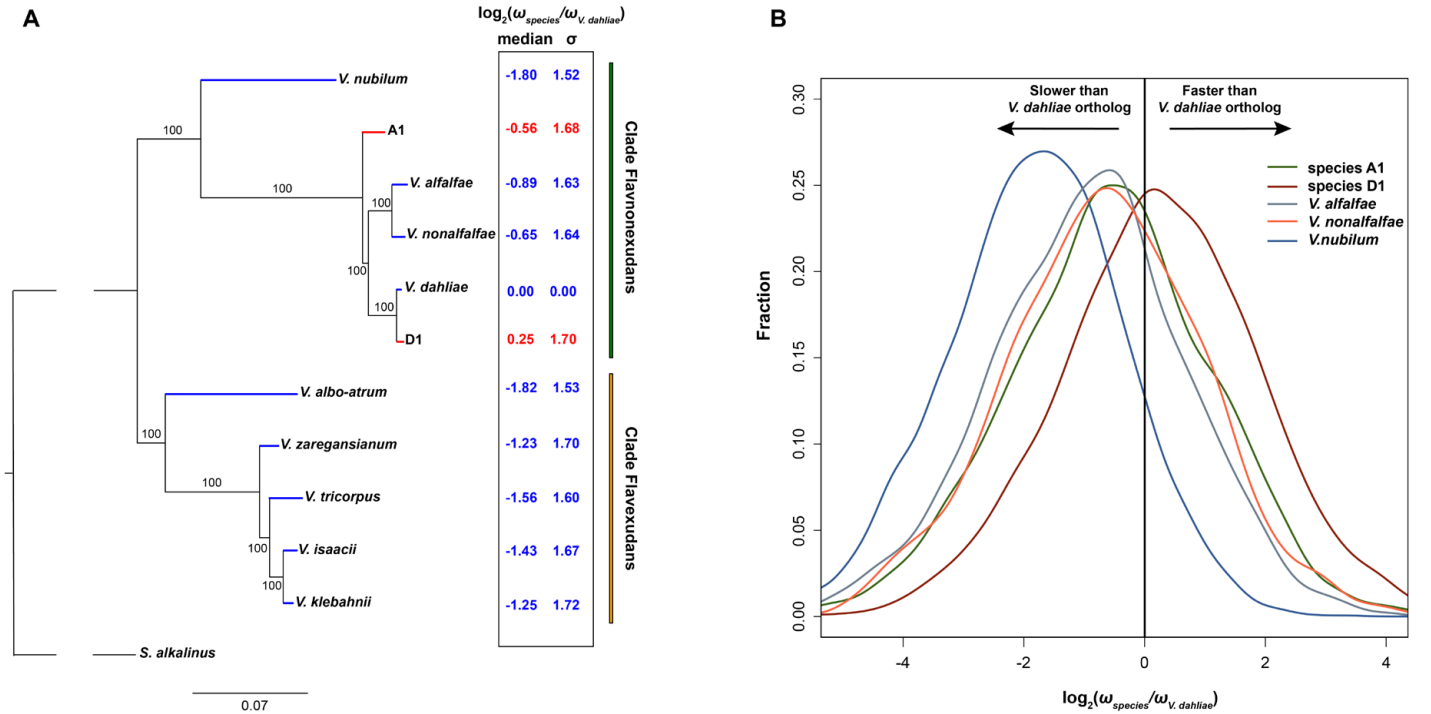

Figure S5 | Gene evolutionary speed comparison between *Verticillium* species. *Ka/Ks* ratios (ω) between *V. dahliae* and other *Verticillium* spp. were compared. (A) Blue branches in the phylogenetic tree represent *Verticillium* species with a haploid evolutionary history, whereas red branches represent species with an allodiploid phase in their evolutionary history. The median difference in evolutionary speed between *V. dahliae* and orthologs was calculated in addition to the standard deviation (σ). (B) The distribution of these differences in evolutionary speed is depicted for species of the *Verticillium* clade Flavnonexudans. For the *Verticillium* species A1 and D1, *V. longisporum* strain VL20 was used.

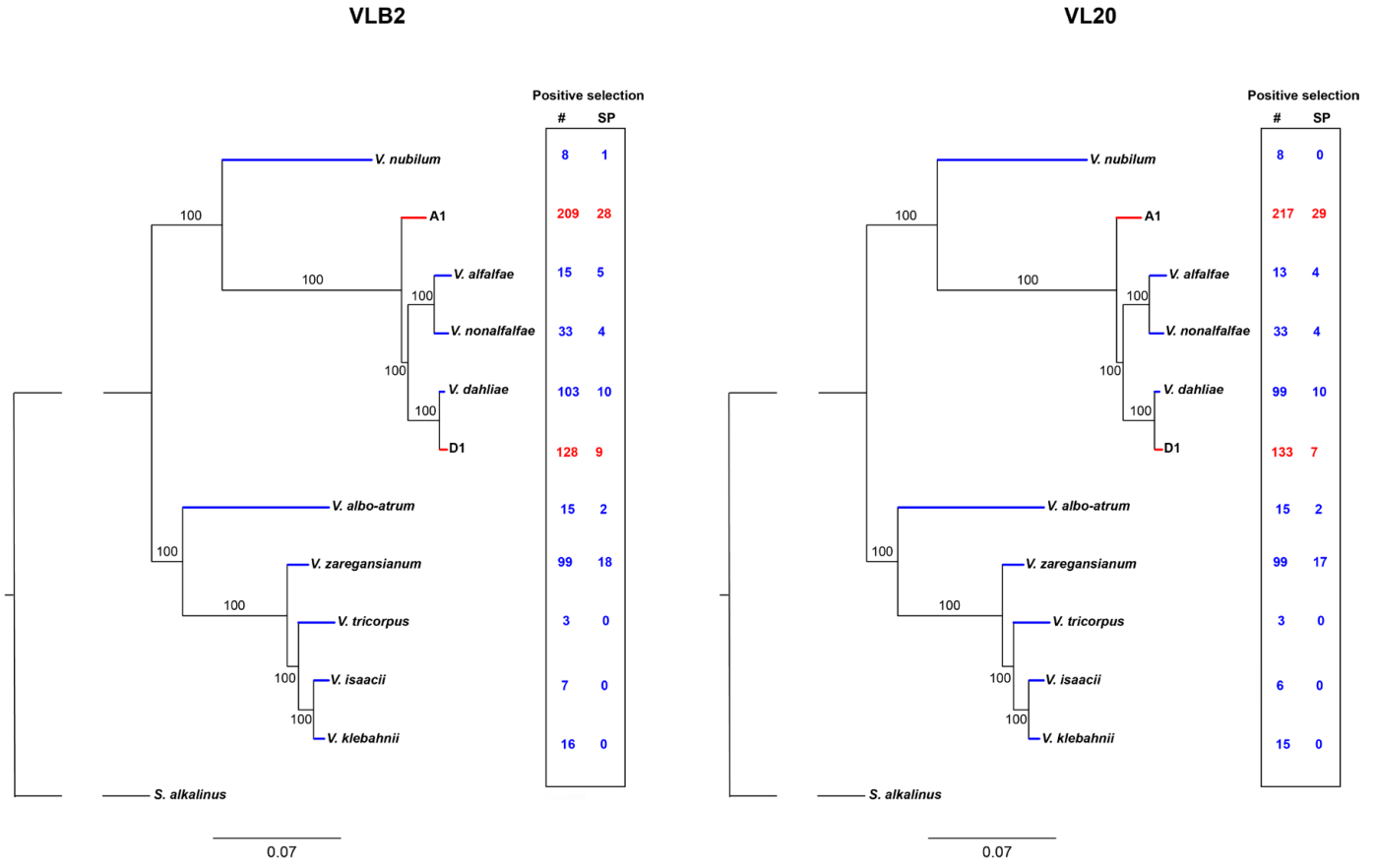

Figure S6 | Genes under positive selection in *Verticillium* species. Genes with one ortholog in every *Verticillium* spp. were tested for positive selection using a *Z*-test ($P<0.05$). # = number of genes under positive selection SP = number of genes encoding secreted proteins under positive selection.

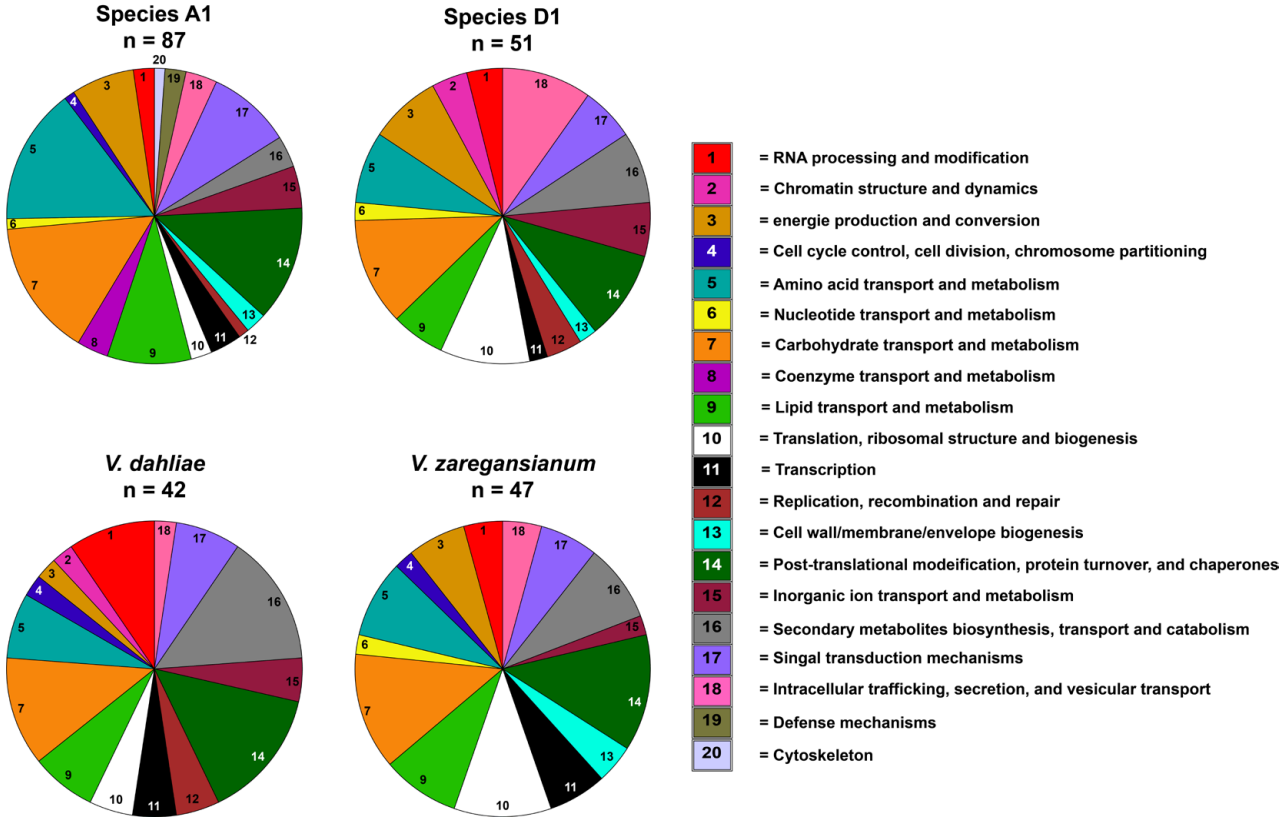

Figure S7 | Relative abundance of Clusters of Orthologous Group (COG) categories for genes under positive selection. Only genes were included were the COG category/categories could be determined. Genes under positive selection had a Z-value > 1.65 (P<0.05). For the *Verticillium* species A1 and D1, *V. longisporum* strain VLB2 was used.

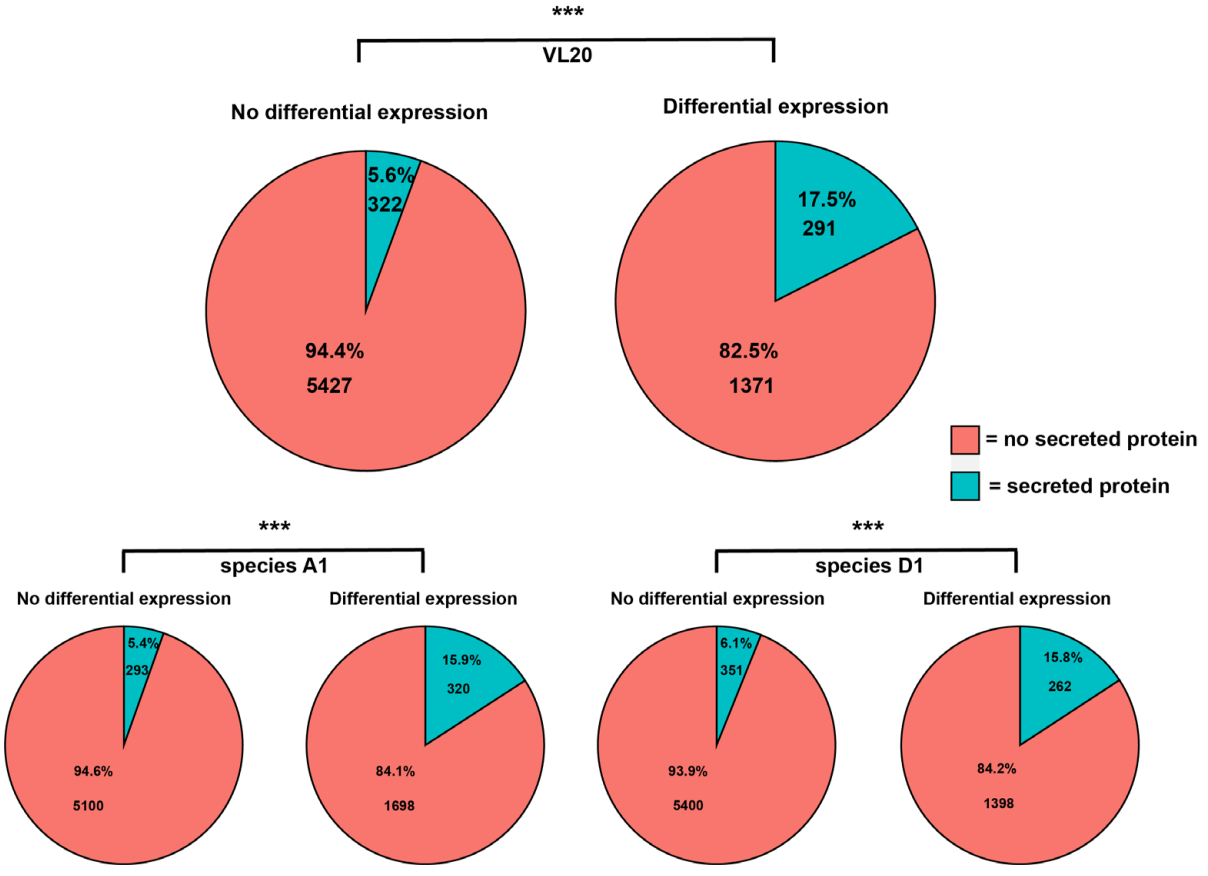

Figure S8 | Differential expression in *V. longisporum* VL20 in relation to genes encoding secreted proteins. Differential expression is calculated for species A1, species D1 and *V. longisporum* (expression A1 and D1 homeologs combined) with *V. dahliae* orthologs. Pie charts show fraction of genes encoding secreted proteins of not-differentially and differentially expressed genes, respectively. Significance of the different distributions was calculated the Fisher's exact test (ns = not significant, *** = $P<0.001$).

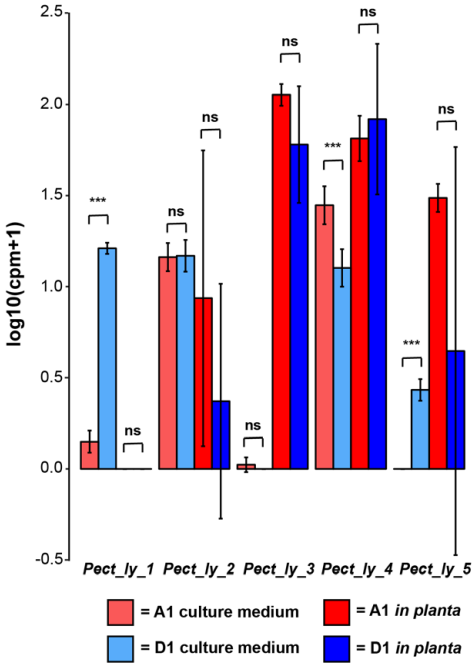

Figure S9 | Expression comparison of genes with a pectate lyase domain (PF03211). Gene expressions are depicted for species A1 and species D1 homeologs of *V. longisporum* cultured in liquid medium and upon oilseed rape colonization, respectively. Bars represent the mean gene expression and error bars represent the standard deviation. The significance of difference in gene expression was calculated using *t*-tests relative to a threshold (TREAT) (McCarthy and Smyth, 2009). Level of significance: ns = not significant and *** = $P<0.001$.

8

Dynamic virulence-related regions of the fungal plant pathogen *Verticillium dahliae* display remarkably enhanced sequence conservation

Jasper R.L. Depotter[†]
Xiaoqian Shi-Kunne[†]
Hélène Missonnier[#]
Tingli Liu[#]
Luigi Faino
Grardy C.M. van den Berg
Thomas A. Wood
Baolong Zhang[*]
Alban Jacques[*]
Michael F. Seidl[$]
Bart P.H.J. Thomma[$]

[†]These authors contributed equally
[#]These authors contributed equally
[*]These authors contributed equally
[$]These authors contributed equally

Abstract

Selection pressure impacts genomes unevenly, as different genes adapt with differential speed to establish an organism's optimal fitness. Plant pathogens co-evolve with their hosts, which implies continuously adaption to evade host immunity. Effectors are secreted proteins that mediate immunity evasion, but may also typically become recognized by host immune receptors. To facilitate effector repertoire alterations, in many pathogens, effector genes reside in dynamic genomic regions that are thought to display accelerated evolution, a phenomenon that is captured by the two-speed genome hypothesis. The genome of the vascular wilt pathogen *Verticillium dahliae* has been proposed to obey a similar two-speed regime with dynamic, lineage-specific regions that are characterized by genomic rearrangements, increased transposable element activity and enrichment in *in planta*-induced effector genes. However, little is known of the origin of, and sequence diversification within, these lineage-specific regions. Based on comparative genomics among *Verticillium* spp. we now show differential sequence divergence between core and lineage-specific genomic regions of *V. dahliae*. Surprisingly, we observed that lineage-specific regions display markedly increased sequence conservation. Since single nucleotide diversity is reduced in these regions, host adaptation seems to be merely achieved through presence/absence polymorphisms. Increased sequence conservation of genomic regions important for pathogenicity is an unprecedented finding for filamentous plant pathogens and signifies the diversity of genomic dynamics in host-pathogen co-evolution.

Introduction

Numerous microbes engage in symbiotic relationships with plants, comprising beneficial, commensalistic and parasitic relationships where each partner evolves towards its optimal fitness. Consequently, parasitic interactions between plants and microbial pathogens evolve as arms races in which plants try to halt microbial ingress while pathogens strive for continued symbiosis (Cook *et al.*, 2015; Jones and Dangl, 2006; Thomma *et al.*, 2011). In such arms races, plant pathogens evolve repertoires of effector proteins, many of which deregulate host immunity, to enable host colonization (de Jonge *et al.*, 2011; Rovenich *et al.*, 2014). Plants, in turn, evolve immune receptors that recognize various molecular patterns that betray microbial invasion; so-called invasion patterns that can also include effectors (Cook *et al.*, 2015). Consequently, pathogen effector repertoires are typically subject to selective forces that often result in rapid diversification.

Effector genes are often not randomly organized in genomes of filamentous plant pathogens (Dong *et al.*, 2015). For instance, effector genes of the potato late blight pathogen *Phytophthora infestans* reside in repeat-rich regions that display increased structural polymorphisms and enhanced levels of positive selection (Haas *et al.*, 2009; Raffaele *et al.*, 2010). Based on this and observations in other pathogenic species, it has been proposed that many pathogens have a bipartite genome architecture with essential household genes residing in the core genome and effector genes co-localizing in repeat-rich compartments; a phenomenon that has been coined a two-speed genome (Croll and McDonald, 2012; Raffaele and Kamoun, 2012; Seidl and Thomma, 2017). Conceivably, such genome compartmentalization increases the evolutionary efficiency as basal functions of core genes are "shielded off" from increased evolutionary dynamics that rapidly diversify effector gene repertoires. Repeat-rich genome regions display signs of such accelerated evolution as they are often enriched for structural variations such as presence/absence polymorphisms (Raffaele *et al.*, 2010) or chromosomal rearrangements (Faino *et al.*, 2016; de Jonge *et al.*, 2013). In addition, increased diversification is also displayed on sequence levels in the form of higher substitution rates (Cuomo *et al.*, 2007; van de Wouw *et al.*, 2010) with a higher fraction of non-synonymous substitutions in genes located in repeat-rich regions compared to core genes (Raffaele *et al.*, 2010; Sperschneider *et al.*, 2015; Stukenbrock *et al.*, 2010).

Verticillium is a genus of Ascomycete fungi, containing notorious plant pathogens of numerous crops, including tomato, cotton, olive and oilseed rape (Inderbitzin and Subbarao, 2014). *Verticillium* spp. are soil-borne fungi that infect their hosts via the roots and then colonize xylem vessels, resulting in vascular occlusion by host depositions and by the physical presence of the pathogen itself (Fradin and Thomma, 2006). Currently, ten *Verticillium* species are described (Inderbitzin *et al.*, 2011a). All these *Verticillium* spp. are haploids, except for *V. longisporum* that is an interspecific hybrid that contains approximately twice the amount of genetic material of haploid

Verticillium spp. (Depotter *et al.*, 2017b; Inderbitzin *et al.*, 2011b). *V. dahliae* is the most notorious plant pathogen within the *Verticillium* genus, causing disease on hundreds of plant species (Inderbitzin and Subbarao, 2014). Similarly, *V. albo-atrum*, *V. alfalfa*, *V. nonalfalfae* and *V. longisporum* are pathogenic, albeit with more confined host ranges (Inderbitzin *et al.*, 2011a; Inderbitzin and Subbarao, 2014). The remaining *Verticillium* spp., namely *V. isaacii*, *V. klebahnii*, *V. nubilum*, *V. tricorpus* and *V. zaregamsianum,* sporadically cause disease on plants and are considered opportunists with a mainly saprophytic life style rather than genuine plant pathogens (Ebihara *et al.*, 2003; Gurung *et al.*, 2015; Inderbitzin *et al.*, 2011a).

Verticillium spp. are thought to have a predominant, if not exclusive, asexual reproduction as a sexual cycle has never been described for any of the species (Short *et al.*, 2014). However, mating types, meiosis-specific genes and genomic recombination between clonal lineages have been observed for *V. dahliae*, suggesting that sexual reproduction is either cryptic or ancestral (Milgroom *et al.*, 2014; Short *et al.*, 2014). Nevertheless, mechanisms different from meiotic recombination contribute to the genomic diversity of *V. dahliae*, such as large-scale genomic rearrangements, horizontal gene transfer and transposable element (TE) activity (Faino *et al.*, 2016; de Jonge *et al.*, 2012, 2013; Seidl and Thomma, 2014). Signs of these evolutionary mechanisms converge on particular genomic regions that are enriched in repeats and lineage-specific (LS) sequences (Faino *et al.*, 2016; de Jonge *et al.*, 2013; Klosterman *et al.*, 2011). Intriguingly, also *in planta*-induced effector genes are enriched in these LS regions (de Jonge *et al.*, 2013).

We previously reported that LS regions of *V. dahliae* are largely derived from segmental duplications (Faino *et al.*, 2016). Gene duplications are important sources for functional diversification (Magadum *et al.*, 2013), and thus here we aim to investigate whether and how the nucleotide sequences within the LS regions diverge. To this end, comparative genomics was performed across the *Verticillium* genus to identify genomic regions showing accelerated and reduced rates of sequence diversification to further characterize the two-speed genome of *V. dahliae*.

Material and methods

Genome sequencing and assembly of *Verticillium* isolates

In total, we used 18 *Verticillium* genomes in this study (Table S2). Genomes of *V. albo-atrum* PD747, *V. alfalfae* PD683, *V. dahliae* JR2 and VdLs17, *V. isaacii* PD618, *V. klebahnii* PD401, *V. nubilum* PD621, *V. tricorpus* PD593 and MUCL9792, *V. zaregamsianum* PD739 were previously sequenced and assembled (Faino *et al.*, 2015; Klosterman *et al.*, 2011; Seidl *et al.*, 2015; Shi-Kunne *et al.*, 2018). Furthermore, sequence reads of the two *V. nonalfalfae* isolates (TAB2 and Rec) were publically available (Bioproject PRJNA283258) (Jakše *et al.*, 2018). *Verticillium* strains CQ2, 85S, PD670, PD660, PD659 and PD736 were sequenced in this study. To this end, we isolated genomic DNA from

conidia and mycelium fragments that were harvested from cultures that were grown in liquid potato dextrose agar according to the protocol described by Seidl *et al.* (2015). We sequenced *V. dahliae* strains CQ2 and 85S by single molecule real time (SMRT) sequencing. The PacBio libraries for sequencing on the PacBio RSII platform (Pacific Biosciences of California, CA, USA) were constructed as described previously by Faino *et al.* (2015). Briefly, DNA was mechanically sheared and size selected using the BluePippin preparation system (Sage Science, Beverly, MA, USA) to produce ~20 kb size libraries. The sheared DNA and final library were characterized for size distribution using an Agilent Bioanalyzer 2100 (Agilent Technology, Inc., Santa Clara, CA, USA). The PacBio libraries were sequenced on four SMRT cells per *V. dahliae* isolate using the PacBio RS II instrument at the Beijing Genome Institute (BGI, Hong Kong) for CQ2 and at KeyGene N.V. (Wageningen, the Netherlands) for 85S, respectively. Sequencing was performed using the P6-C4 polymerase-Chemistry combination and a >4 h movie time and stage start. Filtered sub-reads for CQ2 and 85S, were assembled using the HGAP v3 protocol (Table S1) (Chin *et al.*, 2013).

For PD670, PD660, PD659 and PD736, two libraries (500 bp and 5 Kb insert size) were prepared and sequenced using the Illumina High-throughput sequencing platform (KeyGene N.V., Wageningen, The Netherlands). In total, ~18 million paired-end reads (150 bp read length; 500 bp insert size library) and ~16 million mate-paired read (150 bp read length; 5 kb insert size library) were produced per strain. We assembled the genomes using the A5 pipeline (Tritt *et al.*, 2012), and we subsequently filled the remaining sequence gaps using SOAPdenovo2 (Luo *et al.*, 2012). After obtaining the final assemblies, we used QUAST (Gurevich *et al.*, 2013) to calculate genome statistics. Gene annotation for *V. dahliae* strain JR2 and other *Verticillium* spp. were obtained from Faino *et al.* (2015) and Shi-Kunne *et al.* (2018). Genes for *V. isaacii* strain PD660 were annotated with the Maker2 pipeline according to Shi-Kunne *et al.* (2018) (Holt and Yandell, 2011).

Comparative genome analysis

The alignments of *Verticillium* sequences to a reference genome were performed with nucmer, which is part of the mummer package (v3.1) (Kurtz *et al.*, 2004). Here, we used a repeat-masked genome as a reference in order to prevent assigning high sequence identities to repetitive elements. Repetitive elements were identified using RepeatModeler (v1.0.8) based on known repetitive elements and on *de novo* repeat identification, and genomes were subsequently masked using RepeatMasker (v4.0.6; sensitive mode) (Smit *et al.*, 2015).

Linear plots showing alignments within and closely adjacent JR2 LS regions were plotted with the R package genoPlotR (Guy *et al.*, 2011) (Figure 2, S3). The *Verticillium* phylogenetic tree adjacent to the genoPlotR plots was previously generated using 5,228 single-copy orthologs that are conserved among all of the genomes (Shi-Kunne *et al.*, 2018). The phylogenetic tree of *V. dahliae* strains was constructed using REALPHY (Bertels *et al.*, 2014) (Figure S1).

Alignments > 7.5 kb in length were depicted along the reference genome with the R package Rcircos (Figure 3,4) (Zhang *et al.*, 2013a). LS sequences were defined by alignment of different strains to a reference using nucmer (v3.1) (Kurtz *et al.*, 2004) and regions were determined using BEDTools v2.25.0 (Quinlan and Hall, 2010).

Lineage-specific regions of *V. dahliae* and *V. tricorpus* were arbitrarily delimited based on the abundance of LS sequences and increased sequence conservation (Table S8). The pairwise identity of the genome-wide and LS regions between *V. dahliae*/*V. tricorpus* and other haploid *Verticillium* spp. was calculated using nucmer (mum), with dividing the respective query sequences into non-overlapping windows of 500 bp (Table 1). Sequence identities of the coding regions of genes and intergenic regions were retrieved by BLAST (v2.2.31+) searches between strains *V. dahliae* JR2 and *V. nonalfalfae* TAB2 (Figure 6) (Altschul *et al.*, 1990). Hits with a minimal coverage of 80% with each other were selected. Intergenic regions of JR2 were fractioned in 5 kb windows with BEDTools v2.25.0 and similarly blasted to the genome of TAB2 (Figure 6) (Quinlan and Hall, 2010). Hits with a maximal bit-score and minimal alignment of 500 bp to a window were selected. To compare the rate of synonymous and non-synonymous substitutions between the core and LS regions, *Ka* and *Ks* were of orthologs of JR2 and TAB2 were determined using the Nei and Gojobori method (Nei and Gojoborit, 1986) in PAML (v4.8) (Yang, 2007). Significance of positive selection was tested using a Z-test (Stukenbrock and Dutheil, 2012). Z-values >1.65 were considered significant with $P<0.05$. Secreted proteins were predicted by SignalP4 (Petersen *et al.*, 2011).

Pfam function domains of JR2 proteomes were predicted using InterProScan (Jones *et al.*, 2014). Subsequently, Pfam enrichment of genes residing in LS regions was carried out using hypergeometric tests, and significance values were corrected using the Benjamini-Hochberg false discovery method (Benjamini and Hochberg, 1995).

The pan-LS-genome was constructed based on following *Verticillium* isolates: JR2 (*V. dahliae*), PD683 (*V. alfalfae*), PD593 (*V. tricorpus*) and PD401 (*V. klebahnii*). Genome regions of these for species with increased sequence conservation were combined (Table S8). Repeat masked regions were removed from the pan-LS-genome using BEDTools v2.25.0 (Quinlan and Hall, 2010). Additionally, regions in duplicate (≥90% identity, ≥100 bp) in the pan-LS-genome were determined using nucmer (v3.1) (Kurtz *et al.*, 2004) and subsequently removed with using BEDTools v2.25.0 (Quinlan and Hall, 2010). As a result, a pan-LS-genome was constructed without regions in duplicate. The fractions of pan-LS-genome that were present in every individual *Verticillium* strain, was determined using nucmer (v3.1) (Kurtz *et al.*, 2004). The clade pan-LS-genomes were constructed by combining all the pan-LS-genome regions that are present in the *Verticillium* clade isolates, which was then also removed from duplicate regions.

Results

LS sequences reside in four regions of the genome of *V. dahliae* strain JR2

Previously, we identified regions in the genome sequence of *V. dahliae* isolate JR2 that lack synteny to various other *V. dahliae* strains, including the completely sequenced genome of strain VdLs17, and thus these regions have been referred to as LS regions (Faino *et al.*, 2015, 2016). In *V. dahliae* isolate JR2, the majority of these LS sequences cluster into four genomic regions; chromosomes 2 and 4 each contain one LS region, while two distinct LS regions reside on chromosome 5. To further characterize these LS regions, we here pursued high-quality genome assemblies of additional *V. dahliae* strains based on single-molecule real-time (SMRT) using the PacBio RSII system. Since *V. dahliae* strains JR2 and VdLs17 only recently diverged (de Jonge *et al.*, 2013), we selected two *V. dahliae* strains that are more diverged (Figure S1), namely strains CQ2 and 85S isolated from cotton in China and sunflower in France, respectively. We generated 430,378 (~110x coverage) and 500,428 (~130x coverage) filtered sub-reads for strains CQ2 and 85S, respectively, that were assembled into 17 and 40 contigs with a total size of 35.8 and 35.9 Mb, respectively (Table S1), which is similar to the telomere-to-telomere assemblies of strains JR2 (36.2 Mb) and VdLs17 (36.0 Mb) (Faino *et al.*, 2015). Subsequently, the assemblies of strains VdLs17, CQ2 and 85S were individually aligned to JR2 assembly. In total, 2.0%, 7.1% and 6.6% of the JR2 genome was not covered by sequences from VdLs17, CQ2 and 85S respectively, and 1.4% of the JR2 genome sequence could not be identified in any of the three other *V. dahliae* strains. The vast majority (88%, 82% and 91% for VdLs17, CQ2 and 85S, respectively) of these JR2 sequences without alignment is located in the previously identified four LS regions (Figure 1). Thus, despite the addition of more diverged *V. dahliae* strains, intraspecific presence/absence polymorphisms converge on the four previously identified genomic regions that are thus significantly more dynamic than other parts of the genome.

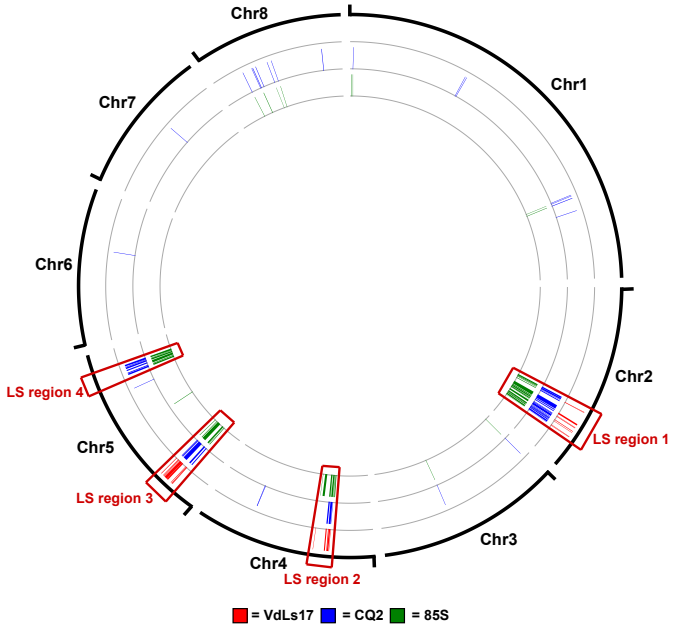

Figure 1 | Locations of lineage-specific (LS) regions in the genome of *V. dahliae* strain JR2. LS regions were determined by individual comparisons to *V. dahliae* strains VdLs17 (red), CQ2 (blue) and 85S (green). Sequences of minimum 7.5 kb without an alignment to at least one of the other isolates are depicted at their respective position on the *V. dahliae* strain JR2 genome.

LS regions share increased sequence identity to other *Verticillium* spp.

To study interspecific sequence conservation, we aligned sequences of the phylogenetically closely related and previously sequenced *V. nonalfalfae* strain TAB2 (Jakše *et al.*, 2018; Shi-Kunne *et al.*, 2018) to the genome assembly of *V. dahliae* strain JR2. While most of the genome of *V. dahliae* JR2 aligns with *V. nonalfalfae* strain TAB2 with a genome-wide average sequence identity of ~92%, particular genomic regions display an increased sequence identity, even up to 100% (Figure S2). Intriguingly, these regions co-localize with the LS regions of *V. dahliae* strain JR2, implying that these LS regions are either derived from a recent horizontal transfer, subject to negative selection that depletes sequence polymorphisms, or encounter lower mutation rates.

In order to evaluate whether LS sequences also display increased sequence conservation when compared with other *Verticillium* spp., we aligned sequences of all other haploid *Verticillium* spp. to the *V. dahliae* JR2 genome assembly. These genomic data were previously generated (Jakše *et al.*, 2018; Shi-Kunne *et al.*, 2018), apart from the data for *V. isaacii* strain PD660 that we sequenced using the Illumina HiSeq2000 platform (Table S2). Genomic sequences of *V. dahliae* (windows of 500 bp) were aligned to the other *Verticillium* spp., displaying median identities ranging from 88 to 95% (Table 1).

These percentages correspond to the phylogenetic distance of the respective species to *V. dahliae*. Sequence identities were similarly calculated in windows for the LS regions. Intriguingly, the LS regions displayed significantly increased sequence identities when compared with the core genome (Figure 2, Table 1), ranging from 92.3% median sequence identity for *V. zaregamsianum*, which is one of the phylogenetically most distantly related species to *V. dahliae*, to 100% median sequence identity for *V. alfalfae* and *V. nonalfalfae*. Thus, based on the genus-wide occurrence and a differential degree of sequence identity that reflects the phylogenetic distance to *V. dahliae*, we conclude that LS regions display increased sequence conservation when compared with the core genome, rather than originate from horizontal transfer events.

Table 1 | Sequence identities between *V. dahliae* (JR2) and other haploid *Verticillium* species (excluding repetitive regions).

Species/strain	Genome-wide[a] (%)	LS regions[a] (%)	# windows aligned to LS regions[b]	*P*-value[c]
V. albo-atrum/PD747	88.8 (4.5)	97.6 (3.7)	146	2.2e-16
V. alfalfae/PD683	94.6 (3.9)	100.0 (3.5)	465	2.2e-16
V. nonalfalfae/TAB2	94.8 (4.1)	100.0 (2.9)	1037	2.2e-16
V. nubilum/PD621	88.4 (3.7)	95.6 (4.3)	144	2.2e-16
V. tricorpus/PD593	89.0 (4.3)	97.2 (4.1)	162	2.2e-16
V. isaacii/PD660	88.8 (4.5)	98.6 (4.4)	189	2.2e-16
V. klebahnii/PD401	88.8 (4.0)	97.8 (5.3)	87	2.2e-16
V. zaregamsianum/PD739	88.8 (3.6)	92.3 (4.2)	38	1.56e-5

[a] The percentage is the median sequence identity and the number between the brackets is the standard deviation.
[b] Windows of 500 bp
[c] The *P*-value was calculated with a two-sided Wilcoxon rank-sum test

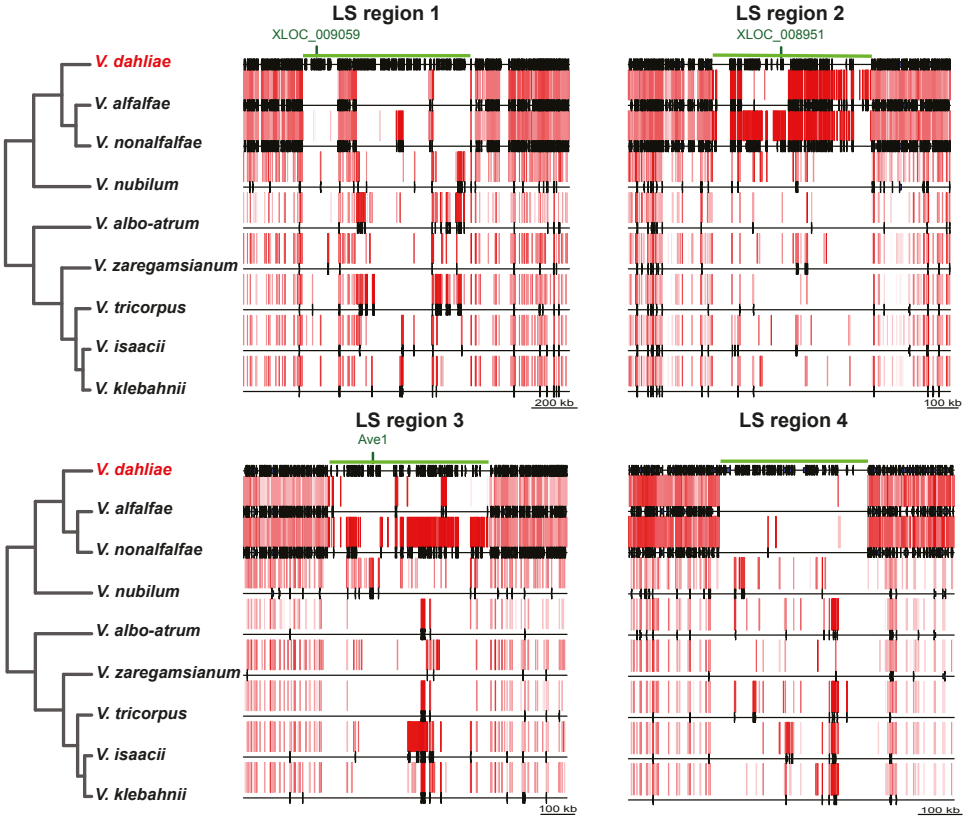

Figure 2 | Interspecific alignments and sequence identity within and immediately adjacent to lineage-specific (LS) regions of *V. dahliae*. The green line indicates the extent of the LS region. The pink/red bars are *Verticillium* sequences alignments to JR2, whereas the intensity of their color represents relative sequence identity for every *Verticillium* spp. individually (higher identity = red, lower identity = pink). The black, vertical stripes on the synteny lines represent predicted gene positions. For *V. dahliae* JR2, all predicted genes are depicted, whereas for other species only genes are depicted if these were successfully aligned. Locations of characterized *V. dahliae* effector genes are indicated: *Ave1*, *XLOC_008951* and *XLOC_009059* (de Jonge *et al.* 2012, 2013). Strains used in this figure: *V. dahliae* JR2, *V. alfalfae* PD683, *V. nonalfalfae* TAB2, *V. nubilum* PD621, *V. albo-atrum* PD747, *V. zaregamsianum* PD739, *V. tricorpus* PD593, *V. isaacii* PD660 and *V. klebahnii* PD401.

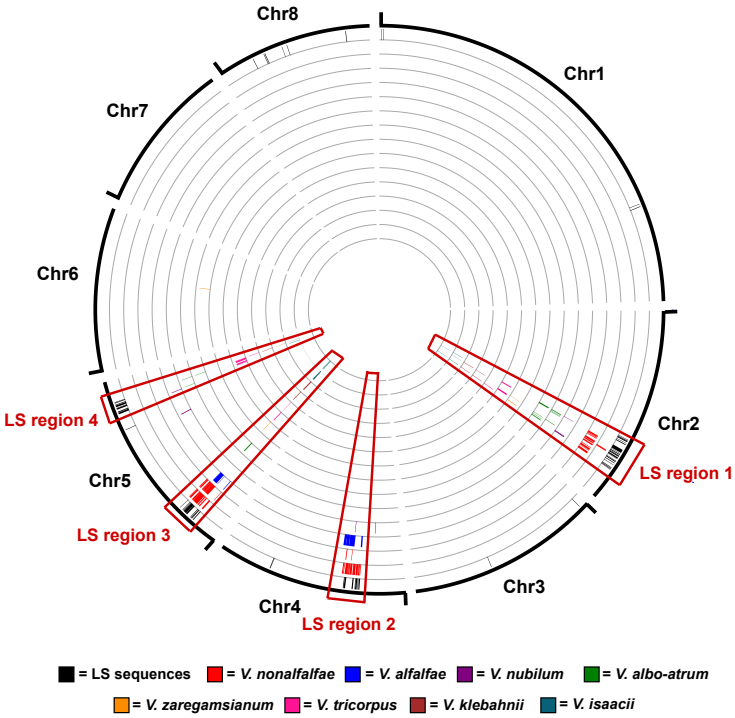

Figure 3 | Regions of particular high sequence identity between *V. dahliae* and other haploid *Verticillium* species. Black bars correspond to lineage-specific sequences of *V. dahliae* strain JR2 (for details, see Figure 1). Sequences (≥7.5 kb) with high sequence identity in any of the other *Verticillium* spp. (≥96% for *V. alfalfae* and *V. nonalfalfae*, ≥90% for all other *Verticillium* spp.) are plotted at the corresponding position on the genome of *V. dahliae* strain JR2. Plotting order for the different *Verticillium* strains from the outside to inside of the circle: *V. dahliae* JR2 *V. nonalfalfae* TAB2 and Rec, *V. alfalfae* PD683, *V. nubilum* PD621, *V. albo-atrum* PD670 and PD747, *V. zaregamsianum* PD736 and PD739, *V. tricorpus* PD593 and MUCL9792, *V. klebahnii* PD401 and PD659, *V. isaacii* PD618 and PD660.

In order to evaluate whether the increased sequence conservation is specific only to LS regions, we aligned *Verticillium* sequences of high identity to the complete *V. dahliae* JR2 genome. For several species we used multiple strains at this stage. While some of these strains were previously sequenced (Table S2) (Jakše *et al.*, 2018; Seidl *et al.*, 2015; Shi-Kunne *et al.*, 2018) others were newly sequenced (*V. albo-atrum* strain PD670, *V. klebahnii* strain PD659 and *V. zaregamsianum* strain PD736) using the Illumina HiSeq2000 platform. Nearly all (99-100%) of the *V. alfalfae* and *V. nonalfalfae* sequences that display >96% identity to *V. dahliae* strain JR2 sequenced localized in LS regions (Figure 3). Similarly, sequences of at least 100 kb with >90% identity of other *Verticillium* spp. mapped to *V. dahliae* JR2 LS regions, ranging from 70% in *V. nubilum* PD621 tot 95% in *V. albo-atrum* PD670 and *V. tricorpus* PD593 (Table S3). In conclusion, increased sequence conservation is a genomic feature that is specifically associated with LS regions in *V. dahliae*.

LS regions with increased sequence conservation are not unique to *V. dahliae*

To investigate whether other *Verticillium* spp. similarly carry LS regions that display increased sequence conservation, we performed alignments using *V. tricorpus* strain PD593 as a reference because of its high degree of completeness, as seven of the nine scaffolds likely represent complete chromosomes (Table S2) (Shi-Kunne *et al.*, 2018). Furthermore, this species belongs to the Flavexudans clade in contrast to *V. dahliae* that belongs to the Flavnonexudans clade. LS sequences of *V. tricorpus* strain PD593 were determined by comparison to *V. tricorpus* strain MUCL9792 (Seidl *et al.*, 2015). In total, 98% of the PD593 genome could be aligned to MUCL9792. However, 48% of the sequences that are specific for *V. tricorpus* strain PD593 resided in one genomic region of 41 kb on scaffold 1 (Figure 4). Like for *V. dahliae* strain JR2, we were able to align sequences of other *Verticillium* spp. with high identity to the *V. tricorpus* strain PD593 genome (Figure 4): *V. isaacii*, *V. klebahnii* and *V. zaregamsianum* display a median genome identity of ~95% to *V. tricorpus*, while other haploid *Verticillium* spp. display ~88-89% median genome identity. Notably, regions that display significant higher sequence identify localized at the LS region on scaffold 1 region, but also to an additional region of 23 kb on scaffold 6 (Figure 4, S3). For *Verticillium* strains with total alignments of at least 100 kb of high-identity sequences, the fraction of high-identity sequences that aligned to the scaffold 1 and 6 genome loci ranged from 49% for *V. nubilum* (PD621) up to 84% for *V. albo-atrum* (PD747) (Table S4). As expected, the sequence identity to six of the eight other haploid *Verticillium* spp. was significantly higher in these two genome loci compared to the genome-wide median (Table S5). No increase in sequence identity was found in alignments with *V. alfalfae* strain PD683 and *V. zaregamsianum* strain PD739 as only few regions with high sequence identity aligned to strain PD593 (Table S4). Strains PD683 and PD739 only aligned 2 and 37 windows of 500 bp, respectively, to scaffold 1 and 6 loci of PD593 (Figure S3, Table S5). In conclusion, LS regions with increased sequence conservation are not unique to *V. dahliae*, but also occur in *V. tricorpus*, and thus likely in other *Verticillium* spp. as well.

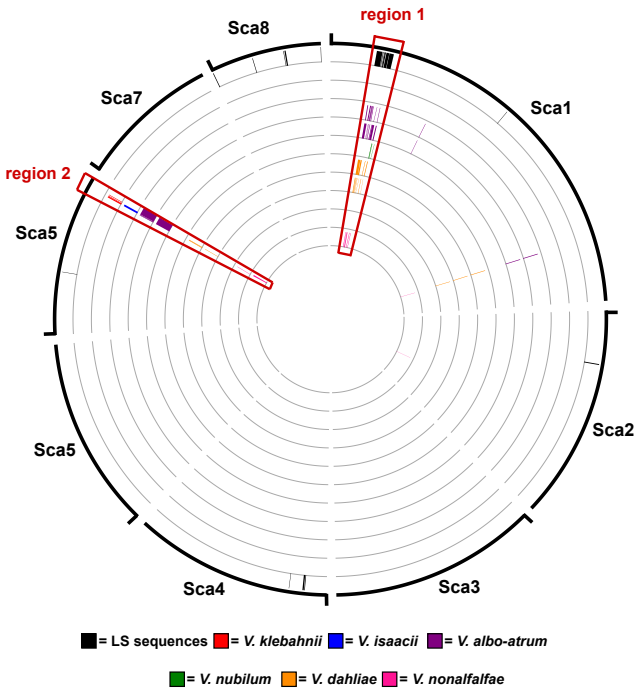

Figure 4 | Regions of particular high sequence identity between *V. tricorpus* and other haploid *Verticillium* species. The eight biggest scaffolds of PD593 are depicted, as these comprise over 99.5% of the genome. Black bars correspond to LS sequences (≥7.5 kb) in the PD593 genome without alignments to *V. tricorpus* strain MUCL9792. Sequences (≥7.5 kb) with relatively high sequence identity in any of the other *Verticillium* spp. (≥96% *V. isaacii, V. klebahnii* and *V. zaregamsianum*, ≥90% for all other *Verticillium* spp.) are plotted at the corresponding position on the genome of *V. tricorpus* strain PD593. Plotting order for the different *Verticillium* strains from the outside to inside of the circle: *V. tricorpus* PD593, *V. klebahnii* PD659, *V. isaacii* PD660, *V. albo-atrum* PD670 and PD747, *V. nubilum* PD621, *V. dahliae* JR2, VdLs17 and 85S, *V. nonalfalfae* TAB2 and Rec. Non-depicted *Verticillium* strains did not have sequences (≥7.5 kb) with previously mention identity to PD593.

The pan-LS-genome distribution across the *Verticillium* genus.

The increased conservation of LS sequences in two diverged *Verticillium* species indicates that the origin of many of the LS regions is ancestral and predates their speciation. Hence, we constructed a pan-LS-genome to determine the distribution of conserved sequences across the *Verticillium* genus. To compose a pan-LS-genome, we combined regions with increased sequence conservation of four *Verticillium* spp., namely *V. dahliae* strain JR2, *V. alfalfae* strain PD683, *V. tricorpus* strain PD593 and *V. klebahnii* strain PD401, motivated by their high assembly contiguity and distribution throughout the *Verticillium* genus (Inderbitzin *et al.*, 2011a; Shi-Kunne *et al.*, 2018). After removal of repetitive and duplicated sequences, we obtained a pan-LS-genome of ~2 Mb, of which 60% occurs in genomes of clade Flavexudans and 72% in clade Flavnonexudans (clade pan-LS-genomes) (Figure 5). Next, the distribution of the pan-LS-genome and the clade pan-LS-genomes was evaluated for all *Verticillium* strains individually (Figure 5 and Table S6). The proportion of the LS-pan-genome differed

markedly between *Verticillium* strains and ranged from 12% for *V. nubilum* strain PD621 up to 58% for *V. dahliae* strain JR2 (Figure 5). Notably, by using a limited number of isolates in the consensus reconstruction, retentions are likely biased towards strains that are phylogenetically closer related to the species that were used to compose the pan-genome: *V. alfalfa*, *V. dahliae*, *V. klebahnii* and *V. nonalfalfae*. However, *V. albo-atrum* strains contained considerably more of the pan-LS-genome compared to *V. zaregamsianum* and *V. isaacii* strains, despite its phylogenetically more distant relation to *V. klebahnii* and *V. tricorpus* (Figure 5). Moreover, LS contents do not only differ considerably between species but also within species as we also observed large intra-specific differences. For example, the genome of *V. dahliae* strain VdLs17 contains less than two thirds of the content present in the LS regions of the strain JR2 genome despite the recent divergence of the two strains (Figure 5, S1) (Faino *et al.*, 2015). Thus, sequences with increased conservation are genus-wide associated with dynamic genomic regions of *Verticillium* spp. as their contents vary greatly between and within species.

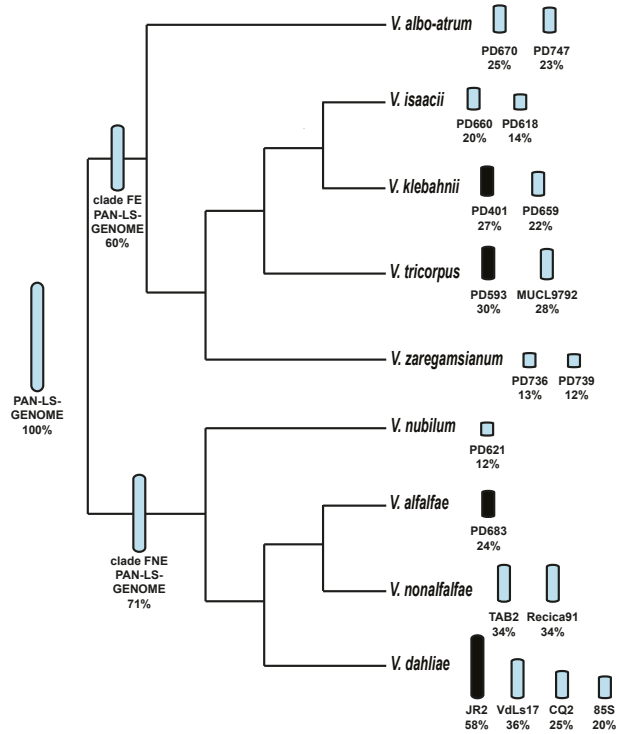

Figure 5 | Diversity of pan-LS-genome contents across the *Verticillium* genus. A pan-LS-genome was constructed based on sequences from *Verticillium* isolates JR2, PD683, PD593 and PD401 (black bars). The bar size next to the species names in the *Verticillium* phylogenetic tree is representative for the amount of the pan-LS-genome that is present in the individual isolates. All isolates of the clade Flavexudans (FE in figure) in this study were used to calculate the percentage of the pan-LS-genome that is present in clade Flavexudans. Similarly, the portion of the Flavnonexudans (FNE in figure) in the pan-LS-genome was calculated with all isolates of the clade Flavnonexudans used in this study.

Increased sequence conservation is not driven by negative selection

The depletion of sequence polymorphisms in LS regions may be driven by negative selection on genes with particular functions that happen to reside in these regions. Hence, we screened LS regions in the genome of *V. dahliae* strain JR2 for enrichment of particular protein domains (Pfam). In total, 13 Pfam domains with various functions are enriched in the LS region genes (Table S7). However, if the negative selection on particular LS genes is responsible for observed increased sequence conservation, depletion of polymorphisms should only concern protein-coding sequences. To test this hypothesis, we compared the sequence identity of coding and intergenic regions between *V. dahliae* and *V. nonalfalfae,* which revealed that increased sequence conservation is also observed in intergenic regions (Figure 6), indicating that increased sequence conservation is likely not driven by negative selection acting on protein-coding genes.

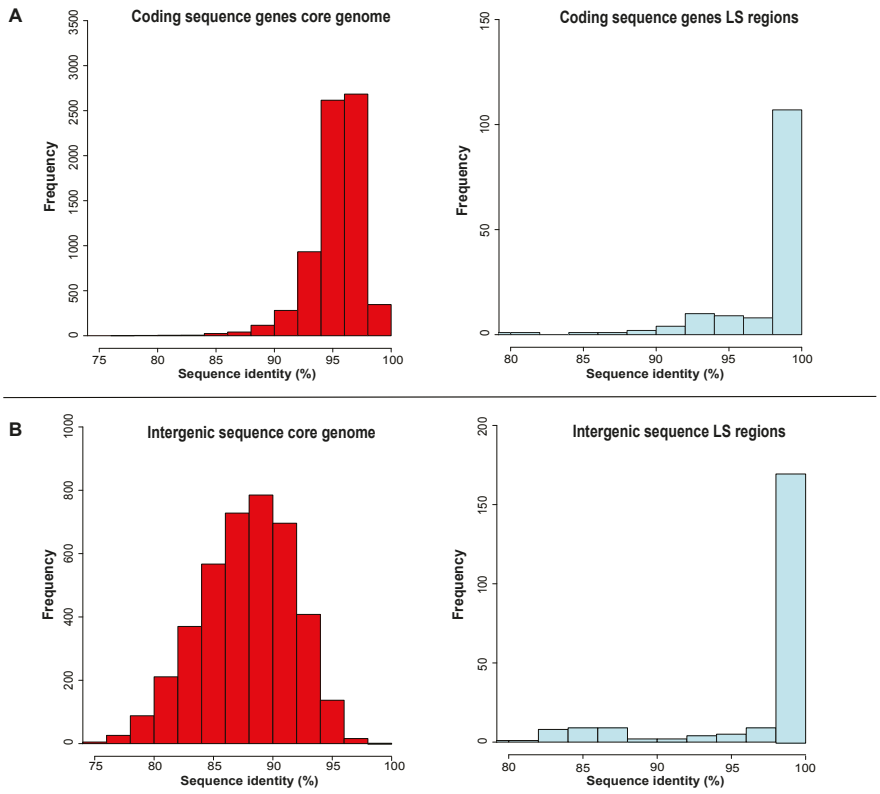

Figure 6 | Sequence identity of *V. dahliae* JR2 core and lineage-specific (LS) regions with *V. nonalfalfae* (TAB2) for coding and intergenic sequences. (A) Coding sequence of JR2 genes were aligned to coding sequences of TAB2 genes. Matching coding sequences of genes that minimally covered 80% of each other were selected and sequence identity between their homologs was determined. (B) For the intergenic regions, windows of 5 kb were constructed for JR2 core and LS regions. The sequence identity distribution is significantly different between core and LS regions and this for both the coding sequence of genes and intergenic regions (two-sided Wilcoxon rank-sum test, $p<0.0001$).

To see how selection impacts the evolution of LS region genes, we determined the rates of non-synonymous (*Ka*) and synonymous (*Ks*) substitutions for genes that reside in LS regions versus those that reside in the core genome. In total, 48% (68 out of 142) of the LS genes could not be used for *Ka* and *Ks* determination, as we did not observe any substitutions when compared to their corresponding *V. nonalfalfae* orthologs. In contrast, within the core almost all genes (8,583 out of 8,584) display nucleotide substitutions with their respective *V. nonalfalfae* orthologs. The *Ka* was not different (two-sided Wilcoxon rank-sum test, $P<0.05$) between LS (median=0.015, $n=74$) and core (median=0.015, $n=8583$) genes (Figure 7). In contrast, the *Ks* of LS genes (median=0.12, $n=74$) was significantly lower than of core genes (median=0.16, $n=8583$). Consequently, LS genes (median=0.38, $n=60$) have significantly higher *Ka*/*Ks* values than core genes (median=0.09, $n=8289$), calculated for genes that have both synonymous and non-synonymous substitutions compared with their *V. nonalfalfae* orthologs. In total, 15 of the 74 tested genes displayed *Ka*/*Ks*>1, which is a higher proportion than the 100 of the 8,583 core genes with *Ka*/*Ks*>1 (Fisher's exact test, $P<0.05$). Two LS and two core genes with *Ka*/*Ks*>1 were predicted to contain an N-terminal signal peptide, which is a typical characteristic of an effector protein. However, due to the limited sequence divergence in the LS regions, positive selection on the genes with *Ka*/*Ks*>1 was not significant based on a *Z*-test, whereas in the core genome 21 genes were found to be under positive selection ($P<0.05$). In conclusion, despite increased sequence conservation, genes in LS regions display symptoms of more diversifying selection than the core genome as *Ka*/*Ks* ratios were significantly higher for LS region genes.

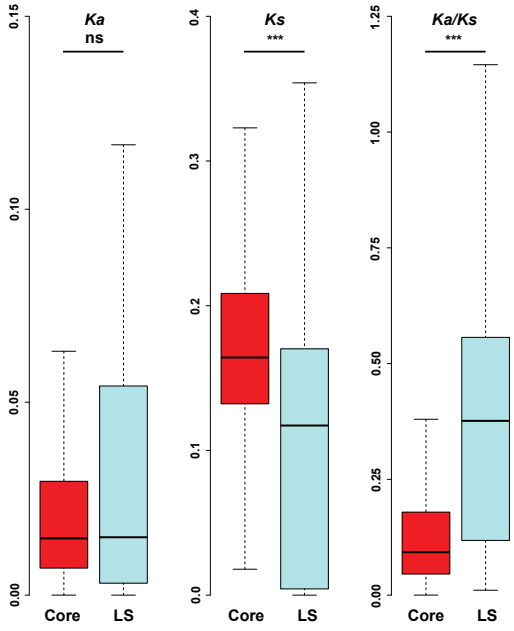

Figure 7 | Comparison of substitutions of *V. dahliae* (JR2) and *V. nonalfalfae* (TAB2) orthologs between core and lineage-specific (LS) regions. The distribution of non-synonymous substitution rates (*Ka*), synonymous substitution rates (*Ks*) and *Ka*/*Ks* ratios are depicted for *V. dahliae* genes aligned to *V. nonalfalfae* orthologs. Outliers are not depicted. Significance of the different distributions was calculated the two-sided Wilcoxon rank-sum test (ns = not significant, *** = $P<0.001$).

Discussion

Genomes of many filamentous plant pathogens are thought to obey the two-speed evolution model (Croll and McDonald, 2012; Dong *et al.*, 2015; Möller and Stukenbrock, 2017). Similarly, *V. dahliae* has been suggested to evolve under a two-speed regime, as LS regions display signs of accelerated evolution as they are hot-spots for structural variation and TE activity (Faino *et al.*, 2015, 2016; de Jonge *et al.*, 2013). Additionally, we establish here that LS regions display abundant presence/absence polymorphisms between closely and even distantly related *V. dahliae* strains (Figure 1, S1) (Faino *et al.*, 2016; de Jonge *et al.*, 2013). Intriguingly, however, genomic sequences that are present within LS regions display increased sequence conservation when compared with other *Verticillium* spp. (Figure 2,3,S2; Table 1). Generally, sequences with increased identities between distinct taxa can originate from horizontal transfer, a phenomenon that has been implicated in the pathogenicity of various filamentous plant pathogens (Soanes and Richards, 2014). For instance, *Pyrenophora tritici-repentis*, the causal agent of wheat tan spot, acquired a gene from the fungal wheat pathogen *Phaeosphaeria nodorum* enabling the production of the host-specific toxin ToxA that mediates pathogenicity on wheat (Friesen *et al.*, 2006). However, the increased sequence identity of LS sequences in *V. dahliae* is likely not a consequence of horizontal transfer as homologous sequences are found in all *Verticillium* spp., and the degree of sequence conservation with these *Verticillium* spp. corresponds to their phylogenetic distance to *V. dahliae* (Table 1). Intriguingly, the increased sequence conservation is not a consequence of negative selection on coding regions, as intergenic regions display similarly increased levels of sequence conservation (Figure 6). In addition, genes residing in LS regions display higher *Ka*/*Ks* ratios compared to core genes, indicating the higher diversifying selection acting on these genes (Figure 7) (Sperschneider *et al.*, 2015). In conclusion, the increased sequence conservation is likely caused by lower mutation rates in LS regions, as horizontal DNA transfer and negative selection are unlikely explanations.

Lower levels of synonymous substitutions were similarly found in the repeat-rich dispensable chromosomes of the fungal wheat pathogen *Zymoseptoria tritici* (Stukenbrock *et al.*, 2010). However, this observation was not attributed to lower mutation rates, but rather the consequence of a lower effective population size of these dispensable chromosomes (Stukenbrock *et al.*, 2010). Increased sequence conservation caused by lower substitution rates as observed in our study is an unprecedented for repeat-rich regions of filamentous pathogens. In contrast, previously increased substitution rates have often been associated with the two-speed genome evolution (Cuomo *et al.*, 2007; Dong *et al.*, 2015). For example, repeat-induced point (RIP) mutagenesis increases sequence divergence of particular effector genes of the oilseed rape pathogen *Leptosphaeria maculans* that are localized adjacent to TEs (van de Wouw *et al.*, 2010). However, accelerated evolution through SNPs is not consistently observed for all two-speed genomes, as no significant difference in SNP frequencies between core and repeat-rich genomic regions was found for *P. infestans* (Raffaele *et al.*, 2010).

Increased sequence conservation of LS regions seems counter-intuitive in the light of the two-speed genome model as increased variation of pathogenicity-related genes facilitates rapid evasion of host immunity. Nonetheless, an effector gene subjected to increased sequence conservation stood the test of time. The *Ave1* effector gene resides in an LS region of *V. dahliae* strain JR2 and is highly conserved as an identical copy was found in *V. alfalfae* strain VaMs102, a strain with an average nucleotide identity of 92% (de Jonge *et al.*, 2012). Moreover, no *Ave1* allelic variation is hitherto found in the *V. dahliae* population as well as in *V. alfalfae* and *V. nonalfalfae* (de Jonge *et al.*, 2012; Song *et al.*, 2017). Conceivably, sequence conservation makes an effector gene an easy target for recognition by the host and also Ave1 is a target for immunity recognition by tomato receptor Ve1 (Fradin *et al.*, 2009). Thus, effector catalogue diversification must be achieved through different means. Indeed, instead through SNPs, *V. dahliae* alters its effector repertoires through presence/absence polymorphisms (de Jonge *et al.*, 2013), leading to large diversities in LS region contents between strains (Figure 5, Table S6). Hence, the evasion of Ve1-mediated recognition in tomato is exclusively observed through the absence of the *Ave1* gene in *V. dahliae* strains (de Jonge *et al.*, 2012).

Mechanisms that can explain the observed lower SNP frequency rates locally, in repeat-rich genomic regions, remain unknown. SNPs often originate from the wrong nucleotide insertion by DNA polymerase and there is no immediate reason why this should be different in LS regions. Possibly, the depletion of SNPs can be associated with a differential epigenetic organisation of LS regions, as repeat-rich regions in other filamentous pathogens are associated with densely organised chromatin, referred to as heterochromatin (Galazka and Freitag, 2014). For instance, the repeat-rich conditionally dispensable chromosomes of *Z. tritici* are enriched for histone modifications associated with heterochromatin, in contrast to core chromosomes that were largely euchromatic, i.e. transcriptionally active (Schotanus *et al.*, 2015). The link between chromatin and structural variation is under debate and controversial (Seidl *et al.*, 2016). In general, heterochromatin is thought to suppress genomic structural alterations as recombination is repressed in heterochromatic regions of many eukaryotic genomes. However, heterochromatic regions in the filamentous pathogens *Z. tritici* are enriched for structural variations as they are enriched for duplications and deletions (Seidl *et al.*, 2016). *V. dahliae* LS regions display similar features with enrichment of repeats, segmental duplications and presence/absence polymorphisms, hence LS regions can be anticipated to be heterochromatic (Figure 1) (Faino *et al.*, 2016; de Jonge *et al.*, 2013). Further research is needed to investigate whether differences in chromatin organisation may affect SNP frequencies in filamentous pathogens in general, and may explain lower rates of SNP frequencies in *V. dahliae* LS regions.

Conclusions

The two-speed genome is an intuitive evolutionary model for filamentous pathogens, as genes important for pathogenicity benefit from frequent alternations to guarantee the continuation of symbiosis with the host. However, filamentous pathogens comprise a heterogeneous group of organisms with diverse lifestyles (Dean *et al.*, 2012; Kamoun *et al.*, 2015). Consequently, it is not surprising that accelerated evolution is driven by different mechanisms between species. Moreover, not all filamentous pathogens appear to adhere to the two-speed genome model (Derbyshire *et al.*, 2017). In *V. dahliae*, acceleration evolution is merely achieved through presence/absence polymorphisms, as nucleotide sequences are highly conserved in LS regions. The dependency of host adaptation on presence/absence polymorphisms may lead to a more rapid immunity evasion than sequence alterations through SNPs (Daverdin *et al.*, 2012). Thus, the quick nature of host immunity evasion through the deletion of effector genes can be evolutionary advantageous over allelic diversification, especially for pathogens with a small effective population size.

Acknowledgements

The authors would like to thank the Marie Curie Actions program of the European Commission that financially supports the research of J.R.L.D. Work in the laboratories of B.P.H.J.T. and M.F.S. is supported by the Research Council Earth and Life Sciences (ALW) of the Netherlands Organization of Scientific Research (NWO). H.M. was supported by French Ministry of Higher Education and Research: CIFRE 2013/1431.

Supplementary material

Table S1 | *V. dahliae* strain CQ2 and 85S genome assemblies.

		CQ2*	85S*
SMRT cells		4	4
Filtered subreads		430,378	500,428
Coverage (n-fold)		110x	130x
HGAP3 assembly	Size (bp)	35,818,019	35,931,336
	Contigs	17	40
	Longest contig	7,864,170	6,633,769
	N_{50} (bp)	3,754,186	3,176,090
	No. of Ns/100 kb	0	0

*Including the mitochondrial contig.

Table S2 | Assembly statistics of the *Verticillium* genomes used in this study.

Species	Strain name	Genome size (Mb)	#Ns/100 kb	N50 (Mb)	# Contigs (≥0 bp)	# Scaffolds (≥1000 bp)
V. albo-atrum	PD670	37.4	56.67	3.7	107	72
	PD747	36.5	16.26	3.9	34	19
V. alfalfae	PD683	32.7	19.36	4.5	40	14
V. dahliae	VdLs17	36.0	0	5.9	8	8
	JR2	36.2	0	4.2	8	8
	CQ2	35.8	0	3.8	17	17
	85S	35.9	0	3.2	40	40
V. nonalfalfae	Rec	33.0	35.4	0.9	1026	795
	TAB2	34.3	897.53	1.8	793	167
V. nubilum	PD621	37.9	9.13	4.7	246	189
V. tricorpus	MUCL9792	36.0	229,64	4,7	255	53
	PD593	35.0	14.52	4.4	71	9
V. isaacii	PD618	35.8	62.48	3.1	239	122
	PD660	36.0	37.53	2.5	114	43
V. klebahnii	PD659	36.2	59.47	3.6	120	60
	PD401	36.0	35.30	3.2	79	37
V. zaregamsianum	PD736	37.1	62.7	2.0	125	62
	PD739	37.1	55.38	3.5	75	32

Table S3 | Sequences of other haploid *Verticillium* spp. with high identity to *V. dahliae* JR2.

Species	Strain name	Amount of high identity sequences (kb)	Fraction that align to LS regions (%)
V. albo-atrum[b]	PD670	209	94.6
	PD747	160	91.9
V. alfalfae[a]	PD683	473	99.5
V. nonalfalfae[a]	Rec	662	100.0
	TAB2	705	99.9
V. nubilum[b]	PD621	147	69.6
V. tricorpus[b]	MUCL9792	92	76.1
	PD593	304	95.3
V. isaacii[b]	PD618	153	89.5
	PD660	202	89.9
V. klebahnii[b]	PD659	193	86.6
	PD401	142	81.9
V. zaregamsianum[b]	PD736	54	52.4
	PD739	68	86.8

[a] Sequences with an identity of >95% with *V. dahliae* JR2
[b] Sequences with an identity of >90% with *V. dahliae* JR2

Table S4 | Sequences of other haploid *Verticillium* spp. with high identity to *V. tricorpus* PD593.

Species	Strain name	Amount of high identity sequences (kb)	Fraction that align to LS regions (%)
V. albo-atrum[b]	PD670	510	83.4
	PD747	527	83.8
V. alfalfae[b]	PD683	46	1.3
V. dahliae[b]	VdLs17	153	80.6
	JR2	285	81.1
	CQ2	36	3.1
	85S	67	2.1
V. nonalfalfae[b]	Rec	322	70.0
	TAB2	60	30.0
V. nubilum[b]	PD621	133	49.4
V. isaacii[a]	PD618	63	32.6
	PD660	100	60.4
V. klebahnii[a]	PD659	105	62.5
	PD401	49	18.8
V. zaregamsianum[a]	PD736	44	9.8
	PD739	40	7.3

[a] Sequences with an identity of >95% with *V. tricorpus* PD593
[b] Sequences with an identity of >90% with *V. tricorpus* PD593

Table S5 | Sequence identities between *V. tricorpus* (PD593) and other haploid *Verticillium* species excluding repetitive regions.

Species/strain	Genome-wide[a] (%)	Conserved regions[a] (%)	# windows aligned to conserved regions[b]	*P*-value[c]
V. albo-atrum/PD747	89.6 (5.2)	100 (3.1)	606	2.2e-16
V. alfalfae/PD683	88.2 (4.0)	86.4 (1.9)	2	0.35
V. dahliae/JR2	88.8 (4.5)	97.6 (3.4)	172	2.2e-16
V. nonalfalfae/TAB2	88.4 (4.1)	99.4 (4.8)	25	7.9e-11
V. nubilum/PD621	88.3 (3.9)	95.1 (4.2)	64	2.2e-16
V. isaacii/PD660	94.6 (4.0)	98.8 (4.0)	133	2.2e-16
V. klebahnii/PD401	94.8 (4.0)	98.8 (3.5)	182	2.2e-16
V. zaregamsianum/PD739	94.8 (4.0)	94.0 (3.5)	37	0.14

[a]The percentage is the median sequence identity and the number between the brackets is the standard deviation.
[b] Windows are 500 bp in size.
[c]The *P*-value was calculated with a two-sided Wilcoxon rank sum test

Table S6 | Presence of constructed dynamic regions in individual *Verticillium* strains.

Species	Strain	Consensus	Clade FE[1] consensus	Clade FNE[2] consensus
V. albo-atrum	PD670	25%	41%	21%
	PD747	23%	38%	17%
V. alfalfae	PD683	24%	9%	34%
V. dahliae	VdLs17	36%	27%	51%
	JR2	58%	39%	81%
	CQ2	25%	12%	35%
	85S	20%	8%	28%
V. nonalfalfae	Rec	34%	28%	48%
	TAB2	34%	21%	47%
V. nubilum	PD621	12%	16%	17%
V. tricorpus	MUCL9792	28%	48%	15%
	PD593	30%	50%	19%
V. isaacii	PD618	14%	24%	15%
	PD660	20%	34%	17%
V. klebahnii	PD659	22%	38%	16%
	PD401	27%	46%	14%
V. zaregamsianum	PD736	13%	21%	11%
	PD739	12%	20%	12%

[1]: FE = Flavexudans
[2]: FNE = Flavnonexudans

Table S7 | Pfam domain enrichments for genes located in the lineage-specific regions of *V. dahliae* JR2.

Pfam domain	Description	*P*-value
PF11917	Protein of unknown function	5e-07
PF12520	Protein of unknown function	1e-05
PF14602	Hexapeptide repeat of succinyl-transferase	9e-04
PF14441	OTT_1508-like deaminase	2e-03
PF12796	Ankyrin repeats	2e-03
PF17111	N-terminal domain of STAND proteins	2e-03
PF00069	Protein kinase domain	3e-03
PF04667	cAMP-regulated phosphoprotein	2e-02
PF01636	APH Phosphotransferase	2e-02
PF13854	Kelch motif	3e-02
PF00172	Zinc finger	3e-02
PF12464	Maltose acetyltransferase	3e-02
PF05729	NACHT domain	5e-02

Table S8 | Genome regions used for pan-LS-genome construction.

Species/strain	Chromosome/scaffold	Start and end position
V. dahliae/JR2	Chr2	2871432-3666484
	Chr4	937294-1480748
	Chr5	560178-1061663
	Chr5	3387969-3743452
V. alfalfae/PD683	Sca11	1-171020
	Sca12	1-105165
	Sca13	1-98982
V. tricorpus/PD589	Sca1	971738-1381898
	Sca6	3245714-3479666
V. klebahnii/PD401	Sca6	1566798-1795658
	Sca21	200168-272356
	Sca22	1-101836

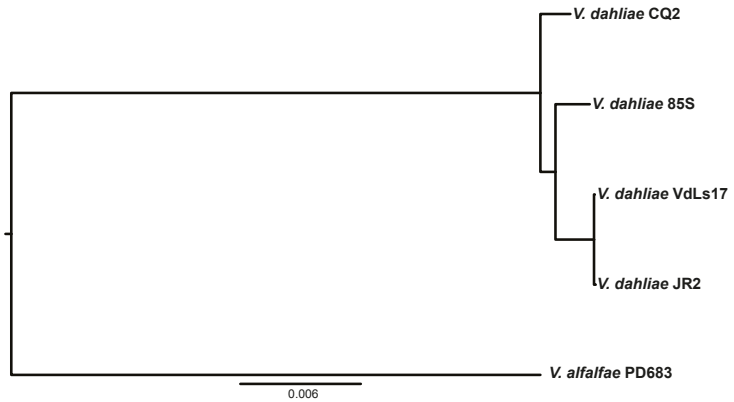

Figure S1 | Phylogenetic relationship between *V. dahliae* isolates used in this study. The phylogenetic analysis of all the *V. dahliae* strains was inferred by whole genome alignments. *V. alfalfae* was used as outgroups species.

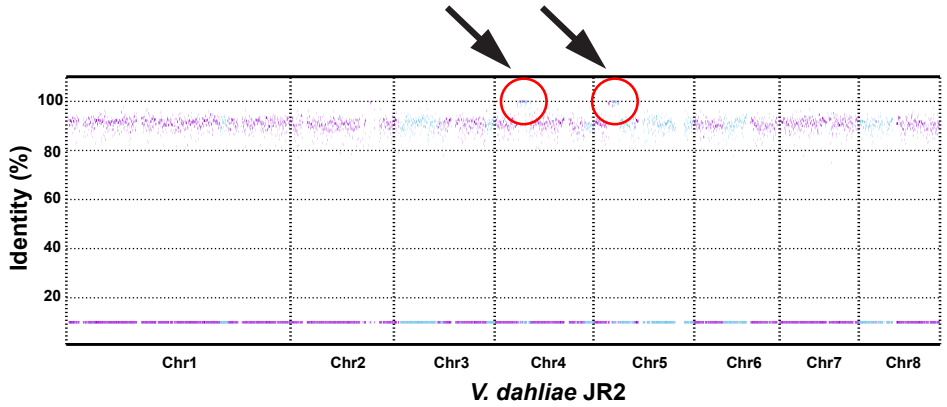

Figure S2 | Whole-genome coverage plot displaying identity of aligned sequences of *V. nonalfalfae* TAB2 to *V. dahliae* JR2. Aligned genomic regions are displayed and purple and blue colors indicate forward-forward alignments and forward-reverse alignments (inversions), respectively. Genome regions with black arrows indicate 99-100% sequence identity.

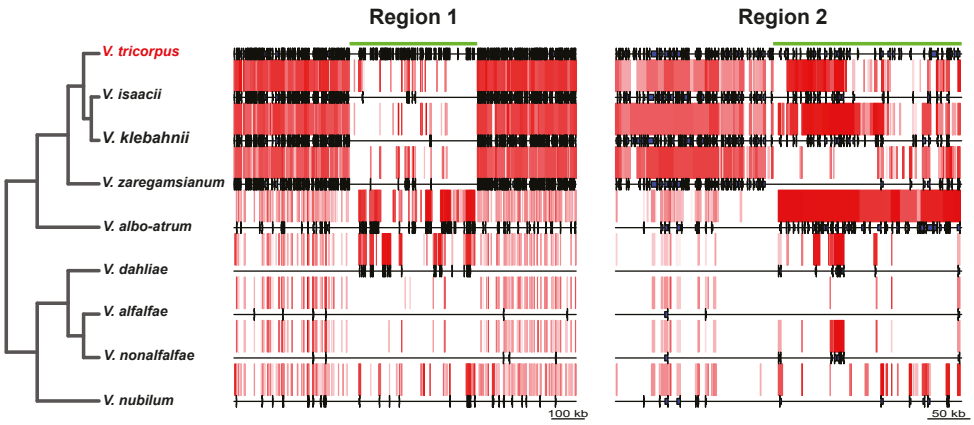

Figure S3 | Interspecific alignments and sequence identity within and immediately adjacent to lineage-specific regions of *V. tricorpus*. The green line indicates the extent of the LS region. The pink/red bars are *Verticillium* sequences alignments to PD593, whereas the intensity of their color represents relative sequence identity for every *Verticillium* spp. individually (higher identity = red, lower identity = pink). The black, vertical stripes on the synteny lines represent predicted gene positions. For *V. tricorpus* PD593, all predicted genes are depicted, whereas for other species only genes are depicted from successfully aligned sequences. Strains used in this figure: *V. tricorpus* PD593, *V. isaacii* PD660, *V. klebahnii* PD401, *V. zaregamsianum* PD739, *V. albo-atrum* PD747, *V. dahliae* JR2, *V. alfalfae* PD683, *V. nonalfalfae* TAB2 and *V. nubilum* PD621.

9

General discussion

Introduction

Many microbes live intimately with plants and establish symbiotic relationships, ranging from mutualistic to pathogenic (Vandenkoornhuyse *et al.*, 2015). Pathogens are especially well-known for engaging in everlasting arms races for continued symbiosis with their hosts (Cook *et al.*, 2015; Jones and Dangl, 2006). In these arms races, pathogens evolve effector proteins to subvert host immunity, thereby successfully achieving host colonization. In turn, plants attempt to re-establish immunity through recognition of patterns that betray pathogen invasion (Cook *et al.*, 2015). Consequently, plant pathogen effector genes often undergo rapid evolutionary changes to prevent host recognition. Genetic variation can be achieved through sexual reproduction, where the recombination of effector repertoires between two individuals can lead to novel allele combinations required for evasion of host immunity responses. However, success of sexual recombination in host immunity evasion depends on the diversity of the pathogen population (McDonald and Linde, 2002). Concretely, if no allele is present in the pathogen population that facilitates immunity evasion upon host recognition, the symbiosis between pathogen and plant will be interrupted leading to avirulence. Although, a recent report for the wheat pathogen *Zymoseptoria tritici* suggests that sexual recombination can even occur with an avirulent parent on a resistant host, maintaining avirulence alleles in subsequent populations (Kema *et al.*, 2018), plant pathogens must rely on alternative evolutionary mechanisms that allow swift adaptation to guarantee continued symbiosis with their host, such as single nucleotide polymorphisms (SNPs), horizontal gene transfer (HGT) and insertions or deletions (indels) (Seidl and Thomma, 2014). Moreover, numerous plant pathogens solely depend on these alternative mechanisms as they are evolutionary successful without sex (McDonald and Linde, 2002). Although mutagenesis through these alternative mechanisms can lead to evolutionary success, genetic alterations can also have deleterious effects on organismal fitness. Thus, mutagenesis rates must be counter-acted by sufficiently large effective population sizes. Conceivably, as plant pathogens often need rapid adaptation of effector repertoires, higher mutation rates specifically for effector genes would reduce the effective population size required for continued symbiosis with hosts.

Genome evolution in filamentous pathogens

Filamentous plant pathogens often exhibit compartmentalized genomes consisting of gene-rich core regions and accessory genome regions that are gene-sparse. The latter are generally associated with the pathogenic lifestyle of filamentous pathogen as genes, including those that encode effector proteins, often reside in accessory genome regions (Dong *et al.*, 2015). Genome compartmentalization is considered advantageous as it

facilitates rapid evolution of pathogenicity-related genes without affecting the core genes with more elementary functions (Croll and McDonald, 2012). The uneven distribution of variation in genomes of filamentous pathogens was coined as the two-speed genome model (Croll and McDonald, 2012; Raffaele and Kamoun, 2012). Accessory genome regions can comprise complete chromosomes; so-called conditionally dispensable chromosomes (CDCs) (Ma *et al.*, 2010; Goodwin *et al.*, 2011), such as for the tomato wilt pathogen *Fusarium oxysporum* f.sp. *lycopersici* that contains various CDCs that mediate pathogenicity on tomato (Ma *et al.*, 2010; Vlaardingerbroek *et al.*, 2016). Alternatively, accessory genome regions can be embedded within core genome regions, as illustrated for the fungal smut pathogen *Ustilago maydis* (Kämper *et al.*, 2006; Schirawski *et al.*, 2010) and the vascular wilt pathogen *Verticillium dahliae* (de Jonge *et al.*, 2012, 2013). *V. dahliae* contains dynamic, lineage-specific (LS) genome regions that are enriched for *in planta*-induced effector genes (Faino *et al.*, 2016; de Jonge *et al.*, 2013). In other pathogens, effector proteins may reside in sub-telomeric regions that are repeat-rich and devoid of elementary genes, such as the *Avr-Pit*a effector gene of the rice blast fungus *Magnaporthe oryzae* (Khang *et al.*, 2008; Orbach *et al.*, 2000).

The advantage of accessory genome regions comprising complete chromosomes may be their capacity to be transferred horizontally between otherwise reproducibly isolated strains. Although not yet demonstrated in nature, CDCs were horizontally transferred between *F. oxysporum* strains under laboratory conditions (Ma *et al.*, 2010). However, even when accessory genome regions are embedded in the core genome, HGT transfer between otherwise reproducibly isolated filamentous pathogens can occur. For instance, effector gene *ToxA* mediates pathogenicity on wheat and was horizontally acquired by the causal agent of wheat tan spot, *Pyrenophora tritici-repentis*, from the fungal wheat pathogen *Phaeosphaeria nodorum* (Friesen *et al.*, 2006). Recently, *ToxA* was also identified in a repeat-rich region of a third wheat pathogen, *Bipolaris sorokiniana* (McDonald *et al.*, 2018). Furthermore, the occurrence of accessory genome regions on separate chromosomes may facilitate their rapid evolution through structural rearrangements without impacting the synteny of core genome regions through inversions or translocations (Stukenbrock, 2013). Synteny loss of core genome regions can be disadvantageous for sexual organisms as it reduces recombination frequencies during meiosis. In contrast, the often lineage-specific character of accessory genome regions results that homologous recombination is less resourceful to generate variation. Hence, variation in CDCs is frequently generated through structural rearrangements (Croll *et al.*, 2013; Croll and McDonald, 2012; Stukenbrock *et al.*, 2010). For instance, in the sexually reproducing fungal wheat pathogen *Z. tritici*, extensive structural rearrangements and loss of CDCs occur during meiosis, whereas core chromosomes are not lost during meiosis and less frequently undergo structural rearrangements (Croll *et al.*, 2013). In contrast, asexual pathogens do not engage in meiosis and, thus, chromosomes may consequently accumulate more rearrangements even if this leads to the inversion or translocation of core genome regions. Extensive structural genomic

alterations are observed in the evolution of the asexual fungus *V. dahliae* where chromosomes that comprise core regions are continuously recombined (Faino *et al.*, 2016; de Jonge *et al.*, 2013).

The association of rapidly evolving accessory genome regions with repeats suggests that transposable elements (TEs) play a pivotal role in the accelerated evolution of accessory regions (Seidl and Thomma, 2017). Transposable elements may lead to genetic variation directly through their activity, which is suggested by the enrichment for active transposons *V. dahliae* LS regions (Faino *et al.*, 2016). Transposons are mobile genomic elements that can move through the genome in a copy-paste (retro-transposons) or a cut-paste (DNA transposon) fashion. Transposable elements can disrupt gene activity through insertion in promoter or open reading frame sequences. Such insertions can facilitate immunity evasion as observed for the barley smut fungus *Ustilago hordei* (Ali *et al.*, 2014). Interruption of the promoter of effector gene *UhAvr1* reduced *UhAvr1* expression and likely led to the evasion of *U. hordei* recognition by barley plants harbouring resistance gene *Ruh1* as the same *UhAvr1* alleles were present in virulent and avirulent *U. hordei* strains (Ali *et al.*, 2014). The activity of retro-transposons can not only disrupt gene functions but also lead to the birth of novel effector genes through gene retro-duplication followed by functional diversification (Fouche *et al.*, 2018). For instance, effector genes *Avrk1* and *Avra10* from barley powdery mildew *Blumeria graminis* f.sp. *hordei* belong to a gene family of more than 1,350 homologs of which the expansion has been association with retro-transposon proliferation (Amselem *et al.*, 2015). In addition to the retro-duplications, excision of TEs also causes double-stranded DNA breaks that may lead to non-faithful repair, especially between genome regions with highly similar sequences (Seidl and Thomma, 2014). Consequently, ectopic rearrangements can result in translocations, inversions, duplications, or deletions of genome regions. *V. dahliae* LS regions are hot-spots for large ectopic chromosomal rearrangements and are enriched for presence/absence polymorphisms and segmental duplications (Faino *et al.*, 2016; de Jonge *et al.*, 2013).

Although TEs are a source of genetic variation, direct contributions of TEs on the actual speed of evolution of accessory genome regions remain largely obscure (Seidl and Thomma, 2017). The most convincing means of TEs contributing to accelerated evolutionary speed is through repeat-induced point mutation (RIP), which is a fungal defence mechanism against TEs (Rouxel *et al.*, 2011). Repeat-induced point mutation actively induces point mutations in TEs, which can also affect adjacent regions through leakage of the RIP process. Effector genes of the *Brassica* blackleg pathogen *Leptosphaeria maculans* that reside in close proximity of TEs encountered increased levels of point mutagenesis through RIP leakage, which facilitated rapid diversification (Rouxel *et al.*, 2011; van de Wouw *et al.*, 2010). This impact of RIP on effector evolution is currently only demonstrated for *L. maculans* and can only occur in filamentous pathogens with a sexual reproduction, as RIP is associated with meiosis (Selker, 2002).

Thus, increased levels of SNPs in repeat-rich regions are certainly not observed in all filamentous pathogens. For instance, in *Phytophthora infestans*, the causal agent of potato late blight, repeat-rich regions are not enriched for SNPs, yet more genes display signs of diversifying selection (Raffaele *et al.*, 2010). Intriguingly, SNP levels in the accessory LS regions of *V. dahliae* are even lower than the core genome (**Chapter 8**). In contrast to increased point mutagenesis through RIP, a mechanism to explain this observation in an asexual fungus is yet to be found.

Sequence conservation of effector genes is remarkable as effector genes are typically also targets for pathogen recognition by the plant immune system (Jones and Dangl, 2006). For instance, *V. dahliae* effector gene *Ave1* is such an effector gene under conserved sequence evolution and is a target for recognition by tomato immune receptor Ve1 (Fradin *et al.*, 2009; de Jonge *et al.*, 2012). Host immunity evasion that involves effector genes with increased sequence conservation is therefore achieved through presence/absence polymorphisms (de Jonge *et al.*, 2013). Consequently, the non-specific nature of deletions makes that effector genes are largely or completely removed from the genome. In contrast, immunity evasion through SNPs leads to effector genes remaining present in the genome that can potentially further contribute to pathogenicity. Thus, as SNPs levels are reduced, *V. dahliae* LS regions must evolve new effector genes through the integration of novel genes. For instance, new effector genes can be obtained from HGT, such as effector gene *Ave1* that was acquired from plants (de Jonge *et al.*, 2012). Alternatively, new effector genes might find their origin in the core genome. For instance, the chitin-binding lysine motif (LysM) effector Vd2LysM resides in an LS region and likely newly emerged, as it is hitherto only found in *V. dahliae* strain VdLS17 (de Jonge *et al.*, 2013; Kombrink *et al.*, 2017). Hypothetically, Vd2LysM may have evolved from core LysM domain-containing genes as VdLS17 contains three *V. dahliae* conserved core LysM effectors that are not expressed *in planta* and are not needed for full virulence (Kombrink *et al.*, 2017).

Although *V. dahliae* is able to generate variation in LS regions through alternative means, the question remains what the evolutionary advantage would be of sequence conservation in LS regions. As LS regions mainly consist of segmental duplications, lower SNP levels conserve homology within and between LS regions (Faino *et al.*, 2016). Homology conservation facilitates ectopic recombination; hence, the majority of synteny breakpoints between *V. dahliae* strains occur in LS regions (Faino *et al.*, 2016; de Jonge *et al.*, 2013). As chromosomal rearrangements occur extensively and are an important driver of genomic variation in *V. dahliae*, conservation of LS sequences may be evolutionarily beneficial.

Allodiploidization in filamentous plant pathogens

A powerful evolutionary mechanism of haploid filamentous plant pathogens is allodiploidization, when interspecific hybridization leads to a stable diploid state. A difference with other evolutionary mechanisms in filamentous pathogens is that the impact is not more abundantly displayed in accessory genome regions, but has major evolutionary consequences for the core genome region. Interspecific hybridization generally occurs between distinct, yet closely related, species (Mallet, 2007). Thus, the acquisition of a complete chromosome set of both parents makes that these hybrid filamentous pathogens contain most core genes in copy. In contrast, the LS nature of accessory genome regions makes that allodiploid pathogens generally did not acquire accessory regions in copy (Croll and McDonald, 2012). The inheritance of distinct accessory genome regions of both parents can lead to novel pathogenicity features similar to homoploid hybridization (**Chapter 6**, Stukenbrock 2016b). For instance, effector repertoire exchange between races of the Brassicaceae pathogen *Albugo candida,* due to homoploid hybridization, enabled host infections by normally non-infecting races (McMullan *et al.*, 2015).

Although accessory genome regions are associated with the fast evolution of effector repertoires, core regions also contain genes important for pathogenicity. For instance, two necrosis- and ethylene-inducing-like protein genes in *V. dahliae* are required for full virulence on tomato and *Arabidopsis thaliana*, yet they reside in a core genome region (Santhanam *et al.*, 2013). These pathogenicity genes may reside in the core as they have an elementary role in organismal survival. As core genome regions contain genes important for pathogenicity, the occurrence of core genes in copy may facilitate the functional diversification leading to alterations in pathogenicity traits of filamentous pathogens (**Chapter 7**). Alternatively, core genes can evolve new functions that contribute to pathogenicity. This high evolutionary potential of allodiploidization makes that filamentous pathogens often evolve distinct pathogenicity traits from their parents (**Chapter 6**).

Although allodiploidy is an evolutionary mechanism that can increase the adaptive potential of organisms, only few examples of stable allodiploid or allopolyploid in filamentous plant pathogens have been described. For instance, in the fungal phylum of ascomycetes, only *V. longisporum* and *Botrytis allii* are known as stable allodiploids (Inderbitzin *et al.*, 2011b; Nielsen and Yohalem, 2001; Staats *et al.*, 2005). How is it possible that so few examples are observed? Firstly, allodiploidy may not be viable due to genomic incompatibilities between the parental genomes, which can be too large to overcome by post-hybridization genome alterations (Matute *et al.*, 2010; Orr, 2005). Secondly, alterations in chromosome number may lead to reproductive isolation from parental populations (Stukenbrock, 2016b). Thirdly, allopolyploids must occur in a niche where they are competitive with other organisms (Stukenbrock, 2016b). Conceivably, being able to colonize a suitable niche is a challenging event for recent allodiploids,

as their newly acquired allodiploid state likely still lacks genomic adaptation to a particular niche. Hence, allodiploids may initially live on the edge of existence, as a period of niche adaption is required before they can emerge (Schranz *et al.*, 2012). Finally, commonly allopolyploids evolve towards their original ploidy by elimination of redundant gene copies (Robertson *et al.* 2017; Maere *et al.* 2005; **Chapter 7**). Ploidy reversal is an additional reason why so little allopolyploid ascomycete pathogens may be observed, as little evidence remains to detect ancient allopolyploid states (Campbell *et al.*, 2016).

The emergence of a new allodiploid pathogen: *V. longisporum*

Allodiploidization contributed to the emergence of a new *Verticillium* pathogen, *V. longisporum*, with different pathogenicity features from other *Verticillium* spp. (**Chapter 2**). As *V. longisporum* is the only *Verticillium* spp. that can cause disease on *Brassica* crops (Eynck *et al.*, 2007), the most likely first description of *V. longisporum* disease was in 1953 on Brussels sprout (Isaac, 1957). However, the exact time of the interspecific hybridization events remains unclear. *V. longisporum* hybridized at least three times with the hitherto unfound haploid *Verticillium* species A1 consistently as one of the two hybridization parents (Inderbitzin *et al.*, 2011b). Species A1 strains hybridized with *V. dahliae*-like strain D1 and with two different *V. dahliae* strains (D2 and D3), respectively (Inderbitzin *et al.*, 2011b). The three events must have occurred recently and around the same time, as species A1 alleles were identical across *V. longisporum* lineages for several marker genes (Inderbitzin *et al.*, 2011b). The presence of most genes in copy in the *V. longisporum* genome confirmed the likely recent origin of this hybrid as allopolyploidization events are generally followed by extensive gene loss (Maere *et al.* 2005; **Chapter 7**).

In its relatively recent allodiploid history, *V. longisporum* evolved as a pathogen on oilseed rape, causing disease symptoms different from any other *Verticillium* disease (Heale and Karapapa, 1999). *V. longisporum* causes stem striping symptoms in the final stage of the oilseed rape growing season. Hence, the common name "Verticillium stem striping" was coined to describe this disease (**Chapter 2**). The first observation of Verticillium stem striping symptoms on oilseed rape occurred at the end of the 1960s in Sweden (Kroeker, 1970). Oilseed rape production has considerably expanded in Europe in the last four decades, as the total production area was over eight times larger in 2010 than it was in 1970 (FAOSTAT, 2018). Along with this expansion, Verticillium stem striping became a well-established disease in continental Europe. In the UK, oilseed rape production similarly expanded from virtually no production in the 1970s to current annual production area of around 700,000 ha (Wood *et al.*, 2013). However, Verticillium stem striping was only reported in 2007 for the first time, much later than in continental Europe (Gladders *et al.*, 2011). This emergence in the UK was not

caused by a new hybridization event, but by *V. longisporum* strains of the hybridization between *Verticillium* species A1 and D1 (**Chapter 3**). *V. longisporum* A1/D1 is generally the most virulent lineage on oilseed rape (Novakazi *et al.*, 2015) and the UK strains were found to be as virulent as the previously characterised A1/D1 strains (**Chapter 4**). The UK population was genotypically more diverse than *V. longisporum* populations of different countries, which is remarkable for a recently emerged organism (**Chapter 3**). This indicates that host or environmental conditions caused Verticillium stem striping to emerge, rather than the spread of a particularly successful *V. longisporum* genotype with high virulence on oilseed rape. Weather conditions can have a significant impact on plant disease development (**Chapter 1**). Alternatively, the emergence of Verticillium stem striping may be due to host alterations (**Chapter 1**). Considerable differences in stem striping development were observed between British oilseed rape cultivars in field trials (**Chapter 5**). Conceivably, when more resistant cultivars like Incentive and Vision are used under practical conditions, the marginal development of striping symptoms may have resulted that the disease remained unnoticed. It is only by the use of susceptible cultivars like Harper and Quartz that the disease is obviously present. Thus, I conclude that the sudden emergence of Verticillium stem striping in the UK is likely caused by the use of more susceptible oilseed rape cultivars in recent years.

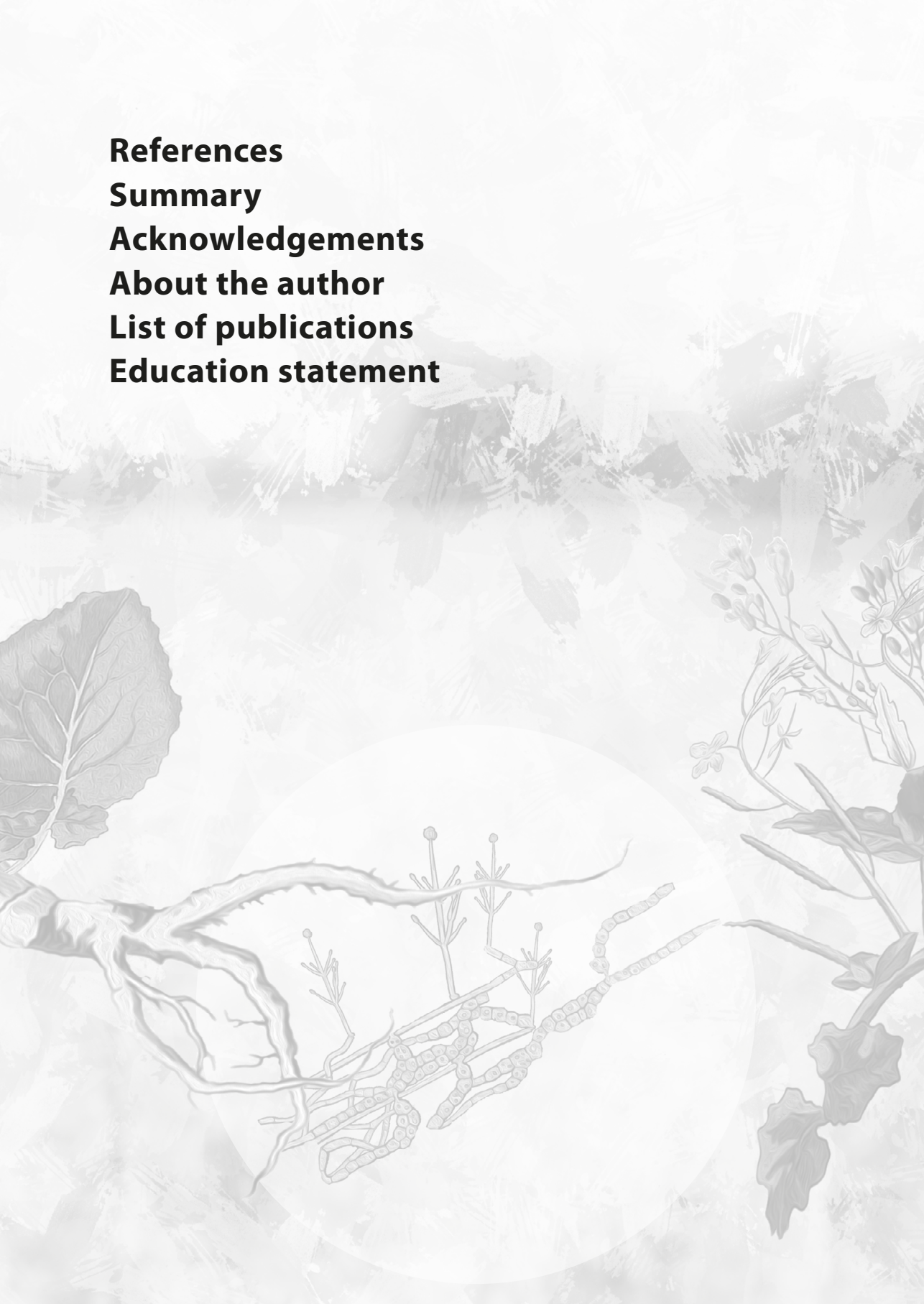

References

Acharya, B.R. and Assmann, S.M. (2009) Hormone interactions in stomatal function. *Plant Mol. Biol.* **69**, 451–462.

Adams, K.L., Cronn, R., Percifield, R. and Wendel, J.F. (2003) Genes duplicated by polyploidy show unequal contributions to the transcriptome and organ-specific reciprocal silencing. *Proc. Natl. Acad. Sci. USA* **100**, 4649–4654.

Akama, S., Shimizu-Inatsugi, R., Shimizu, K.K. and Sese, J. (2014) Genome-wide quantification of homeolog expression ratio revealed nonstachastic gene regulation in synthetic allopolyploid *Arabidopsis*. *Nucleic Acids Res.* **42**, e46.

Albalat, R. and Cañestro, C. (2016) Evolution by gene loss. *Nat. Rev. Genet.* **17**, 379–391.

Ali, S., Laurie, J.D., Linning, R., Cervantes-Chávez, J.A., Gaudet, D. and Bakkeren, G. (2014) An immunity-triggering effector from the barley smut fungus *Ustilago hordei* resides in an Ustilaginaceae-specific cluster bearing signs of transposable element-assisted evolution. *PLoS Pathog.* **10**, e1004223.

Altschul, S.F., Gish, W., Miller, W., Myers, E.W. and Lipman, D.J. (1990) Basic local alignment search tool. *J. Mol. Biol.* **215**, 403–410.

Aminnejad, M., Diaz, M., Arabatzis, M., Castañeda, E., Lazera, M., Velegraki, A., Marriott, D., Sorrell, T.C. and Meyer, W. (2012) Identification of novel hybrids between *Cryptococcus neoformans* var. *grubii* VNI and *Cryptococcus gattii* VGII. *Mycopathologia* **173**, 337–346.

Amselem, J., Vigouroux, M., Oberhaensli, S., et al. (2015) Evolution of the *EKA* family of powdery mildew avirulence-effector genes from the ORF 1 of a LINE retrotransposon. *BMC Genomics* **16**, 917.

Anderson, P.K., Cunningham, A.A., Patel, N.G., Morales, F.J., Epstein, P.R. and Daszak, P. (2004) Emerging infectious diseases of plants: pathogen pollution, climate change and agrotechnology drivers. *Trends Ecol. Evol.* **19**, 535–544.

Andrade-Piedra, J.L., Forbes, G.A., Shtienberg, D., Grünwald, N.J., Chacón, M.G., Taipe, M.V., Hijmans, R.J. and Fry, W.E. (2005) Qualification of a plant disease simulation model: performance of the LATEBLIGHT model across a broad range of environments. *Phytopathology* **95**, 1412–1422.

Atallah, Z.K., Maruthachalam, K. and Subbarao, K.V. (2012) Sources of *Verticillium dahliae* affecting lettuce. *Phytopathology* **102**, 1071–1078.

Atallah, Z.K., Maruthachalam, K., du Toit, L., Koike, S.T., Davis, R.M., Klosterman, S.J., Hayes, R.J. and Subbarao, K.V. (2010) Population analyses of the vascular plant pathogen *Verticillium dahliae* detect recombination and transcontinental gene flow. *Fungal Genet. Biol.* **47**, 416–422.

Babadoost, M., Chen, W., Bratsch, A.D. and Eastman, C.E. (2004) *Verticillium longisporum* and *Fusarium solani*: two new species in the complex of internal discoloration of horseradish roots. *Plant Pathol.* **53**, 669–676.

Bandelt, H.-J., Forster, P. and Röhl, A. (1999) Median-joining networks for inferring intraspecific phylogenies. *Mol. Biol. Evol.* **16**, 37–48.

Bao, W., Kojima, K.K. and Kohany, O. (2015) Repbase Update, a database of repetitive elements in eukaryotic genomes. *Mob. DNA* **6**, 11.

Barbara, D.J., Morton, A. and Miller, N.J. (2005) Isolation of microsatellite markers from an interspecific hybrid isolate of the fungal plant pathogen *Verticillium dahliae*. *Mol. Ecol. Notes* **5**, 854–856.

Barker, M.S., Arrigo, N., Baniaga, A.E., Li, Z. and Levin, D.A. (2015) On the relative abundance of autopolyploids and allopolyploids. *New Phytol.* **210**, 391–398.

te Beest, M., Roux, J.J. Le, Richardson, D.M., Brysting, A.K., Suda, J., Kubešová, M. and Pyšek, P. (2012) The more the better? The role of polyploidy in facilitating plant invasions. *Ann. Bot.* **109**, 19–45.

Bell, A.A. and Wheeler, M.H. (1986) Biosynthesis and functions of fungal melanins. *Annu. Rev. Phytopathol.* **24**, 411–451.

Benjamini, Y. and Hochberg, Y. (1995) Controlling the false discovery rate : a practical and powerful approach to multiple testing. *J R Stat. Soc B* **57**, 289–300.

Berry, P., Cook, S., Ellis, S., Gladders, P. and Roques, S. (2014) *HGCA Oilseed rape guide* (**Boys, E.**, ed.). Stoneleigh Park, Kenilworth, Warwickshire: HGCA Publications.

Bertels, F., Silander, O.K., Pachkov, M., Rainey, P.B. and van Nimwegen, E. (2014) Automated reconstruction of whole-genome phylogenies from short-sequence reads. *Mol. Biol. Evol.* **31**, 1077–1088.

Bertier, L., Leus, L., D'hondt, L., de Cock, A.W.A.M. and Höfte, M. (2013) Host adaptation and speciation through hybridization and polyploidy in *Phytophthora*. *PLoS One* **8**, e85385.

Bhat, R.G. and Subbarao, K.V. (1999) Host range specificity in *Verticillium dahliae*. *Phytopathology* **89**, 1218–1225.

Bhat, R.G. and Subbarao, K.V. (2001) Reaction of broccoli to isolates of *Verticillium dahliae* from various hosts. *Plant Dis.* **85**, 141–146.

Blanc, G. and Wolfe, K.H. (2004) Functional divergence of duplicated genes formed by polyploidy during *Arabidopsis* evolution. *Plant Cell* **16**, 1679–1691.

Bonanomi, G., Antignani, V., Pane, C. and Scala, F. (2007) Supression of soilborne fungal diseases with organic amendments. *J. Plant Pathol.* **89**, 311–324.

Bourke, P.M.A. (1964) Emergence of potato blight, 1843-46. *Nature* **203**, 805–808.

Bovers, M., Hagen, F., Kuramae, E.E., Diaz, M.R., Spanjaard, L., Dromer, F., Hoogveld, H.L. and Boekhout, T. (2006) Unique hybrids between the fungal pathogens *Cryptococcus neoformans* and *Cryptococcus gattii*. *FEMS Yeast Res* **6**, 599–607.

Bowden, J., Gregory, P.H. and Johnson, C.G. (1971) Possible wind transport of coffee leaf rust across the Atlantic Ocean. *Nature* **229**, 500–501.

Brasier, C. (2000) The rise of the hybrid fungi. *Nature* **405**, 134–135.

Brasier, C.M. (2001) Rapid evolution of introduced plant pathogens via interspecific hybridization. *Bioscience* **51**, 123–133.

Brasier, C.M. (2008) The biosecurity threat to the UK and global environment from international trade in plants. *Plant Pathol.* **57**, 792–808.

Brasier, C.M. and Kirk, S.A. (2001) Comparative aggressiveness of standard and variant hybrid alder phytophthoras, *Phytophthora cambivora* and other *Phytophthora* species on bark of *Alnus*, *Quercus* and other woody hosts. *Plant Pathol.* **50**, 218–229.

Brasier, C.M. and Kirk, S.A. (2010) Rapid emergence of hybrids between the two subspecies of *Ophiostoma novo-ulmi* with a high level of pathogenic fitness. *Plant Pathol.* **59**, 186–199.

Brasier, C.M., Kirk, S. a., Pipe, N.D. and Buck, K.W. (1998) Rare interspecific hybrids in natural populations of the Dutch elm disease pathogens *Ophiostoma ulmi* and *O. novo-ulmi*. *Mycol. Res.* **102**, 45–57.

Brasier, C.M., Rose, J. and Gibbs, J.N. (1995) An unusual *Phytophthora* associated with widespread alder mortality in Britain. *Plant Pathol.* **44**, 999–1007.

Brown, J.K.M. and Hovmøller, M.S. (2002) Aerial dispersal of pathogens on the global and continental scales and its impact on plant disease. *Science* **297**, 537–541.

Buggs, R.J.A., Elliott, N.M., Zhang, L., Koh, J., Viccini, L.F., Soltis, D.E. and Soltis, P.S. (2010) Tissue-specific silencing of homoeologs in natural populations of the recent allopolyploid *Tragopogon mirus*. *New Phytol.* **186**, 175–183.

Burt, A., Carter, D.A., Koenig, G.L., White, T.J. and Taylor, J.W. (1996) Molecular markers reveal cryptic sex in the human pathogen *Coccidioides immitis*. *Proc. Natl. Acad. Sci. USA* **93**, 770–773.

Butler, M.J. and Day, A.W. (1998) Destruction of fungal melanins by ligninases of *Phanerochaete chrysosporium* and other white rot fungi. *Int. J. Plant Sci.* **159**, 989–995.

Callaghan, S. and Guest, D. (2015) Globalisation, the founder effect, hybrid *Phytophthora* species and rapid evolution: new headaches for biosecurity. *Australas. Plant Pathol.* **44**, 255–262.

Campbell, M.A., Ganley, A.R.D., Gabaldón, T. and Cox, M.P. (2016) The case of the missing ancient fungal polyploids. *Am. Nat.* **188**, 602–614.

Carder, J.H. and Barbara, D.J. (1994) Molecular variation within some Japanese isolates of *Verticillium dahliae*. *Plant Pathol.* **43**, 947–950.

Caten, C.E. (1981) Parasexual processes in fungi. In *The Fungal Nucleus*. (**Gull, K.** and **Oliver, S.G.**, eds), pp. 191–214. Cambridge University Press, Cambridge.

CFIA (2015) Verticillium wilt-*Verticillium longisporum*. Canadian Food Inspection Agency. Available at: http://www.inspection.gc.ca/plants/plant-pests-invasive-species/diseases/verticillim-wilt/eng/1420746212959/1420746213803. Accessed: 22 February 2016.

Chakraborty, S. and Newton, A.C. (2011) Climate change, plant diseases and food security: an overview. *Plant Pathol.* **60**, 2–14.

Chin, C.-S., Alexander, D.H., Marks, P., et al. (2013) Nonhybrid, finished microbial genome assemblies from long-read SMRT sequencing data. *Nat. Methods* **10**, 563–569.

Christen, O., Evans, E., Nielsson, C. and Haldrup, C. (1999) Oilseed rape cropping systems in NW Europe. In: *Proceedings of the 10th Internation al Rapeseed Congress, Canberra, Australia*.

Colhoun, J. (1973) Effects of environmental factors on plant disease. *Annu. Rev. Phytopathol.* **11**, 343–364.

Collins, A., Okoli, C.A.N., Morton, A., Parry, D., Edwards, S.G. and Barbara, D.J. (2003) Isolates of *Verticillium dahliae* pathogenic to crucifers are of at least three distinct molecular types. *Phytopathology* **93**, 364–376.

Cook, D.E., Mesarich, C.H. and Thomma, B.P.H.J. (2015) Understanding plant immunity as a surveillance system to detect invasion. *Annu. Rev. Phytopathol.* **53**, 541–563.

Cowling, W.A. (2007) Genetic diversity in Australian canola and implications for crop breeding for changing future environments. *F. Crop. Res.* **104**, 103–111.

Cox, M.P., Dong, T., Shen, G., Dalvi, Y., Scott, D.B. and Ganley, A.R.D. (2014) An interspecific fungal hybrid reveals cross-kingdom rules for allopolyploid gene expression patterns. *PLoS Genet.* **10**, e1004180.

Craven, K.D., Blankenship, J.D., Leuchtmann, A., Hignight, K. and Schardl, C.L. (2001) Hybrid fungal endophytes symbiotic with the grass *Lolium pratense*. *Sydowia* **53**, 44–73.

Croll, D. and Laine, A.-L. (2016) What the population genetic structures of host and pathogen tell us about disease evolution. *New Phytol.* **2012**, 537–539.

Croll, D. and McDonald, B.A. (2012) The accessory genome as a cradle for adaptive evolution in pathogens. *PLoS Pathog.* **8**, e1002608.

Croll, D., Zala, M. and McDonald, B.A. (2013) Breakage-fusion-bridge cycles and large insertions contribute to the rapid evolution of accessory chromosomes in a fungal pathogen. *PLoS Genet.* **9**, e1003567.

Cuomo, C.A., Güldener, U., Xu, J.-R., et al. (2007) The *Fusarium graminearum* genome reveals a link between localized polymorphism and pathogen specialization. *Science* **317**, 1400–1402.

Daebeler, F., Amelung, D. and Zeise, K. (1988) *Verticillium*-Welke an Winterraps - Auftreten und Bedeutung. *Nachrichtenblatt Pflanzenschutzd. DDR* **42**, 71–73.

Danecek, P., Auton, A., Abecasis, G., et al. (2011) The variant call format and VCFtools. *Bioinformatics* **27**, 2156–2158.

Danielsson, J., Reva, O. and Meijer, J. (2007) Protection of oilseed rape (*Brassica napus*) toward fungal pathogens by strains of plant-associated *Bacillus amyloliquefaciens*. *Microb. Ecol.* **54**, 134–140.

Daverdin, G., Rouxel, T., Gout, L., Aubertot, J.-N., Fudal, I., Meyer, M., Parlange, F., Carpezat, J. and Balesdent, M.-H. (2012) Genome structure and reproductive behaviour influence the evolutionary potential of a fungal phytopathogen. *PLoS Pathog.* **8**, e1003020.

Dean, R., van Kan, J.A.L., Pretorius, Z.A., et al. (2012) The top 10 fungal pathogens in molecular plant pathology. *Mol. Plant Pathol.* **13**, 414–430.

Debode, J., Clewes, E., De Backer, G. and Höfte, M. (2005a) Lignin is involved in the reduction of *Verticillium dahliae* var. *longisporum* inoculum in soil by crop residue incorporation. *Soil Biol. Biochem.* **37**, 301–309.

Debode, J., Declercq, B. and Höfte, M. (2005b) Identification of cauliflower cultivars that differ in susceptibility to *Verticillium longisporum* using different inoculation methods. *J. Phytopathol.* **153**, 257–263.

Debode, J., Van Poucke, K., França, S.C., Maes, M., Höfte, M. and Heungens, K. (2011) Detection of multiple *Verticillium* species in soil using density flotation and real-time polymerase chain reaction. *Plant Dis.* **95**, 1571–1580.

Depotter, J.R.L., Deketelaere, S., Inderbitzin, P., von Tiedemann, A., Höfte, M., Subbarao, K.V., Wood, T.A. and Thomma, B.P.H.J. (2016a) *Verticillium longisporum* , the invisible threat to oilseed rape and other brassicaceous plant hosts. *Mol. Plant Pathol.* **17**, 1004–1016.

Depotter, J.R.L., Rodriguez-Moreno, L., Thomma, B.P.H.J. and Wood, T.A. (2017a) The emerging British *Verticillium longisporum* population consists of aggressive *Brassica* pathogens. *Phytopathology* **107**, 1399–1405.

Depotter, J.R.L., Seidl, M.F., van den Berg, G.C.M., Thomma, B.P.H.J. and Wood, T.A. (2017b) A distinct and genetically diverse lineage of the hybrid fungal pathogen *Verticillium longisporum* population causes stem striping in British oilseed rape. *Environ. Microbiol.* **19**, 3997–4009.

Depotter, J.R.L., Seidl, M.F., Wood, T.A. and Thomma, B. (2016b) Interspecific hybridization impacts host range and pathogenicity of filamentous microbes. *Curr. Opin. Microbiol.* **32**, 7–13.

Derbyshire, M., Denton-Giles, M., Hegedus, D., et al. (2017) The complete genome sequence of the phytopathogenic fungus *Sclerotinia sclerotiorum* reveals insights into the genome architecture of broad host range pathogens. *Genome Biol. Evol.* **9**, 593–618.

Diepenbrock, W. (2000) Yield analysis of winter oilseed rape (*Brassica napus* L.): a review. *F. Crop. Res.* **67**, 35–49.

Dixelius, C., Happstadius, I. and Berg, G. (2005) Verticillium wilt on *Brassica* oilseed crops – a Swedish perspective. *J. Swed. Seed Assoc.* **115**, 36–48.

Dong, S., Raffaele, S. and Kamoun, S. (2015) The two-speed genomes of filamentous pathogens: waltz with plants. *Curr. Opin. Genet. Dev.* **35**, 57–65.

Doyle, J.J., Flagel, L.E., Paterson, A.H., Rapp, R.A., Soltis, D.E., Soltis, P.S. and Wendel, J.F. (2008) Evolutionary genetics of genome merger and doubling in plants. *Annu. Rev. Genet.* **42**, 443–461.

Dunker, S., Keunecke, H., Steinbach, P. and von Tiedemann, A. (2008) Impact of *Verticillium longisporum* on yield and morphology of winter oilseed rape (*Brassica napus*) in relation to systemic spread in the plant. *J. Phytopathol.* **156**, 698–707.

Dutech, C., Barrès, B., Bridier, J., Robin, C., Milgroom, M.G. and Ravigné, V. (2012) The chestnut blight fungus world tour: successive introduction events from diverse origins in an invasive plant fungal pathogen. *Mol. Ecol.* **21**, 3931–3946.

Dutech, C., Fabreguettes, O., Capdevielle, X. and Robin, C. (2010) Multiple introductions of divergent genetic lineages in an invasive fungal pathogen, *Cryphonectria parasitica*, in France. *Heredity* **105**, 220–228.

Dutheil, J.Y., Mannhaupt, G., Schweizer, G., Sieber, C.M.K., Münsterkötter, M., Güldener, U., Schirawski, J. and Kahmann, R. (2016) A tale of genome compartmentalization: the evolution of virulence clusters in smut fungi. *Genome Biol. Evol.* **8**, 681–704.

Earl, D.A. and vonHoldt, B.M. (2012) STRUCTURE HARVESTER: a website and program for visualizing STRUCTURE output and implementing the Evanno method. *Conserv. Genet. Resour.* **4**, 359–361.

Eastburn, D.M. and Chang, R.J. (1994) *Verticillium dahliae*: a causal agent of root discoloration of horseradish in Illinois. *Plant Dis.* **78**, 496–498.

Ebihara, Y., Nagao, H., Uematsu, S., Moriwaki, J. and Kimishima, E. (2003) First report of *Verticillium tricorpus* isolated from potato tubers in Japan. *Mycoscience* **44**, 481–488.

Edgar, R.C. (2004) MUSCLE: multiple sequence alignment with high accuracy and high throughput. *Nucleic Acids Res.* **32**, 1792–1797.

Ellendorff, U., Fradin, E.F., de Jonge, R. and Thomma, B.P.H.J. (2009) RNA silencing is required for *Arabidopsis* defence against Verticillium wilt disease. *J. Exp. Bot.* **60**, 591–602.

Emanuelsson, O., Nielsen, H., Brunak, S. and von Heijne, G. (2000) Predicting subcellular localization of proteins based on their N-terminal amino acid sequence. *J. Mol. Biol.* **300**, 1005–1016.

Evanno, G., Regnaut, S. and Goudet, J. (2005) Detecting the number of clusters of individuals using the software STRUCTURE : a simulation study. *Mol. Ecol.* **14**, 2611–2620.

Excoffier, L., Smouse, P.E. and Quattro, J.M. (1992) Analysis of molecular variance inferred from metric distances among DNA haplotypes: application to human mitochondrial DNA restriction data. *Genetics* **131**, 479–491.

Eynck, C., Koopmann, B., Grunewaldt-Stoecker, G., Karlovsky, P. and von Tiedemann, A. (2007) Differential interactions of *Verticillium longisporum* and *V. dahliae* with *Brassica napus* detected with molecular and histological techniques. *Eur. J. Plant Pathol.* **118**, 259–274.

Eynck, C., Koopmann, B., Karlovsky, P. and von Tiedemann, A. (2009a) Internal resistance in winter oilseed rape inhibits systemic spread of the vascular pathogen *Verticillium longisporum*. *Phytopathology* **99**, 802–811.

Eynck, C., Koopmann, B. and von Tiedemann, A. (2009b) Identification of *Brassica* accessions with enhanced resistance to *Verticillium longisporum* under controlled and field conditions. *J. Plant Dis. Prot.* **116**, 63–72.

Faino, L., Seidl, M.F., Datema, E., van den Berg, G.C.M., Janssen, A., Wittenberg, A.H.J. and Thomma, B.P.H.J. (2015) Single-molecule real-time sequencing combined with optical mapping yields completely finished fungal genome. *MBio* **6**, e00936-15.

Faino, L., Seidl, M.F., Shi-Kunne, X., Pauper, M., Berg, G.C.M. van den, Wittenberg, A.H.J. and Thomma, B.P.H.J. (2016) Transposons passively and actively contribute to evolution of the two-speed genome of a fungal pathogen. *Genome Res.* **26**, 1091–1100.

FAOSTAT (2016) Statistical database. Food and Agriculture Organization of the United Nations: Statistics Division. Available at: http://faostat3.fao.org. Accessed: 23 May 2018.

Ferree, P.M. and Prasad, S. (2012) How can satellite DNA divergence cause reproductive isolation? Let us count the chromosomal ways. *Genet. Res. Int.* **2012**, 430136.

Feurtey, A., Gladieux, P., Hood, M.E., Snirc, A., Cornille, A., Rosenthal, L. and Giraud, T. (2016) Strong phylogeographic co-structure between the anther-smut fungus and its white campion host. *New Phytol.* **212**, 668–679.

Fisher, M.C., Henk, D.A., Briggs, C.J., Brownstein, J.S., Madoff, L.C., McCraw, S.L. and Gurr, S.J. (2012) Emerging fungal threats to animal, plant and ecosystem health. *Nature* **484**, 186–194.

Fitt, B.D.L., Brun, H., Barbetti, M.J. and Rimmer, S.R. (2006) World-wide importance of phoma stem canker (*Leptosphaeria maculans* and *L. biglobosa*) on oilseed Rape (*Brassica napus*). *Eur. J. Plant Pathol.* **114**, 3–15.

Floerl, S., Druebert, C., Majcherczyk, A., Karlovsky, P., Kües, U. and Polle, A. (2008) Defence reactions in the apoplastic proteome of oilseed rape (*Brassica napus* var. *napus*) attenuate *Verticillium longisporum* growth but not disease symptoms. *BMC Plant Biol.* **8**, 129.

Fordyce, C. and Green, R.J. (1964) Mechanisms of variation in *Verticillium albo-atrum*. *Phytopathology* **54**, 795–798.

Fouche, S., Plissonneau, C. and Croll, D. (2018) The birth and death of effectors in rapidly evolving filamentous pathogen genomes. *Curr. Opin. Microbiol.* **46**, 34–42.

Fradin, E.F., Abd-El-Haliem, A., Masini, L., van den Berg, G.C.M., Joosten, M.H.A.J. and Thomma, B.P.H.J. (2011) Interfamily transfer of tomato *Ve1* mediates *Verticillium* resistance in Arabidopsis. *Plant Physiol.* **156**, 2255–2265.

Fradin, E.F. and Thomma, B.P.H.J. (2006) Physiology and molecular aspects of Verticillium wilt diseases caused by *V. dahliae* and *V. albo-atrum*. *Mol. Plant Pathol.* **7**, 71–86.

Fradin, E.F., Zhang, Z., Ayala, J.C.J., Castroverde, C.D.M., Nazar, R.N., Robb, J., Liu, C.-M. and Thomma, B.P.H.J. (2009) Genetic dissection of Verticillium wilt resistance mediated by tomato Ve1. *Plant Physiol.* **150**, 320–332.

França, S.C., Spiessens, K., Pollet, S., Debode, J., De Rooster, L., Callens, D. and Höfte, M. (2013) Population dynamics of *Verticillium* species in cauliflower fields: influence of crop rotation, debris removal and ryegrass incorporation. *Crop Prot.* **54**, 134–141.

Friesen, T.L., Stukenbrock, E.H., Liu, Z., et al. (2006) Emergence of a new disease as a result of interspecific virulence gene transfer. *Nat. Genet.* **38**, 953–956.

Fulton, T.M., Chunwongse, J. and Tanksley, S.D. (1995) Microprep protocol for extraction of DNA from tomato and other herbaceous plants. *Plant Mol. Biol. Report.* **13**, 207–209.

Galazka, J.M. and Freitag, M. (2014) Variability of chromosome structure in pathogenic fungi - of " ends and odds ." *Curr. Opin. Microbiol.* **20**, 19–26.

Garbelotto, M. and Gonthier, P. (2013) Biology, epidemiology, and control of *Heterobasidion* species worldwide. *Annu. Rev. Phytopathol.* **51**, 39–59.

Garbelotto, M., Ratcliff, A., Bruns, T.D., Cobb, F.W. and Otrosina, W.J. (1996) Use of taxon-specific competitive-priming PCR to study host specificity, hybridization, and intergroup gene flow in intersterility groups of *Heterobasidion annosum*. *Phytopathology* **86**, 543–551.

Garber, R.H. and Houston, B.R. (1966) Penetration and development of *Verticillium albo-atrum* in the cotton plant. *Phytopathology* **56**, 1121–1126.

Gibson, B. and Liti, G. (2015) *Saccharomyces pastorianus*: genomic insights inspiring innovation for industry. *Yeast* **32**, 17–27.

Gladders, P., Ritchie, F., Barbara, D., Clarkson, J., Chantry, T., Taylor, M. and Turner, J. (2013) Importance and management of Verticillium wilt in winter oilseed rape. HGCA Project Report 512. Online publication. AHDB. https:// cereals.ahdb.org.uk/publications/2013/august/22/importance-and-management- of-verticillium-wilt-in-winter-oilseed-rape.aspx

Gladders, P., Smith, J.A., Kirkpatrick, L., Clewes, E., Grant, C., Barbara, D., Barnes, A. V and Lane, C.R. (2011) First record of Verticillium wilt (*Verticillium longisporum*) in winter oilseed rape in the UK. *New Dis. Reports* **23**, 8.

Gladieux, P., Vercken, E., Fontaine, M.C., Hood, M.E., Jonot, O., Couloux, A. and Giraud, T. (2011) Maintenance of fungal pathogen species that are specialized to different hosts: allopatric divergence and introgression through secondary contact. *Mol. Biol. Evol.* **28**, 459–471.

Gonthier, P., Nicolotti, G., Linzer, R., Guglielmo, F. and Garbelotto, M. (2007) Invasion of European pine stands by a North American forest pathogen and its hybridization with a native interfertile taxon. *Mol. Ecol.* **16**, 1389–1400.

Gonthier, P., Warner, R., Nicolotti, G., Mazzaglia, A. and Garbelotto, M.M. (2004) Pathogen introduction as a collateral effect of military activity. *Mycol. Res.* **108**, 468–470.

Goodwin, S.B., M'Barek, S.B., Dhillon, B., et al. (2011) Finished genome of the fungal wheat pathogen *Mycosphaerella graminicola* reveals dispensome strucutre, chromosome plasticity, and stealth pathogenesis. *PLoS Genet.* **7**, e1002070.

Gordon, J.L., Byrne, K.P. and Wolfe, K.H. (2009) Additions, losses, and rearrangements on the evolutionary route from a reconstructed ancestor to the modern *Saccharomyces cerevisiae* genome. *PLoS Genet.* **5**, e1000485.

Goss, E.M., Cardenas, M.E., Myers, K., Forbes, G.A., Fry, W.E., Restrepo, S. and Grünwald, N.J. (2011) The plant pathogen *Phytophthora andina* emerged via hybridization of an unknown *Phytophthora* species and the irish potato famine pathogen, *P. infestans*. *PLoS One* **6**, e24543.

Greig, D. (2009) Reproductive isolation in *Saccharomyces*. *Heredity* **102**, 39–44.

Gross, A., Hosoya, T. and Queloz, V. (2014) Population structure of the invasive forest pathogen *Hymenoscyphus pseudoalbidus*. *Mol. Ecol.* **23**, 2943–2960.

Grover, C.E., Gallagher, J.P., Szadkowski, E.P., Yoo, M.J., Flagel, L.E. and Wendel, J.F. (2012) Homoeolog expression bias and expression level dominance in allopolyploids. *New Phytol.* **196**, 966–971.

Grum-Grzhimaylo, A.A., Debets, A.J.M., van Diepeningen, A.D., Georgieva, M.L. and Bilanenko, E.N. (2013) *Sodiomyces alkalinus*, a new holomorphic alkaliphilic ascomycete within the *Plectosphaerellaceae*. *Persoonia* **31**, 147–158.

Gu, Z., Nicolae, D., Lu, H.-S. and Li, W.-H. (2002) Rapid divergence in expression between duplicate genes inferred from microarray data. *Trends Genet.* **18**, 609–613.

Guindon, S. and Gascuel, O. (2003) A simple, fast, and accurate algorithm to estimate large phylogenies by maximum likelihood. *Syst. Biol.* **52**, 696–704.

Gupta, R., Lee, S.E., Agrawal, G.K., Rakwal, R., Park, S., Wang, Y. and Kim, S.T. (2015) Understanding the plant-pathogen interactions in the context of proteomics-generated apoplastic proteins inventory. *Front. Plant Sci.* **6**, 352.

Gurevich, A., Saveliev, V., Vyahhi, N. and Tesler, G. (2013) QUAST: quality assessment tool for genome assemblies. *Bioinformatics* **29**, 1072–1075.

Gurung, S., Short, D.P.G., Hu, X., Sandoya, G. V, Hayes, R.J., Koike, S.T. and Subbarao, K.V. (2015) Host range of *Verticillium isaacii* and *Verticillium klebahnii* from artichoke, spinach and lettuce. *Plant Dis.* **99**, 933–938.

Guy, L., Kultima, J.R. and Andersson, S.G.E. (2011) genoPlotR: comparative gene and genome visualization in R. *Bioinformatics* **26**, 2334–2335.

Haas, B.J., Kamoun, S., Zody, M.C., et al. (2009) Genome sequence and analysis of the Irish potato famine pathogen *Phytophthora infestans*. *Nature* **461**, 393–398.

Happstadius, I., Ljungberg, A., Kristiansson, B. and Dixelius, C. (2003) Identification of *Brassica oleracea* germplasm with improved resistance to Verticillium wilt. *Plant Breed.* **122**, 30–34.

Harrell, F.E.J. and Dupont, C. (2016) Hmisc: Harrell Miscellaneous. Hmisc: Harrell Miscellaneous. R package version 4.0–2 [WWW document]. URL https://CRAN.R-project.org/package5Hmisc.

Hastie, A.C. (1973) Hybridization of *Verticillium albo-atrum* and *Verticillium dahliae*. *Trans. Br. Mycol. Soc.* **60**, 511–523.

Haubold, B. and Hudson, R.R. (2000) LIAN 3.0: detecting linkage disequilibrium in multilocus data. Linkage Analysis. *Bioinformatics* **16**, 847–848.

Hayes, R.J., McHale, L.K., Vallad, G.E., Truco, M.J., Michelmore, R.W., Klosterman, S.J., Maruthachalam, K. and Subbarao, K.V. (2011) The inheritance of resistance to Verticillium wilt caused by race 1 isolates of *Verticillium dahliae* in the lettuce cultivar La Brillante. *Theor. Appl. Genet.* **123**, 509–517.

He, Y., Fukushige, H., Hildebrand, D.F. and Gan, S. (2002) Evidence supporting a role of jasmonic acid in *Arabidopsis* leaf senescence. *Plant Physiol.* **128**, 876–884.

Heale, J.B. and Karapapa, V.K. (1999) The *Verticillium* threat to Canada's major oilseed crop: canola. *Can. J. Plant Pathol.* **21**, 1–7.

Hellsten, U., Khokha, M.K., Grammer, T.C., Harland, R.M., Richardson, P. and Rokhsar, D.S. (2007) Accelerated gene evolution and subfunctionalization in the pseudotetraploid frog *Xenopus laevis*. *BMC Biol.* **5**, 31.

Hoegg, S., Brinkmann, H., Taylor, J.S. and Meyer, A. (2004) Phylogenetic timing of the fish-specific genome duplication correlates with the diversification of teleost fish. *J. Mol. Evol.* **59**, 190–203.

Hoff, K.J., Lange, S., Lomsadze, A., Borodovsky, M. and Stanke, M. (2016) BRAKER1: unsupervised RNA-seq-based genome annotation with GeneMark-ET and AUGUSTUS. *Bioinformatics* **32**, 767–769.

Holt, C. and Yandell, M. (2011) MAKER2 : an annotation pipeline and genome- database management tool for second- generation genome projects. *BMC Bioinformatics* **12**, 491.

Hovmøller, M.S., Walter, S., Bayles, R.A., et al. (2016) Replacement of the European wheat yellow rust population by new races from the centre of diversity in the near-Himalayan region. *Plant Pathol.* **65**, 402–411.

Hubbard, A., Lewis, C.M., Yoshida, K., et al. (2015) Field pathogenomics reveals the emergence of a diverse wheat yellow rust population. *Genome Biol.* **16**, 23.

Huerta-Cepas, J., Szklarczyk, D., Forslund, K., et al. (2016) eggNOG 4.5: a hierarchical orthology framework with improved functional annotations for eukaryotic, prokaryotic and viral sequences. *Nucleic Acids Res.* **44**, D286–D293.

Hurtado-Gonzales, O.P., Aragon-Caballero, L.M., Flores-Torres, J.G., Man in 't Veld, W. and Lamour, K.H. (2009) Molecular comparison of natural hybrids of *Phytophthora nicotianae* and *P. cactorum* infecting loquat trees in Peru and Taiwan. *Mycologia* **101**, 496–502.

Husson, C., Aguayo, J., Revellin, C., Frey, P., Ioos, R. and Marçais, B. (2015) Evidence for homoploid speciation in *Phytophthora alni* supports taxonomic reclassification in this species complex. *Fungal Genet. Biol.* **77**, 12–21.

Inderbitzin, P., Bostock, R.M., Davis, R.M., Usami, T., Platt, H.W. and Subbarao, K.V. (2011a) Phylogenetics and taxonomy of the fungal vascular wilt pathogen *Verticillium*, with the descriptions of five new species. *PLoS One* **6**, e28341.

Inderbitzin, P., Davis, R.M., Bostock, R.M. and Subbarao, K.V. (2013) Identification and differentiation of *Verticillium* species and *V. longisporum* lineages by simplex and multiplex PCR assays. *PLoS One* **8**, e65990.

Inderbitzin, P., Davis, R.M., Bostock, R.M. and Subbarao, K.V. (2011b) The ascomycete *Verticillium longisporum* is a hybrid and a plant pathogen with an expanded host range. *PLoS One* **6**, e18260.

Inderbitzin, P. and Subbarao, K.V. (2014) *Verticillium* systematics and evolution: how confusion impedes Verticillium wilt management and how to resolve it. *Phytopathology* **104**, 564–574.

Ingram, R. (1968) *Verticillium dahliae* var. *longisporum*, a stable diploid. *Trans. Br. Mycol. Soc.* **51**, 339–341.

Isaac, I. (1957) Verticillium wilt of Brussels sprout. *Ann. Appl. Biol.* **45**, 276–283.

Iven, T., König, S., Singh, S., et al. (2012) Transcriptional activation and production of tryptophan-derived secondary metabolites in *Arabidopsis* roots contributes to the defense against the fungal vascular pathogen *Verticillium longisporum*. *Mol. Plant* **5**, 1389–1402.

Jackson, C.W. and Heale, J.B. (1985) Relationship between DNA content and spore volume in sixteen isolates of *Verticillium lecanii* and two new diploids of *V. dahliae* (= *V. dahliae* var. *longisporum* Stark). *J. Gen. Microbiol.* **131**, 3229–3236.

Jakobsson, M. and Rosenberg, N.A. (2007) CLUMPP : a cluster matching and permutation program for dealing with label switching and multimodality in analysis of population structure. *Bioinformatics* **23**, 1801–1806.

Jakše, J., Jelen, V., Radišek, S., et al. (2018) Genome sequence of a lethal strain of xylem-invading *Verticillium nonalfalfae*. *Genome Announc.* **6**, e01458-17.

Jiao, Y., Wickett, N.J., Ayyampalayam, S., et al. (2011) Ancestral polyploidy in seed plants and angiosperms. *Nature* **473**, 97–100.

Joaquim, T.R. and Rowe, R.C. (1990) Reassessment of vegetative compatibility relationships among strains of *Verticillium dahliae* using nitrate-nonutilizing mutants. *Phytopathology* **80**, 1160–1166.

Johansson, A., Goud, J.-K.C. and Dixelius, C. (2006a) Plant host range of *Verticillium longisporum* and microsclerotia density in Swedish soils. *Eur. J. Plant Pathol.* **114**, 139–149.

Johansson, A., Staal, J. and Dixelius, C. (2006b) Early responses in the *Arabidopsis-Verticillium longisporum* pathosystem are dependent on *NDR1*, JA- and ET-associated signals via cytosolic NPR1 and *RFO1*. *Mol. Plant-Microbe Interact.* **19**, 958–969.

Jones, J.D.G. and Dangl, J.L. (2006) The plant immune system. *Nature* **444**, 323–329.

Jones, P., Binns, D., Chang, H.-Y., et al. (2014) InterProScan 5: genome-scale protein function classification. *Bioinformatics* **30**, 1236–1240.

de Jonge, R., Bolton, M.D., Kombrink, A., van den Berg, G.C.M., Yadeta, K.A. and Thomma, B.P.H.J. (2013) Extensive chromosomal reshuffling drives evolution of virulence in an asexual pathogen. *Genome Res.* **23**, 1271–1282.

de Jonge, R., Bolton, M.D. and Thomma, B.P.H.J. (2011) How filamentous pathogens co-opt plants: the ins and outs of fungal effectors. *Curr. Opin. Plant Biol.* **14**, 400–406.

de Jonge, R., van Esse, H.P., Maruthachalam, K., et al. (2012) Tomato immune receptor Ve1 recognizes effector of multiple fungal pathogens uncovered by genome and RNA sequencing. *Proc. Natl. Acad. Sci. USA* **109**, 5110–5115.

Kamble, A., Koopmann, B. and von Tiedemann, A. (2013) Induced resistance to *Verticillium longisporum* in *Brassica napus* by beta-aminobutyric acid. *Plant Pathol.* **62**, 552–561.

Kamoun, S., Furzer, O., Jones, J.D.G., et al. (2015) The top 10 oomycete pathogens in molecular plant pathology. *Mol. Plant Pathol.* **16**, 413–434.

Kämper, J., Kahmann, R., Bölker, M., et al. (2006) Insights from the genome of the biotrophic fungal plant pathogen *Ustilago maydis*. *Nature* **444**, 97–101.

Karapapa, V.K., Bainbridge, B.W. and Heale, J.B. (1997) Morphological and molecular characterization of *Verticillium longisporum* comb. nov., pathogenic to oilseed rape. *Mycol. Res.* **101**, 1281–1294.

Karapapa, V.K. and Typas, M.A. (2001) Molecular characterization of the host-adapted pathogen *Verticillium longisporum* on the basis of a group-I intron found in the nuclear SSU-rRNA gene. *Curr. Microbiol.* **42**, 217–224.

Katoh, K. and Standley, D.M. (2013) MAFFT multiple sequence alignment software version 7: improvements in performance and usability. *Mol. Biol. Evol.* **30**, 772–780.

Kawchuk, L.M., Hachey, J., Lynch, D.R., et al. (2001) Tomato *Ve* disease resistance genes encode cell surface-like receptors. *Proc. Natl. Acad. Sci. USA* **98**, 6511–6515.

Kema, G.H.J., Mirzadi Gohari, A., Aouini, L., et al. (2018) Stress and sexual reproduction affect the dynamics of the wheat pathogen effector AvrStb6 and strobilurin resistance. *Nat. Genet.* **50**, 375–380.

Kemmochi, L., Kobayashi, I., Tsuchiya, M., Sakai, H. and Shimizu, M. (2000) Breeding materials for resistance to Verticillium wilt in Japanese cabbage. *J. Japanese Soc. Hortic. Sci.* **69**, 483–491.

Keunecke, H. (2009) Einfluss von Kohlfliegenbefall auf die Infektion und Schadwirkung von *Verticillium longisporum* und *Phoma lingam* an Raps. PhD thesis, University of Göttingen (in German).

Khang, C.H., Park, S.-Y., Lee, Y.-H., Valent, B. and Kang, S. (2008) Genome organization and evolution of the *AVR-Pita* avirulence gene family in the *Magnaporthe grisea* species complex. *Mol. Plant-Microbe Interact.* **21**, 658–670.

Kimura, M. and Ohta, T. (1974) On some principles governing molecular evolution. *Proc. Natl. Acad. Sci. USA* **71**, 2848–2852.

Klebahn, H. (1913) Beiträge zur Kenntnis der Fungi imperfecti. 1. Eine Verticillium- Krankheit auf Dahlien. *Mycol. Centbl.* **3**, 49–66.

Klosterman, S.J., Subbarao, K.V., Kang, S., et al. (2011) Comparative genomics yields insights into niche adaptation of plant vascular wilt pathogens. *PLoS Pathog.* **7**, e1002137.

Knecht, K., Seyffarth, M., Desel, C., Thurau, T., Sherameti, I., Lou, B., Oelmüller, R. and Cai, D. (2010) Expression of *BvGLP-1* encoding a germin-like protein from sugar beet in *Arabidopsis thaliana* leads to resistance against phytopathogenic fungi. *Mol. Plant-Microbe Interact.* **23**, 446–457.

Knüfer, J., Lopisso, D.T., Koopmann, B., Karlovsky, P. and von Tiedemann, A. (2017) Assessment of latent infection with *Verticillium longisporum* in field-grown oilseed rape by qPCR. *Eur. J. Plant Pathol.* **147**, 819–831.

Koike, S.T., Subbarao, K.V., Davis, R.M., Gordon, T.R. and Hubbard, J.C. (1994) Verticillium wilt of cauliflower in California. *Plant Dis.* **78**, 1116–1121.

Kombrink, A., Rovenich, H., Shi-Kunne, X., et al. (2017) *Verticillium dahliae* LysM effectors differentially contribute to virulence on plant hosts. *Mol. Plant Pathol.* **18**, 596–608.

König, S., Feussner, K., Kaever, A., Landesfeind, M., Thurow, C., Karlovsky, P., Gatz, C., Polle, A. and Feussner, I. (2014) Soluble phenylpropanoids are involved in the defense response of *Arabidopsis* against *Verticillium longisporum*. *New Phytol.* **202**, 823–837.

Kroeker, G. (1970) Vissnesjuka pa rabs och rybs i Skane orsakad av *Verticillium*. [*Verticillium* on oilseed rape and turnip rape in Scania caused by *Verticillium*.]. *Sven. Frötidning* **19**, 10–13.

Krogh, A., Larsson, B., von Heijne, G. and Sonnhammer, E.L.L. (2001) Predicting transmembrane protein topology with a hidden Markov model: application to complete genomes. *J. Mol. Biol.* **305**, 567–580.

Kurtz, S., Phillippy, A., Delcher, A.L., Smoot, M., Shumway, M., Antonescu, C. and Salzberg, S.L. (2004) Versatile and open software for comparing large genomes. *Genome Biol.* **5**, R12.

Lam, K.-K., Labutti, K., Khalak, A. and Tse, D. (2015) FinisherSC: a repeat-aware tool for upgrading de-novo assembly using long reads. *Bioinformatics* **31**, 3207–3209.

Lemaire, C., De Gracia, M., Leroy, T., Michalecka, M., Lindhard-Pedersen, H., Guerin, F., Gladieux, P. and Le Cam, B. (2016) Emergence of new virulent populations of apple scab from nonagricultural disease reservoirs. *New Phytol.* **209**, 1220–1229.

Leroy, T., Caffier, V., Celton, J.M., Anger, N., Durel, C.E., Lemaire, C. and Le Cam, B. (2016) When virulence originates from nonagricultural hosts: evolutionary and epidemiological consequences of introgressions following secondary contacts in *Venturia inaequalis*. *New Phytol.* **210**, 1443-1452.

Levin, A.G., Lavee, S. and Tsror, L. (2003) Epidemiology of *Verticillium dahliae* on olive (cv. Picual) and its effect on yield under saline conditions. *Plant Pathol.* **52**, 212–218.

Levinson, G. and Gutman, G.A. (1987) Slipped-strand mispairing: a major mechanism for DNA sequence evolution. *Mol. Biol. Evol.* **4**, 203–221.

Li, H. (2013) Aligning sequence reads, clone sequences and assembly contigs with BWA-MEM. *arXiv*, 1303.3997.

Li, H., Handsaker, B., Wysoker, A., Fennell, T., Ruan, J., Homer, N., Marth, G., Abecasis, G. and Durbin, R. (2009) The Sequence Alignment/Map format and SAMtools. *Bioinformatics* **25**, 2078–2079.

Li, Y., Zhang, Q., Zhang, J., Wu, L., Qi, Y. and Zhou, J.M. (2010) Identification of microRNAs involved in pathogen-associated molecular pattern-triggered plant innate immunity. *Plant Physiol.* **152**, 2222–2231.

Liao, Y., Smyth, G.K. and Shi, W. (2013) The Subread aligner: fast, accurate and scalable read mapping by seed-and-vote. *Nucleic Acids Res.* **41**, e108.

Lockman, B., Mascheretti, S., Schechter, S. and Garbelotto, M. (2014) A first generation *Heterobasidion* hybrid discovered in *Larix lyalli* in Montana. *Dis. Notes* **98**, 1003.

Lohaus, R. and Van de Peer, Y.(2016) Of dups and dinos: evolution at the K/Pg boundary. *Curr. Opin. Plant Biol.* **30**, 62–69.

Lomsadze, A., Burns, P.D. and Borodovsky, M. (2014) Integration of mapped RNA-Seq reads into automatic training of eukaryotic gene finding algorithm. *Nucleic Acids Res.* **42**, e119.

Lopisso, D.T., Knüfer, J., Koopmann, B. and von Tiedemann, A. (2017) The vascular pathogen *Verticillium longisporum* does not affect water relations and plant responses to drought stress of its host, *Brassica napus*. *Phytopathology* **107**, 444-454.

Louis, V.L., Despons, L., Friedrich, A., et al. (2012) *Pichia sorbitophila*, an interspecies yeast hybrid, reveals early steps of genome resolution after polyploidization. *G3* **2**, 299–311.

Luo, R., Liu, B., Xie, Y., et al. (2012) SOAPdenovo2: an empirically improved memory-efficient short-read de novo assembler. *Gigascience* **1**, 18.

Lynch, M. and Conery, J.S. (2001) The evolutionary fate and consequences of duplicate genes. *Science* **290**, 1151–1155.

Ma, L.-J., van der Does, H.C., Borkovich, K.A., et al. (2010) Comparative genomics reveals mobile pathogenicity chromosomes in *Fusarium*. *Nature* **464**, 367–373.

Maere, S., De Bodt, S., Raes, J., Casneuf, T., Montagu, M. Van, Kuiper, M. and Van de Peer, Y. (2005) Modeling gene and genome duplications in eukaryotes. *Proc. Natl. Acad. Sci. USA* **102**, 5454–5459.

Magadum, S., Banerjee, U., Murugan, P., Gangapur, D. and Ravikesavan, R. (2013) Gene duplication as a major force in evolution. *J. Genet.* **92**, 155–161.

Mallet, J. (1995) A species definition for the modern synthesis. *Trends Ecol. Evol.* **10**, 294–299.

Mallet, J. (2007) Hybrid speciation. *Nature* **446**, 279–283.

Mallet, J. (2005) Hybridization as an invasion of the genome. *Trends Ecol. Evol.* **20**, 229–237.

Man in 't Veld, W.A., Veenbaas-Rijks, W.J., Ilieva, E., de Cock, A.W.A.M., Bonants, P.J.M. and Pieters, R. (1998) Natural hybrids of *Phytophthora nicotianae* and *Phytophthora cactorum* demonstrated by isozyme analysis and random amplified polymorphic DNA. *Phytopathology* **88**, 922–929.

Man in 't Veld, W.A., de Cock, A.W.A.M. and Summerbell, R.C. (2007) Natural hybrids of resident and introduced *Phytophthora* species proliferating on multiple new hosts. *Eur. J. Plant Pathol.* **117**, 25–33.

Man in 't Veld, W.A, Rosendahl, K.C.H.M. and Hong, C. (2012) *Phytophth*ora x*serendipita* sp. nov. and *P. xpelgrandis*, two destructive pathogens generated by natural hybridization. *Mycologia* **104**, 1390–1396.

Marcet-Houben, M. and Gabaldón, T. (2015) Beyond the whole-genome duplication: phylogenetic evidence for an ancient interspecies hybridization in the baker's yeast lineage. *PLOS Biol.* **13**, e1002220.

Marín-Rodríguez, M.C., Orchard, J. and Seymour, G.B. (2002) Pectate lyases, cell wall degradation and fruit softening. *J. Exp. Bot.* **53**, 2115–2119.

Matute, D.R., Butler, I.A., Turissini, D.A. and Coyne, J.A. (2010) A test of the snowball theory for the rate of evolution of hybrid incompatibilities. *Science* **329**, 1518–1521.

McCarthy, D.J., Chen, Y. and Smyth, G.K. (2012) Differential expression analysis of multifactor RNA-Seq experiments with respect to biological variation. *Nucleic Acids Res.* **40**, 4288–4297.

McCarthy, D.J. and Smyth, G.K. (2009) Testing significance relative to a fold-change threshold is a TREAT. *Bioinformatics* **25**, 765–771.

McDonald, B.A. and Linde, C. (2002) Pathogen population genetics, evolutionary potential, and durable resistance. *Annu. Rev. Phytopathol.* **40**, 349–379.

McDonald, B.A. and Stukenbrock, E.H. (2016) Rapid emergence of pathogens in agro-ecosystems: global threats to agricultural sustainability and food security. *Philos. Trans. R. Soc. B* **371**, 20160026.

McDonald, J.H. and Kreitman, M. (1991) Adaptive protein evolution at the *Adh* locus in *Drosophila*. *Nature* **351**, 652–654.

McDonald, M.C., Ahren, D., Simpfendorfer, S., Milgate, A. and Solomon, P.S. (2018) The discovery of the virulence gene *ToxA* in the wheat and barley pathogen *Bipolaris sorokiniana*. *Mol. Plant Pathol.* **19**, 432–439.

McGrath, C.L., Gout, J.F., Johri, P., Doak, T.G. and Lynch, M. (2014) Differential retention and divergent resolution of duplicate genes following whole-genome duplication. *Genome Res.* **24**, 1665–1675.

McMullan, M., Gardiner, A., Bailey, K., et al. (2015) Evidence for suppression of immunity as a driver for genomic introgressions and host range expansion in races of *Albugo candida*, a generalist parasite. *Elife* **4**, e04550.

Meier, J.I., Marques, D.A., Mwaiko, S., Wagner, C.E., Excoffier, L. and Seehausen, O. (2017) Ancient hybridization fuels rapid cichlid fish adaptive radiations. *Nat. Commun.* **8**, 14363.

Meirmans, P.G. and van Tienderen, P.H. (2004) GENOTYPE and GENODIVE: two programs for the analysis of genetic diversity of asexual organisms. *Mol. Ecol. Notes* **4**, 792–794.

Melero-Vara, J.M., Blanco-López, M.A., Bejarano-Alcázar, J. and Jiménez-Díaz, R.M. (1995) Control of Verticillium wilt of cotton by means of soil solarization and tolerant cultivars in southern Spain. *Plant Pathol.* **44**, 250–260.

Menardo, F., Praz, C., Wyder, S., et al. (2016) Hybridization of powdery mildew strains gives raise to pathogens on novel agricultural crop species. *Nat. Genet.*, **48**, 201-205.

Milgroom, M.G., Jiménez-Gasco, M.d.M., Olivares-García, C., Drott, M.T. and Jiménez-Díaz, R.M. (2014) Recombination between clonal lineages of the asexual fungus *Verticillium dahliae* detected by genotyping by sequencing. *PLoS One* **9**, e106740.

Mixão, V. and Gabaldón, T. (2017) Hybridization and emergence of virulence in opportunistic human yeast pathogens. *Yeast*, **35**, 5-20.

Möller, M. and Stukenbrock, E.H. (2017) Evolution and genome architecture in fungal plant pathogens. *Nat. Rev. Microbiol.* **15**, 756–771.

Moon, C.D., Craven, K.D., Leuchtmann, a., Clement, S.L. and Schardl, C.L. (2004) Prevalence of interspecific hybrids amongst asexual fungal endophytes of grasses. *Mol. Ecol.* **13**, 1455–1467.

Morales, L. and Dujon, B. (2012) Evolutionary role of interspecies hybridization and genetic exchanges in yeasts. *Microbiol. Mol. Biol. Rev.* **76**, 721–739.

Müller, H. and Berg, G. (2008) Impact of formulation procedures on the effect of the biocontrol agent *Serratia plymuthica* HRO-C48 on Verticillium wilt in oilseed rape. *BioControl* **53**, 905–916.

Nagao, H., Wakatabe, D. and Iijima, T. (1994) Difficulty to establish vegetative compatibility of Japanese isolates of *Verticillium dahliae* Kleb. using melanin-synthesis deficient mutants. *J. Gen. Appl. Microbiol.* **40**, 277–285.

Narisawa, K., Ohki, K.T. and Hashiba, T. (2000) Suppression of clubroot and *Verticillium* yellows in Chinese cabbage in the field by the root endophytic fungus, *Heteroconium chaetospira*. *Plant Pathol.* **49**, 141–146.

Narisawa, K., Tokumasu, S. and Hashiba, T. (1998) Suppression of clubroot formation in Chinese cabbage by the root endophytic fungus, *Heteroconium chaetospira*. *Plant Pathol.* **47**, 206–210.

Narisawa, K., Usuki, F. and Hashiba, T. (2004) Control of *Verticillium* yellows in Chinese cabbage by the dark septate endophytic fungus LtVB3. *Phytopathology* **94**, 412–418.

Nechwatal, J. and Lebecka, R. (2013) Genetic and phenotypic analyses of *Pythium* isolates from reed suggest the occurrence of a new species, *P. phragmiticola*, and its involvement in the generation of a natural hybrid. *Mycoscience* **55**, 134–143.

Nechwatal, J. and Mendgen, K. (2009) Evidence for the occurrence of natural hybridization in reed-associated *Pythium* species. *Plant Pathol.* **58**, 261–270.

Nei, M. (1973) Analysis of gene diversity in subdivided populations. *Proc. Nat. Acad. Sci.* **70**, 3321–3323.

Nei, M. and Gojoborit, T. (1986) Simple methods for estimating the numbers of synonymous and nonsynonymous nucleotide substitutions. *Mol. Biol. Evol.* **3**, 418–426.

Nei, M., Maruyama, T. and Chakraborty, R. (1975) The bottleneck effect and genetic variability in populations. *Evolution* **29**, 1–10.

Newcombe, G., Stirling, B. and Bradshaw, H.D. Jr (2001) Abundant pathogenic variation in the new hybrid rust *Melampsora* x*columbiana* on hybrid poplar. *Phytopathology* **91**, 981–985.

Newcombe, G., Stirling, B., McDonald, S. and Bradshaw, H.D. Jr (2000) *Melampsora* ×*columbiana*, a natural hybrid of *M . medusae* and *M . occidenta*lis. *Mycol. Res.* **104**, 261–274.

Niazi, A., Manzoor, S., Asari, S., Bejai, S., Meijer, J. and Bongcam-Rudloff, E. (2014) Genome analysis of *Bacillus amyloliquefaciens* subsp. *plantarum* UCMB5113: a rhizobacterium that improves plant growth and stress management. *PLoS One* **9**, e104651.

Nielsen, K. and Yohalem, D.S. (2001) Origin of a polyploid *Botrytis* pathogen through interspecific hybridization between *Botrytis aclada* and *B . byssoidea*. *Mycologia* **93**, 1064–1071.

Nirenberg, H.I., Gerlach, W.F. and Gräfenhan, T. (2009) *Phytophthora* x *pelgrandis*, a new natural hybrid pathogenic to *Pelargonium grandiflorum* hort. *Mycologia* **101**, 220–231.

Njoroge, S.M.C., Vallad, G.E., Park, S.-Y., Kang, S., Koike, S.T., Bolda, M., Burman, P., Polonik, W. and Subbarao, K.V. (2011) Phenological and phytochemical changes correlate with differential interactions of *Verticillium dahliae* with broccoli and cauliflower. *Phytopathology* **101**, 523–534.

Novakazi, F., Inderbitzin, P., Sandoya, G., Hayes, R.J., von Tiedemann, A. and Subbarao, K.V. (2015) The three lineages of the diploid hybrid *Verticillium longisporum* differ in virulence and pathogenicity. *Phytopathology* **105**, 662–673.

Obermeier, C., Hossain, M.A., Snowdon, R., Knüfer, J., von Tiedemann, A. and Friedt, W. (2013) Genetic analysis of phenylpropanoid metabolites associated with resistance against *Verticillium longisporum* in *Brassica napus*. *Mol. Breed.* **31**, 347–361.

Ohtaka, N. and Narisawa, K. (2008) Molecular characterization and endophytic nature of the root-associated fungus *Meliniomyces variabilis* (LtVB3). *J. Gen. Plant Pathol.* **74**, 24–31.

Okoli, C.A.N., Carder, J.H. and Barbara, D.J. (1994) Restriction fragment length polymorphisms (RFLPs) and the relationships of some host-adapted isolates of *Verticillium dahliae*. *Plant Pathol.* **43**, 33–40.

Oliva, R.F., Kroon, L.P.N.M., Chacón, G., Flier, W.G., Ristaino, J.B. and Forbes, G.A. (2010) *Phytophthora andina* sp. nov., a newly identified heterothallic pathogen of solanaceous hosts in the Andean highlands. *Plant Pathol.* **59**, 613–625.

Orbach, M.J., Farrall, L., Sweigard, J.A., Chumley, F.G. and Valent, B. (2000) A telomeric avirulence gene determines dfficacy for the rice blast resistance gene *Pi-ta*. *Plant Cell* **12**, 2019–2032.

Ordonez, N., Seidl, M.F., Waalwijk, C., Drenth, A., Kilian, A., Thomma, B.P.H.J., Ploetz, R.C. and Kema, G.H.J. (2015) Worse comes to worst: bananas and panama disease-when plant and pathogen clones meet. *PLoS Pathog.* **11**, e1005197.

Orr, H.A. (2005) The genetic basis of reproductive isolation: insights from *Drosophila*. *Proc. Natl. Acad. Sci. USA* **102**, 6522–6526.

Ortiz-Merino, R.A., Kuanyshev, N., Braun-Galleani, S., Byrne, K.P., Porro, D., Branduardi, P. and Wolfe, K.H. (2017) Evolutionary restoration of fertility in an interspecies hybrid yeast, by whole-genome duplication after a failed mating-type switch. *PLoS Biol.* **15**, e2002128.

Pantou, M.P., Strunnikova, O.K., Shakhnazarova, V.Y., Vishnevskaya, N.A., Papalouka, V.G. and Typas, M.A. (2005) Molecular and immunochemical phylogeny of *Verticillium* species. *Mycol. Res.* **109**, 889–902.

Peakall, R. and Smouse, P.E. (2006) GENALEX 6: Genetic analysis in Excel. Population genetic software for teaching and research. *Mol. Ecol. Notes* **6**, 288–295.

Peakall, R. and Smouse, P.E. (2012) GenAlEx 6.5 : genetic analysis in Excel . Population genetic software for teaching and research-an update. *Bioinformatics* **28**, 2537–2539.

Pegg, G.F. and Brady, B.L. (2002) *Verticillium wilts*. Wallingford, Oxfordshire: CABI Publishing.

Peris, D., Moriarty, R.V., Alexander, W.G., et al. (2017) Hybridization and adaptive evolution of diverse *Saccharomyces* species for cellulosic biofuel production. *Biotechnol. Biofuels* **10**, 78.

Petersen, T.N., Brunak, S., von Heijne, G. and Nielsen, H. (2011) SignalP 4.0: discriminating signal peptides from transmembrane regions. *Nat. Methods* **8**, 785–786.

Petit, R.J., Mousadik, A.E. and Pons, O. (1998) Identifying populations for consevation on the basis of genetic markers. *Conserv. Biol.* **12**, 844–855.

Phanstiel, D.H., Boyle, A.P., Araya, C.L. and Snyder, M.P. (2014) Sushi.R: flexible, quantitative and integrative genomic visualizations for publication-quality multi-panel figures. *Bioinformatics* **30**, 2808–2810.

Ploetz, R.C., Kema, G.H.J. and Ma, L.-J. (2015) Impact of diseases on export and smallholder production of banana. *Annu. Rev. Phytopathol.* **53**, 269–288.

Powelson, R.L. and Carter, G.E. (1973) Efficacy of soil fumigants for control of Verticillium wilt of potatoes. *Am. Potato J.* **50**, 162–167.

Price, J.S., Hobson, R.N., Neale, M.A. and Bruce, D.M. (1996) Seed losses on commercial harvesting of oilseed rape. *J. Agric. Eng. Res.* **65**, 183–191.

Pritchard, J.K., Stephens, M. and Donnelly, P. (2000) Inference of population structure using multilocus genotype data. *Genetics* **155**, 945–959.

Pryszcz, L.P., Németh, T., Saus, E., Ksiezopolska, E., Hegedűsová, E., Nosek, J., Wolfe, K.H., Gacser, A. and Gabaldón, T. (2015) The genomic aftermath of hybridization in the opportunistic pathogen *Candida metapsilosis*. *PLoS Genet.* **11**, e1005626.

Puhalla, J.E. (1979) Classification of isolates of *Verticillium dahliae* based on heterokaryon incompatibility. *Phytopathology* **69**, 1186–1189.

Pullman, G.S., DeVay, J.E. and Garber, R.H. (1981) Soil solarization and thermal death: a logarithmic relationship between time and temperature for four soilborne plant pathogens. *Phytopathology* **71**, 959–964.

Qin, Q.-M., Vallad, G.E., Wu, B.M. and Subbarao, K.V. (2006) Phylogenetic analyses of phytopathogenic isolates of *Verticillium* spp. *Phytopathology* **96**, 582–592.

Quinlan, A.R. and Hall, I.M. (2010) BEDTools: A flexible suite of utilities for comparing genomic features. *Bioinformatics* **26**, 841–842.

R Core Team (2015) R: a language and environment for statistical computing. R foundation for statistical computing, Vienna, Austria. Available at: https://www.R-project.org/. Accessed: 23 May 2018.

Raffaele, S., Farrer, R.A., Cano, L.M., et al. (2010) Genome evolution following host jumps in the Irish potato famine pathogen lineage. *Science* **330**, 1540–1543.

Raffaele, S. and Kamoun, S. (2012) Genome evolution in filamentous plant pathogens: why bigger can be better. *Nat. Rev. Microbiol.* **10**, 417–430.

Ralhan, A., Schöttle, S., Thurow, C., Iven, T., Feussner, I., Polle, A. and Gatz, C. (2012) The vascular pathogen *Verticillium longisporum* requires a jasmonic acid-independent COI1 function in roots to elicit disease symptoms in *Arabidopsis* shoots. *Plant Physiol.* **159**, 1192–1203.

Ratzinger, A., Riediger, N., von Tiedemann, A. and Karlovsky, P. (2009) Salicylic acid and salicylic acid glucoside in xylem sap of *Brassica napus* infected with *Verticillium longisporum*. *J. Plant Res.* **122**, 571–579.

Refrégier, G., Hood, M.E. and Giraud, T. (2010) No evidence of reproductive character displacement between two sister fungal species causing anther smut disease in *Silene*. *Int. J. Plant Sci.* **171**, 847–859.

Reusche, M., Klásková, J., Thole, K., et al. (2013) Stabilization of cytokinin levels enhances *Arabidopsis* resistance against *Verticillium longisporum*. *Mol. Plant-Microbe Interact.* **26**, 850–860.

Reusche, M., Thole, K., Janz, D., Truskina, J., Rindfleisch, S., Drubert, C., Polle, A., Lipka, V. and Teichmann, T. (2012) *Verticillium* infection triggers VASCULAR-RELATED NAC DOMAIN7-dependent *de novo* xylem formation and enhances drought tolerance in *Arabidopsis*. *Plant Cell* **24**, 3823–3837.

Reusche, M., Truskina, J., Thole, K., et al. (2014) Infections with the vascular pathogens *Verticillium longisporum* and *Verticillium dahliae* induce distinct disease symptoms and differentially affect drought stress tolerance of *Arabidopsis thaliana*. *Environ. Exp. Bot.* **108**, 23–37.

Ribeiro, R.A., and Lovato, M.B. (2007) Comparative analysis of different DNA extraction protocols in fresh and herbarium specimens of the genus *Dalbergia*. *Genet. Mol. Res.* **6**, 173–187.

Ristaino, J.B. (2002) Tracking historic migrations of the Irish potato famine pathogen, *Phytophthora infestans*. *Microbes Infect.* **4**, 1369–1377.

Robertson, F.M., Gundappa, M.K., Grammes, F., et al. (2017) Lineage-specific rediploidization is a mechanism to explain time-lags between genome duplication and evolutionary diversification. *Genome Biol.* **18**, 111.

Robinson, J.T., Thorvaldsdóttir, H., Winckler, W., Guttman, M., Lander, E.S., Getz, G. and Mesirov, J.P. (2011) Integrative Genomics Viewer. *Nat. Biotechnol.* **29**, 24–6.

Robinson, M.D., McCarthy, D.J. and Smyth, G.K. (2009) edgeR: a Bioconductor package for differential expression analysis of digital gene expression data. *Bioinformatics* **26**, 139–140.

Roos, J., Bejai, S., Mozūraitis, R. and Dixelius, C. (2015) Susceptibility to *Verticillium longisporum* is linked to monoterpene production by TPS23/27 in *Arabidopsis*. *Plant J.* **81**, 572–585.

Roos, J., Bejai, S., Oide, S. and Dixelius, C. (2014) *RabGAP22* is required for defense to the vascular pathogen *Verticillium longisporum* and contributes to stomata immunity. *PLoS One* **9**, e88187.

Rosenberg, N.A. (2004) DISTRUCT : a program for the graphical display of population structure. *Mol. Ecol. Notes* **4**, 137–138.

Rouxel, T., Grandaubert, J., Hane, J.K., et al. (2011) Effector diversification within compartments of the *Leptosphaeria maculans* genome affected by Repeat-Induced Point mutations. *Nat. Commun.* **2**, 202.

Rovenich, H., Boshoven, J.C. and Thomma, B.P.H.J. (2014) Filamentous pathogen effector functions: of pathogens, hosts and microbiomes. *Curr. Opin. Plant Biol.* **20**, 96–103.

Rygulla, W., Friedt, W., Seyis, F., Lühs, W., Eynck, C., von Tiedemann, A. and Snowdon, R.J. (2007a) Combination of resistance to *Verticillium longisporum* from zero erucic acid *Brassica oleracea* and oilseed *Brassica rapa* genotypes in resynthesized rapeseed (*Brassica napus*) lines. *Plant Breed.* **126**, 596–602.

Rygulla, W., Snowdon, R.J., Eynck, C., Koopmann, B., von Tiedemann, A., Lühs, W. and Friedt, W. (2007b) Broadening the genetic basis of *Verticillium longisporum* resistance in *Brassica napus* by interspecific hybridization. *Phytopathology* **97**, 1391–1396.

Rygulla, W., Snowdon, R.J., Friedt, W., Happstadius, I., Cheung, W.Y. and Chen, D. (2008) Identification of quantitative trait loci for resistance against *Verticillium longisporum* in oilseed rape (*Brassica napus*). *Phytopathology* **98**, 215–221.

Santhanam, P., van Esse, H.P., Albert, I., Faino, L., Nürnberger, T. and Thomma, B.P.H.J. (2013) Evidence for functional diversification within a fungal NEP1-like protein family. *Mol. Plant-Microbe Interact.* **26**, 278–286.

Sarosh, B.R., Danielsson, J. and Meijer, J. (2009) Transcript profiling of oilseed rape (*Brassica napus*) primed for biocontrol differentiate genes involved in microbial interactions with beneficial *Bacillus amyloliquefaciens* from pathogenic *Botrytis cinerea*. *Plant Mol. Biol.* **70**, 31–45.

Schirawski, J., Mannhaupt, G., Münch, K., et al. (2010) Pathogenicity determinants in smut fungi revealed by genome comparison. *Science* **330**, 1546–1548.

Scholthof, K.-B.G. (2007) The disease triangle: pathogens, the environment and society. *Nat. Rev. Microbiol.* **5**, 152–156.

Schotanus, K., Soyer, J.L., Connolly, L.R., Grandaubert, J., Happel, P., Smith, K.M., Freitag, M. and Stukenbrock, E.H. (2015) Histone modifications rather than the novel regional centromeres of *Zymoseptoria tritici* distinguish core and accessory chromosomes. *Epigenetics Chromatin* **8**, 41.

Schranz, M.E., Mohammadin, S. and Edger, P.P. (2012) Ancient whole genome duplications, novelty and diversification: the WGD Radiation Lag-Time Model. *Curr. Opin. Plant Biol.* **15**, 147–153.

Schuelke, M. (2000) An economic method for the fluorescent labeling of PCR fragments. *Nat. Biotechnol.* **18**, 233–234.

Seehausen, O. (2004) Hybridization and adaptive radiation. *Trends Ecol. Evol.* **19**, 198–207.

Seidl, M.F., Cook, D.E. and Thomma, B.P.H.J. (2016) Chromatin biology impacts adaptive evolution of filamentous plant pathogens. *PLoS Pathog.* **12**, e1005920.

Seidl, M.F., Faino, L., Shi-Kunne, X., van den Berg, G.C.M., Bolton, M.D. and Thomma, B.P.H.J. (2015) The genome of the saprophytic fungus *Verticillium tricorpus* reveals a complex effector repertoire resembling that of its pathogenic relatives. *Mol. Plant-Microbe Interact.* **28**, 362–373.

Seidl, M.F. and Thomma, B.P.H.J. (2014) Sex or no sex: evolutionary adaptation occurs regardless. *BioEssays* **36**, 335–345.

Seidl, M.F. and Thomma, B.P.H.J. (2017) Transposable elements direct the coevolution between plants and microbes. *Trends Genet.* **33**, 842–851.

Selker, E.U. (2002) Repeat-induced gene silencing in fungi. *Advances in Genetics*. **46** , 439–450.

Seoighe, C. and Wolfe, K.H. (1998) Extent of genomic rearrangement after genome duplication in yeast. *Proc. Natl. Acad. Sci. USA* **95**, 4447–52.

Seyis, F., Snowdon, R.J., Lühs, W. and Friedt, W. (2003) Molecular characterization of novel resynthetised rapeseed (*Brassica napus*) lines and analysis of their genetic diversity in comparison with spring rapeseed cultivars. *Plant Breed.* **122**, 473–478.

Shaner, G. and Finney, R.E. (1977) The effect of nitrogen fertilization on the expression of slow-mildewing resistance in knox wheat. *Phytopathology* **77**, 1051–1056.

Shen, D., Suhrkamp, I., Wang, Y., Liu, S., Menkhaus, J., Verreet, J., Fan, L. and Cai, D. (2014) Identification and characterization of microRNAs in oilseed rape (*Brassica napus*) responsive to infection with the pathogenic fungus *Verticillium longisporum* using *Brassica* AA (*Brassica rapa*) and CC (*Brassica oleracea*) as reference genomes. *New Phytol.*, 577–594.

Shetty, K.G., Subbarao, K.V., Huisman, O.C. and Hubbard, J.C. (2000) Mechanism of broccoli-mediated Verticillium wilt reduction in cauliflower. *Phytopathology* **90**, 305–310.

Shi-Kunne, X., Faino, L., van den Berg, G.C.M., Thomma, B.P.H.J. and Seidl, M.F. (2018) Evolution within the fungal genus *Verticillium* is characterized by chromosomal rearrangements and gene losses. *Environ. Microbiol.* **20**, 1362-1373.

Shi, X., Ng, D.W.-K., Zhang, C., Comai, L., Ye, W. and Chen, Z.J. (2012) *Cis-* and *trans*-regulatory divergence between progenitor species determines gene-expression novelty in *Arabidopsis* allopolyploids. *Nat. Commun.* **3**, 950.

Short, D.P.G., Gurung, S., Hu, X., Inderbitzin, P. and Subbarao, K.V. (2014) Maintenance of sex-related genes and the co-occurrence of both mating types in *Verticillium dahliae*. *PLoS One* **9**, e112145.

Siebold, M. and von Tiedemann, A. (2013) Effects of experimental warming on fungal disease progress in oilseed rape. *Glob. Chang. Biol.* **19**, 1736–1747.

Siebold, M. and von Tiedemann, A. (2012) Potential effects of global warming on oilseed rape pathogens in Northern Germany. *Fungal Ecol.* **5**, 62–72.

Simão, F.A., Waterhouse, R.M., Ioannidis, P., Kriventseva, E. V. and Zdobnov, E.M. (2015) BUSCO: assessing genome assembly and annotation completeness with single-copy orthologs. *Bioinformatics* **31**, 3210–3212.

Simms, D., Cizdziel, P., Chomczynski, P. (1993) TRIzol: a new reagent for optimal single-step isolation of RNA. *Focus* **15**, 99-102.

Singh, S., Braus-Stromeyer, S.A., Timpner, C., et al. (2010) Silencing of *Vlaro2* for chorismate synthase revealed that the phytopathogen *Verticillium longisporum* induces the cross-pathway control in the xylem. *Appl. Microbiol. Biotechnol.* **85**, 1961–1976.

Smit, A.F.A., Hubley, R. and Green, P. (2015) RepeatMasker Open-4.0. Available at: http://www.repeatmasker.org. Accessed: 23 May 2018.

Soanes, D. and Richards, T.A. (2014) Horizontal gene transfer in eukaryotic plant pathogens. *Annu. Rev. Phytopathol.* **52**, 583–614.

Soltis, D.E., Albert, V.A., Leebens-Mack, J., et al. (2009) Polyploidy and angiosperm diversification. *Am. J. Bot.* **96**, 336–348.

Song, Y., Zhang, Z., Boshoven, J.C., et al. (2017) Tomato immune receptor Ve1 recognizes surface-exposed co-localized N- and C-termini of *Verticillium dahliae* effector Ave1. Available at: https://www.biorxiv.org/content/early/2017/01/26/103473. Accessed 23 May 2018.

Sperschneider, J., Gardiner, D.M., Thatcher, L.F., Lyons, R., Singh, K.B., Manners, J.M. and Taylor, J.M. (2015) Genome-wide analysis in three *Fusarium* pathogens identifies rapidly evolving chromosomes and genes associated with pathogenicity. *Genome Biol. Evol.* **7**, 1613–1627.

Spiers, A.G. and Hopcroft, D.H. (1994) Comparative studies of the poplar rusts *Melampsora medusae*, *M. larici-populina* and their interspecific hybrid *M. medusae-populina*. *Mycol. Res.* **98**, 889–903.

Sriswasdi, S., Takashima, M., Manabe, R., Ohkuma, M., Sugita, T. and Iwasaki, W. (2016) Global deceleration of gene evolution following recent genome hybridizations in fungi. *Genome Res.* **26**, 1081–1090.

Staats, M., van Baarlen, P. and van Kan, J.A.L. (2005) Molecular phylogeny of the plant pathogenic genus *Botrytis* and the evolution of host specificity. *Mol. Biol. Evol.* **22**, 333–346.

Stadler, M. and von Tiedemann, A. (2014) Biocontrol potential of *Microsphaeropsis ochracea* on microsclerotia of *Verticillium longisporum* in environments differing in microbial complexity. *BioControl* **59**, 449–460.

Stamatakis, A. (2014) RAxML version 8: a tool for phylogenetic analysis and post-analysis of large phylogenies. *Bioinformatics* **30**, 1312–1313.

Stanke, M., Diekhans, M., Baertsch, R. and Haussler, D. (2008) Using native and syntenically mapped cDNA alignments to improve de novo gene finding. *Bioinformatics* **24**, 637–644.

Stapleton, J.J. (2000) Soil solarization in various agricultural production systems. *Crop Prot.* **19**, 837–841.

Stark, C. (1961) Das Auftrete der *Verticillium*-Tracheomykosen in Hamburger Gartenbaukulturen. *Gartenbauwissenschaft* **2**, 493–528.

Stefanini, I., Dapporto, L., Berná, L., Polsinelli, M., Turillazzi, S. and Cavalieri, D. (2016) Social wasps are a *Saccharomyces* mating nest. *Proc. Natl. Acad. Sci. USA* **113**, 2247–2251.

Stergiopoulos, I., Kourmpetis, Y.A.I., Slot, J.C., Bakker, F.T., de Wit, P.J.G.M. and Rokas, A. (2012) In silico characterization and molecular evolutionary analysis of a novel superfamily of fungal effector proteins. *Mol. Biol. Evol.* **29**, 3371–3384.

Steventon, L.A., Fahleson, J., Hu, Q. and Dixelius, C. (2002) Identification of the causal agent of Verticillium wilt of winter oilseed rape in Sweden, *V . longisporum*. *Mycol. Res.* **106**, 570–578.

Stukenbrock, E.H. (2016a) Hybridization speeds up the emergence and evolution of a new pathogen species. *Nat. Genet.* **48**, 113–115.

Stukenbrock, E.H. (2013) Evolution, selection and isolation: a genomic view on speciation in fungal plant pathogens. *New Phytol.* **199**, 895–907.

Stukenbrock, E.H. (2016b) The role of hybridization in the evolution and emergence of new fungal plant pathogens. *Phytopathology* **106**, 104–112.

Stukenbrock, E.H., Banke, S., Javan-Nikkhah, M. and McDonald, B.A. (2007) Origin and domestication of the fungal wheat pathogen *Mycosphaerella graminicola* via sympatric speciation. *Mol. Biol. Evol.* **24**, 398–411.

Stukenbrock, E.H., Christiansen, F.B., Hansen, T.T., Dutheil, J.Y. and Schierup, M.H. (2012) Fusion of two divergent fungal individuals led to the recent emergence of a unique widespread pathogen species. *Proc. Natl. Acad. Sci. USA* **109**, 10954–10959.

Stukenbrock, E.H. and Dutheil, J.Y. (2012) Comparing fungal genomes: insight into functional and evolutionary processes. *Methods Mol. Biol.* **835**, 531–548.

Stukenbrock, E.H., Jørgensen, F.G., Zala, M., Hansen, T.T., McDonald, B.A. and Schierup, M.H. (2010) Whole-genome and chromosome evolution associated with host adaptation and speciation of the wheat pathogen *Mycosphaerella graminicola*. *PLoS Genet.* **6**, e1001189.

Subbarao, K.V. (2002) Methyl bromide alternatives: meeting the deadlines. *Phytopathology* **92**, 1334–1336.

Subbarao, K.V., Chassot, A., Gordon, T.R., Hubbard, J.C., Bonello, P., Mullin, R., Okamoto, D., Davis, R.M. and Koike, S.T. (1995) Genetic relationships and cross pathogenicities of *Verticillium dahliae* isolates from cauliflower and other crops. *Phytopathology* **85**, 1105–1112.

Subbarao, K.V. and Hubbard, J.C. (1999) Evaluation of broccoli residue incorporation into field soil for Verticillium wilt control in Cauliflower. *Plant Dis.* **83**, 124–129.

Subbarao, K.V. and Hubbard, J.C. (1996) Interactive effects of broccoli residue and temperature on *Verticillium dahliae* microsclerotia in soil and on wilt in Cauliflower. *Phytopathology* **86**, 1303–1310.

Thomma, B.P.H.J., Nürnberger, T. and Joosten, M.H.A.J. (2011) Of PAMPs and effectors: the blurred PTI-ETI dichotomy. *Plant Cell* **23**, 4–15.

Timpner, C., Braus-Stromeyer, S.A., Tran, V.T. and Braus, G.H. (2013) The Cpc1 regulator of the cross-rathway control of amino acid biosynthesis is required for pathogenicity of the vascular pathogen *Verticillium longisporum*. *Mol. Plant-Microbe Interact.* **26**, 1312–1324.

Tirosh, I., Reikhav, S., Levy, A.A. and Barkai, N. (2009) A yeast hybrid provides insight into the evolution of gene expression regulation. *Science* **324**, 659–662.

Tran, V.T., Braus-Stromeyer, S.A., Timpner, C. and Braus, G.H. (2013) Molecular diagnosis to discriminate pathogen and apathogen species of the hybrid *Verticillium longisporum* on the oilseed crop *Brassica napus*. *Appl. Microbiol. Biotechnol.* **97**, 4467–4483.

Tritt, A., Eisen, J.A., Facciotti, M.T. and Darling, A.E. (2012) An integrated pipeline for de novo assembly of microbial genomes. *PLoS One* **7**, e42304.

Typas, M.A. and Heale, J.B. (1976) Heterokaryosis and the role of cytoplasmic inheritance in dark resting structure formation in *Verticillium* spp. *Mol. Gen. Genet.* **146**, 17–26.

Tyvaert, L., França, S.C., Debode, J. and Höfte, M. (2014) The endophyte *Verticillium* Vt305 protects cauliflower against Verticillium wilt. *J. Appl. Microbiol.* **116**, 1563–1571.

Untergasser, A., Cutcutache, I., Koressaar, T., Ye, J., Faircloth, B.C., Remm, M. and Rozen, S.G. (2012) Primer3-new capabilities and interfaces. *Nucleic Acids Res.* **40**, e115.

Van de Peer, Y., Mizrachi, E. and Marchal, K. (2017) The evolutionary significance of polyploidy. *Nat. Rev. Genet.*, **18**, 411-424.

Vandenkoornhuyse, P., Quaiser, A., Duhamel, M., Le Van, A. and Dufresne, A. (2015) The importance of the microbiome of the plant holobiont. *New Phytol.* **206**, 1196–1206.

Vanneste, K., Baele, G., Maere, S. and Van de Peer, Y. (2014a) Analysis of 41 plant genomes supports a wave of successful genome duplications in association with the Cretaceous-Paleogene boundary. *Genome Res.*, 1334–1347.

Vanneste, K., Maere, S. and Van de Peer, Y. (2014b) Tangled up in two: a burst of genome duplications at the end of the Cretaceous and the consequences for plant evolution. *Philos. Trans. R. Soc. B* **369**, 20130353.

Vargas-Machuca, R., Martin, C. and Galindez, W. (1987) Recovery of *Verticillium dahliae* from weed plants in farmers' fields in Peru. *Plant Dis.* **71**, 756–758.

Veronese, P., Narasimhan, M.L., Stevenson, R.A., Zhu, J.-K., Weller, S.C., Subbarao, K.V. and Bressan, R.A. (2003) Identification of a locus controlling Verticillium disease symptom response in *Arabidopsis thaliana*. *Plant J.* **35**, 574–587.

Vlaardingerbroek, I., Beerens, B., Schmidt, S.M., Cornelissen, B.J.C. and Rep, M. (2016) Dispensable chromosomes in *Fusarium oxysporum* f. sp *lycopersici*. *Mol. Plant Pathol.* **17**, 1455–1466.

Watanabe, T.,)zawa, M. and Sakai, R. (1973) A new disease of Chinese cabbage caused by *Verticillium albo-atrum* and some factors related to the incidence of the disease. *Ann. Phytopathol. Soc. Japan* **39**, 344–349.

Webb, A.E., Walsh, T.A. and O'Connell, M.J. (2017) VESPA: very large-scale evolutionary and selective pressure analyses. *PeerJ Comput. Sci.* **3**, e118.

Wellings, C.R., McIntosh, R.A. and Walker, J. (1987) *Puccinia striiformis* f. sp. *tritici* in Eastern Australia - possible means of entry and implications for plant quarantine. *Plant Pathol.* **36**, 239–241.

Wilhelm, S. (1955) Longevity of Verticillium wilt fungus in the laboratory and field. *Phytopathology* **45**, 180–181.

Williams, P.D. (2010) Darwinian interventions : taming pathogens through evolutionary ecology. *Trends Parasitol.* **26**, 83–92.

Wittkop, B., Snowdon, R.J. and Friedt, W. (2009) Status and perspectives of breeding for enhanced yield and quality of oilseed crops for Europe. *Euphytica* **170**, 131–140.

Wittstock, U. and Halkier, B.A. (2002) Glucosinolate research in the *Arabidopsis* era. *Trends Plant Sci.* **7**, 263–270.

Witzel, K., Hanschen, F.S., Klopsch, R., Ruppel, S., Schreiner, M. and Grosch, R. (2015) *Verticillium longisporum* infection induces organ-specific glucosinolate degradation in *Arabidopsis thaliana*. *Front. Plant Sci.* **6**, 1–11.

Wolfe, K.H. (2001) Yesterday's polyploids and the mystery of diploidization. *Nat. Rev. Genet.* **2**, 333–341.

Wong, S., Butler, G. and Wolfe, K.H. (2002) Gene order evolution and paleopolyploidy in hemiascomycete yeasts. *Proc. Natl. Acad. Sci. USA* **99**, 9272–9277.

Wood, T., Teakle, G. and Mackay, I. (2013) An introduction to the contemporary breeding of oil seed rape. *Lipid Technol.* **25**, 251–254.

Woolliams, G.E. (1966) Host range and symptomatology of *Verticillium dahliae* in economic, weed, and native plants in interior British Columbia. *Can. J. Plant Sci.* **46**, 661–669.

van de Wouw, A.P., Cozijnsen, A.J., Hane, J.K., Brunner, P.C., McDonald, B.A., Oliver, R.P. and Howlett, B.J. (2010) Evolution of linked avirulence effectors in *Leptosphaeria maculans* is affected by genomic environment and exposure to resistance genes in host plants. *PLoS Pathog.* **6**, e1001180.

Xiao, C.L. and Subbarao, K.V. (1998) Relationships between *Verticillium dahliae* inoculum density and wilt incidence, severity, and growth of cauliflower. *Phytopathology* **88**, 1108–1115.

Xiao, C.L., Subbarao, K.V., Schulbach, K.F. and Koike, S.T. (1998) Effects of crop rotation and irrigation on *Verticillium dahliae* microsclerotia in soil and wilt in cauliflower. *Phytopathology* **88**, 1046–1055.

Yadeta, K.A., Hanemian, M., Smit, P., Hiemstra, J.A., Pereira, A., Marco, Y. and Thomma, B.P.H.J. (2011) The *Arabidopsis thaliana* DNA-binding protein AHL19 mediates Verticillium wilt resistance. *Mol. Plant-Microbe Interact.* **24**, 1582–1591.

Yadeta, K.A., Valkenburg, D.-J., Hanemian, M., Marco, Y. and Thomma, B.P.H.J. (2014) The Brassicaceae-specific *EWR1* gene provides resistance to vascular wilt pathogens. *PLoS One* **9**, e88230.

Yang, Z. (2007) PAML 4: phylogenetic analysis by maximum likelihood. *Mol. Biol. Evol.* **24**, 1586–1591.

Yohalem, D.S., Nielsen, K. and Nicolaisen, M. (2003) Taxonomic and nomenclatural clarification of the onion neck rotting *Botrytis* species. *Mycotaxon* **85**, 175–182.

Yoo, M.-J., Szadkowski, E. and Wendel, J.F. (2013) Homoeolog expression bias and expression level dominance in allopolyploid cotton. *Heredity* **110**, 171–180.

Yu, J.M., Cafarov, I.H. and Babadoost, M. (2016) Morphology, molecular identity, and pathogenicity of *Verticillium dahliae* and *V. longisporum* associated with internally discolored horseradish roots. *Plant Dis.* **100**, 749–757.

Zare, R., Gams, W., Starink-Willemse, M. and Summerbell, R.C. (2007) *Gibellulopsis*, a suitable genus for *Verticillium nigrescens*, and *Musicillium*, a new genus for *V. theobromae*. *Nov. Hedwigia* **85**, 463–489.

Zeise, K. and von Tiedemann, A. (2002) Host specialization among vegetative compatibility groups of *Verticillium dahliae* in relation to *Verticillium longisporum*. *J. Phytopathol.* **150**, 112–119.

Zeise, K. and von Tiedemann, A. (2001) Morphological and physiological differentiation among vegetative compatibility groups of *Verticillium dahliae* in relation to *V. longisporum*. *J. Phytopathol.* **149**, 469–475.

Zhang, B., Yang, Y., Chen, T., et al. (2012) Island cotton *Gbve1* gene encoding a receptor-like protein confers resistance to both defoliating and non-Defoliating isolates of *Verticillium dahliae*. *PLoS One* **7**, e51091.

Zhang, H., Meltzer, P. and Davis, S. (2013a) RCircos: an R package for Circos 2D track plots. *BMC Bioinformatics* **14**, 244.

Zhang, N., Castlebury, L.A., Miller, A.N., et al. (2006) An overview of the systematics of the *Sordariomycetes* based on a four-gene phylogeny. **98**, 1076–1087.

Zhang, Y., Wang, X., Yang, S., Chi, J., Zhang, G. and Ma, Z. (2011) Cloning and characterization of a *Verticillium* wilt resistance gene from *Gossypium barbadense* and functional analysis in *Arabidopsis thaliana*. *Plant Cell Rep.* **30**, 2085–2096.

Zhang, Z., Fradin, E., de Jonge, R., van Esse, H.P., Smit, P., Liu, C.-M. and Thomma, B.P.H.J. (2013b) Optimized agroinfiltration and virus-induced gene silencing to study Ve1-mediated *Verticillium* resistance in tobacco. *Mol. Plant-Microbe Interact.* **26**, 182–190.

Zhou, L., Hu, Q., Johansson, a. and Dixelius, C. (2006) *Verticillium longisporum* and *V. dahliae*: infection and disease in *Brassica napus*. *Plant Pathol.* **55**, 137–144.

Zolan, M.E. (1995) Chromosome-length polymorphism in fungi. *Microbiol. Rev.* **59**, 686–698.

Summary

Emerging plant diseases pose a threat to agricultural and natural ecosystems. Understanding the mechanisms behind such emergences is important in order to control them and prevent them from occurring in the future. Diseases can emerge because of several reasons, which are discussed in **Chapter 1**. Diseases emerge in pristine ecosystems through new pathogen introductions. Alternatively, alterations in the pathogen, host or environment may cause the balance of longer established plant/pathogen interactions to shift, which may lead to the emergence of disease.

Verticillium diseases cause considerable losses worldwide annually, and affect major crops such as tomato, cotton and oilseed rape. **Chapter 2** focuses on one particular *Verticillium* pathogen, namely *V. longisporum*, an allodiploid species that is specialized on brassicaceous hosts. Similar to other *Verticillium* pathogens, *V. longisporum* causes wilt symptoms on *Brassica* horticulture crops. However, on oilseed rape *V. longisporum* does not induce wilting, but rather induces stem striping symptoms.

Verticillium stem striping is an emerging disease in the UK as it was reported for the first time only in 2007, but is currently present in most regions in England. In **Chapter 3**, UK *V. longisporum* isolates were genotyped along with isolates from various countries in continental Europe, Japan and USA. UK isolates belong to the *V. longisporum* lineage that contains hybrids between the hitherto unfound *Verticillium* species A1 and species D1. Collectively, lineage A1/D1 consists of two populations; one that is abundant in Western Europe (including all UK samples) and one that is abundant more eastern in Europe. Both A1/D1 populations originate from the same hybridization event and diverged after hybridization for currently unknown reasons.

In **Chapter 4**, the UK *V. longisporum* isolates were further characterized through pathogenicity tests under glasshouse conditions. The UK isolates were as virulent as previously characterized *V. longisporum* A1/D1 isolates on various *Brassica* hosts. However, as previously demonstrated, the virulence of A1/D1 isolates is distinct from *V. longisporum* strains from other hybridization events. Generally, the virulence was positively correlated with fungal colonization levels in the stem of infected plants.

The impact of *V. longisporum* for UK oilseed rape production was assessed in **Chapter 5**, as hitherto a significant impact of *Verticillium* stem striping on yield was never demonstrated. The oilseed rape cultivars Incentive and Vision developed few symptoms upon *V. longisporum* challenge, whereas Harper and especially Quartz displayed abundant stem striping. The impact of *V. longisporum* on yield was variable over the two cropping years with one-year significant losses for all cultivars, whereas in the other year no significant losses were observed.

V. longisporum emerged as a new pathogen through hybridization and colonized a host range that differs from the host range of other *Verticillium* pathogens. **Chapter 6** describes the impact of hybridization as an evolutionary mechanism for filamentous microbes. New allele combinations with or without whole genome duplication upon hybridization can be invigorating for pathogens, leading to new disease emergences. Hybrid pathogens often developed distinct traits from their parents, such as an altered host range or higher virulence.

The impact of hybridization on *V. longisporum* was further investigated in **Chapter 7** by elucidating how these novel pathogenicity traits may evolve. *V. longisporum* received two complete chromosome sets from different *Verticillium* species that rearranged with each other. Consequently, *V. longisporum* genomes have a mosaic structure as chromosomes consist of sections of both parental origins. Furthermore, genes in *V. longisporum* generally have a higher diversification rate than the genes in haploid *Verticillium* spp., likely due to the presence of most genes in two copies. Hybridization also combined gene transcriptome patterns of two parental species leading to a novel transcription pattern in *V. longisporum*.

As a side step, genome evolution of a notorious non-hybrid *Verticillium* pathogen, *Verticillium dahliae*, was studied. Previously, *V. dahliae* was suggested to evolve according to the two-speed genome model, as strains of this species carry lineage-specific regions that are hotspots for presence/absence polymorphisms, chromosomal rearrangements, active transposable elements and *in planta*-induced effector genes. Moreover, lineage-specific regions are enriched for segmental duplications. In **Chapter 8** the sequence diversification of lineage-specific regions was investigated. Intriguingly, these regions display increased sequence conservation that affects both coding and non-coding regions. Such sequence conservation of accessory genome regions is an unprecedented finding in filamentous pathogens.

Two-speed genome evolution in filamentous pathogens is further discussed in **Chapter 9**. Filamentous pathogens employ a variety of evolutionary mechanisms to generate genomic variation, especially in accessory genome regions. The diversity by which rapid evolution is achieved in filamentous pathogens to evade host immunity can be appointed to differences in lifestyle within this heterogeneous group of organisms.

Acknowledgements

Today WE graduate. It would be a fallacy to believe that "I did it all by myself". As a PhD student you get the opportunity to steer your own project, however, you depend on so many people. I was fortunate to collaborate with and to be supported by very talented and driven people along the way. They enabled me to successfully complete my project and stand here today. In this section I want to thank all those people involved in my professional and personal life. To prevent a dry enumeration of names, I will often thank people in an anecdotal fashion. With this, it is not my intention to belittle the impact they had.

Phytopathology, studying the interaction between plants and pathogenic microbes, seems to many of my family and friends an unusual, slightly random topic to study. My interest in biology might be innate and further nurtured by my environment; however, it was prof. Monica Höfte who incited my fascination for plant diseases. I want to thank you for the way your face lit up during your lectures and how you convinced us that plant/microbe interactions were the only thing that mattered. Monica was also the one who told me: "one of the best phytopathologists in the world is Bart Thomma", a sign for me to contact him. Sara, thank you for helping me to put my motivation to do a PhD on paper. It made me a better applicant.

Thank you Seventh Framework Program of the European Union for financing the Max-CROP PhD training program that I was part of. The European Union provides great opportunities for scientists and builds bridges between research institutes across national boundaries. I was not alone in this program. I shared this training opportunity with four other diligent early-stage researchers. Aurélie, Ioannis, Mathilde and Tryntsje, it was a pleasure to attend the various courses and term reviews with you all. The highlight of our collaboration for me was the PhD outreach activity, where we joined forces and organized a great event. Lesley, thank you for being the materfamilias of Max-CROP.

Living in the UK was grand. I want to thank the suicide squad – i.e. Ahmed, Allyson, Andrew and Natalie- for being my family for five months. With you guys, I experienced the student life I never had. I will make sure you all get a thesis copy, not to read, but as a souvenir. Rosa and Ricardo, I bow deeply to you guys. You are the Italian friends everyone should have. Rico, we are so compatible, you like cooking and I like eating. Rosa, you are a guide professionally and personally. You taught me how to clone DNA and that you should stop working when your girlfriend is in the hospital.

Working at NIAB was epic. I had so many great colleagues. I will miss Anne's ecstasy for nanopore sequencing, Chris' opera voice during Spyfall, Serena's love for travelling, Simon's calmness, Sandra's sense of humor, Amelia's guinea pigs, Rebecca's terrible days, Richard's chat about the weather, Denise's passion for hula hoops, Krystyna's warnings to never have kids, Nicole's flexibility with the qPCR machine, Benedetta's

tolerance for singing in the lab, Richard's care for thrips, Garry's interest in how Laura is doing in the Netherlands... Most importantly, Tom, I want to thank you for your guidance and supervision. Initially, I could not keep up with your fast pace of speech, yet I eventually managed and understood that you generally trusted me and did not want to interfere too much in my research. Thank you for that trust.

Living in the Netherlands was not that foreign to me. I sincerely regret that I did not manage to teach Dutch people proper Flemish. Only our neighbor Willy sometimes uses the word "allez" and Sander says "yoghurt" the right way... I will have to come back. Laura and I made great friends: Fenne and Max, who wanted to spend time with us despite our geeky fascination for orchids; Xiaoqian and Tim, who shared our interest in food and board games; Sander and Kim, who changed our perception of cats.

Working at Wageningen University was luxurious. I embarked into the world of bio-informatics and had excellent guides: Sander, who murdered me when I changed files without using scripts; Xiaoqian, who had all the files I needed and Hesham, who did the quick maths. Fabian, I want to thank you for giving me a very biased view on how easy it is to supervise a student. It was a delight to work with you and you gave the project a real boost. Furthermore, I also quickly realized that bioinformaticians are in the vulnerable position of being dependent on wet lab people as, without them, there are no data to analyze. Grardy and Luis, I want to thank you for all the culturing, extractions and PCR's you did for my project. All other *Verticillium* group members, unfortunately I was only privileged to work a relatively short amount of time with many of you. During my first four months stay in Wageningen, I enjoyed working with Luigi, David, Jordi, Hanna, Mireille and Eduardo. When I rejoined the Phytopathology lab in 2017, these people already left or left soon after my arrival. However, many inspiring colleagues remained, who had an unparalleled drive for science: Nick with whom I discussed which Nordic beers we liked the most, Jinling who thought that "Jappie" was a more suitable name for me, Martin who proved that you also can make a train of two people during a conference after party, Hui who gave "see you tomorrow" a completely different connotation, Yin whom I had a great time with visiting Ljubljana, Malaika who has to endure more of me in the future... In the conclusion of my PhD, Edgar, Gabriel and Nelia started their PhD journey. I wish you all the success for your project. Also Jasper and Katharina, who spent a lot of their time in plant breeding, I wish you all the best. Finally, I want to thank two people who were elementary for my research. Michael, you joined my project as co-supervisor after two years. I want to thank you for your guidance, especially; you're so well read that you are an inexhaustible source of research ideas. Bart, I find your drive and enthusiasm really inspirational. Your high expectations helped me to become a better researcher. I wish you all the best for the new upcoming chapter in your professional career.

Han and San, my siblings and best buddies, I always look forward to our weekly (Hanne) or bimonthly (Sander) skype chats. Sander, thank you for being our personal taxi driver and the help moving me from Belgium to the UK, from Belgium to the Netherlands, from the Netherlands to the UK, from the UK to the Netherlands, from the Netherlands to the Netherlands and finally from the Netherlands to Germany.

Mum and dad, as Kahlil Gibran said, "your children are not your children". When I moved to the UK to start my PhD, Hanne and Sander spread there wings soon after and live currently in Antwerp and Ghent, respectively. Desperate as you are, you adopted a disabled cat to fill the void. Just know that our confidence in what we undertake is due to your diligence in our upbringing.

Other family members, I thank you for your support and visits, which required trips to exotic places. I will never forget drinking champers with the "omatjes" whilst punting on the Cam, quaffing wine in a London cellar with uncle Ides and tasting more wine with aunt Veerle and uncle Johan in their caravan in Ede.

To my British family, I felt very welcomed. I have great memories drinking Ethiopian coffee with John during the Amsterdam coffee festival, drinking milky tea in the flat of "the boys" when Sarah moved in and Hannah, your biscottis need no words.

Drumrolls... Laura, I will definitely not write that I love you and that you are the most important person in my life. As you told me, this would be highly inappropriate and embarrassing, as so many strangers will read this. Let me just say that you are my dearest.

About the author

Jasper R.L. Depotter was born in Bruges, Belgium on the 6th of June 1991. As a boisterous young child, Jasper already took an interest in agriculture. He was eager to join his granddad at his modestly sized farm, where sheep, chickens and ducks were kept. Moreover, at home, Jasper was occupied with initially rabbit, and later duck breeding. Jasper combined this interest for agriculture with a propensity for sciences at school. Consequently, during his final two years at Sint-Lodewijks secondary school in Bruges, he majored in sciences and maths. In 2009, Jasper moved to Ghent to embark on a bioengineering degree at Ghent University. After two years of his degree with a broad formation in maths and sciences, Jasper specialized in agriculture, learning about animal and plant production systems. In 2012, Jasper obtained his BSc degree in bioengineering cum laude. Jasper continued to study in Ghent and began an MSc degree in bioengineering with the emphasis on agriculture. In the first year, Jasper attended courses addressing a wide range of agronomic topics, from plant breeding to European agricultural policies. During the summer, Jasper went to Ames, Iowa, USA, for a six-week long internship at Iowa State University, where he completed a rotation project contributing to experimental horticulture trials. In the final year of his MSc degree, Jasper specialized in phytopathology during his thesis. For one year, he joined the research group of prof. dr. ir. Monica Höfte and studied the interaction between pathogenic and beneficial *Verticillium* strains in the host tomato. This thesis study incited Jasper's interest in interactions between plants and microbes. Consequently, Jasper looked for a PhD project to continue his research in phytopathology. Having worked with *Verticillium* pathogens, Jasper contacted prof. dr. ir. Bart P.H.J. Thomma and enquired for PhD opportunities in his lab. Coincidentally, prof. Thomma had an open "sandwich" PhD position, which was a collaboration between the National Institute of Agricultural Botany and Wageningen University. Jasper obtained this position and thus, after completing his MSc degree with magna cum laude, he moved to Cambridge, UK, for two years. After a further two years in Wageningen, the Netherlands, Jasper completed his PhD thesis, of which the result can be seen here. Jasper graduates with the exciting prospect of starting a postdoc position studying smut pathogens in the terrestrial microbiology laboratory of prof. dr. Gunther Doehlemann, at the University of Cologne.

List of publications

Depotter, J.R.L., van den Berg, G.C.M., Wood, T.A., Thomma, B.P.H.J. and Seidl, M.F. (2018) The mitochondrial genome of the hybrid fungal pathogen *Verticillium longisporum* has a bi-parental origin. In preparation.

Depotter, J.R.L., van Beveren, F., Rodriguez-Moreno, L., van den Berg, G.C.M., Wood, T.A., Thomma, B.P.H.J. and Seidl, M.F. (2018) Homogenization of sub-genome secretome gene expression patterns in the allodiploid fungus *Verticillium longisporum*. Submitted

Depotter, J.R.L., Shi-Kunne, X., Missonnier, H., Liu, T., Faino, L., van den Berg, G.C.M., Wood, T.A., Zhang, B., Jacques, A., Seidl, M.F., Thomma, B.P.H.J. (2018) Dynamic virulence-related regions of the fungal plant pathogen *Verticillium dahliae* display remarkably enhanced sequence conservation. Submitted.

Depotter, J.R.L., Thomma, B.P.H.J. and Wood, T.A. (2018) Measuring the impact of *Verticillium longisporum* on oilseed rape (*Brassica napus*) yield in field trials in the United Kingdom. *European Journal of Plant Pathology*. Accepted.

Depotter, J.R.L., Rodriguez-Moreno, L., Thomma, B.P.H.J. and Wood, T.A. (2017) The emerging British *Verticillium longisporum* population consists of aggressive *Brassica* pathogens. *Phytopathology* 107, 1399-1405.

Depotter, J.R.L., Seidl, M.F., van den Berg, G.C.M., Thomma, B.P.H.J. and Wood, T.A. (2017) A distinct and genetically diverse lineage of the hybrid fungal pathogen *Verticillium longisporum* population causes stem striping in British oilseed rape. *Environmental Microbiology* 19, 3997-4009.

Depotter, J.R.L., Seidl, M.F., Wood, T.A. and Thomma, B.P.H.J. (2016) Interspecific hybridization impacts host range and pathogenicity of filamentous microbes. *Current Opinion in Microbiology* 32, 7-13.

Depotter, J.R.L., Deketelaere, S., Inderbitzin, P., von Tiedemann, A., Höfte, M., Subbarao, K.V., Wood, T.A. and Thomma, B.P.H.J. (2016) *Verticillium longisporum*, the invisible threat to oilseed rape and other brassicaceous plant hosts. *Molecular Plant Pathology* 17, 1004-1016.

Education Statement of the Graduate School Experimental Plant Sciences

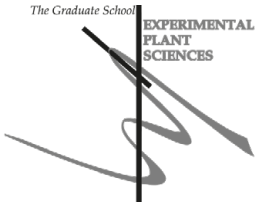

Issued to: **Jasper R.L. Depotter**
Date: **14 September 2018**
Group: **Laboratory of Phytopathology**
University: **Wageningen University & Research**

1) Start-up phase

	date
► **First presentation of your project**	
Population and pathogenicity dynamics of the *Brassica* pathogen *Verticillium longisporum*	23 Feb 2015
► **Writing or rewriting a project proposal**	
Population and pathogenicity dynamics of the *Brassica* pathogen *Verticillium longisporum*	24 Oct 2014
► **Writing a review or book chapter**	
Verticillium longisporum, the invisible threat to oilseed rape and other brassicaceous plant hosts. Molecular Plant Pathology, (2016) **17**(7), 1004-1016, DOI: 10.1111/mmp.12350	2016
Interspecific hybridization impacts host range and pathogenicity of filamentous microbes. Current Opinion in Microbiology, (2016) **32**:7-13, DOI:10.1016/j.mib.2016.04.005	2016
► **MSc courses**	
► **Laboratory use of isotopes**	
Subtotal Start-up Phase	*7.8 credits**

2) Scientific Exposure

	date
► **EPS PhD student days**	
EPS PhD day 'Get2Gether', Soest, NL	09-10 Feb 2017
EPS PhD day 'Get2Gether', Soest, NL	15-16 Feb 2018
► **EPS theme symposia**	
EPS Theme 2 symposium 'Interactions between Plants and Biotic Agents', together with Willie Commelin Scholten day, Utrecht, NL	20 Feb 2015
EPS Theme 2 symposium 'Interactions between Plants and Biotic Agents', together with Willie Commelin Scholten day, Wageningen, NL	23 Jan 2017
EPS Theme 2 symposium 'Interactions between Plants and Biotic Agents', together with Willie Commelin Scholten day, Amsterdam, NL	24 Jan 2018
► **National meetings (e.g. Lunteren days) and other National Platforms**	
Annual meeting 'Experimental Plant Sciences', Lunteren, NL	13-14 Apr 2015
Annual meeting 'Experimental Plant Sciences', Lunteren, NL	10-11 Apr 2017
Annual meeting 'Experimental Plant Sciences', Lunteren, NL	09-10 Apr 2018
► **Seminars (series), workshops and symposia**	
Seminar: prof. dr. Yves van de Peer, The evolutionary significance of gene and genome duplications	02 Feb 2015
Seminar: prof. dr. ir. Monica Höfte, Towards understanding rice brown spot, a disease induced by physiological stress	06 Feb 2015
Seminar: Chih-Hang Wu, Helper NLR proteins of the NRC family in solanaceous plants	05 Mar 2015
Seminar: dr. Alisdair Fernie, Tomato metabolomics in 2015, the difference a genome makes	11 Mar 2015

	Seminar: dr. Will Cuddy, Wheat yellow rust in Australasia	29 Jun 2015
	Symposium: COST Action SUSTAIN on pathogen-informed crop improvement, Wageningen, NL	08-10 Apr 2015
	Symposium: NIAB Open Day 2015, Cambridge, the United Kingdom	23 Jun 2015
	Symposium: NIAB Director's Day 2015, Cambridge, the United Kingdom	26 Jun 2015
	Mini-symposium: Applied phytopathology - from the lab to the field, Wageningen, NL	01 Mar 2017
	Workshop: Max-CROP training, Cambridge, the United Kingdom	10-12 Feb 2015
	Workshop: Max-CROP training, Wageningen, the Netherlands	05-08 May 2015
	Workshop: Max-CROP training Midterm review, Cambridge, the United Kingdom	24 Nov 2015
	Workshop: Max-CROP training Midterm review, Cambridge, the United Kingdom	21-22 Nov 2016
	Workshop: Netherlands Society for Evolutionary Biology (NLSEB) meeting, Ede, NL	11 Apr 2018
▶	**Seminar plus**	
▶	**International symposia and congresses**	
	12th International Verticillium Symposium, Ljubljana, Slovenia	06-09 Oct 2016
	29th Fungal Genetics Conference, Pacific Grove, CA, USA	14-19 Mar 2017
▶	**Presentations**	
	Poster: Verticillium was introduced at least twice in the U.K.	23 Jun 2015
	Poster: Verticillium stem striping: an emergent disease on oilseed rape in the UK	28 Jun 2016
	Poster: Divergent evolution of the hybrid fungal pathogen *Verticillium longisporum*	16 Mar 2017
	Talk: Agri-Tech Pollinator event: *Verticillium longisporum,* detection and diagnostics in UK oilseed rape	19 Jan 2016
	Talk: 12th International Verticillium Symposium: Population structure of the *Verticillium* striping pathogen of oilseed rape; *Verticillium longisporum*	07 Oct 2016
	Talk: Mini-symposium applied phytopathology: divergent evolution within a hybrid fungal pathogen species	01 Mar 2017
	Talk: Host-Microbe Genetics Meeting: Dynamics and conservation in the compartmentalised genome of *Verticillium*	27 Oct 2017
▶	**IAB interview**	
▶	**Excursions**	
	Subtotal Scientific Exposure	*18.7 credits**

3) In-Depth Studies		*date*
▶	**EPS courses or other PhD courses**	
	Postgraduate course 'Genome Assembly', Wageningen, NL	28-29 Apr 2015
	NIAB-CJBS Entrepeneurship course, Cambridge, the United Kingdom	14-16 Jun 2017
	Data analyses and visualizations in R (for biologists), Wageningen, NL	12-13 Dec 2016
▶	**Journal club**	
	Participation in literature discussion group, Laboratory of Phytopathology	2015-2018
▶	**Individual research training**	
	Training course: Disease management in oilseed rape, Artis, Cambridge, the United Kingdom	12 Nov 2014
	Training course: Crop agronomy for cereals and oilseed rape, Artis, Cambridge, the United Kingdom	28 Jan 2015
	Quantitative methods in plant breeding, NIAB, Cambridge, the United Kingdom	Sept-Dec 2015
	Subtotal In-Depth Studies	*5.2 credits**

4) Personal development	*date*
► **Skill training courses**	
Green shoots communication skills course, Cambridge, the United Kingdom	05-07 Jan 2015
PhD Workshop Carousel: Scientific discussion and reasoning, Finding and acquiring small grants and writing proposals, Wageningen, NL	17 Apr 2015
Didactical courses WUR: online activerende werkvormen, Wageningen, NL	19 May 2015
EPS introduction course, Wageningen, NL	29 Sep 2016
Mobilising your scientific network, Wageningen, NL	17 & 24 Oct 2017
Last stretch of PhD programme, Wageningen, NL	22 Sep 2017
Philosophy and ethics of food science and technology, Wageningen, NL	Jan-Feb 2018
► **Organisation of PhD students day, course or conference**	
Organisation conference NIAB PhD outreach activity, the United Kingdom	20-21 Nov 2017
► **Membership of Board, Committee or PhD council**	
Subtotal Personal Development	*5.7 credits**

TOTAL NUMBER OF CREDIT POINTS*	*37.4*

Herewith the Graduate School declares that the PhD candidate has complied with the educational requirements set by the Educational Committee of EPS which comprises of a minimum total of 30 ECTS credits

** A credit represents a normative study load of 28 hours of study.*

This work was supported by the Framework Program 7 (FP7-PEOPLE) of the European Commission (Project ID: 607178). The work was carried out in the Laboratory of Phytopathology, Wageningen University, the Netherlands, and in the Department of Crops and Agronomy, National Institute of Agricultural Botany, the United Kingdom.

Cover & layout design: Iliana Boshoven-Gkini || AgileColor.com
Printed by: Proefschriftmaken, Vianen, The Netherlands || Proefschriftmaken.nl